CHARACTERIZATION OF THE *HELICOBACTER PYLORI* VACUOLATING CYTOTOXIN MEDIATED INDUCTION OF MITOCHONDRIAL CELL DEATH MECHANISM

BY

PRASHANT JAIN

DISSERTATION

Submitted in partial fulfillment of the requirements
for the degree of Doctor of Philosophy in Microbiology
in the Graduate College of the
University of Illinois at Urbana-Champaign, 2012

Urbana, Illinois

Doctoral Committee:

Professor Steven R. Blanke, Chair
Professor Abigail A. Salyers
Professor James M. Slauch
Assistant Professor Rachel J. Whitaker

Abstract

The *Helicobacter pylori* vacuolating cytotoxin (VacA) is a paradigm for microbial virulence factors that target and disable host cell mitochondria. VacA intoxication triggers mitochondrial dysfunction and metabolic stress, but the mechanisms underlying these perturbations in mitochondrial function are poorly understood. In this dissertation, we report that infection of gastric epithelial cells with *H. pylori* results in the transition of cellular mitochondria from a predominantly filamentous network state to small punctiform organelles, suggesting that *H. pylori* uncouples the dynamic balance between mitochondrial fusion and division that normally exists within healthy cells. *H. pylori* infection induces excessive mitochondrial recruitment of the endogenous host protein Drp1, which plays a critical role in the regulation of mitochondrial division within uninfected healthy cells. The dynamic balance between mitochondrial division and fusion is important for maintaining proper functionality of the network. However, increased mitochondrial fragmentation could result in metabolic stress and cell death. Among *H. pylori* factors, the vacuolating cytotoxin (VacA) was demonstrated to be both essential and sufficient to disrupt mitochondrial dynamics. Importantly, specific inhibition of Drp1 activity blocks VacA-induced fragmentation of mitochondrial network, as well as activation of mitochondria dependent cell death program (apoptosis), a hallmark of *H. pylori* infection. Importantly, Drp1 mediated mitochondrial fission preceded and was required for Bax activation, which is critical for VacA dependent cell death mechanism.

However, the complete mechanism underlying VacA mediated Bax activation, particularly the nature of cellular changes initiated by VacA that linked the de-regulation of mitochondrial network dynamics to engagement of host apoptotic machinery, was not entirely clear. Additional studies reported in Chapter 3 of this dissertation demonstrate that VacA induces the activation and mitochondrial recruitment of the endogenous stress sensor protein Bid (BH3 interacting death domain agonist). Within VacA intoxicated cells, Bid was important for the activation of Bax and mitochondrial cell death mechanism. Importantly, Drp1 GTPase activity was required for Bid activation within VacA intoxicated cells. Our results therefore indicate that cellular stress as a result of excessive fission is possibly translated to Bax mediated mitochondrial outer membrane permeabilization through the stress sensor Bid. Furthermore, Drp1 dependent mitochondrial fission also resulted in the increase in cytosolic calcium levels, which was required for the activation of the calcium dependent cysteine protease called calpain. The proteolytic activity of calpain was required for processing of Bid to yield the mitochondrial targeting active fragment called t-Bid (truncated Bid).

We Hypothesize that *H. pylori* mediated deregulation of mitochondrial dynamics promotes bacterial colonization by generating a novel class of dysfunctional host cells that are energetically crippled, and unable to respond appropriately to infection with *H. pylori* at the epithelial barrier.

Acknowledgements

I would like to express my sincere gratitude to my advisor, Professor Steven Blanke, for his unwavering support and guidance throughout these years. He always showed tremendous faith in my abilities, especially during tough phases in my research. His mentorship provided me with renewed vigor and confidence that helped me complete this dissertation.

I am also grateful to Professor Abigail Salyers, Professor James Slauch and Professor Rachel Whitaker in my thesis committee for their support and encouragement. I thank them for taking the time to guide me and read my thesis despite their busy schedules.

I wish to thank the members of Blanke Lab, whom I consider more as friends rather than colleagues, for the pleasant memories of wonderful times I had working with them. I am fortunate to have worked with a highly motivated and intelligent group of people who have had considerable influence in shaping my thoughts and personality since the time I joined the lab. I have greatly benefited from the vast expertise of my friends and the stimulating conversations we had over the years.

I wish to thank Dr. Barbara Pilas and Dr. Bernard Montez of the University of Illinois R. J. Carver Biotechnology Center Flow Cytometry Facility for their technical expertise and assistance in carrying out flow cytometry analysis.

I would like to express my sincere gratitude to our Microbiology office manager Debra LeBaugh and Office support specialist Diane Tsevelekos for their support and help throughout the years.

Lastly, I would like to thank my family for providing me with the support and strength to face life's challenges. My parents have always been my source of strength and have provided me with confidence and clarity during tough times. My dad, a doctor in the Indian Army, is a man of strong principles and character. He has always impressed upon me the importance of being focused and considerate in any task I undertake. My mother has been my eternal source of comfort and has taught me to live life with confidence and purpose. But more than anything, my parents have inspired me to be a good and caring human being. My sister was my role model growing up. Her perseverance and hard work in everything she did constantly inspired me to work harder towards achieving my potential. Finally, I want to thank my wife, who for the last many years has endured my pain and celebrated my success. I could not have asked for a more sincere and caring companion than her and thank the almighty for bringing us together. I feel extremely blessed to have such a wonderful family and thank them for their love and support. I therefore dedicate this thesis to my dear family. My accomplishments so far would not have been possible without their blessings.

Table of Contents

Chapter 1: Introduction

1.1 *HELICOBACTER PYLORI*

Nearly 25 years ago, researchers Barry Marshall and Robin Warren discovered the causative agent of peptic ulcer disease as the bacterium *Helicobacter pylori* (82, 83). This discovery shattered the popular perception of that the harsh acidic environment of stomach is inhospitable for bacterial colonization. In a dramatic demonstration of Koch's postulates, Dr. Marshall quelled these doubts by ingesting *H. pylori* culture and subsequently developing peptic ulcer disease. Following anti-biotic treatment, he cured the peptic ulcer, proving to the scientific community that the disease resulted from *H. pylori* colonization. The discovery not only led to the re-evaluation of the treatment of gastro-intestinal disorders, but also spawned numerous initiatives to identify probable bacterial causes to diseases considered incurable. For their path breaking discovery and for confirming the infectious etiology of peptic ulcer disease, Barry Marshall and Robin Warren were jointly awarded the Nobel Prize in Physiology or Medicine in 2005 (1, 42, 105).

Since the discovery of *Helicobacter pylori* as a gastro-intestinal pathogen, studies have revealed that a significant proportion of world population is infected with this bacterium, estimated close to 50-60% in developed countries and nearing 100% in some developing nations. *H. pylori* is a gram negative microaerophile known to colonize the gastric mucosa (Fig. 1.1), which provides a protective environment for the bacterium, subsequently allowing for bacterial

attachment to stomach epithelia (Fig. 1.2) and development of pathology. Infection with *H. pylori* is generally thought to occur during childhood, either through oral-oral or fecal-oral routes of transmission (39) and in the absence of therapeutic intervention, can last for up to the lifetime of host (43). Although chronic infection with *H. pylori* is largely manifested as pan-gastritis or gastric inflammation and are predominantly asymptomatic, close to 10-20% of infected individuals develop more serious outcomes like gastric and duodenal ulcers. Notably, close to 1-2% of infected individuals progress to a state of MALT (Mucosa Associated Lymphoid Tissue) lymphoma and gastric adenocarcinoma (144), which is the second largest cause of cancer related deaths worldwide (61), therefore resulting in the classification of *H. pylori* as a group 1 human carcinogen (NIH Consensus Conference, 1994). The fact that the rate of infection clearly outpaces the incidence of disease indicates that *H. pylori* mediated disease is complex and multi-factorial. Studies have suggested that successful treatment of *H. pylori* infection resulted in almost 70% reduction in disease incidence (101). Thus, the understanding of *H. pylori* pathobiology has gained considerable interest, particularly with regards to understanding the mechanism by which the bacteria is able to persist within the harsh environment of human stomach for extended periods of time.

1.1.1 *Helicobacter pylori* pathogenesis.

In addition to being the most successful bacterium to colonize the stomach, *H. pylori* is also the first organism with complete genome sequenced from 2 unrelated strains (4, 6, 122). The 1.67 megabases of *H. pylori* genome

code for 1590 predicted ORFs. Despite the small genome, *H. pylori* strains isolated from unrelated patients display remarkable genetic heterogeneity, with every isolate appearing to have a unique DNA fingerprint (22). The genetic diversity observed within *H. pylori* could possibly help the bacteria evolve strategies to remodel the host gastric epithelia and make it more conducive for successful colonization.

In order to successfully colonize the host gastric epithelia, *H. pylori* has to overcome environmental stress like the acidic pH, as well as host immune defenses. The production of urease by the bacterium, helps in converting urea at the site of colonization into ammonium ions, which significantly elevate the pH and help in bacterial survival (116). Additionally, *H. pylori* harbor an arsenal of protein toxins that directly modulate the functions of the host cells in order to assist in stable colonization within the site of infection. One such toxin is the product of the cytotoxin associated gene A (*cagA*) (63) which is directly injected into the host cytoplasm by a type IV secretion system, and activates the NF-kB signaling cascade, resulting in the release of inflammatory mediators like IL-8 (63). Additionally, virulent strains of *H. pylori* also secrete an exotoxin called VacA (Vacuolating cytotoxin A), which as discussed in detail below initiate multiple changes within the host epithelial cells, aiding in bacterial persistence and colonization (76).

1.2 VACUOLATING CYTOTOXIN (VacA)

VacA is the only known exotoxin produced by *Helicobacter pylori* and was initially identified as a protein in the *H. pylori* culture filtrate which was able to form large intra-cellular vacuoles within cultured mammalian epithelial cells (76). Several studies examining the role of VacA in *H. pylori* colonization have established the importance of VacA, not only in the initial colonization of the bacteria, but also in persistence of *H. pylori* within the host stomach (111). VacA has been directly implicated in the development of gastric and duodenal ulcers (44). In fact, VacA, introduced orally into mice was able to generate ulcerative lesions similar to those found following *H. pylori* infection (81, 121). Moreover, *H. pylori* colonization was greatly attenuated in isogenic VacA knockout strains, compared to wild type strains, underlining the importance of VacA in *H. pylori* pathogenesis (111).

1.2.1 VacA expression and secretion.

VacA is encoded by the chromosomal gene *vacA* (26, 29, 113) and is produced in active form by ~ 50% of *H. pylori* clinical isolates (5). VacA is initially produced as a 140 kDa pro-toxin, which contains a classic leader peptide to Sec-dependent secretion in Gram negative bacteria (113, 121). The Carboxy-terminus of VacA displays a region with significant sequence homology to a family of gram negative bacterial autotransporters (93). Processing of the pro-toxin, likely involving cleavage of the leader peptide in the bacterial periplasm, yields an 88 kDa mature toxin, that is secreted to the extracellular space as a

soluble protein, facilitated by transport across the bacterial outer membrane by a Type V autotransporter mechanism (93) (Fig. 1.3). Additionally, VacA can also remain associated with the bacterial surface within spatially organized domains (65).

1.2.2 VacA general properties.

VacA (88 kDa monomer) assembles as single or double layer, heat resistant oligomers in solution at physiological pH (23, 24, 27, 79, 137). Analysis of 2-D crystals, as well as electron microscopy and metal replica analysis have confirmed that oligomers are composed of either 6-8 monomers (single layer) or 12-14 monomers (double layer) (2, 40, 79, 107). The monomers assemble in the form of either a single layer or double layer of symmetrically arranged petals around a central ring, giving rise to a flower shaped oligomeric structure (79) (Fig. 1.4). The VacA oligomer is pH sensitive. Protease sensitivity assays, as well as circular dichroism and fluorescence spectroscopy measurements have indicated that VacA oligomer reversibly dissociates into monomers at acidic or alkaline pH, and possibly undergoes significant conformational rearrangements thereafter (27, 31, 35, 88).

VacA belongs to a class of intracellularly acting toxins called A-B toxins or class 3 toxins (33). Showing similarity to A-B toxins, VacA monomers consist of 2 domains, a 55 kDa domain (p55), analogous to B moiety, responsible for binding to cell surface receptors and facilitating the entry of the catalytic A moiety, which in the case of VacA is a 33 kDa domain (p33) (84, 106). However studies have

suggested that VacA does not entirely follow the classical A-B toxin model, as cellular vacuolation, a marker for intracellular VacA action, required the co-expression of both p33 domain and a small portion of p55 domain within transfected HeLa cells, whereas expression of either p33 or p55 alone failed to induce vacuolation (142). Studies also show that VacA monomers assemble as higher ordered oligomers within vacuolated cells, suggesting that inter-molecular interaction between monomers may be critical for VacA intra-cellular function (134).

1.2.3 VacA alleles.

The *vacA* gene is polymorphic (127) (Fig. 1.5), with allelic variation directly linked to VacA production and disease incidence within *H. pylori* infected individuals (8, 9). The first region of allelic variation resides within 'secretion signal' or 's region'. *H. pylori* strains containing the s1 allele are associated with increased VacA production and virulence, indicated by increased gastric disease incidence in infected individuals, when compared to the s2 allele variants (8, 9). The second region of allelic variation within *vacA* gene lies in the 'middle region' or 'm region', with the m1 and m2 allelic variants displaying differential, cell type specific binding abilities (98). While both s1m1 and s1m2 are associated with disease causing strains as compared to the non disease associated s2 allele, the m region allele variants (m1 and m2) are associated with differential tendency to develop gastric ulcer disorders (7-9). Individuals infected with *H. pylori* strains harboring m1 *vacA* allele are more prone to gastric epithelial damage and gastric adenocarcinoma than those infected with *H. pylori* strains harboring m2 allele

(75). Further investigations into *vacA* allelic variations have recently led to the discovery of a third allelic variant called ‘intermediate’ or i-variant, which lies between the signal and middle region (108). Similar to the earlier variants, between the i1 and i2 variants, only the i1 variant is significantly associated with risk of gastroduodenal diseases in *H. pylori* infected individuals (94, 108). While the correlation between *vacA* allelic variations to gastric disease state is exciting, further investigations need to be conducted to understand the pathophysiology behind these correlations.

1.2.4 Mechanisms of VacA cellular intoxication.

In order to colonize a host, bacterial pathogens rely on numerous strategies, either involving changes within the pathogens themselves, or, effective remodeling of host cells and tissues by a group of protein effectors called toxins. Various toxins modulate host cell functions through action on host cell surface (receptors), or via traversing host cell membrane and acting directly on vital intracellular organelles. Depending on their mechanism of action on host cells, toxins are classified into Class 1, 2 or 3.

Class 1 toxins, which include superantigens, primarily from *S. aureus* and *S. pyogenes*, act at the level of host plasma membrane of immune cells, resulting in the production of pro-inflammatory cytokines (77). This group also contains heat stable toxins from *E. coli*, which modulate host cell intracellular signaling by binding to host cell receptors (56).

Class 2 toxins, similar to Class 1 toxins, also interact with host cell membrane. However, they are distinct in their mode of action. These toxins form pores on the host plasma membrane, thereby inducing membrane permeability changes which ultimately disrupt retention of macromolecules and small solutes within cells. Pores formed by Class 2 toxins can range from small pores (1-2 nm) to larger pores (approx. 35 nm). Apart from eliciting effects on host osmolarity, Class 2 toxins are also shown to modulate cytokine release, activate cellular proteases and host apoptotic programs. Class 2 toxins include Listerolysin O (LLO) from *L. monocytogenes*, Streptolysin O (SLO) from *S. pneumomoniae,* and aerolysin secreted by *Aeromonas hydrophila*, which have been shown to confer anti-phagocytic properties to the bacterium and damage host tissues by virtue of their pore forming activity (11, 46, 59).

A third class of protein effectors produced by certain pathogenic organisms involve proteins that interact with host cells and have broad degradative properties. Members of this class include proteases, chitinases, nucleases and lipases, which are typically involved in the degradation of extracellular matrix and membrane components of host cells. A well known example of this class of protein effectors is *Bacteroides fragilis* enterotoxin (BFT) (87). This zinc-dependent metalloprotease cleaves a number of extracellular matrix proteins *in vitro* leading to diarrhea and fluid accumulation in ligated ileal loops. Infact, the internalization of a number of enteric pathogens such as *Salmonella sp*., *E. coli*, and *enterococcus sp*. is shown to be enhanced due to the proteolytic activity of BFT (132).

The classes of toxins mentioned above are not required to enter the host cell to modulate host cell functions. However, protein effectors of several pathogens are required to be transported directly into the host cell cytosol, in order to elicit their modulatory functions (14, 45, 114, 135). The direct injection of bacterial factors into host cells is shown to be mediated by the bacterial Type III and Type IV secretion systems, which are adaptations of the flagellar biosynthetic machinery and conjugative pilus machinery, respectively (14, 48). This fourth class of toxin is distinct from the other classes mentioned earlier, as they modulate the function of only the host cells with which they are in intimate contact, as opposed to the capability of a distal mode of action demonstrated by toxins from classes 1, 2 and 3.

Another class of toxins is called the AB intracellularly-acting toxins. The enzymatic activity of AB toxins lies in the A moiety, which covalently modifies the intracellular targets to modulate host functions (36). The B moiety is involved in binding to the host cell membrane and facilitating the translocation of A moiety into the host cytosol (10). The diphtheria toxin from *C. diphtheriae*, cholera toxin from *V. cholerae,* and shiga toxin from different sources including *E. coli* (O157:H7) and *S. dysenteriae* are typical examples A-B group of toxins.

The mechanism of action of VacA, especially in relation to cellular vacuolation, is considered very similar to that of an A-B toxin (60, 107). However, studies aimed at identifying VacA domains essential for induction of cellular vacuolation have demonstrated the requirement of both p33 domain, and a small portion of p55 domain for VacA to elicit its vacuolating activity (142). Therefore,

mechanism of cellular action of VacA has features which are not typical of an A-B toxin. Infact, VacA is shown to share specific features that belong to different classes of toxins mentioned earlier. The ability of VacA to modulate cellular interactions in polar epithelial membranes from the cell surface is similar to the mechanism of action of Class 1 toxins (24). Moreover, the ability of VacA to form membrane channels is reminiscent of Class 2 pore forming toxins (119). Interestingly, studies have demonstrated the important role of VacA channel activity in cellular vacuolation. It is therefore hypothesized that VacA induced cellular vacuolation could be a result of the toxin's ability to act both as an intracellular acting A-B toxin, as well as a pore forming class 2 toxin (24).

1.2.5 Cellular effects of VacA.

VacA is a paradigm for multi-functional intracellular-acting toxins (24) (Fig. 1.6). The cellular effects of VacA intoxication range from increased anion permeability of the cell membrane, loss of trans epithelial electrical resistance (TER), to membrane depolarization and cellular vacuolation and modulation of cellular apoptotic signaling mechanisms and immune cell functions (37, 102, 104, 119, 123, 133). An important biochemical function related to most of these cellular effects of VacA is the formation of channels on cell membrane. The membrane channels formed by VacA are known to mimic anion selective channels found within human cells (32).

Previous studies suggest a very important role anion channels formed by VacA in promoting efficient colonization and persistence of *H. pylori* within the

host. Increased paracellular permeability following channel formation could lead to release of low molecular weight nutrients such as pyruvate, as well as ions like Nickel and Iron, which help sustain bacterial infection and promote colonization in the nutrient starved host environment (100, 119, 123). VacA anion channel function has been implicated in the modulation of tight junctions in polarized epithelial monolayers, thereby decreasing the trans epithelial electrical resistance (TER). Furthermore, VacA anion channels formed within intracellular sites, such as membranes of late endosomes and mitochondria, is shown to result in vacuolation and mitochondrial membrane depolarization, respectively (119, 124, 133).

However, studies have also reported VacA cellular activities, which do not rely on toxin channel activity. These cellular activities involve modulation of cellular signaling mechanisms involved in immune cell functions. VacA intoxication is shown to result in the upregulation of expression of proinflammatory molecules such as cyclooxygenase-2 (COX-2) and prostaglandin E_2 (PGE_2), through the activation of mitogen activated protein kinases such as p38 and ERK1/2, as well as activating transcription factor 2 (ATF2) signaling pathway (64, 91).

Previous reports indicate that the immunomodulatory effects of VacA range from immunosuppressive functions, such as inhibition of T-cell proliferation (52, 117), to pro-inflammatory functions, such as those involving TNF-α and IL-6 by Mast cells (34, 118), as well as COX-2 by neutrophils and macrophages (64). Furthermore, VacA is also shown to interfere with antigen presentation by B cells

and phagosome maturation within macrophages (3, 89, 145). Infact, the recruitment and retention of the tryptophan-aspartate-containing coat protein 1 (TACO or coronin 1) within phagosomes is thought to impair the phagocytic clearance of *H. pylori* (145).

1.2.6 Cellular vacuolation induced by VacA.

Cultured mammalian cells develop large cytoplasmic vacuoles following intoxication with VacA. *H. pylori* and VacA induced vacuolation has been reported both *in vitro* and *in vivo* within various cell types, including primary gastric epithelial cells, as well as gastric biopsies from infected individuals (62, 76, 115, 125).

Induction of cellular vacuolation by VacA is potentiated by brief acidification followed by reneutralization of the toxin (process referred to as acid activation), and the presence of weak base like ammonium ions (26, 35). Investigations into the characteristics of VacA induced vacuoles have revealed the presence of Rab7 (small GTP binding protein), lysosomal proteins LAMP1 and Lgp110 on the vacuolar membrane, suggesting that the vacuoles were derived from late endosomal and lysosomal compartments within the cells (99, 100). Consistent with their origin, the vacuoles have an intraluminal acidic pH, which enables the vacuolar accumulation of weak bases, including dyes such as acridine orange and neutral red, which has been extensively used to visualize and quantify cellular vacuolation (30).

VacA anion channel function is important for vacuolation activity of the toxin as demonstrated by the inhibition of vacuolation activity using NPPB (anion channel inhibitor) and the absence of cellular vacuolation in cells intoxicated with channel mutants of VacA (84, 119, 129, 141). A current model for the mechanism of VacA-induced vacuole formation proposes that VacA binds to the plasma membrane, internalizes, and inserts into endosomal membranes to form anion-selective membrane channels, a notion supported by localization of VacA to the limiting vacuolar membranes (109, 119). VacA channel activity is proposed to result in an influx of anions into the endosomes (123), which stimulates increased proton pumping by the vacuolar ATPases. However, since protons are relatively permeable and have a tendency to leak out of the vacuolar membranes, the concerted action of VacA channel activity and electrogenic vacuolar ATPase is thought to result in accumulation of protonated, membrane-permeant weak bases such as ammonium ions inside endosomes, resulting in their osmotic swelling and transformation into vacuoles (53). Direct evidence for this mechanism of VacA induced vacuolation comes from TEM studies done on isolated endosomes showing the essentiality of VacA channel activity (using VacA channel mutants) for osmotic swelling of endosomes (53).

1.3 VacA AND APOPTOSIS

Apoptosis is a highly conserved, genetically encoded cell death program. Apoptotic cell death is involved in several important functions such as removal of excess or damaged cells, infected cells, cancerous cells, as well as regulation of host immune responses and various other physiologically important functions

(41, 55, 69, 96, 128). Importantly, deregulation of apoptotic mechanism is known to result in several pathologies, including cancer and neurodegenerative disorders (13, 78, 146).

The signals leading to activation of apoptotic mechanism typically involve phosphorylation cascades originating from cell surface receptors, or could originate from DNA damage as well as other signals. Within vertebrate cells, apoptosis proceeds through mainly two forms of signaling pathways, an “Intrinsic pathway” and an “Extrinsic pathway”, each of which activate cell death mechanism by activating Executioner Caspase 3 and Caspase 7 (97, 120). The Intrinsic pathway involves the release of cytochrome *c* (Cyt *c*), an apoptogenic factor, from the mitochondria to cytosol following mitochondrial outer membrane permeabilization (MOMP). Cyt *c* binds to monomeric apoptotic activation factor (APAF1), leading to APAF1 oligomerization and creation of Apoptosome, which recruits Caspase 9, which in turn activates Caspases 3 and 7 (Fig. 1.7). The extrinsic pathway involves the activation of Caspase 8 through a death receptor ligation mechanism. Although Caspase 8 is known to directly cleave and activate Caspases 3 and 7, studies have clearly demonstrated that Caspase 8 can proteolytically process and activate the BCL-2 homology 3 (BH3)-interacting domain death agonist (BID). BID, a BH3 only protein, translocates to mitochondria, where it activates pro-death effector Bcl-2 protein BAX. Activation of BAX results in MOMP, thereby inducing cell death by a mechanism involving Cyt *c* dependent Caspase 3 and 7 activation (20).

Persistent infection with *Helicobacter pylori* has been strongly associated with induction of apoptosis within the gastric mucosa (72, 73, 80, 90, 130, 136). Infact, induction of host cell apoptosis is considered as a hallmark of *H. pylori* infection, and studies have demonstrated *H. pylori* mediated cell death within *in vitro* models of infection, as well as within murine and gerbil models of infection (68, 103). Although multiple virulence factors produced by *H. pylori* have been shown to mediate pro-apoptotic functions, the exotoxin VacA has been shown to be both essential (74) and sufficient (28) for activation of cell death mechanism within host cells.

Several studies have shown that VacA is a mitochondrial targeting toxin (12). Our study, as well as earlier reports have demonstrated that a VacA-GFP chimera, consisting of an N-terminal 1-319 residues of mature VacA (49, 67), when expressed internally within AZ-521 gastric epithelial cells, as well as in HeLa cells, localized to the mitochondria and induced changes correlated with mitochondrial damage, as well as cell death. Moreover, significant portion of purified VacA when externally applied to cultured mammalian cells, localized to the mitochondria (133). Importantly, a recent study reported that the N-terminal p34 fragment of VacA is imported into the mitochondria and inserts in the mitochondrial inner membrane (38). Additionally, another study reports that the p55 subunit is imported along with the p33 subunit, across the mitochondrial outer membrane (47).

Studies aimed at understanding the functional consequences of VacA-mitochondrial targeting suggested a toxin induced activation of mitochondrial cell

death mechanism (15, 49, 50, 67, 70, 133, 140). Subsequent to binding plasma membrane sphingomyelin (57, 58), and potentially additional components (138, 139), VacA is internalized and localized to cellular mitochondria. One of the early consequences of VacA-mitochondrial targeting was the decrease in mitochondrial transmembrane potential, indicative of the loss of mitochondrial inner membrane integrity (133, 140). This was followed by mitochondrial outer membrane permeabilization (MOMP), resulting in the release of Cyt *c* to the cytosol (133). Interestingly, significant reduction in mitochondrial depolarization as well as cell death activation was observed when mitochondrial targeting of VacA was blocked using the drug cytochalasin-D (51), thereby strongly indicating the importance of VacA-mitochondrial targeting in the mechanism of toxin induced cell death.

Similar to their important role in VacA induced cellular vacuolation, VacA anion channel activity was also important for the toxin mediated mitochondrial depolarization and Cyt *c* release into cytosol. Studies carried out in cells that were intoxicated with VacA anion channel mutants, VacA P9A and VacA G14A, or with purified VacA in the presence of a specific anion channel blocker 5-nitro-2-(3-propylphenylamino)-benzoic acid (NPPB) (67, 133), demonstrated significant reduction in mitochondrial transmembrane potential loss and Cyt *c* release. Consistent with the important role of mitochondrial transmembrane potential and Cyt *c* in mitochondrial energetics, as well as cellular apoptosis mechanism, these studies also demonstrated the importance of VacA anion channel function in cell death activation following toxin intoxication.

Numerous studies have been carried to elucidate the mechanism of VacA induced mitochondrial depolarization and MOMP, which play an important role in VacA mediated cell death mechanism. Interestingly, VacA intoxication of mitochondria isolated from HeLa cells resulted in loss of mitochondrial transmembrane potential, but not mitochondrial Cyt *c* release (140). This study therefore suggested that VacA was sufficient to induce mitochondrial depolarization, but required other host cellular effectors for MOMP and Cyt *c* release. Infact, this study identified the cellular pro-apoptotic effector Bcl2-associated-X protein (Bax) as the host effector required for VacA induced MOMP. Importantly, mouse embryonic fibroblast (MEF) in which the *bax* gene was knocked out, displayed almost complete absence of Cyt *c* release, as well as significant reduction in cell death, following VacA intoxication.

Induction of host mitochondrial damage and cell death can be beneficial for *H. pylori* colonization and long term persistence. *H. pylori* infection is routinely associated with increased gastric pH (85). Several studies have directly attributed this to *H. pylori* mediated changes in the physiology and survival of gastric parietal cells, which are the major sources of gastric acid. It has been shown that *H. pylori* induces apoptosis in isolated, non-transformed Parietal cells (92). Also, significant reduction in acid secretion by Parietal cells has been reported following treatment with either culture supernatants isolated from cultures of toxigenic *H. pylori* strains (71), or purified VacA (131). Furthermore, *H. pylori* induced cell death has also been reported in RAW 264.7 macrophages (86). In addition to macrophage killing, *H. pylori* is also shown to prevent

phagosome maturation by mediating increased retention of TACO (coronin 1) in a VacA dependent manner (145). Furthermore, the limited damage to gastric epithelium seen in *H. pylori* infected stomach could possibly result in release of essential nutrients from host cells, which could aid in bacterial persistence within a nutrient-starved environment.

Interestingly, a recent study demonstrated significant cross-talk between CagA and VacA, two *H. pylori* virulence factors associated with increased cellular damage and disease pathology. This study showed that CagA significantly counteracted VacA mediated apoptosis, by two different mechanisms, depending on the tyrosine phosphorylation status of CagA within host cells (95). While the phosphorylated CagA interfered with intracellular trafficking of VacA, thereby preventing it from reaching mitochondria, the non-phosphorylated CagA, inhibited VacA induced apoptosis directly at the level of mitochondria. It is hypothesized that by directly counteracting the VacA induced apoptotic effects, CagA aids in the survival of *H. pylori* adhered to the gastric mucosa, thereby protecting the colonization niche. At the same time, *H. pylori* can modulate the host innate and adaptive immune response through deregulation of survival mechanism of surrounding host cells in a VacA dependent manner.

1.4 GAP IN KNOWLEDGE

Mitochondrial health is closely linked to cell viability, as these organelles produce the energy required for cellular function while at the same time functioning as regulators of programmed cell death (55). Accordingly,

mitochondrial dysfunction has been increasingly linked to several human pathologies, including those associated with cancer (13), inflammatory disorders (146), and degenerative diseases (78). Several pathogenic microbes target mitochondria (12, 110), but the extent to which pathogen-mediated mitochondrial dysfunction promotes bacterial colonization and survival within the host or contributes to the pathophysiology associated with bacterial infection is largely unexplored.

Infection with the gastric pathogen *H. pylori* is routinely associated with host cell mitochondrial damage and activation of cellular apoptosis (90). For *H. pylori*, an increase in cell death within the gastric mucosa may alter the host niche in several ways, including the loss of specialized cells, such as gastric parietal cells, but also increased cellular proliferation, and gastric atrophy that precedes metaplasia, dysplasia, and ultimately cancer (25). Earlier studies have clearly identified the vacuolating cytotoxin (VacA) as a critical mediator of *H. pylori* induced host cell death. VacA induces mitochondrial damage resulting in mitochondrial dysfunction and activation of mitochondrial dependent cell death mechanism. Interestingly, although VacA is shown to be sufficient in inducing mitochondrial depolarization, it requires cellular pro-death effector Bax to induce MOMP and downstream cell death mechanism (140). Thus far, the exact relationship between VacA induced mitochondrial depolarization (dysfunction) and subsequent Bax activation is not clear. Moreover, the cellular signaling mechanism involved in VacA induced Bax activation and mitochondrial recruitment is not entirely understood. Earlier studies have clearly shown that

VacA targets mitochondria, and forms channels by inserting into the mitochondrial inner membrane (38, 47). VacA channels have been shown to be important for both toxin induced mitochondrial dysfunction, as well as cellular Bax activation (67, 133, 140). However, the relationship between direct association of VacA with the mitochondria and cellular Bax activation is not yet clear.

1.5 SIGNIFICANCE OF THIS STUDY

Within this study, we report that VacA disrupts the morphological dynamics of mitochondria as a mechanism to induce gastric epithelial cell death. Mitochondria exist in several overall morphologies, which are linked to the health of the cell, and change in a dynamic fashion through frequent and repetitive cycles of fission and fusion that occur in response to cellular energy demands and environmental challenges (126). De-regulation of mitochondrial dynamics has increasingly been linked to the pathologies resulting from inflammatory and neurodegenerative disorders (21), as well as several cancers (54). However, the extent to which the morphological dynamics of mitochondria may be targeted by pathogenic microbes during host infection, or are associated with the pathophysiology of some infectious diseases, is largely unexplored. Our studies revealed that VacA induces activation of the dynamin-related protein 1 (Drp1), which is a critical regulator of mitochondrial fission within cells (16-19, 66, 112). Moreover, inhibition of VacA-mediated Drp1-dependent fission prevented activation of the pro-apoptotic Bcl-2–associated X (Bax) protein, MOMP, and death of intoxicated cells. Studies to elucidate the mechanism of VacA induced Drp1 activation indicated that VacA channel activity was important for Drp1

mitochondrial translocation and mitochondrial fragmentation. Importantly, Drp1 activity was not required for VacA induced mitochondrial depolarization (dysfunction), suggesting that VacA induced mitochondrial dysfunction is possibly a trigger for Drp1 mediated fission.

The results from this study demonstrate that apoptosis of gastric epithelial cells during *Hp* infection is triggered by VacA-induced disruption of mitochondrial morphological dynamics through Drp1-mediated fission. Future work will be required to reveal whether other pathogens also promote apoptosis within host cells by targeting the morphological dynamics of mitochondria.

Although our study clearly demonstrates the role of Drp1 mediated de-regulation of mitochondrial dynamics in activation of cellular Bax, the exact mechanism involved was not entirely clear. Our study here demonstrates that VacA induces the activation and mitochondrial recruitment of the endogenous stress sensor protein Bid (BH3 interacting death domain agonist), a BH3 domain-only member of Bcl-2 family of proteins, which is known to target the mitochondria and activate Bax in certain cell death mechanisms (143). Within VacA intoxicated cells, Bid was important for the activation of Bax and mitochondrial cell death mechanism. Importantly, Drp1 GTPase activity was required for Bid activation within VacA intoxicated cells. Our results therefore indicate that cellular stress as a result of excessive fission is possibly translated to Bax mediated mitochondrial outer membrane permeabilization through the stress sensor Bid. Studies aimed at characterizing the mechanism of VacA mediated Bid activation indicated a non-canonical pathway, independent of

caspase-8 activity, but dependent on rise in cytosolic calcium levels. Cellular calcium rise resulted in activation of the calcium dependent protease calpain, which induced a site specific proteolytic processing required for Bid activation. Importantly, Drp1 dependent mitochondrial fission was required for the rise in cellular calcium levels. The molecular mechanism underlying fission induced rise in cytosolic calcium is presently not clear. Further studies would aim towards characterizing the relationship between Drp1 mediated mitochondrial fission and de-regulation of cellular calcium homeostasis.

Figures

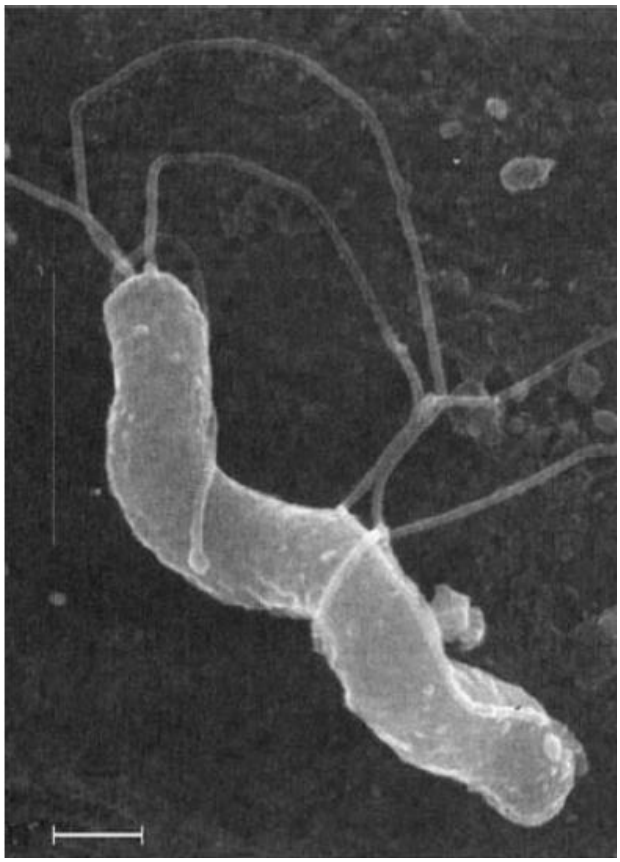

Figure 1.1 *Helicobacter pylori* (*H. pylori*).

Electron micrograph of *Helicobacter pylori* depicting its spiral shape and flagella.

(Source: Lucinda J. Thompson, Department of Microbiology and Immunology, Stanford, CA, USA.)

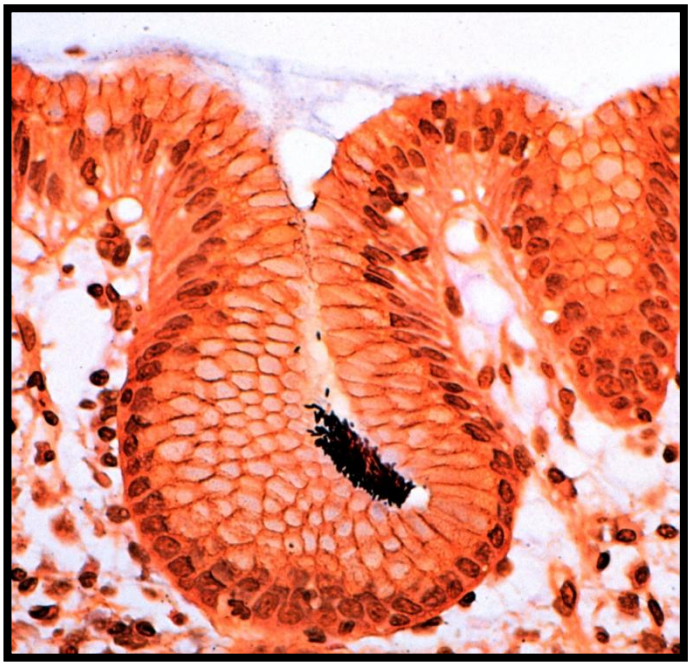

Figure 1.2 *H. pylori* in a gastric pit.

Photomicrograph of a section of a biopsy taken from a 35-year-old man and stained with Genta stain, shows a gastric pit filled with *H. pylori.*

(Pictures taken by Robert M. Genta and David Y. Graham at the Medical Center, Houston, TX.)

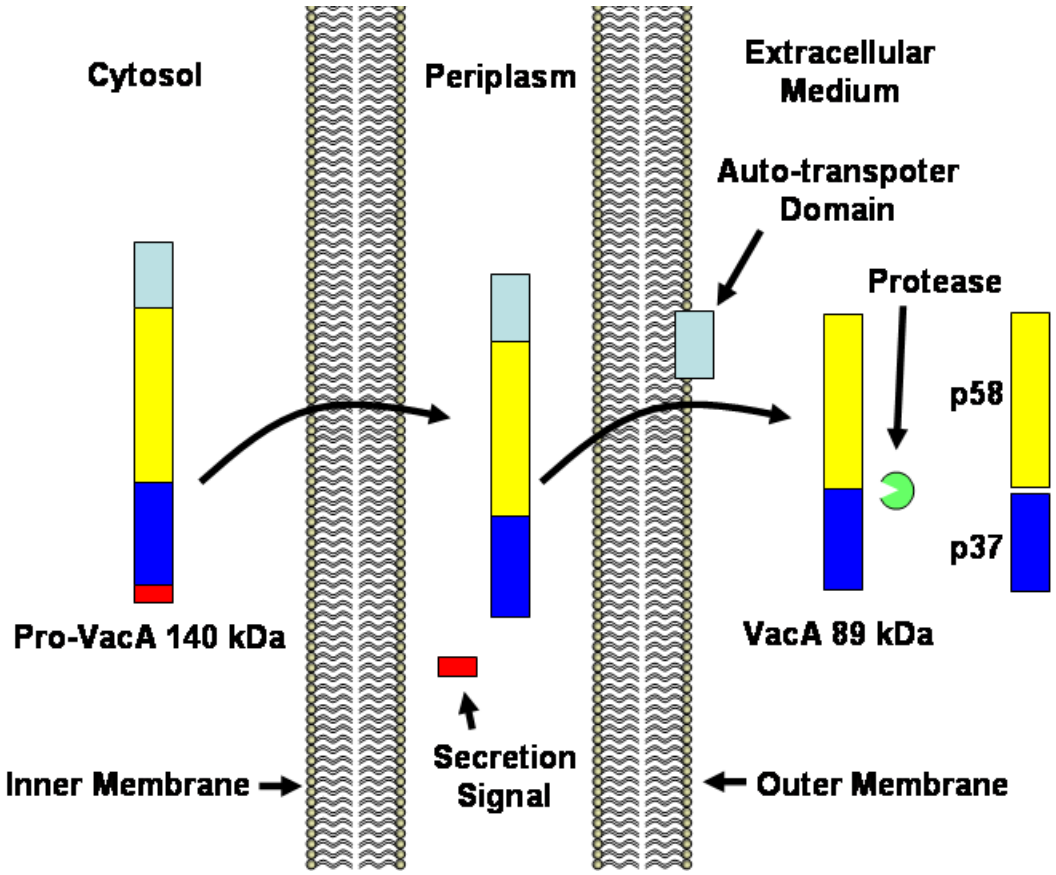

Figure 1.3 Schematic cross-section of *H. pylori* showing VacA secretion.

VacA is produced in the cytosol as a 140 kilo Dalton pro-toxin (left). A secretion signal is cleaved from the amino-terminus after Sec-dependent translocation to the periplasm. The carboxyl-terminal auto-transporter domain then inserts into the outer membrane, facilitating translocation of the mature, 89 kilo Dalton VacA. VacA is often cleaved between amino acids 311 and 312 to form the subunits p37 and p58, which remain associated.

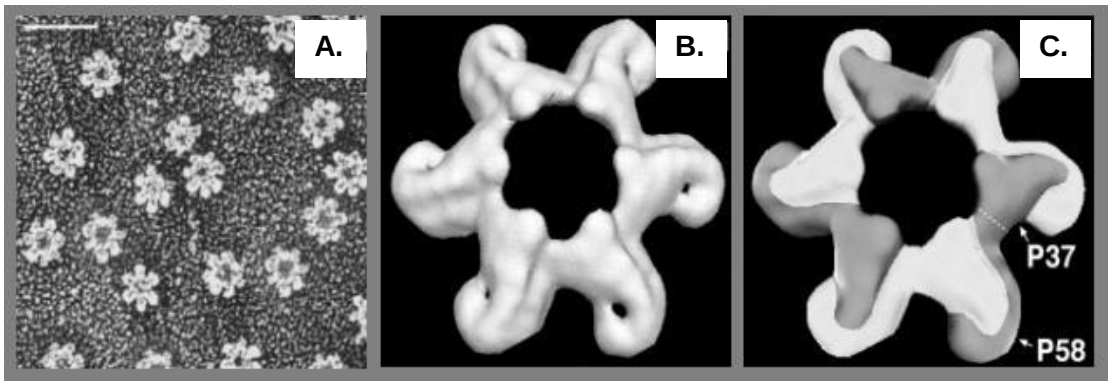

Figure 1.4 Structure of VacA.

Electron micrograph of purified VacA (Scale bar = 50nM). (B) Three-dimensional top view of wild type VacA replicas. (C) Model of possible interactions between VacA monomers in the oligomeric structure and possible interaction between p33 (previously p37) and p55 (previously p58) fragments of VacA.

(Source: Reyrat, J. M. et al. 1999. 3D imaging of the 58 kDa cell binding subunit of the *Helicobacter pylori* cytotoxin. J Mol Biol 290:459-70.)

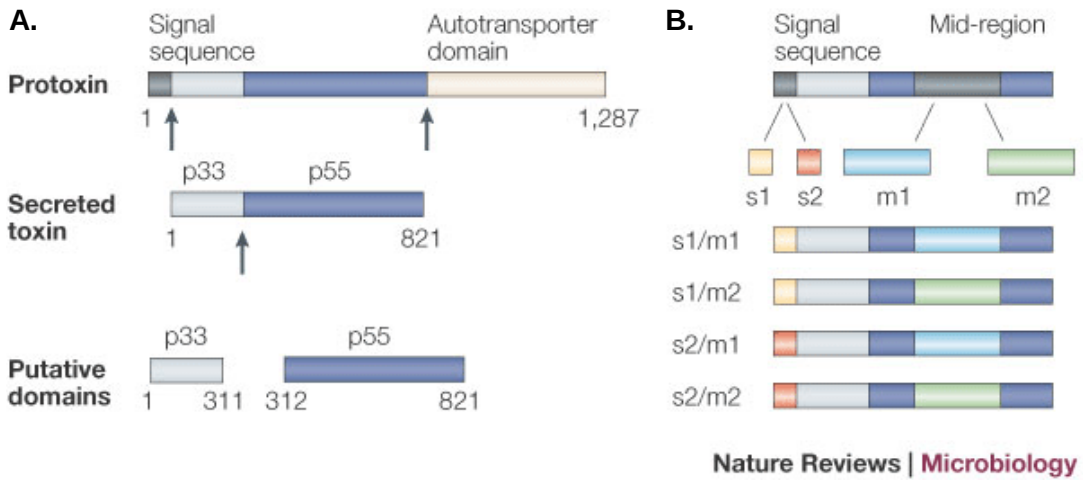

Figure 1.5 *vacA* gene structure and allelic diversity.

(A) The amino-terminal signal sequence and carboxy-terminal domain are cleaved from the 140-kDa VacA protoxin to yield an 88-kDa mature toxin that is secreted into the extracellular space via an autotransporter mechanism.

(B) The structure of the *vacA* gene and the secretion and proteolytic processing of the VacA protein.

(Source: Cover, T. L., and S. R. Blanke. 2005. *Helicobacter pylori* VacA, a paradigm for toxin multifunctionality. Nat Rev Microbiol 3:320-32.)

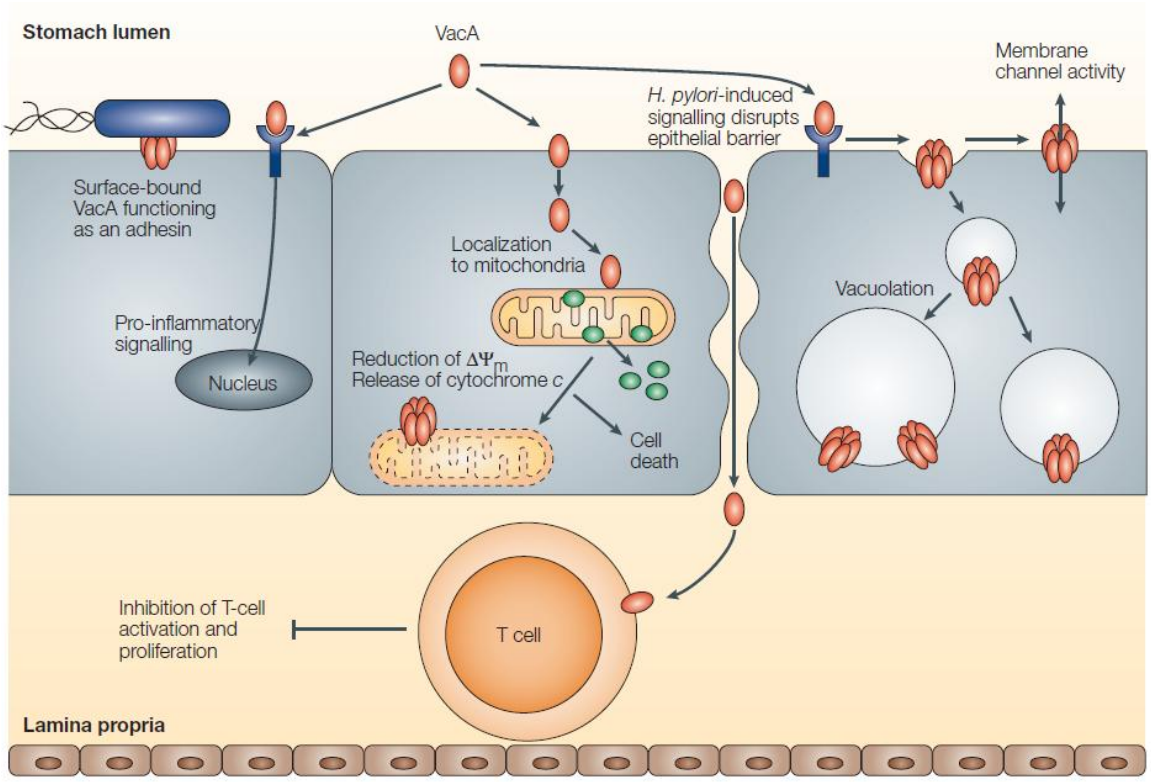

Figure 1.6 VacA: a paradigm for toxin multifunctionality.

Intoxication of gastric epithelial cells with VacA results in alterations in mitochondrial membrane permeability and apoptosis, stimulation of pro-inflammatory signaling, increased permeability of plasma membrane and alterations in endocytic compartments.

(Source: Cover, T. L., and S. R. Blanke. 2005. *Helicobacter pylori* VacA, a paradigm for toxin multifunctionality. Nat Rev Microbiol 3:320-32.)

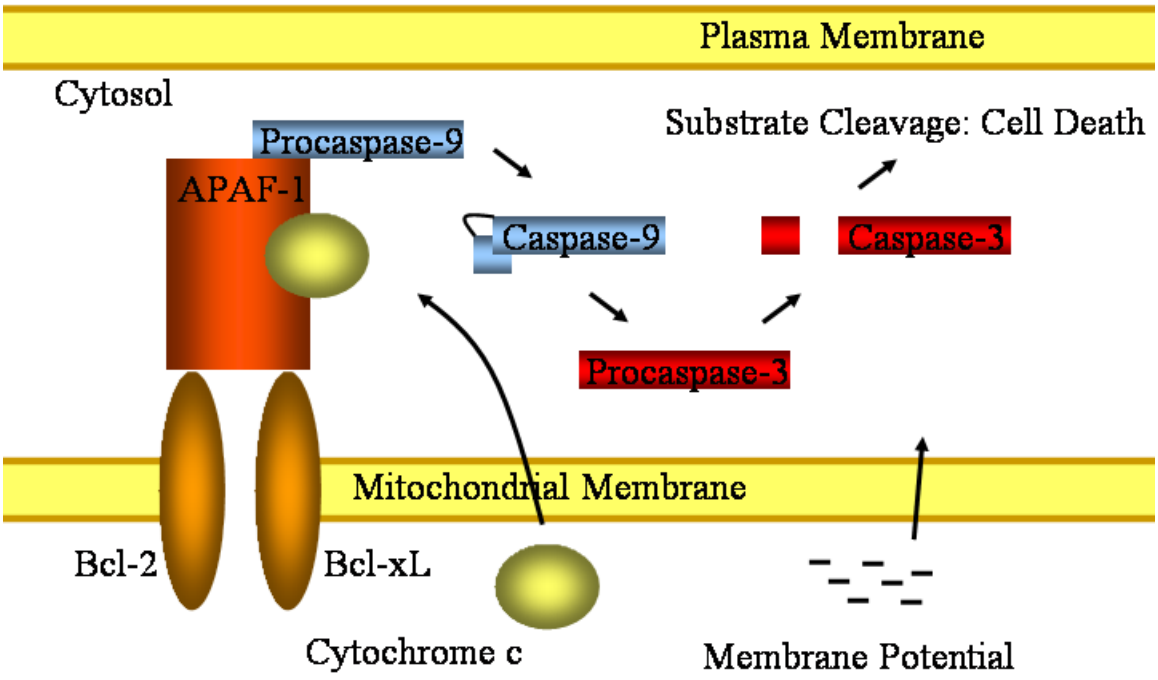

Figure 1.7 The apoptosis cascade.

A schematic cross-section of a human cell showing elements of the apoptosis cascade. Two of the earliest events in mitochondrial-mediated apoptosis are loss of the transmembrane potential and release of cytochrome c. Bcl family proteins are thought to play a role in the maintenance (or disruption) of the membrane potential, but the part which this potential loss plays in apoptosis is not clear. Cytochrome c is released by an unknown mechanism to the cell cytosol, where it interacts with APAF-1 and procaspase-9 to form the apoptosome. This complex cleaves procaspase-9 to form caspase-9, which in turn cleaves caspace-3. A caspase cleavage cascade results in wide-spread substrate cleavage, nuclear fragmentation, DNA damage and cell death.

References

1. **Abbott, A.** 2005. Gut feeling secures medical Nobel for Australian doctors. Nature **437:**801.

2. **Adrian, M., T. L. Cover, J. Dubochet, and J. E. Heuser.** 2002. Multiple oligomeric states of the *Helicobacter pylori* vacuolating toxin demonstrated by cryo-electron microscopy. J Mol Biol **318:**121-33.

3. **Allen, L. A., L. S. Schlesinger, and B. Kang.** 2000. Virulent strains of *Helicobacter pylori* demonstrate delayed phagocytosis and stimulate homotypic phagosome fusion in macrophages. J Exp Med **191:**115-28.

4. **Alm, R. A., L. S. Ling, D. T. Moir, B. L. King, E. D. Brown, P. C. Doig, D. R. Smith, B. Noonan, B. C. Guild, B. L. deJonge, G. Carmel, P. J. Tummino, A. Caruso, M. Uria-Nickelsen, D. M. Mills, C. Ives, R. Gibson, D. Merberg, S. D. Mills, Q. Jiang, D. E. Taylor, G. F. Vovis, and T. J. Trust.** 1999. Genomic-sequence comparison of two unrelated isolates of the human gastric pathogen *Helicobacter pylori*. Nature **397:**176-80.

5. **Atherton, J. C.** 1997. The clinical relevance of strain types of *Helicobacter pylori*. Gut **40:**701-3.

6. **Atherton, J. C.** 1997. *Helicobacter pylori* unmasked--the complete genome sequence. Eur J Gastroenterol Hepatol **9:**1137-40.

7. **Atherton, J. C.** 2006. The pathogenesis of *Helicobacter pylori*-induced gastro-duodenal diseases. Annu Rev Pathol **1:**63-96.

8. **Atherton, J. C., P. Cao, R. M. Peek, Jr., M. K. Tummuru, M. J. Blaser, and T. L. Cover.** 1995. Mosaicism in vacuolating cytotoxin alleles of *Helicobacter pylori*. Association of specific vacA types with cytotoxin production and peptic ulceration. J Biol Chem **270:**17771-7.

9. **Atherton, J. C., R. M. Peek, Jr., K. T. Tham, T. L. Cover, and M. J. Blaser.** 1997. Clinical and pathological importance of heterogeneity in vacA, the vacuolating cytotoxin gene of *Helicobacter pylori*. Gastroenterology **112:**92-9.

10. **Barth, H., K. Aktories, M. R. Popoff, and B. G. Stiles.** 2004. Binary bacterial toxins: biochemistry, biology, and applications of common Clostridium and Bacillus proteins. Microbiol Mol Biol Rev **68:**373-402, table of contents.

11. **Birmingham, C. L., V. Canadien, N. A. Kaniuk, B. E. Steinberg, D. E. Higgins, and J. H. Brumell.** 2008. Listeriolysin O allows *Listeria monocytogenes* replication in macrophage vacuoles. Nature **451:**350-4.

12. **Blanke, S. R.** 2005. Micro-managing the executioner: pathogen targeting of mitochondria. Trends Microbiol **13:**64-71.

13. **Brandon, M., P. Baldi, and D. C. Wallace.** 2006. Mitochondrial mutations in cancer. Oncogene **25:**4647-62.

14. **Burns, D. L.** 1999. Biochemistry of type IV secretion. Curr Opin Microbiol **2:**25-9.

15. **Calore, F., C. Genisset, A. Casellato, M. Rossato, G. Codolo, M. D. Esposti, L. Scorrano, and M. de Bernard.** 2010. Endosome-mitochondria juxtaposition during apoptosis induced by *H. pylori* VacA. Cell Death Differ **17:**1707-16.

16. **Cassidy-Stone, A., J. E. Chipuk, E. Ingerman, C. Song, C. Yoo, T. Kuwana, M. J. Kurth, J. T. Shaw, J. E. Hinshaw, D. R. Green, and J. Nunnari.** 2008. Chemical inhibition of the mitochondrial division dynamin reveals its role in Bax/Bak-dependent mitochondrial outer membrane permeabilization. Dev Cell **14:**193-204.

17. **Cerveny, K. L., Y. Tamura, Z. Zhang, R. E. Jensen, and H. Sesaki.** 2007. Regulation of mitochondrial fusion and division. Trends Cell Biol **17:**563-9.

18. **Chang, C. R., and C. Blackstone.** 2010. Dynamic regulation of mitochondrial fission through modification of the dynamin-related protein Drp1. Ann N Y Acad Sci **1201:**34-9.

19. **Chen, H., and D. C. Chan.** 2005. Emerging functions of mammalian mitochondrial fusion and fission. Hum Mol Genet **14 Spec No. 2:**R283-9.

20. **Chipuk, J. E., and D. R. Green.** 2008. How do BCL-2 proteins induce mitochondrial outer membrane permeabilization? Trends Cell Biol **18:**157-64.

21. **Cho, D. H., T. Nakamura, and S. A. Lipton.** 2010. Mitochondrial dynamics in cell death and neurodegeneration. Cell Mol Life Sci **67:**3435-47.

22. **Covacci, A., S. Falkow, D. E. Berg, and R. Rappuoli.** 1997. Did the inheritance of a pathogenicity island modify the virulence of *Helicobacter pylori*? Trends Microbiol **5:**205-8.

23. **Cover, T. L.** 1996. The vacuolating cytotoxin of *Helicobacter pylori*. Mol Microbiol **20:**241-6.

24. **Cover, T. L., and S. R. Blanke.** 2005. *Helicobacter pylori* VacA, a paradigm for toxin multifunctionality. Nat Rev Microbiol **3:**320-32.

25. **Cover, T. L., and M. J. Blaser.** 1999. *Helicobacter pylori* factors associated with disease. Gastroenterology **117:**257-61.

26. **Cover, T. L., and M. J. Blaser.** 1992. Purification and characterization of the vacuolating toxin from *Helicobacter pylori*. J Biol Chem **267:**10570-5.

27. **Cover, T. L., P. I. Hanson, and J. E. Heuser.** 1997. Acid-induced dissociation of VacA, the *Helicobacter pylori* vacuolating cytotoxin, reveals its pattern of assembly. J Cell Biol **138:**759-69.

28. **Cover, T. L., U. S. Krishna, D. A. Israel, and R. M. Peek, Jr.** 2003. Induction of gastric epithelial cell apoptosis by *Helicobacter pylori* vacuolating cytotoxin. Cancer Res **63:**951-7.

29. **Cover, T. L., M. K. Tummuru, P. Cao, S. A. Thompson, and M. J. Blaser.** 1994. Divergence of genetic sequences for the vacuolating cytotoxin among *Helicobacter pylori* strains. J Biol Chem **269:**10566-73.

30. **Cover, T. L., S. G. Vaughn, P. Cao, and M. J. Blaser.** 1992. Potentiation of *Helicobacter pylori* vacuolating toxin activity by nicotine and other weak bases. J Infect Dis **166:**1073-8.

31. **Czajkowsky, D. M., H. Iwamoto, T. L. Cover, and Z. Shao.** 1999. The vacuolating toxin from *Helicobacter pylori* forms hexameric pores in lipid bilayers at low pH. Proc Natl Acad Sci U S A **96:**2001-6.

32. **Czajkowsky, D. M., H. Iwamoto, G. Szabo, T. L. Cover, and Z. Shao.** 2005. Mimicry of a host anion channel by a *Helicobacter pylori* pore-forming toxin. Biophys J **89:**3093-101.

33. **de Bernard, M., D. Burroni, E. Papini, R. Rappuoli, J. Telford, and C. Montecucco.** 1998. Identification of the *Helicobacter pylori* VacA toxin domain active in the cell cytosol. Infect Immun **66:**6014-6.

34. **de Bernard, M., A. Cappon, L. Pancotto, P. Ruggiero, J. Rivera, G. Del Giudice, and C. Montecucco.** 2005. The *Helicobacter pylori* VacA cytotoxin activates RBL-2H3 cells by inducing cytosolic calcium oscillations. Cell Microbiol **7:**191-8.

35. **de Bernard, M., E. Papini, V. de Filippis, E. Gottardi, J. Telford, R. Manetti, A. Fontana, R. Rappuoli, and C. Montecucco.** 1995. Low pH activates the vacuolating toxin of *Helicobacter pylori*, which becomes acid and pepsin resistant. J Biol Chem **270:**23937-40.

36. **De Haan, L., and T. R. Hirst.** 2004. Cholera toxin: a paradigm for multi-functional engagement of cellular mechanisms. Mol Membr Biol **21:**77-92.

37. **Debellis, L., E. Papini, R. Caroppo, C. Montecucco, and S. Curci.** 2001. *Helicobacter pylori* cytotoxin VacA increases alkaline secretion in gastric epithelial cells. Am J Physiol Gastrointest Liver Physiol **281:**G1440-8.

38. **Domanska, G., C. Motz, M. Meinecke, A. Harsman, P. Papatheodorou, B. Reljic, E. A. Dian-Lothrop, A. Galmiche, O. Kepp, L. Becker, K. Gunnewig, R. Wagner, and J. Rassow.** 2010. *Helicobacter pylori* VacA toxin/subunit p34: targeting of an anion channel to the inner mitochondrial membrane. PLoS Pathog **6:**e1000878.

39. **Dunn, B. E., H. Cohen, and M. J. Blaser.** 1997. *Helicobacter pylori*. Clin Microbiol Rev **10:**720-41.

40. **El-Bez, C., M. Adrian, J. Dubochet, and T. L. Cover.** 2005. High resolution structural analysis of *Helicobacter pylori* VacA toxin oligomers by cryo-negative staining electron microscopy. J Struct Biol **151:**215-28.

41. **Ellis, R. E., J. Y. Yuan, and H. R. Horvitz.** 1991. Mechanisms and functions of cell death. Annu Rev Cell Biol **7:**663-98.

42. **Enserink, M.** 2005. Physiology or medicine. Triumph of the ulcer-bug theory. Science **310:**34-5.

43. **Everhart, J. E.** 2000. Recent developments in the epidemiology of *Helicobacter pylori*. Gastroenterol Clin North Am **29:**559-78.

44. **Figura, N., P. Guglielmetti, A. Rossolini, A. Barberi, G. Cusi, R. A. Musmanno, M. Russi, and S. Quaranta.** 1989. Cytotoxin production by *Campylobacter pylori* strains isolated from patients with peptic ulcers and from patients with chronic gastritis only. J Clin Microbiol **27:**225-6.

45. **Finlay, B. B., and P. Cossart.** 1997. Exploitation of mammalian host cell functions by bacterial pathogens. Science **276:**718-25.

46. **Fivaz, M., L. Abrami, Y. Tsitrin, and F. G. van der Goot.** 2001. Aerolysin from *Aeromonas hydrophila* and related toxins. Curr Top Microbiol Immunol **257:**35-52.

47. **Foo, J. H., J. G. Culvenor, R. L. Ferrero, T. Kwok, T. Lithgow, and K. Gabriel.** 2010.Both the p33 and p55 subunits of the *Helicobacter pylori* VacA toxin are targeted to mammalian mitochondria. J Mol Biol **401:**792-8.

48. **Galan, J. E., and A. Collmer.** 1999. Type III secretion machines: bacterial devices for protein delivery into host cells. Science **284:**1322-8.

49. **Galmiche, A., J. Rassow, A. Doye, S. Cagnol, J. C. Chambard, S. Contamin, V. de Thillot, I. Just, V. Ricci, E. Solcia, E. Van Obberghen, and P. Boquet.** 2000. The N-terminal 34 kDa fragment of *Helicobacter pylori* vacuolating cytotoxin targets mitochondria and induces cytochrome c release. EMBO J **19:**6361-70.

50. **Ganten, T. M., E. Aravena, J. Sykora, R. Koschny, J. Mohr, J. Rudi, W. Stremmel, and H. Walczak.** 2007. *Helicobacter pylori*-induced apoptosis in T cells is mediated by the mitochondrial pathway independent of death receptors. Eur J Clin Invest **37:**117-25.

51. **Gauthier, N. C., V. Ricci, P. Gounon, A. Doye, M. Tauc, P. Poujeol, and P. Boquet.** 2004. Glycosylphosphatidylinositol-anchored proteins and actin cytoskeleton modulate chloride transport by channels formed by the *Helicobacter pylori* vacuolating cytotoxin VacA in HeLa cells. J Biol Chem **279:**9481-9.

52. **Gebert, B., W. Fischer, E. Weiss, R. Hoffmann, and R. Haas.** 2003. *Helicobacter pylori* vacuolating cytotoxin inhibits T lymphocyte activation. Science **301:**1099-102.

53. **Genisset, C., A. Puhar, F. Calore, M. de Bernard, P. Dell'Antone, and C. Montecucco.** 2007. The concerted action of the *Helicobacter pylori* cytotoxin VacA and of the v-ATPase proton pump induces swelling of isolated endosomes. Cell Microbiol **9:**1481-90.

54. **Grandemange, S., S. Herzig, and J. C. Martinou.** 2009. Mitochondrial dynamics and cancer. Semin Cancer Biol **19:**50-6.

55. **Green, D. R., and G. Kroemer.** 2004. The pathophysiology of mitochondrial cell death. Science **305:**626-9.

56. **Greenberg, R. N., M. Hill, J. Crytzer, W. J. Krause, S. L. Eber, F. K. Hamra, and L. R. Forte.** 1997. Comparison of effects of uroguanylin, guanylin, and Escherichia coli heat-stable enterotoxin STa in mouse intestine and kidney: evidence that uroguanylin is an intestinal natriuretic hormone. J Investig Med **45:**276-82.

57. **Gupta, V. R., H. K. Patel, S. S. Kostolansky, R. A. Ballivian, J. Eichberg, and S. R. Blanke.** 2008. Sphingomyelin functions as a novel receptor for *Helicobacter pylori* VacA. PLoS Pathog **4:**e1000073.

58. **Gupta, V. R., B. A. Wilson, and S. R. Blanke.** 2010. Sphingomyelin is important for the cellular entry and intracellular localization of *Helicobacter pylori* VacA. Cell Microbiol **12:**1517-33.

59. **Hara, H., I. Kawamura, T. Nomura, T. Tominaga, K. Tsuchiya, and M. Mitsuyama.** 2007. Cytolysin-dependent escape of the bacterium from the phagosome is required but not sufficient for induction of the Th1 immune response against *Listeria monocytogenes* infection: distinct role of Listeriolysin O determined by cytolysin gene replacement. Infect Immun **75:**3791-801.

60. **Hazes, B., and R. J. Read.** 1997. Accumulating evidence suggests that several AB-toxins subvert the endoplasmic reticulum-associated protein degradation pathway to enter target cells. Biochemistry **36:**11051-4.

61. **Herrera, V., and J. Parsonnet.** 2009. *Helicobacter pylori* and gastric adenocarcinoma. Clin Microbiol Infect **15:**971-6.

62. **Hessey, S. J., J. Spencer, J. I. Wyatt, G. Sobala, B. J. Rathbone, A. T. Axon, and M. F. Dixon.** 1990. Bacterial adhesion and disease activity in Helicobacter associated chronic gastritis. Gut **31:**134-8.

63. **Higashi, H., R. Tsutsumi, S. Muto, T. Sugiyama, T. Azuma, M. Asaka, and M. Hatakeyama.** 2002. SHP-2 tyrosine phosphatase as an intracellular target of *Helicobacter pylori* CagA protein. Science **295:**683-6.

64. **Hisatsune, J., E. Yamasaki, M. Nakayama, D. Shirasaka, H. Kurazono, Y. Katagata, H. Inoue, J. Han, J. Sap, K. Yahiro, J. Moss, and T. Hirayama.** 2007. *Helicobacter pylori* VacA enhances prostaglandin E2 production through induction of cyclooxygenase 2 expression via a p38 mitogen-activated protein kinase/activating transcription factor 2 cascade in AZ-521 cells. Infect Immun **75:**4472-81.

65. **Ilver, D., S. Barone, D. Mercati, P. Lupetti, and J. L. Telford.** 2004. *Helicobacter pylori* toxin VacA is transferred to host cells via a novel contact-dependent mechanism. Cell Microbiol **6:**167-74.

66. **Ingerman, E., E. M. Perkins, M. Marino, J. A. Mears, J. M. McCaffery, J. E. Hinshaw, and J. Nunnari.** 2005. Dnm1 forms spirals that are structurally tailored to fit mitochondria. J Cell Biol **170:**1021-7.

67. **Jain, P., Z. Q. Luo, and S. R. Blanke.** 2011. *Helicobacter pylori* vacuolating cytotoxin A (VacA) engages the mitochondrial fission machinery to induce host cell death. Proc Natl Acad Sci U S A.

68. **Jones, N. L., A. S. Day, H. Jennings, P. T. Shannon, E. Galindo-Mata, and P. M. Sherman.** 2002. Enhanced disease severity in *Helicobacter pylori*-infected mice deficient in Fas signaling. Infect Immun **70:**2591-7.

69. **Kerr, J. F., A. H. Wyllie, and A. R. Currie.** 1972. Apoptosis: a basic biological phenomenon with wide-ranging implications in tissue kinetics. Br J Cancer **26:**239-57.

70. **Kimura, M., S. Goto, A. Wada, K. Yahiro, T. Niidome, T. Hatakeyama, H. Aoyagi, T. Hirayama, and T. Kondo.** 1999. Vacuolating cytotoxin purified from *Helicobacter pylori* causes mitochondrial damage in human gastric cells. Microb Pathog **26:**45-52.

71. **Kobayashi, H., S. Kamiya, T. Suzuki, K. Kohda, S. Muramatsu, T. Kurumada, U. Ohta, M. Miyazawa, N. Kimura, N. Mutoh, T. Shirai, A. Takagi, S. Harasawa, N. Tani, and T. Miwa.** 1996. The effect of *Helicobacter pylori* on gastric acid secretion by isolated parietal cells from a guinea pig. Association with production of vacuolating toxin by *H. pylori*. Scand J Gastroenterol **31:**428-33.

72. **Kodama, M., T. Fujioka, R. Kodama, K. Takahashi, T. Kubota, K. Murakami, and M. Nasu.** 1998. p53 expression in gastric mucosa with *Helicobacter pylori* infection. J Gastroenterol Hepatol **13:**215-9.

73. **Konturek, P. C., P. Pierzchalski, S. J. Konturek, H. Meixner, G. Faller, T. Kirchner, and E. G. Hahn.** 1999. *Helicobacter pylori* induces apoptosis in gastric mucosa through an upregulation of Bax expression in humans. Scand J Gastroenterol **34:**375-83.

74. **Kuck, D., B. Kolmerer, C. Iking-Konert, P. H. Krammer, W. Stremmel, and J. Rudi.** 2001. Vacuolating cytotoxin of *Helicobacter pylori* induces apoptosis in the human gastric epithelial cell line AGS. Infect Immun **69:**5080-7.

75. **Letley, D. P., J. L. Rhead, R. J. Twells, B. Dove, and J. C. Atherton.** 2003. Determinants of non-toxicity in the gastric pathogen *Helicobacter pylori*. J Biol Chem **278:**26734-41.

76. **Leunk, R. D., P. T. Johnson, B. C. David, W. G. Kraft, and D. R. Morgan.** 1988. Cytotoxic activity in broth-culture filtrates of *Campylobacter pylori*. J Med Microbiol **26:**93-9.

77. **Li, H., A. Llera, and R. A. Mariuzza.** 1998. Structure-function studies of T-cell receptor-superantigen interactions. Immunol Rev **163:**177-86.

78. **Lin, M. T., and M. F. Beal.** 2006. Mitochondrial dysfunction and oxidative stress in neurodegenerative diseases. Nature **443:**787-95.

79. **Lupetti, P., J. E. Heuser, R. Manetti, P. Massari, S. Lanzavecchia, P. L. Bellon, R. Dallai, R. Rappuoli, and J. L. Telford.** 1996. Oligomeric and subunit structure of the *Helicobacter pylori* vacuolating cytotoxin. J Cell Biol **133:**801-7.

80. **Mannick, E. E., L. E. Bravo, G. Zarama, J. L. Realpe, X. J. Zhang, B. Ruiz, E. T. Fontham, R. Mera, M. J. Miller, and P. Correa.** 1996. Inducible nitric oxide synthase, nitrotyrosine, and apoptosis in *Helicobacter pylori* gastritis: effect of antibiotics and antioxidants. Cancer Res **56:**3238-43.

81. **Marchetti, M., B. Arico, D. Burroni, N. Figura, R. Rappuoli, and P. Ghiara.** 1995. Development of a mouse model of *Helicobacter pylori* infection that mimics human disease. Science **267:**1655-8.

82. **Marshall, B. J., J. A. Armstrong, D. B. McGechie, and R. J. Glancy.** 1985. Attempt to fulfil Koch's postulates for pyloric Campylobacter. Med J Aust **142:**436-9.

83. **Marshall, B. J., D. B. McGechie, P. A. Rogers, and R. J. Glancy.** 1985. Pyloric Campylobacter infection and gastroduodenal disease. Med J Aust **142:**439-44.

84. **McClain, M. S., H. Iwamoto, P. Cao, A. D. Vinion-Dubiel, Y. Li, G. Szabo, Z. Shao, and T. L. Cover.** 2003. Essential role of a GXXXG motif for membrane channel formation by *Helicobacter pylori* vacuolating toxin. J Biol Chem **278:**12101-8.

85. **McColl, K. E., E. el-Omar, and D. Gillen.** 1998. Interactions between *H. pylori* infection, gastric acid secretion and anti-secretory therapy. Br Med Bull **54:**121-38.

86. **Menaker, R. J., P. J. Ceponis, and N. L. Jones.** 2004. *Helicobacter pylori* induces apoptosis of macrophages in association with alterations in the mitochondrial pathway. Infect Immun **72:**2889-98.

87. **Miyoshi, S., and S. Shinoda.** 2000. Microbial metalloproteases and pathogenesis. Microbes Infect **2:**91-8.

88. **Molinari, M., C. Galli, M. de Bernard, N. Norais, J. M. Ruysschaert, R. Rappuoli, and C. Montecucco.** 1998. The acid activation of *Helicobacter pylori* toxin VacA: structural and membrane binding studies. Biochem Biophys Res Commun **248:**334-40.

89. **Molinari, M., M. Salio, C. Galli, N. Norais, R. Rappuoli, A. Lanzavecchia, and C. Montecucco.** 1998. Selective inhibition of Ii-dependent antigen presentation by *Helicobacter pylori* toxin VacA. J Exp Med **187:**135-40.

90. **Moss, S. F., J. Calam, B. Agarwal, S. Wang, and P. R. Holt.** 1996. Induction of gastric epithelial apoptosis by *Helicobacter pylori*. Gut **38:**498-501.

91. **Nakayama, M., M. Kimura, A. Wada, K. Yahiro, K. Ogushi, T. Niidome, A. Fujikawa, D. Shirasaka, N. Aoyama, H. Kurazono, M. Noda, J. Moss, and T. Hirayama.** 2004. *Helicobacter pylori* VacA activates the p38/activating transcription factor 2-mediated signal pathway in AZ-521 cells. J Biol Chem **279:**7024-8.

92. **Neu, B., P. Randlkofer, M. Neuhofer, P. Voland, A. Mayerhofer, M. Gerhard, W. Schepp, and C. Prinz.** 2002. *Helicobacter pylori* induces apoptosis of rat gastric parietal cells. Am J Physiol Gastrointest Liver Physiol **283:**G309-18.

93. **Nguyen, V. Q., R. M. Caprioli, and T. L. Cover.** 2001. Carboxy-terminal proteolytic processing of *Helicobacter pylori* vacuolating toxin. Infect Immun **69:**543-6.

94. **Ogiwara, H., D. Y. Graham, and Y. Yamaoka.** 2008. vacA i-region subtyping. Gastroenterology **134:**1267; author reply 1268.

95. **Oldani, A., M. Cormont, V. Hofman, V. Chiozzi, O. Oregioni, A. Canonici, A. Sciullo, P. Sommi, A. Fabbri, V. Ricci, and P. Boquet.** 2009. *Helicobacter pylori* counteracts the apoptotic action of its VacA toxin by injecting the CagA protein into gastric epithelial cells. PLoS Pathog **5:**e1000603.

96. **Oltvai, Z. N., and S. J. Korsmeyer.** 1994. Checkpoints of dueling dimers foil death wishes. Cell **79:**189-92.

97. **Ow, Y. P., D. R. Green, Z. Hao, and T. W. Mak.** 2008. Cytochrome *c*: functions beyond respiration. Nat Rev Mol Cell Biol **9:**532-42.

98. **Pagliaccia, C., M. de Bernard, P. Lupetti, X. Ji, D. Burroni, T. L. Cover, E. Papini, R. Rappuoli, J. L. Telford, and J. M. Reyrat.** 1998. The m2 form of the *Helicobacter pylori* cytotoxin has cell type-specific vacuolating activity. Proc Natl Acad Sci U S A **95:**10212-7.

99. **Papini, E., M. de Bernard, E. Milia, M. Bugnoli, M. Zerial, R. Rappuoli, and C. Montecucco.** 1994. Cellular vacuoles induced by *Helicobacter pylori* originate from late endosomal compartments. Proc Natl Acad Sci U S A **91:**9720-4.

100. **Papini, E., B. Satin, N. Norais, M. de Bernard, J. L. Telford, R. Rappuoli, and C. Montecucco.** 1998. Selective increase of the permeability of polarized epithelial cell monolayers by *Helicobacter pylori* vacuolating toxin. J Clin Invest **102:**813-20.

101. **Parsonnet, J., D. Vandersteen, J. Goates, R. K. Sibley, J. Pritikin, and Y. Chang.** 1991. *Helicobacter pylori* infection in intestinal- and diffuse-type gastric adenocarcinomas. J Natl Cancer Inst **83:**640-3.

102. **Patel, H. K., D. C. Willhite, R. M. Patel, D. Ye, C. L. Williams, E. M. Torres, K. B. Marty, R. A. MacDonald, and S. R. Blanke.** 2002. Plasma membrane cholesterol modulates cellular vacuolation induced by the *Helicobacter pylori* vacuolating cytotoxin. Infect Immun **70:**4112-23.

103. **Peek, R. M., Jr., H. P. Wirth, S. F. Moss, M. Yang, A. M. Abdalla, K. T. Tham, T. Zhang, L. H. Tang, I. M. Modlin, and M. J. Blaser.** 2000. *Helicobacter pylori* alters gastric epithelial cell cycle events and gastrin secretion in Mongolian gerbils. Gastroenterology **118:**48-59.

104. **Pelicic, V., J. M. Reyrat, L. Sartori, C. Pagliaccia, R. Rappuoli, J. L. Telford, C. Montecucco, and E. Papini.** 1999. *Helicobacter pylori* VacA cytotoxin associated with the bacteria increases epithelial permeability independently of its vacuolating activity. Microbiology **145 (Pt 8):**2043-50.

105. **Pincock, S.** 2005. Nobel Prize winners Robin Warren and Barry Marshall. Lancet **366:**1429.

106. **Reyrat, J. M., S. Lanzavecchia, P. Lupetti, M. de Bernard, C. Pagliaccia, V. Pelicic, M. Charrel, C. Ulivieri, N. Norais, X. Ji, V. Cabiaux, E. Papini, R. Rappuoli, and J. L. Telford.** 1999. 3D imaging of the 58 kDa cell binding subunit of the *Helicobacter pylori* cytotoxin. J Mol Biol **290:**459-70.

107. **Reyrat, J. M., V. Pelicic, E. Papini, C. Montecucco, R. Rappuoli, and J. L. Telford.** 1999. Towards deciphering the *Helicobacter pylori* cytotoxin. Mol Microbiol **34:**197-204.

108. **Rhead, J. L., D. P. Letley, M. Mohammadi, N. Hussein, M. A. Mohagheghi, M. Eshagh Hosseini, and J. C. Atherton.** 2007. A new *Helicobacter pylori* vacuolating cytotoxin determinant, the intermediate region, is associated with gastric cancer. Gastroenterology **133:**926-36.

109. **Ricci, V., P. Sommi, R. Fiocca, M. Romano, E. Solcia, and U. Ventura.** 1997. *Helicobacter pylori* vacuolating toxin accumulates within the endosomal-vacuolar compartment of cultured gastric cells and potentiates the vacuolating activity of ammonia. J Pathol **183:**453-9.

110. **Rudel, T., O. Kepp, and V. Kozjak-Pavlovic.** 2010. Interactions between bacterial pathogens and mitochondrial cell death pathways. Nat Rev Microbiol **8:**693-705.

111. **Salama, N. R., G. Otto, L. Tompkins, and S. Falkow.** 2001. Vacuolating cytotoxin of *Helicobacter pylori* plays a role during colonization in a mouse model of infection. Infect Immun **69:**730-6.

112. **Santel, A., and S. Frank.** 2008. Shaping mitochondria: The complex posttranslational regulation of the mitochondrial fission protein DRP1. IUBMB Life **60:**448-55.

113. **Schmitt, W., and R. Haas.** 1994. Genetic analysis of the *Helicobacter pylori* vacuolating cytotoxin: structural similarities with the IgA protease type of exported protein. Mol Microbiol **12:**307-19.

114. **Silhavy, T. J.** 1997. Death by lethal injection. Science **278:**1085-6.

115. **Smoot, D. T., J. H. Resau, M. H. Earlington, M. Simpson, and T. L. Cover.** 1996. Effects of *Helicobacter pylori* vacuolating cytotoxin on primary cultures of human gastric epithelial cells. Gut **39:**795-9.

116. **Stingl, K., K. Altendorf, and E. P. Bakker.** 2002. Acid survival of *Helicobacter pylori*: how does urease activity trigger cytoplasmic pH homeostasis? Trends Microbiol **10:**70-4.

117. **Sundrud, M. S., V. J. Torres, D. Unutmaz, and T. L. Cover.** 2004. Inhibition of primary human T cell proliferation by *Helicobacter pylori* vacuolating toxin (VacA) is independent of VacA effects on IL-2 secretion. Proc Natl Acad Sci U S A **101:**7727-32.

118. **Supajatura, V., H. Ushio, A. Wada, K. Yahiro, K. Okumura, H. Ogawa, T. Hirayama, and C. Ra.** 2002. Cutting edge: VacA, a vacuolating cytotoxin of *Helicobacter pylori*, directly activates mast cells for migration and production of proinflammatory cytokines. J Immunol **168:**2603-7.

119. **Szabo, I., S. Brutsche, F. Tombola, M. Moschioni, B. Satin, J. L. Telford, R. Rappuoli, C. Montecucco, E. Papini, and M. Zoratti.** 1999. Formation of anion-selective channels in the cell plasma membrane by the toxin VacA of *Helicobacter pylori* is required for its biological activity. Embo J **18:**5517-27.

120. **Tait, S. W., and D. R. Green.** 2010. Mitochondria and cell death: outer membrane permeabilization and beyond. Nat Rev Mol Cell Biol **11:**621-32.

121. **Telford, J. L., P. Ghiara, M. Dell'Orco, M. Comanducci, D. Burroni, M. Bugnoli, M. F. Tecce, S. Censini, A. Covacci, Z. Xiang, and et al.** 1994. Gene structure of the *Helicobacter pylori* cytotoxin and evidence of its key role in gastric disease. J Exp Med **179:**1653-58.

122. **Tomb, J. F., O. White, A. R. Kerlavage, R. A. Clayton, G. G. Sutton, R. D. Fleischmann, K. A. Ketchum, H. P. Klenk, S. Gill, B. A. Dougherty, K. Nelson, J. Quackenbush, L. Zhou, E. F. Kirkness, S. Peterson, B. Loftus, D. Richardson, R. Dodson, H. G. Khalak, A. Glodek, K. McKenney, L. M. Fitzegerald, N. Lee, M. D. Adams, E. K. Hickey, D. E. Berg, J. D. Gocayne, T. R. Utterback, J. D. Peterson, J. M. Kelley, M. D. Cotton, J. M. Weidman, C. Fujii, C. Bowman, L. Watthey, E. Wallin, W. S. Hayes, M. Borodovsky, P. D. Karp, H. O. Smith, C. M. Fraser, and J. C. Venter.** 1997. The complete genome sequence of the gastric pathogen *Helicobacter pylori*. Nature **388:**539-47.

123. **Tombola, F., C. Carlesso, I. Szabo, M. de Bernard, J. M. Reyrat, J. L. Telford, R. Rappuoli, C. Montecucco, E. Papini, and M. Zoratti.** 1999. *Helicobacter pylori* vacuolating toxin forms anion-selective channels in planar lipid bilayers: possible implications for the mechanism of cellular vacuolation. Biophys J **76:**1401-9.

124. **Tombola, F., F. Oregna, S. Brutsche, I. Szabo, G. Del Giudice, R. Rappuoli, C. Montecucco, E. Papini, and M. Zoratti.** 1999. Inhibition of the vacuolating and anion channel activities of the VacA toxin of *Helicobacter pylori*. FEBS Lett **460:**221-5.

125. **Tricottet, V., P. Bruneval, O. Vire, J. P. Camilleri, F. Bloch, N. Bonte, and J. Roge.** 1986. Campylobacter-like organisms and surface epithelium abnormalities in active, chronic gastritis in humans: an ultrastructural study. Ultrastruct Pathol **10:**113-22.

126. **Twig, G., B. Hyde, and O. S. Shirihai.** 2008. Mitochondrial fusion, fission and autophagy as a quality control axis: the bioenergetic view. Biochim Biophys Acta **1777:**1092-7.

127. **van Doorn, L. J., C. Figueiredo, R. Sanna, S. Pena, P. Midolo, E. K. Ng, J. C. Atherton, M. J. Blaser, and W. G. Quint.** 1998. Expanding allelic diversity of *Helicobacter pylori* vacA. J Clin Microbiol **36:**2597-603.

128. **Vaux, D. L., G. Haecker, and A. Strasser.** 1994. An evolutionary perspective on apoptosis. Cell **76:**777-9.

129. **Vinion-Dubiel, A. D., M. S. McClain, D. M. Czajkowsky, H. Iwamoto, D. Ye, P. Cao, W. Schraw, G. Szabo, S. R. Blanke, Z. Shao, and T. L. Cover.** 1999. A dominant negative mutant of *Helicobacter pylori* vacuolating toxin (VacA) inhibits VacA-induced cell vacuolation. J Biol Chem **274:**37736-42.

130. **Wagner, S., W. Beil, J. Westermann, R. P. Logan, C. T. Bock, C. Trautwein, J. S. Bleck, and M. P. Manns.** 1997. Regulation of gastric epithelial cell growth by *Helicobacter pylori*: offdence for a major role of apoptosis. Gastroenterology **113:**1836-47.

131. **Wang, F., P. Xia, F. Wu, D. Wang, W. Wang, T. Ward, Y. Liu, F. Aikhionbare, Z. Guo, M. Powell, B. Liu, F. Bi, A. Shaw, Z. Zhu, A. Elmoselhi, D. Fan, T. L. Cover, X. Ding, and X. Yao.** 2008. *Helicobacter pylori* VacA disrupts apical membrane-cytoskeletal interactions in gastric parietal cells. J Biol Chem **283:**26714-25.

132. **Wells, C. L., E. M. van de Westerlo, R. P. Jechorek, B. A. Feltis, T. D. Wilkins, and S. L. Erlandsen.** 1996. *Bacteroides fragilis* enterotoxin modulates epithelial permeability and bacterial internalization by HT-29 enterocytes. Gastroenterology **110:**1429-37.

133. **Willhite, D. C., and S. R. Blanke.** 2004. *Helicobacter pylori* vacuolating cytotoxin enters cells, localizes to the mitochondria, and induces mitochondrial membrane permeability changes correlated to toxin channel activity. Cell Microbiol **6:**143-54.

134. **Willhite, D. C., D. Ye, and S. R. Blanke.** 2002. Fluorescence resonance energy transfer microscopy of the *Helicobacter pylori* vacuolating cytotoxin within mammalian cells. Infect Immun **70:**3824-32.

135. **Winans, S. C., D. L. Burns, and P. J. Christie.** 1996. Adaptation of a conjugal transfer system for the export of pathogenic macromolecules. Trends Microbiol **4:**64-8.

136. **Xia, H. H., and N. J. Talley.** 2001. Apoptosis in gastric epithelium induced by *Helicobacter pylori* infection: implications in gastric carcinogenesis. Am J Gastroenterol **96:**16-26.

137. **Yahiro, K., T. Niidome, T. Hatakeyama, H. Aoyagi, H. Kurazono, P. I. Padilla, A. Wada, and T. Hirayama.** 1997. *Helicobacter pylori* vacuolating cytotoxin binds to the 140-kDa protein in human gastric cancer cell lines, AZ-521 and AGS. Biochem Biophys Res Commun **238:**629-32.

138. **Yahiro, K., T. Niidome, M. Kimura, T. Hatakeyama, H. Aoyagi, H. Kurazono, K. Imagawa, A. Wada, J. Moss, and T. Hirayama.** 1999. Activation of *Helicobacter pylori* VacA toxin by alkaline or acid conditions increases its binding to a 250-kDa receptor protein-tyrosine phosphatase beta. J Biol Chem **274:**36693-9.

139. **Yahiro, K., A. Wada, M. Nakayama, T. Kimura, K. Ogushi, T. Niidome, H. Aoyagi, K. Yoshino, K. Yonezawa, J. Moss, and T. Hirayama.** 2003. Protein-tyrosine phosphatase alpha, RPTP alpha, is a *Helicobacter pylori* VacA receptor. J Biol Chem **278:**19183-9.

140. **Yamasaki, E., A. Wada, A. Kumatori, I. Nakagawa, J. Funao, M. Nakayama, J. Hisatsune, M. Kimura, J. Moss, and T. Hirayama.** 2006. *Helicobacter pylori* vacuolating cytotoxin induces activation of the proapoptotic proteins Bax and Bak, leading to cytochrome *c* release and cell death, independent of vacuolation. J Biol Chem **281:**11250-9.

141. **Ye, D., and S. R. Blanke.** 2000. Mutational analysis of the *Helicobacter pylori* vacuolating toxin amino terminus: identification of amino acids essential for cellular vacuolation. Infect Immun **68:**4354-7.

142. **Ye, D., D. C. Willhite, and S. R. Blanke.** 1999. Identification of the minimal intracellular vacuolating domain of the *Helicobacter pylori* vacuolating toxin. J Biol Chem **274:**9277-82.

143. **Yin, X. M.** 2006. Bid, a BH3-only multi-functional molecule, is at the cross road of life and death. Gene **369:**7-19.

144. **Zarrilli, R., V. Ricci, and M. Romano.** 1999. Molecular response of gastric epithelial cells to *Helicobacter pylori*-induced cell damage. Cell Microbiol **1:**93-9.

145. **Zheng, P. Y., and N. L. Jones.** 2003. *Helicobacter pylori* strains expressing the vacuolating cytotoxin interrupt phagosome maturation in macrophages by recruiting and retaining TACO (coronin 1) protein. Cell Microbiol **5:**25-40.

146. **Zhou, R., A. S. Yazdi, P. Menu, and J. Tschopp.** 2011. A role for mitochondria in NLRP3 inflammasome activation. Nature **469:**221-5.

Chapter 2: *Helicobacter pylori* VacA engages the mitochondrial apoptotic machinery by inducing Drp1-mediated mitochondrial fission

2.1 INTRODUCTION

Mitochondria preserve cell viability by functioning both as centers for energy production, as well as central regulators of calcium homeostasis, apoptosis, and development. Some pathogenic microbes usurp the mitochondrial apoptotic machinery (4) which, depending on the pathogen and host cell type, can block cell death to preserve a colonization niche or, alternatively, induce cell death to promote escape from an intracellular niche or circumvent immune clearance (44). For the gastric pathogen *Helicobacter pylori* (*Hp*), chronic infection is associated with increased apoptosis within the gastric mucosa of humans (40), mice (31), and Mongolian gerbil models (43). Increased apoptosis may alter the gastric environment to promote *Hp* persistence (11), while at the same time, contribute to gastric disease, including peptic ulcers and gastric adenocarcinoma (12). Earlier studies have indicated that the vacuolating cytotoxin (VacA), an *Hp* virulence factor that is important for *Hp* colonization (45) and disease pathogenesis (20), is essential (35) and sufficient (14) for inducing gastric epithelial cell death.

Several studies investigating the mechanism of VacA induced cell death indicate that VacA is a mitochondrial-targeting toxin. Subsequent to binding

plasma membrane sphingomyelin (27, 28), and potentially additional protein components (59, 60), VacA is internalized and induces mitochondrial dysfunction and mitochondrial outer membrane permeabilization (MOMP) (56). Intracellular VacA localizes to mitochondria (22, 56), and isolated mitochondria rapidly import purified VacA beyond the outer membrane (17, 19, 22), resulting in dissipation of the mitochondrial trans-membrane potential ($\Delta\Psi_m$) (61). VacA-dependent MOMP occurs after $\Delta\Psi_m$ dissipation (56), and requires activation of the eukaryotic pro-apoptotic effector Bax (61). However, the underlying mechanism by which VacA triggers Bax-dependent MOMP has not been identified.

Within this study, we report that VacA disrupts the morphological dynamics of mitochondria as a mechanism to induce gastric epithelial cell death. Mitochondria exist in several overall morphologies, which are linked to the health of the cell, and change in a dynamic fashion through frequent and repetitive cycles of fission and fusion that occur in response to cellular energy demands and environmental challenges (52). De-regulation of mitochondrial dynamics has increasingly been linked to the pathologies resulting from inflammatory and neurodegenerative disorders (10), as well as several cancers (25). However, the extent to which the morphological dynamics of mitochondria may be targeted by pathogenic microbes during host infection, or are associated with the pathophysiology of some infectious diseases, is largely unexplored. Our studies revealed that VacA induces activation of the dynamin-related protein 1 (Drp1), which is a critical regulator of mitochondrial fission within cells. Moreover, inhibition of VacA-mediated Drp1-dependent fission prevented activation of the

pro-apoptotic Bcl-2–associated X (Bax) protein, MOMP, and death of intoxicated cells. *Hp* disruption of mitochondrial dynamics during infection is a here-to-fore unrecognized strategy by which a pathogenic microbe engages the host's apoptotic machinery.

The text of the chapter 2 is similar to similar to the text of paper published in the journal Proceedings of the National Academy of Sciences (Jain P, Luo ZQ and Blanke SR. 2011. *Helicobacter pylori* vacuolating cytotoxin (VacA) engages the mitochondrial fission machinery to induce host cell death. Proc Natl Acad Sci USA; 108 (38): 16032-7).

2.2 MATERIALS AND METHODS

Bacterial Strains. *Hp* 60190 (*cag* PAI$^+$*, vacA* s1/m1; 49503; ATCC; Manassas, VA) was cultured in bisulfite- and sulfite-free brucella broth (BSFB) containing 5 μg vancomycin/mL (Sigma Aldrich; St. Louis, MO), on a rotary platform shaker for 48 h at 37 °C, under 5% CO_2 and 10% O_2. *Hp* VM022 (*ΔvacA*) (53) and *Hp* VM084 (*ΔvacA::vacA*) were kind gifts from Dr. Timothy Cover (Vanderbilt University Medical Center; Nashville, TN) (37). *Hp* 60190 derived strains producing VacA (P9A) and VacA (G14A) were constructed and cultivated as described previously (37, 56). *Hp* 26695 (*cag* PAI$^+$, *vacA* s1/m1) was obtained from ATCC (700392). *Hp* G27 (*cag* PAI$^+$, *vacA* s1/m1) (48) was obtained as a kind gift from Dr. Karen Guillemin (University of Oregon; Eugene, OR).

Mammalian Cells. AZ-521 human gastric-cancer derived cell line was obtained from Japan Health Science Foundation (3940; Tokyo, JP) and maintained in MEM (Sigma Aldrich), which when supplemented with glutamine (2 mM), penicillin (100 U/mL), streptomycin sulfate (1 mg/mL) and 10% fetal bovine calf serum, was referred to as "supplemented MEM". HeLa (CCL-2; ATCC), HEp-2 (CCL-23; ATCC) and Madin-Darby Canine Kidney II (MDCK) cells (CCL-34; ATCC) were maintained in supplemented MEM. AGS cells (CRL-1739; ATCC) were maintained in Ham's F-12 Kaighn's modification medium (Cellgro; Manassas, VA), which when supplemented with glutamine (2 mM), penicillin (100 U/mL), streptomycin sulfate (1 mg/mL) (Sigma Aldrich) and 10% fetal bovine calf serum (JRH Biosciences; Lenexa, KS), was referred to as "supplemented Ham's F-12 medium". *bax*$^{+/+}$ and *bax*$^{-/-}$ mouse embryonic fibroblasts (MEFs), obtained as a kind gift from Dr. Wei-Xing Zong (Stony Brook University; Stony Brook, NY), were maintained in DMEM (Cellgro), which when supplemented with glutamine (2 mM), penicillin (100 U/mL), streptomycin sulfate (1 mg/mL) and 10% fetal bovine calf serum, was referred to as "supplemented DMEM". All cell lines were maintained at 37 °C within a humidified atmosphere and under 5% CO_2.

Plasmids. The plasmids pDsRed2-Mito and pAcGFP1-N1 were obtained from Clontech (Mountain View, CA). Plasmids pEGFP-Drp1 and pEGFP-DN-Drp1 (K38A) were a kind gift from Dr. Marina Jendrach (Goethe University; Frankfurt/Main, Germany). Plasmid p34(1-319)-EGFP was kind a gift from Dr. Joachim Rassow (Ruhr-Universität Bochum; Bochum, Germany).

Transfection. Cells were transfected with the indicated plasmids using Lipofectamine-2000 transfection reagent (Invitrogen; Carlsbad, CA), according to manufacturer's instructions.

***Hp* Infection of Mammalian Cells.** Monolayers of mammalian cells, at 37 °C within a humidified environment under 5% CO_2, were incubated with the indicated *Hp* strains and at the indicated MOI. At the end of incubation, monolayers were washed with PBS pH 7.2, and processed for the indicated analyses.

Analysis of Mitochondrial Fragmentation within AZ-521, AGS and Mouse Embryonic Fibroblast Cells. Mammalian cells plated in 8-well culture slides (BD Biosciences; Franklin Lakes, NJ), that had been transiently transfected with pDsRed2-Mito, a mammalian expression vector that encodes a fusion between red fluorescent protein and the mitochondrial targeting sequence from subunit VIII of the human cytochrome *c* oxidase, were infected with *Hp* (at the indicated MOI), or incubated with VacA (at the indicated concentration) or HPCF (at the indicated concentration), or mock-treated with PBS pH 7.2. At the indicated times, the cells were washed 3 times with PBS pH 7.2, and then fixed by incubation with paraformaldehyde (4%) at 37 °C for 20 min. Mitochondrial morphology was analyzed by DIC-epifluorescence microscopy. Images were processed using DeltaVision SoftWoRx 3.5.1 software suite (Applied Precision; Issaquah, WA). Mitochondrial lengths were measured using Imaris 5.7 software

(Bitplane; St. Paul, MN). Data were rendered as the average mitochondrial lengths obtained by combining data from at least two or three independent experiments. In each independent experiment, 15 cells were analyzed from at least 4 randomly chosen fields for each treatment. Within each cell, at least 3 mitochondria were analyzed and mitochondrial lengths measured. Relative mitochondrial lengths were calculated as the fold change in average mitochondrial length measured in cells treated as indicated relative to those measured in mock-treated cells.

Generation of Polarized MDCK Monolayers. Polarized MDCK monolayers were generated and maintained, as described previously (50). Briefly, MDCK cells (2.5 X 10^5 cells/0.5 mL in supplemented MEM) were seeded onto 12 mm, 3.0 μm-pore polyester tissue culture transwell inserts (Corning; Corning, NY), and incubated at 37 °C and under 5% CO_2, with 1.5 mL supplemented MEM added in the basal chamber. Cell culture medium in the apical chambers was replaced once, 24 h after seeding, with fresh supplemented MEM, while the medium in basal chamber was replaced with fresh supplemented MEM daily. The plates were maintained at 37 °C in humidified atmosphere and under 5% CO_2 for at least 4 days prior to experiments.

To assess the integrity of polarized monolayers, transwell inserts with MDCK cells or mock-seeded transwell inserts (incubated with PBS pH 7.2 alone) were incubated at 37 °C and under 5% CO_2 with biotin-albumin (50 μg/mL, 1.5 mL; Sigma Aldrich) in supplemented MEM in the transwell basal chamber and

supplemented MEM alone (0.5 mL) in the apical chamber. After 1 h, medium from the apical and basal chambers were collected and resolved by SDS gel electrophoresis, followed by Western blot analysis to probe for biotin-albumin using streptavidin-HRP (GE Healthcare; Piscataway, NJ). The presence of biotin-albumin was detected by chemiluminescence using the Super-signal West Femto chemiluminescence detection kit (Thermo Scientific; Rockford, IL).

Analysis of Mitochondrial Fragmentation within HeLa, HEp-2 and Polarized MDCK Cells. HeLa and HEp-2 cells plated in 8-well culture slides, as well as transmembrane polyester inserts containing polarized MDCK monolayers were washed twice with PBS pH 7.2 and fixed by incubation with paraformaldehyde (4%) for 20 min at 37 °C, followed by permeabilization in PBS pH 7.2 containing Triton-X 100 (0.1 %) for 10 min at 4 °C. After washing twice with PBS pH 7.2, cells were probed for the mitochondrial marker Tom-20 by incubation at 4 °C for overnight with anti-Tom 20 mAb (BD Biosciences) in PBS pH 7.2 containing 3% BSA (Sigma Aldrich), followed by incubation at 25 °C for 1 h with mouse anti-IgG conjugated to Alexa Fluor 488 (Invitrogen) in PBS pH 7.2 containing 3% BSA. The cells were washed 3 times with PBS pH 7.2 and mitochondria were visualized by DIC-epifluorescence microscopy.

Preparation of HPCF. The indicated *Hp* strains were grown in 200 mL bisulfite- and sulfite-free brucella broth (BSFB) containing 5 μg vancomycin/mL, in 1 L culture flasks, on a rotary platform shaker at 37 °C, under 5% CO_2 and

10% O_2. After 48 h, *Hp* cultures were harvested by centrifugation at 8,000 g for 30 min at 4 °C. The supernatants were collected, and pellets were decontaminated by autoclaving. The supernatants were cooled to 4 °C, and the total protein was precipitated by slowly dissolving ammonium sulfate (Sigma Aldrich) to 90% saturation with stirring, followed by stirring overnight at 4 °C. The precipitates were collected by centrifugation at 8,000 g for 30 min at 4 °C, and the pellets were resuspended in 10 mM sodium phosphate buffer pH 7.0. The samples were dialyzed at 4 °C into 10 mM sodium phosphate buffer pH 7.0 using the Spectra/Por® membrane (molecular weight cut-off (MWCO) 50,000 Daltons (Da); Spectrum Laboratories; Rancho Dominguez, CA), concentrated approximately 5-fold using an Amicon Ultra Centrifugal Filter Unit (MWCO 50,000 Da; Sigma Aldrich), and filter sterilized using a 0.2 μm vacuum filtration unit (Corning), to obtain the final HPCF.

The presence of full-length VacA within the HPCFs was confirmed by Western blot analysis, using VacA rabbit antiserum (Rockland Immunochemicals; Gilbertsville, PA), followed by incubation with HRP conjugated anti-rabbit IgG secondary antibody (Cell Signaling Technology; Danvers, MA). The presence of VacA was detected by chemiluminescence using the Super-signal West Femto chemiluminescence detection kit. VacA concentrations were normalized using densitometry analysis (UN-SCAN-IT gel analysis software; Silk Scientific Inc.; Orem, Utah) to compare the total pixels of each band against those obtained using known concentrations of purified VacA. The HPCFs were used within several days of preparation, during which time there was no detectable loss of

VacA-induced vacuolation of AZ-521 cells, as determined by quantification of cellular vacuolation (15, 28).

Heat Inactivation of HPCF. HPCFs (5 mg/mL) were incubated in a 37 °C or 95 °C water bath for 30 min, followed by incubation for 10 min at 37 °C. The HPCFs were immediately activated by adding 0.1 v/v 300 mM HCl to HPCF preparation and incubation for 30 min at 37 °C, followed by neutralization with the same volume of 300 mM NaOH. Activated HPCF were incubated with AZ-521 cells at a final concentration of 0.05 mg/mL. At the indicated times, the AZ-521 cells were analyzed for changes in mitochondrial morphology relative to cells that were mock intoxicated with PBS pH 7.2.

Intoxication of Mammalian Cells with VacA or HPCF. Mammalian cells were incubated at 37 °C and within a humidified environment under 5% CO_2 with purified VacA or HPCF (both at the indicated concentrations). At the indicated times, the cells were processed for specific analyses.

Heat Inactivation of *Hp*. *Hp* 60190 (12.5 X 10^8 CFU/mL in 1 mL PBS pH 7.2) were incubated in a 37 °C or 65 °C water bath for 30 min, and then further incubated for 10 min at 37 °C. Immediately, 37 °C- or 65 °C-pretreated *Hp* were incubated with AZ-521 cells (MOI 100) or, alternatively, enumerated by serially diluting in PBS pH 7.2, followed by spread-plating onto fresh F-12 agar plates (supplemented with 5% FBS and 5 μg vancomycin/mL) and incubating the plates

at 37 °C, and under 5% CO_2 and 10% O_2. After 72 h, CFU/mL were determined by direct counting of colonies on the F-12 plates and back calculating the appropriate dilution factor.

Analysis of *Hp* Association with AZ-521 cells. Monolayers (85-95% confluence) of AZ-521 cells, plated at 0.75 X 10^5 cells per well, were incubated with *Hp* 60190, *Hp* VM022 (*ΔvacA*), or *Hp* VM084 (*ΔvacA::vacA*) (all at MOI 100) at 37 °C and under 5% CO_2 and 10% O_2. After 8 h, the cell monolayers were washed twice with PBS pH 7.2. Each monolayer was gently lysed by incubating with 0.1 % Triton X-100 in PBS pH 7.2 (50 μL) for 3 min on ice and collected in 950 μL PBS pH 7.2. The cell associated *Hp* was plated on F-12 media plates supplemented with 10% FBS and 5 μg vancomycin/mL and incubated at 37 °C under 5% CO_2 and 10% O_2. After 72 h, the CFU/mL was determined by the direct counting of colonies on F-12 plates, and back calculating using the appropriate dilution-factor.

Purification of VacA. *H. pylori* 60190 (49503; ATCC) was cultured, and VacA was purified from *Hp* culture filtrate (HPCF; from *Hp* broth culture described earlier) by anion exchange chromatography using Diethyl aminoethyl Sephacel resin (Sigma). VacA was then eluted using 10 mM phosphate buffer pH 7.0, containing 200 mM sodium chloride. All eluted fractions were collected and analyzed by sodium dodecyl sulfate (SDS)-polyacrylamide gel electrophoresis followed by Coomassie brilliant blue staining and immunoblot analysis using

rabbit anti-VacA polyclonal antibody, and purity of the full length toxin in VacA containing fractions was assessed to be on an average of 90-95 % pure. Additionally, a major fraction of impurities constitute breakdown products of full length toxin including p33 and p55 fragments as found out by western blot analysis using polyclonal anti-VacA antibodies showing cross reactive proteins of around 33 and 55 kDa size. Fractions demonstrating the greatest degree of purity were pooled and stored at 4 °C until use. VacA (s1m1) from *Hp* 60190, was purified and activated, as previously described (13).

Heat Inactivation of VacA. Purified VacA (4 μM) was incubated in a 37 °C or 95 °C water bath, followed by further incubation of both samples at 37 °C for 10 min. Immediately, VacA was activated as described previously (13, 27, 56), and incubated with AZ-521 cells (at a final concentration of 250 nM). At the indicated times, the AZ-521 cells were analyzed for changes in mitochondrial morphology relative to cells that were mock intoxicated with PBS pH 7.2.

Inactivation of VacA with Anti-VacA Antibody. Purified VacA (0.1 mg/mL) was pre-incubated on ice with VacA rabbit antiserum (2 mg/mL), a non-specific rabbit antiserum against *Haemophilus ducreyi* cytolethal distending toxin A (CdtA; 2 mg/mL), or PBS pH 7.2. After 30 min, the VacA-containing samples were activated as described previously (13, 27, 56), and immediately incubated at 37 °C with AZ-521 cells (250 nM VacA in each sample). At the indicated times,

the AZ-521 cells were analyzed for changes in mitochondrial morphology relative to cells that were mock intoxicated with PBS pH 7.2.

Expression and Purification of Recombinant VacA Proteins. The recombinant VacA fragments, p33 (residues 1-312) and p55 (residues 312-821), were expressed in *E. coli* (DH5α) and purified as described previously (51).

Analysis of Drp1 Localization to Mitochondria. Mitochondrial localization of Drp1 was analyzed as described previously (33). Mammalian cells that had been transiently transfected with pDsRed2-Mito and plated in 8-well culture slides, were incubated with *Hp* (at the indicated MOI) or purified VacA (at the indicated concentrations), or *Hp* culture filtrates (at the indicated concentrations). At the indicated times, the monolayers were washed 3 times with PBS pH 7.2, fixed by incubation with paraformaldehyde (4%) for 20 min at 37 °C, permeabilized by incubation with PBS pH 7.2 containing Triton-X 100 (0.1%) for 10 min at 4 °C, immunostained for Drp1 using anti-Drp1 mAb (BD Biosciences), and, finally, incubated at 25 °C for 1 h with mouse anti-IgG conjugated to Alexa Fluor 647 (Invitrogen). The cells were imaged using DIC-epifluorescence microscopy. Drp1 localization to mitochondria was quantified using the co-localization module of the DeltaVision SoftWoRx 3.5.1 software suite. Results were expressed as the co-localization index, derived from calculating the Pearson's coefficient of correlation, which in this study was a measure of co-localization between Drp1 and mitochondria in each z plane of the

cell. For each cell, images from an average of 10-20 z planes at a thickness of 0.2 μm were collected. A co-localization index of 1.0 indicates 100% co-localization of Drp1 to mitochondria, whereas a co-localization index of 0.0 indicates the absence of detectable co-localization between Drp1 and mitochondria. Data were rendered as the average co-localization index obtained from analyzing 30 cells from over the course of three independent experiments. In each independent experiment, 10 cells were analyzed from at least 4 randomly chosen fields for each treatment.

Flow Cytometry Assay for Determination of Total Cellular and Activated Bax. AZ-521 cells were detached from tissue culture wells by mild trypsinization for 3 min at 37 °C with Trypsin EDTA (Cellgro), fixed by incubation with paraformaldehyde (4%) for 20 min at 37 °C, followed by permeabilization with saponin (0.1 %) in PBS pH 7.2 containing BSA (0.5%) and anti-Bax 2D2 mAb (1 μg/mL; BD Biosciences) in order to stain for total cellular Bax. Alternatively, the cells were fixed by incubation with paraformaldehyde (4%) for 20 min at 37 °C, followed by permeabilization with saponin (0.1 %) in PBS pH 7.2 containing BSA (0.5%) and anti-Bax Clone 3 mAb in order to stain for activated Bax. After 45 min, the cells were washed 3 times with PBS pH 7.2, followed by incubation with mouse anti-IgG conjugated to Alexa Fluor 488 (1 μg/mL) in PBS pH 7.2 containing saponin (0.1 %) and BSA (0.5%) for 30 min on ice and in the dark. As a negative control, cells were incubated in the presence of mouse anti-IgG conjugated to Alexa Fluor 488 (1 μg/mL) alone. Cells were washed in PBS

pH 7.2 containing saponin (0.1 %) and BSA (0.5%) and resuspended in PBS pH 7.2. Alexa Fluor 488 fluorescence was quantified by flow cytometry in the FL1 channel (525/40 nm band pass filter). 10,000 cells were analyzed for each sample.

Microscopic Analysis of Intracellular Activated Bax. Cells were fixed by incubation with paraformaldehyde (4%) for 20 min at 37 °C, followed by permeabilization on ice with saponin (0.1 %; Sigma Aldrich) in PBS pH 7.2 containing BSA (0.5%) and anti-Bax (Clone 3) mAb (1 μg/mL; BD Biosciences) in order to stain for activated Bax. After 45 min, the cells were washed 3 times with PBS pH 7.2, followed by incubation with mouse anti-IgG conjugated to Alexa Fluor 647 or Alexa Fluor 488 (1 μg/mL) in PBS pH 7.2 containing saponin (0.1 %) and BSA (0.5%) for 1 h on ice in the dark. The cells were visualized by DIC-epifluorescence microscopy, with visible fluorescence indicative of activated Bax. In order to enumerate the number of cells displaying active Bax, imaging was carried out at a constant time of exposure. All images were deconvolved using SoftWoRx constrained iterative deconvolution tool (ratio mode) to remove out of focus signal. Following deconvolution, cells displaying visible fluorescence were considered to contain active Bax, as opposed to the absence of Bax activation in cells that did not display fluorescence. Data were rendered as the percentage of cells displaying active Bax within the entire population, and were obtained by analyzing over 700 cells from randomly chosen fields over the course of two independent experiments.

Analysis of Cyt *c* Release. Cyt *c* release was analyzed as described previously (6). Briefly, Mammalian cells were fixed by incubation with paraformaldehyde (4%) for 20 min at 37 °C, permeabilized by incubation with PBS pH 7.2 containing Triton-X 100 (0.1%) for 10 min at 4 °C, immunostained for Cyt *c* by incubating with anti-Cyt *c* mAb (BD Biosciences), and then further incubated with one of two secondary antibodies. In order to visualize Cyt *c* within cells intoxicated with VacA in the presence or absence of mdivi-1, cells were further incubated with mouse anti-IgG conjugated to Alexa Fluor 488. Alternatively, in order to visualize Cyt *c* within VacA intoxicated cells over-expressing either EGFP-Drp1 or EGFP-DN-Drp1 (K38A), cells were further incubated with mouse anti-IgG conjugated to Alexa Fluor 647. The cells were imaged using DIC-epifluorescence microscopy. Cells with diffuse, non-localized fluorescence were scored as having released (cytosolic) Cyt *c*, while cells with punctate fluorescence localized in the perinuclear regions were scored as having mitochondrial-localized Cyt *c*.

Cell Death. Cell death was measured by flow cytometry, using the Live-Dead viability/cytotoxicity assay kit (Invitrogen) according to manufacturer's instructions.

Analysis of VacA Localization to Mitochondria. AZ521 cells plated in 8-well culture slides were incubated with purified VacA (100 nM). After 30 min, the monolayers were washed 3 times with PBS pH 7.2, fixed by incubation with

paraformaldehyde (4%) for 20 min at 37 °C, permeabilized by incubation with PBS pH 7.2 containing Triton-X 100 (0.1%) for 10 min at 4 °C, immunostained for VacA using anti-VacA rabbit polyclonal Ab, and, mitochondria using anti-Tom 20 mAb and incubated at 25 °C for 2 h. The cells were washed 3 times with PBS pH 7.2 followed by incubation with rabbit anti-IgG conjugated to Alexa Fluor 568 and mouse anti-IgG conjugated to Alexa Fluor 488 for 1 h at 25 °C. The cells were washed 3 times with PBS pH 7.2 and imaged using DIC-epifluorescence microscopy.

Analysis of Mitochondrial Transmembrane Potential ($\Delta\Psi_m$). AZ-521 cells were incubated with TMRE (50 nM; Sigma Aldrich) for 30 min prior to the end of each experiment. The cells were detached by mild trypsinization for 3 min at 37 °C with Trypsin-EDTA and washed two times with PBS pH 7.2. TMRE fluorescence was quantified by flow cytometry in the FL2 channel (575/30 nm band pass filter). 10,000 cells were analyzed for each sample.

Flow Cytometry. Analytical flow cytometry was carried out using a BD FACSCanto II flow analyzer (BD Biosciences) located at the R. J. Carver Biotechnology Center Flow Cytometry Facility (University of Illinois at Urbana-Champaign). The flow cytometer was equipped with 70-μm nozzle, 488 nm line of an air-cooled argon-ion laser, and 400 mV output. The band pass filters used for analysis were 525/40 nm, 575/30 nm and 675/30 nm. Cell analysis was standardized for scatter and fluorescence by using a suspension of fluorescent

beads (Beckman Coulter; Miami, FL). Events were recorded on a log fluorescence scale and the geometric mean as well as percent events was determined using FCS Express analysis software (De Novo Software; Los Angeles, CA). Forward and side scatter properties were considered to exclude non-cellular (debris) events from viable and (or) dead cell populations.

DIC-Epifluorescence Microscopy. Fluorescence and DIC images were collected using a Delta Vision RT microscope (Applied Precision), EX 490/20 and EM 528/38, EX 555/28 and EM 617/73, EX 640/20 and EM 685/40 using Olympus Plan Apo 60X oil objective with NA 1.42 and working distance of 0.17 nm. Images were processed using DeltaVision SoftWoRx 3.5.1 software suite.

Statistical Analysis. Unless otherwise indicated, each experiment was performed at least three independent times. For those data requiring statistical analysis, data were combined from 2 or 3 independent experiments, as indicated, with each independent experiment carried out in triplicate. Statistical analyses were performed using Microsoft Excel (Version 11.0; Microsoft Corporation; Redmond, WA). Unless otherwise noted, error bars represent standard deviations. All *P* values were calculated with the Student's *t* test using paired, two-tailed distribution. $P < 0.05$ indicates statistical significance.

2.3 RESULTS

2.3.1 *Hp* infection and mitochondrial fragmentation.

While studying cellular responses to *Hp*, we observed *Hp*-dependent alterations in the structure of cellular mitochondria, similar to those previously reported in studies of *Hp*-infected human stomach adenocarcinoma (AGS) cells (2). In uninfected AZ-521 gastric epithelial cells, mitochondria were predominantly filamentous networks of interconnected strands (approximately 15-25 µm in length) (Fig. 2.1 A, E). In contrast, at 8 h post-infection with *Hp* 60190, the mitochondrial network structure was highly fragmented, and individual mitochondria were visible as punctate organelles that were significantly shorter in length (1-2 µm) (Fig. 2.1 B, E). The transition from filamentous to punctate structures was also observed with either *Hp* 26695 or *Hp* G27, indicating that *Hp*-dependent fragmentation of mitochondria is not idiosyncratic to a single strain (Fig. 2.2). In addition, *Hp*-dependent fragmentation was recapitulated across cells lines, as observed in studies employing AGS (Fig. 2.3) and polarized Madin-Darby canine kidney II (MDCK) cells (Fig. 2.4 A, B). Fragmentation occurred at multiplicity of infection (MOI) 10, but not at MOI 1 (Fig. 2.5), and was time dependent, with progressive fragmentation of the filamentous network observed between 2 and 8 h post-infection (Fig. 2.6).

2.3.2 VacA is essential for *Hp*-induced mitochondrial fragmentation.

While characterizing *Hp*-dependent mitochondrial alterations, we observed fragmentation of the mitochondrial network in AZ-521 cells that had been

incubated with culture filtrate prepared from *Hp* 60190 (HPCF), but not with HPCF that had been pre-treated at 95 °C (Fig. 2.7). These results suggested that a proteinaceous factor released by *Hp* is responsible for mitochondrial fragmentation observed during infection. Consistent with this idea, fragmentation was not detected in cells incubated with heat-killed *Hp* 60190 (Fig. 2.8).

Studies indicating the involvement of an extracellular, heat-labile factor in *Hp*-mediated mitochondrial network fragmentation prompted us to evaluate a potential role for VacA, which has been previously reported to modulate mitochondrial function (22, 34, 56, 57). In contrast to the extensive fragmentation of mitochondria induced by *Hp* 60190 (Fig. 2.1B), an isogenic *Hp* mutant strain lacking a functional *vacA* gene (*Hp* (*ΔvacA*)) (53) did not induce visible mitochondrial fragmentation within AZ-521 cells (Fig. 2.1 C, E), while the complemented strain (*Hp* (*ΔvacA::vacA*)) (37) induced robust mitochondrial fragmentation (Fig. 2.1 D, E). Differences in the adherence of *Hp* 60190, *Hp* (*ΔvacA*), or *Hp* (*ΔvacA::vacA*) to AZ-521 cells were not observed (Fig. 2.9), suggesting that the inability of *Hp* (*ΔvacA*) to induce mitochondrial fragmentation was not likely due to attenuated cell association. These results support the idea that VacA is essential for *Hp*-dependent mitochondrial fragmentation.

2.3.3 VacA is sufficient to induce mitochondrial fragmentation.

Studies to evaluate the sufficiency of VacA for *Hp*-dependent mitochondrial fragmentation revealed that VacA, which had been purified from

culture filtrates of *Hp* 60190, induced the transition of mitochondrial networks into significantly shorter punctiform organelles (Fig. 2.10), an effect that was abrogated when the toxin was pre-incubated at 95 °C or with VacA antiserum (Fig. 2.11). More convincing, however, were studies conducted with recombinant VacA comprising the toxin's amino- and carboxyl-terminal fragments, called p33 and p55 respectively, that had been expressed separately in *E. coli* and purified (23). The combined p33-p55 fragments induced robust fragmentation, while neither p33 nor p55 alone induced detectable alterations in the mitochondrial network (Fig. 2.12). Together, these results indicate that VacA is sufficient to induce mitochondrial fragmentation.

VacA-mediated mitochondrial fragmentation is not idiosyncratic to AZ-521 cells, as the toxin induced similar morphological changes within AGS cells (Fig. 2.13), as previously observed (41), and polarized MDCK cells (Fig. 2.14). VacA-dependent mitochondrial fragmentation was also visible within human cervical adenocarcinoma (HeLa) and human larynx carcinoma (HEp-2) cells (Fig. 2.13), two non-gastric cell lines that have been previously used to study VacA interactions with mitochondria (17, 22). Within AZ-521 cells, mitochondrial fragmentation was detected with VacA at concentrations as low as 10 nM, but not at 1 nM (Fig. 2.15). Fragmentation was visible within 60 min after exposure of the cells to VacA (250 nM), and progressed to almost entirely punctiform organelles by 150 min (Fig. 2.16).

2.3.4 VacA induces mitochondrial recruitment of Drp1.

Cellular mitochondria exist in a dynamic state, constantly dividing and fusing by opposing processes (55). An important regulator of mitochondrial fission is Drp1 (55), which upon activation is recruited to focal sites of division on the mitochondrial outer membrane (46). Studies to evaluate whether VacA-dependent mitochondrial fragmentation might involve the cellular fission machinery revealed that, compared to mock-intoxicated cells, incubation for 4 h with purified VacA (from *Hp* 60190) resulted in a significant increase in Drp1 localization to mitochondria (Fig. 2.17 A, B). VacA-induced Drp1 localization to mitochondria was dose dependent, with significant increases observed at toxin concentrations as low as 10 nM (Fig. 2.18). A significant increase in mitochondrial localization of Drp1 was also detected in cells infected with *Hp* 60190 and *Hp* (*ΔvacA::vacA*), but not with *Hp* (*ΔvacA*), indicating that increased Drp1 recruitment to mitochondria within infected cells is VacA-dependent (Fig. 2.19). These results suggested a possible involvement of the cellular fission machinery in VacA-dependent mitochondrial network fragmentation.

2.3.5 Drp1 GTPase activity is important for VacA-dependent mitochondrial fragmentation.

A critical step during mitochondrial fission is the assembly of Drp1 into spiral chains at the mitochondrial scission sites (29), which is driven by the intrinsic GTPase activity of Drp1 (21). To evaluate the importance of Drp1 function for VacA-dependent mitochondrial fission, AZ-521 cells were intoxicated

with VacA in the absence or presence of the mitochondrial division inhibitor mdivi-1, which specifically blocks Drp1 self assembly and GTPase activity (8). These studies revealed that mdivi-1 significantly inhibits VacA-dependent mitochondrial fragmentation in AZ-521 cells (Fig. 2.20 A, B), as well as in AGS cells (Fig. 2.21). Mitochondrial fragmentation was also significantly inhibited by mdivi-1 in AZ-521 cells infected with *Hp* 60190 (Fig. 2.22). Together, these data indicate that *Hp*- and VacA-dependent mitochondrial fragmentation requires Drp1 GTPase activity, thereby implicating the involvement of the cellular mitochondrial fission machinery.

2.3.6 Drp1-mitochondrial localization is important for VacA-dependent mitochondrial fragmentation.

Further validation of Drp1 involvement came from studies using AZ-521 cells over-expressing either Drp1 fused to enhanced green fluorescence protein, EGFP-Drp1 or a dominant-negative form of Drp1, EGFP-DN-Drp1 (K38A), which inhibits Drp1 association with the mitochondrial outer membrane (30). VacA-intoxicated cells over-expressing EGFP-DN-Drp1 (K38A) demonstrated significantly reduced mitochondrial fragmentation than those over-expressing EGFP-Drp1 (Fig. 2.23 A, B). These results further support the functional importance of the cellular fission machinery for VacA-mediated mitochondrial fragmentation.

2.3.7 Drp1-dependent mitochondrial fission precedes and is important for VacA-induced Bax activation.

To evaluate whether VacA-mediated mitochondrial fragmentation may be linked to cell death, we first investigated whether Drp1-dependent mitochondrial fission is required for activation of the pro-apoptotic Bcl-2 effector, Bax, as reported within VacA intoxicated cells (61). Notably, several studies have reported significant cross-talk between Drp1- and Bax-mediated cellular processes (32, 54). Within this study, we observed a significant decrease in Bax activation in AZ-521 cells incubated with VacA in the presence of the Drp1 inhibitor mdivi-1 (Fig. 2.24). The overall cellular levels of Bax were unaltered in cells that had been incubated with mdivi-1 and/or VacA (Fig. 2.25). Consistent with the results obtained using mdivi-1, VacA-dependent Bax activation was also inhibited in AZ-521 cells over-expressing EGFP-DN-Drp1 (K38A) (Fig. 2.26). Although mitochondrial fragmentation was clearly visible by 60 min in AZ-521 cells incubated with VacA, (Fig. 2.16), a significant increase in the fraction of cells with activated Bax was not detected until 2 h, and the fraction of cells with activated Bax continued to increase through 8 h (Fig. 2.27). Together, these results suggest that within VacA intoxicated cells, Drp1-mediated mitochondrial fission precedes and is important for Bax activation.

2.3.8 Bax is not essential for Drp1-dependent mitochondrial fission in VacA-intoxicated cells.

Studies to evaluate the essentiality of cellular Bax for mitochondrial network fragmentation revealed clearly visible fragmentation in both *bax*$^{+/+}$ and *bax*$^{-/-}$ mouse embryonic fibroblasts (MEFs) that had been incubated with VacA (Fig. 2.28). These results suggest that Bax is not required for Drp1-dependent mitochondrial fission within VacA-intoxicated cells.

2.3.9 Drp1-dependent fission is important for VacA-induced MOMP.

Within VacA-intoxicated cells, Bax activation is associated with MOMP, as manifested by release of mitochondrial cytochrome *c* (Cyt *c*) into the cytosol (61). Studies to evaluate the relationship between MOMP and Drp1-dependent mitochondrial fission revealed that the fraction of AZ-521 cells with Cyt *c* released from mitochondria into the cytosol had not increased after 1 h incubation with VacA (Fig. 2.29), although mitochondrial fragmentation was evident at this same time point (Fig. 2.16). However, there was a significant increase in the fraction of cells with Cyt *c* released from mitochondria into the cytosol by 2 h, and the fraction continued to increase through 8 h (Fig. 2.29), similar to the kinetics of Bax activation (Fig. 2.27), indicating that VacA-mediated mitochondrial fragmentation precedes MOMP. Cyt *c* release was significantly inhibited in the presence of the Drp1 inhibitor mdivi-1 (Fig. 2.30 A, B). In addition, Cyt *c* release in response to VacA was visibly reduced in cells over-expressing

EGFP-DN-Drp1 (K38A) (Fig. 2.31). These results suggest that enhanced mitochondrial fission promotes MOMP within VacA intoxicated cells.

2.3.10 VacA-mediated Drp1 activation is important for toxin-dependent cell death.

VacA-dependent MOMP precedes and is necessary for cell death (56, 61). Studies to evaluate the importance of Drp1 revealed that cell death was significantly reduced in AZ-521 (Fig. 2.32) or AGS cells (Fig. 2.33) that were incubated with VacA in the presence of mdivi-1. These results indicate that Drp1-dependent fission is important for VacA-induced cell death, and suggest that the disruption of cellular mitochondrial dynamics plays an important role in activation of cell death mechanism following *Hp* infection.

2.3.11 VacA anion channel activity is important for mitochondrial fragmentation.

Anion-selective, membrane channels formed by VacA were earlier reported to be important for toxin-dependent MOMP and cell death (56). Studies to evaluate whether VacA channel activity is also required for toxin-dependent disruption of mitochondrial dynamics revealed the absence of detectable mitochondrial fragmentation in cells exposed to two mutant forms of toxin (Fig. 2.34 A, B), VacA (P9A) or VacA (G14A) (62), each of which had been previously shown to be attenuated in membrane channel-forming activity (38). Additionally, ectopic expression of the amino-terminal p34 domain of VacA, which contains

the residues required for VacA channel activity (38), directly within the cytosol of transiently transfected AZ-521 cells, resulted in morphological changes, including apparent fragmentation in the cellular mitochondrial network (Fig. 2.35). Finally, we confirmed that there was significantly less Bax activation (Fig. 2.36) and cell death (Fig. 2.37) in AZ-521 monolayers exposed to VacA (P9A) or VacA (G14A) than cells exposed to wild-type toxin. These data indicate that VacA membrane channel activity is important for the activation of Drp1-dependent mitochondrial fission within intoxicated cells.

2.4 DISCUSSION

Mitochondrial health is closely linked to cell viability, as these organelles produce the energy required for cellular function while at the same time functioning as regulators of programmed cell death (63). Accordingly, mitochondrial dysfunction has been increasingly linked to several human pathologies, including those associated with cancer (26), inflammatory disorders (5), and degenerative diseases (65).

Here, we demonstrated that *Hp* infection of gastric epithelial cells disrupts the morphological dynamics of mitochondria by a mechanism dependent on the mitochondrial acting exotoxin, VacA. While mitochondrial fragmentation has been previously observed in cells infected with *Hp* (2) or intoxicated with VacA (41), our studies revealed that Drp1-mediated mitochondrial fission precedes and is important for induction of VacA-dependent cell death. For *Hp*, an increase in cell death within the gastric mucosa may alter the host niche in several ways,

including the loss of specialized cells, such as gastric parietal cells, but also increased cellular proliferation, and gastric atrophy that precedes metaplasia, dysplasia, and ultimately cancer (36, 58, 64).

A causal link between Drp1 and the cellular apoptotic machinery has been reported within diverse organisms such as yeast (18) and Drosophila (24). In contrast, down-regulation of Drp1 expression within HeLa or COS-7 cells did not prevent Bax-dependent apoptosis induced by ultraviolet radiation or actinomycin D (42). In addition, a recent report indicated that cell death does not result from the perturbation of mitochondrial dynamics in cells infected with *Listeria monocytogenes* (47), indicating that cell death is not an obligate outcome of disrupting mitochondrial dynamics. Thus, potential roles for Drp1 in mitochondrial-dependent cell death may ultimately be dictated by factors such as cell/tissue type, or the nature of the pro-death stimulus.

Our results indicate that Drp1-mitochondrial localization and GTPase activity is required for activation of Bax in VacA-intoxicated cells (Fig. 2.24). Recent studies have demonstrated that functional crosstalk between Drp1 and Bax exists in some cases (3). One study identified Drp1 as the factor within rat brain extracts that stimulates Bax activity and mitochondrial Cyt *c* release, but in a manner that is independent of its GTPase activity (39), suggesting fundamental differences with Drp1-dependent Bax activation in VacA-intoxicated cells, which requires Drp1 GTPase activity (Fig. 2.24). On the other hand, Bax was reported to co-localize with Drp1 at mitochondrial scission sites (32), and promote sumoylation of Drp1, which is required for stable association of Drp1 with

mitochondria (54). Furthermore, Bax was reported to influence redistribution of Drp1 to mitochondria through release of the mitochondrial effector DDP/TIMM8a (1). Our data indicate that Bax is not required for Drp1-mediated fission, suggesting that within VacA-intoxicated cells, crosstalk between Drp1 and Bax may be uni-directional (e.g. Drp1-dependent fission as a trigger for Bax-mediated MOMP). Currently, we are investigating the mechanism by which Drp1-dependent fission results in Bax activation and MOMP within VacA-intoxicated cells.

The mechanism by which VacA induces Drp1-dependent mitochondrial fission is not clear. Our data indicate that VacA channel activity is required for toxin-dependent mitochondrial fragmentation (Fig. 2.34 A, B), but the cellular site at which toxin channel activity is required for fragmentation has not been identified. Because ectopic expression of p34-EGFP directly within the cytosol of AZ-521 cells alters mitochondrial morphology (Fig. 2.35), it is unlikely that VacA membrane channels formed on the surface of mammalian cells (49) are required for toxin-mediated activation of Drp1-dependent mitochondrial fission. Alternatively, VacA might act directly at mitochondria, as several previous studies reported that a portion of VacA taken up from the cell surface localizes to this organelle (7, 41, 56). Preliminary studies to address a possible relationship between the location of intracellular VacA and the perturbation of mitochondrial dynamics revealed that VacA localization to mitochondria (Fig. 2.38) is evident within AZ-521 cells at 30 min, prior to the earliest time (60 min) that visible mitochondrial fragmentation was detected after exposure to toxin (Fig. 2.16).

While these data are consistent with the idea that VacA may act directly at mitochondria to induce Drp1-mediated fission, we cannot currently rule out the possibility that VacA-mediated mitochondrial fragmentation is triggered independently of toxin localization to mitochondria. In support of this latter possibility, a recent study reported that localization of VacA to mitochondria is delayed within MEFs lacking both Bax and the related effector Bcl-2 homologous antagonist/killer (Bak) (7), although our data clearly indicate that Bax is not required for VacA-induced Drp1-mediated mitochondrial fission (Fig. 2.28).

Preliminary studies to address the relationship between mitochondrial dysfunction and fission within VacA intoxicated cells revealed that Drp1 activity is not required for VacA-mediated dissipation of mitochondrial transmembrane potential ($\Delta\Psi_m$) (Fig. 2.39), suggesting that fission in VacA intoxicated cells is not likely the trigger for mitochondrial dysfunction. However, it remains possible that VacA-induced $\Delta\Psi_m$ dissipation induces Drp1-dependent fission. Support for this idea comes from unrelated studies which demonstrated that mitochondrial depolarization in HeLa cells induced a sustained cytosolic calcium rise, followed by calcineurin mediated dephosphorylation of Drp1 at Ser637 as a mechanism to drive Drp1 translocation to mitochondria (9). VacA is sufficient to induce $\Delta\Psi_m$ dissipation (61) and increases in cytosolic calcium (16), but a potential link between elevated cellular calcium or calcineurin action and Drp1-dependent mitochondrial fission within VacA-intoxicated cells remains to be evaluated.

In summary, these results demonstrate that apoptosis of gastric epithelial cells during *Hp* infection is triggered by VacA-induced disruption of mitochondrial morphological dynamics through Drp1-mediated fission, which both precedes and is required for Bax-dependent remodeling of the mitochondrial outer membrane. Future work will be required to reveal whether other pathogens also promote host cell death by targeting the morphological dynamics of mitochondria.

Figures

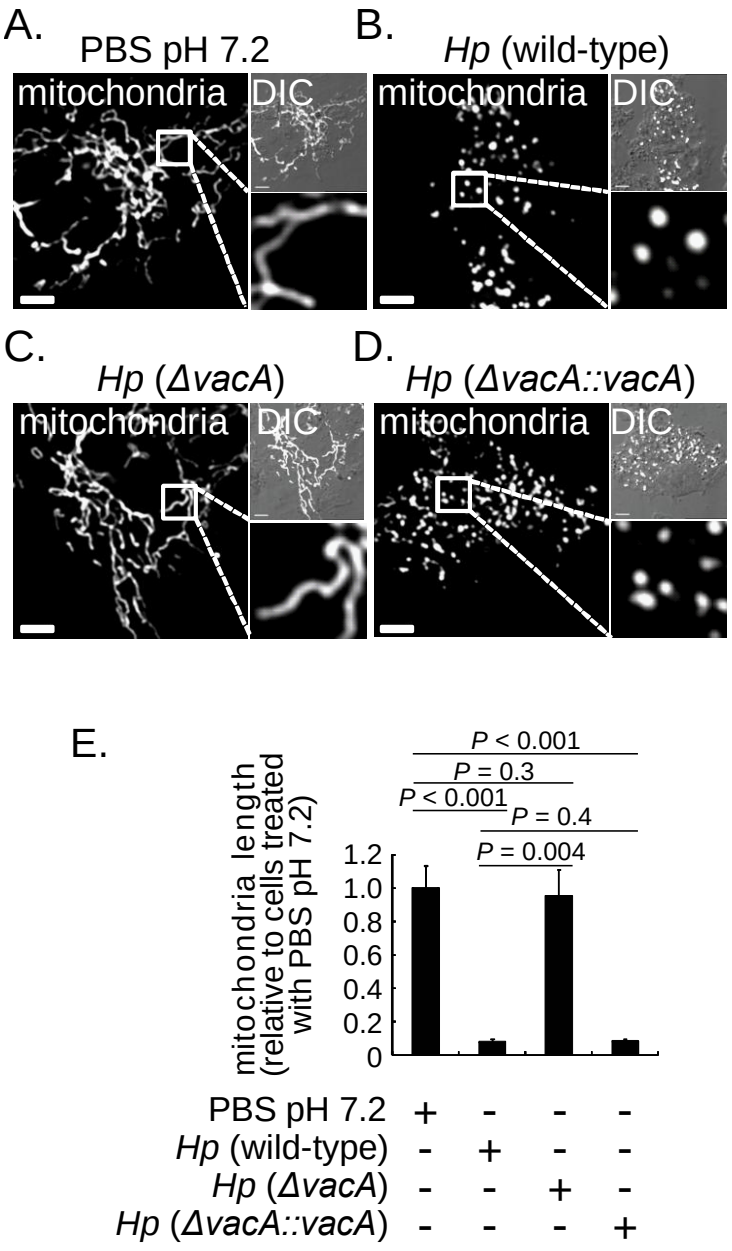

Figure 2.1 *H. pylori* induces mitochondrial fragmentation within AZ-521 cells in a VacA dependent manner.

AZ-521 cells transfected with pDsRed2-Mito were incubated at 37 °C and under 5% CO_2 for 8 h with *Hp* 60190 (B), *Hp* VM022 (*ΔvacA*) (C), *Hp* VM084 (*ΔvacA::vacA*) (D) or mock-infected with PBS pH 7.2 (A). (A-D) Scale bar = 5 µm. (E) Data from A-D were rendered as mitochondrial length relative to mock infected cells. Data were combined from 3 independent experiments where, in each, 45 randomly chosen mitochondria were analyzed (3 mitochondria in each of the 15 cells). Error bars indicate standard deviations.

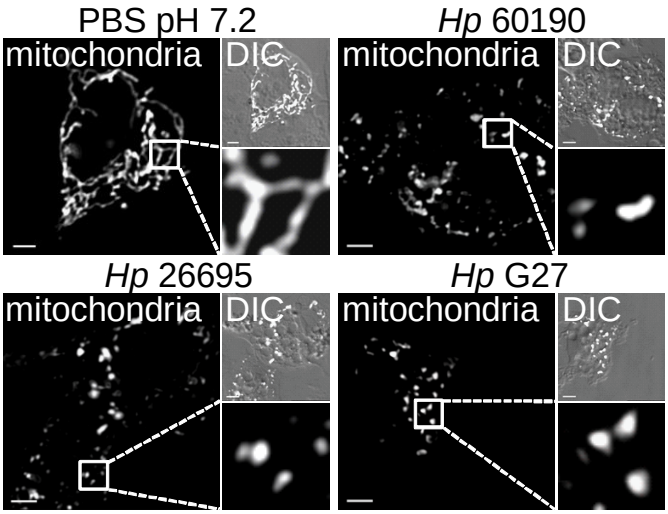

Figure 2.2 *H. pylori* induced mitochondrial fragmentation within AZ-521 cells is not idiosyncratic to a particular *Hp* strain.

AZ-521 cells transfected with pDsRed2-Mito were incubated at 37 °C and under 5% CO_2 for 8 h with *Hp* 60190, *Hp* 26695 and *Hp* G27, each at MOI 100 or mock-infected with PBS pH 7.2. The cells were evaluated for mitochondrial fragmentation by DIC-epifluorescence microscopy. Images reveal the morphology of fluorescently stained mitochondria and are representative of those collected from 2 independent experiments. Scale bar = 5 µm.

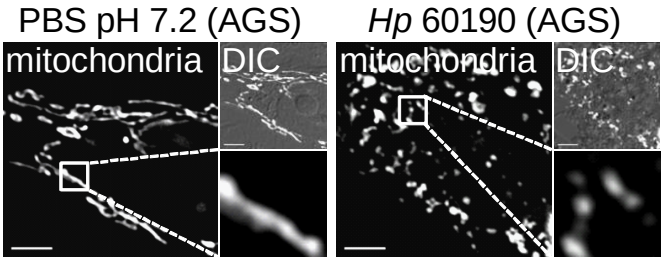

Figure 2.3 *H. pylori* induces mitochondrial fragmentation within AGS gastric epithelial cells.

AGS cells transfected with pDsRed2-Mito were incubated at 37 °C and under 5% CO_2 for 8 h with *Hp* 60190 (MOI 100) or mock-infected with PBS pH 7.2. The cells were evaluated for mitochondrial fragmentation by DIC-epifluorescence microscopy. Images reveal the morphology of fluorescently stained mitochondria and are representative of those collected from 3 independent experiments. Scale bar = 5 µm.

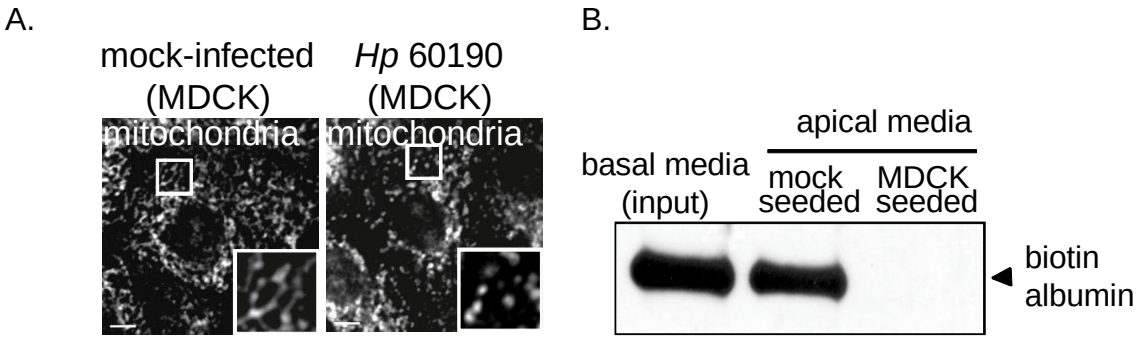

Figure 2.4 *H. pylori* induces mitochondrial fragmentation within polarized MDCK cells.

(A) Polarized MDCK cells were incubated at 37 °C and under 5% CO_2 for 8 h with *Hp* 60190 (MOI 100) or mock-infected with PBS pH 7.2. The cells were fixed, permeabilized and immunostained with Tom-20 as a mitochondrial marker. The cells were evaluated for mitochondrial fragmentation by DIC-epifluorescence microscopy. Images reveal the morphology of fluorescently stained mitochondria and are representative of those collected from 2 independent experiments. Scale bar = 5 µm.

(B) The integrity of the polarized MDCK monolayer was evaluated by monitoring the passage of biotin-BSA (50 µg/mL) from the transwell basal chamber through either the MDCK monolayer or mock-seeded transwell inserts (in the absence of cells) into the apical chamber. The presence of biotin-BSA within the apical or basal chamber was assessed by Western blot analysis, using the streptavidin-HRP conjugate, and chemiluminescence signal development. The Western blot data are representative of those collected from two independent experiments, each with two independent MDCK monolayers.

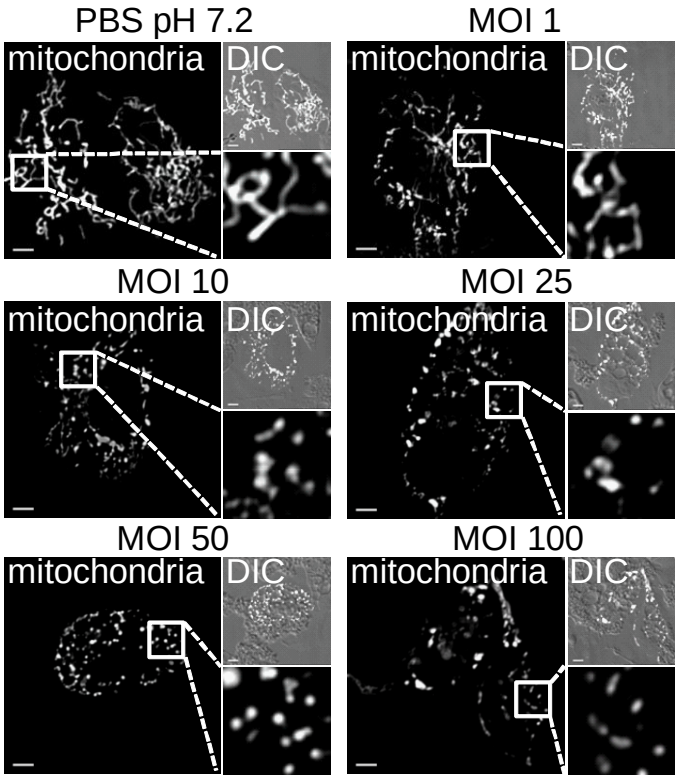

Figure 2.5 *H. pylori* induces mitochondrial fragmentation within AZ-521 cells in an MOI dependent manner.

AZ-521 cells transfected with pDsRed2-Mito were incubated at 37 °C and under 5% CO_2 for 8 h with *Hp* 60190 at the indicated MOI or mock-infected with PBS pH 7.2. The cells were evaluated for mitochondrial fragmentation by DIC-epifluorescence microscopy. Images reveal the morphology of fluorescently stained mitochondria and are representative of those collected from 3 independent experiments. Scale bar = 5 µm.

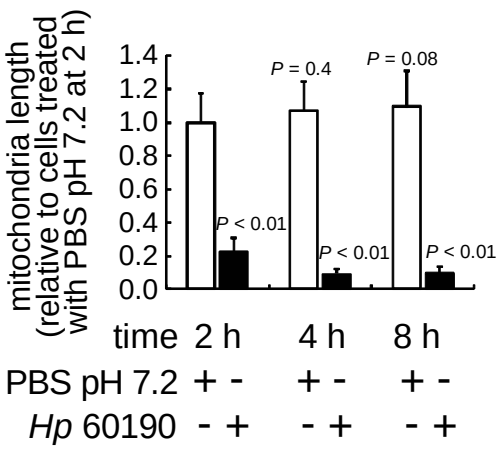

Figure 2.6 *H. pylori* induces mitochondrial fragmentation within AZ-521 cells in a time dependent manner.

AZ-521 cells transfected with pDsRed2-Mito were incubated at 37 °C and under 5% CO_2 for indicated time periods with *Hp* 60190 at MOI 100 or mock-infected with PBS pH 7.2. The cells were evaluated for mitochondrial fragmentation by DIC-epifluorescence microscopy. Mitochondrial lengths were measured using Imaris 5.7 (Bitplane) software. Data are representative of those collected from 3 independent experiments where, in each, 45 randomly chosen mitochondria were analyzed (3 mitochondria in each of the 15 cells). Error bars indicate standard deviations. Statistical difference was calculated for differences in mitochondrial lengths between *Hp* infected cells or cells treated with PBS pH 7.2 at the indicated time periods and cells treated with PBS pH 7.2 for 2 h.

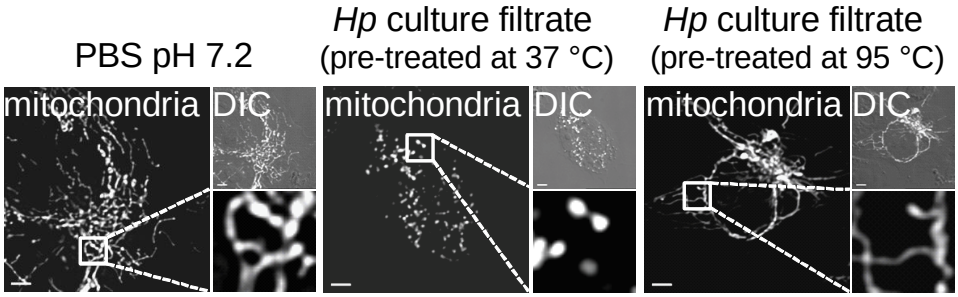

Figure 2.7 A proteinaceous factor within *Hp* culture filtrate is responsible for mitochondrial fragmentation within AZ-521 cells.

AZ-521 cells transfected with pDsRed2-Mito were incubated at 37 °C and under 5% CO_2 for 8 h with *Hp* culture filtrate that had been preincubated at 37 °C or 95 °C, or mock-treated with PBS pH 7.2. The cells were evaluated for mitochondrial fragmentation by DIC-epifluorescence microscopy. Images reveal the morphology of fluorescently stained mitochondria and are representative of those collected from 3 independent experiments. Scale bar = 5 µm.

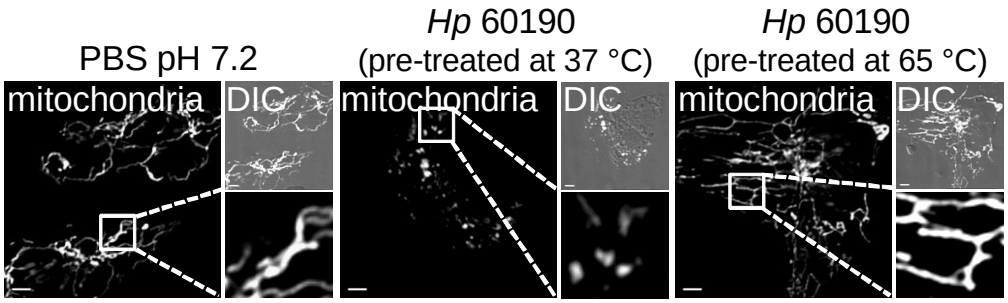

Figure 2.8 Analysis of *Hp* dependent mitochondrial fragmentation.

AZ-521 cells transfected with pDsRed2-Mito were incubated at 37 °C and under 5% CO_2 for 8 h with *Hp* 60190 at MOI 100 that had been preincubated at 37 °C or 65 °C, or mock-treated with PBS pH 7.2. The cells were evaluated for mitochondrial fragmentation by DIC-epifluorescence microscopy. Images reveal the morphology of fluorescently stained mitochondria and are representative of those collected from 3 independent experiments. Scale bar = 5 µm.

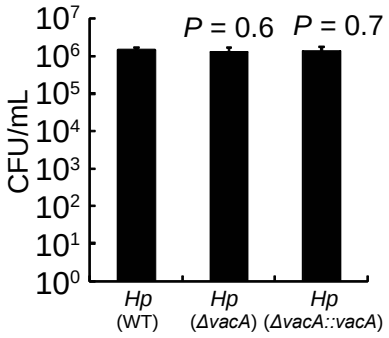

Figure 2.9 Analysis of the association of *vacA*$^+$ and *vacA*$^-$ *Hp* strains with AZ-521 cells.

AZ-521 cells were incubated at 37 °C and under 5% CO_2 with *Hp* 60190, *Hp* VM022 (*ΔvacA*), *Hp* VM084 (*ΔvacA::vacA*) (all at MOI 100), or mock-infected with PBS pH 7.2. After 1 h, the monolayers were washed 2 times with PBS pH 7.2, lysed, and *Hp* associated with AZ-521 cells in each treatment was quantified by dilution plating and direct CFU counting. Data are rendered as the average CFU/mL obtained from combining data collected from two independent experiments, each conducted in triplicate. Error bars indicate standard deviations. Statistical significance was calculated for differences in CFU/mL between *Hp* 60190 (WT) and *Hp* VM022 (*ΔvacA*) or *Hp* VM084 (*ΔvacA::vacA*).

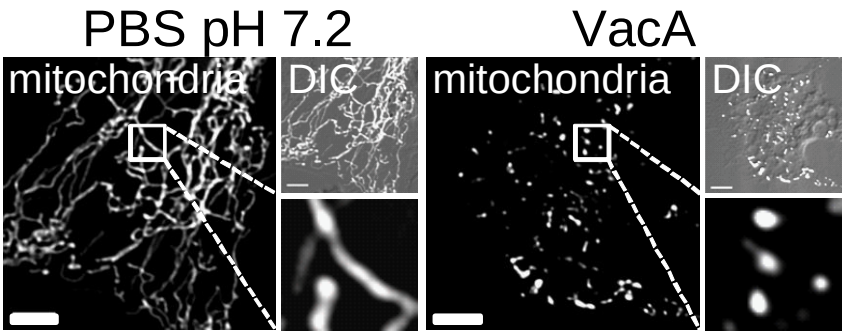

Figure 2.10 VacA induces mitochondrial fragmentation within AZ-521 gastric epithelial cells.

AZ-521 cells transfected with pDsRed2-Mito were incubated at 37 °C and under 5% CO_2 for 4 h with purified VacA (250 nM) or mock-treated with PBS pH 7.2. The cells were evaluated for mitochondrial fragmentation by DIC-epifluorescence microscopy. Images reveal the morphology of fluorescently stained mitochondria and are representative of those collected from 3 independent experiments. Scale bar = 5 µm.

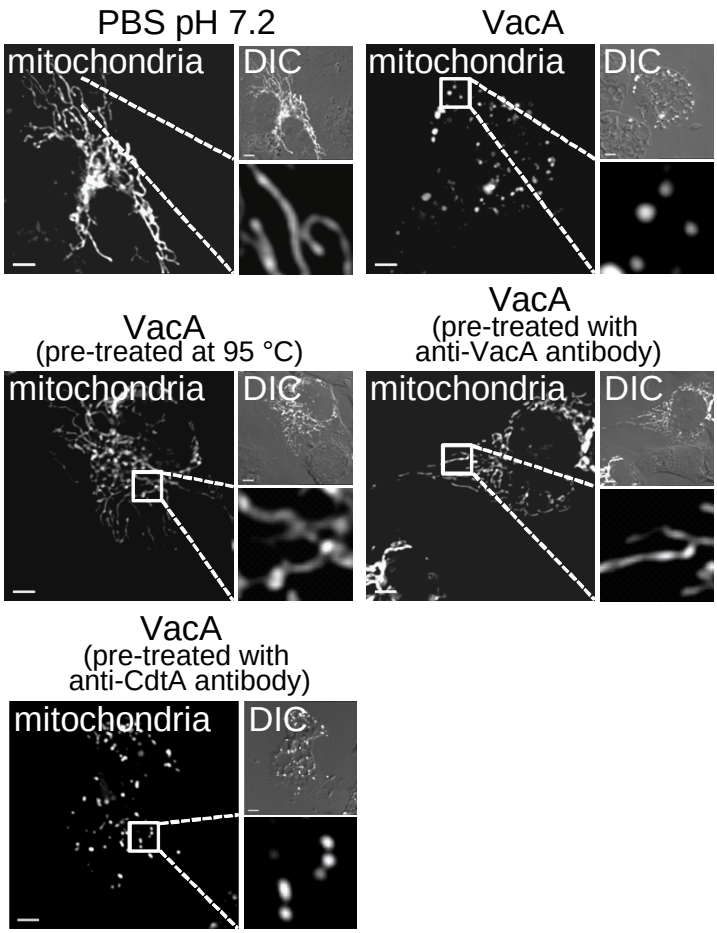

Figure 2.11 VacA is important for the induction of mitochondrial fragmentation within AZ-521 cells.

AZ-521 cells transfected with pDsRed2-Mito were incubated at 37 °C and under 5% CO_2 for 4 h with VacA (250 nM) that had been preincubated at 37 °C or 95 °C, or, for 30 min on ice with VacA antiserum (2 mg/mL) or a non-specific *H. ducreyi* CdtA antiserum (2 mg/mL). Additionally, the cells were mock-treated with PBS pH 7.2. The cells were evaluated for mitochondrial fragmentation by DIC-epifluorescence microscopy. Images reveal the morphology of fluorescently stained mitochondria and are representative of those collected from 3 independent experiments. Scale bar = 5 µm.

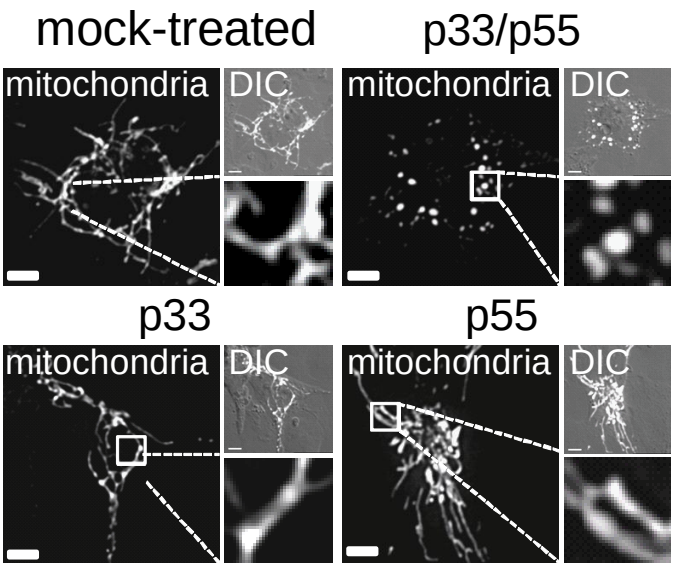

Figure 2.12 VacA is sufficient for the induction of mitochondrial fragmentation within AZ-521 cells.

AZ-521 cells transfected with pDsRed2-Mito were incubated at 37 °C and under 5% CO_2 for 4 h with recombinant p33, p55 or p33 plus p55 (each at 250 nM). Additionally, the cells were mock-treated with 25 mM HEPES pH 8.8 containing 5% glycerol and 0.1 nM β-ME. The cells were evaluated for mitochondrial fragmentation by DIC-epifluorescence microscopy. Images reveal the morphology of fluorescently stained mitochondria and are representative of those collected from 2 independent experiments. Scale bar = 5 µm.

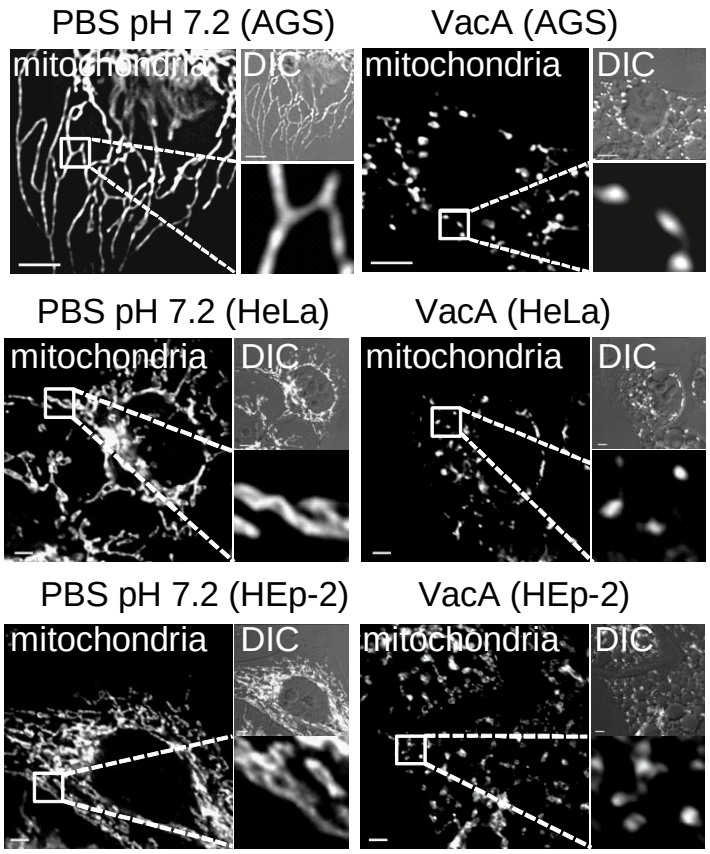

Figure 2.13 VacA induces mitochondrial fission in AGS, HeLa and HEp-2 cells.

AGS cells that had been previously transfected with pDsRed2-Mito, or HeLa and HEp-2 cells, were incubated at 37 °C and under 5% CO_2 with VacA (250 nM for AGS cells; 500 nM for HeLa and HEp-2 cells). Additionally, the cells were mock intoxicated with PBS pH 7.2. After 4 h (AGS), or 8 h (HeLa and HEp-2) the cells were fixed (AGS) or, fixed, permeabilized, and immunostained for Tom-20 as a mitochondrial marker (HeLa and HEp-2), and cellular mitochondria were visualized by DIC-epifluorescence microscopy. The images reveal the morphology of fluorescently stained mitochondria, and are representative of those collected from three independent experiments. Scale bar = 5 μm.

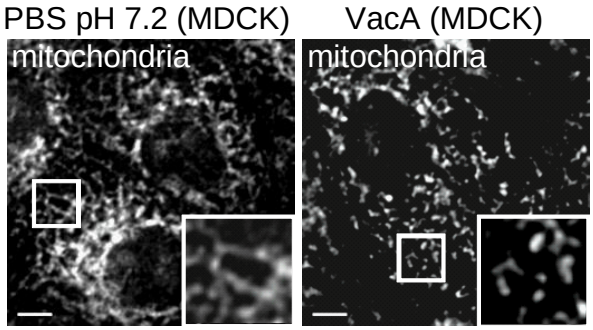

Figure 2.14 VacA induces mitochondrial fission in polarized MDCK cells.

Polarized MDCK cells were incubated at 37 °C and under 5% CO_2 with VacA (500 nM). Additionally, the cells were mock intoxicated with PBS pH 7.2. After 4 h the cells were fixed, permeabilized, and immunostained for Tom-20 as a mitochondrial marker and cellular mitochondria were visualized by DIC-epifluorescence microscopy. The images reveal the morphology of fluorescently stained mitochondria, and are representative of those collected from two independent experiments. Scale bar = 5 μm.

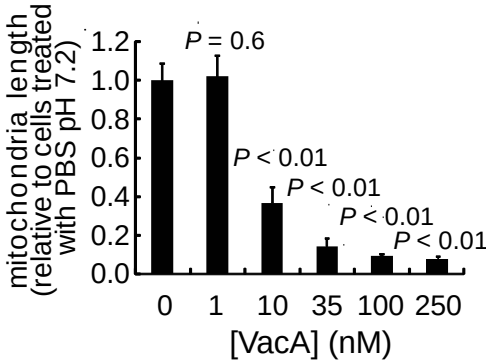

Figure 2.15 VacA induces mitochondrial fragmentation within AZ-521 gastric cells in a toxin dose dependent manner.

AZ-521 cells transfected with pDsRed2-Mito were incubated at 37 °C and under 5% CO_2 for 4 h with purified VacA at the indicated concentrations or mock-treated with PBS pH 7.2. The cells were evaluated for mitochondrial fragmentation by DIC-epifluorescence microscopy. Mitochondrial lengths were measured using Imaris 5.7 (Bitplane) software. The data are rendered as the average mitochondrial length obtained by combining data from three independent experiments where, in each, 45 randomly chosen mitochondria were analyzed (3 mitochondria in each of the 15 cells). Statistical significance was calculated for differences in mitochondrial lengths between cells incubated with VacA at the indicated concentrations and cells that were mock intoxicated with PBS pH 7.2.

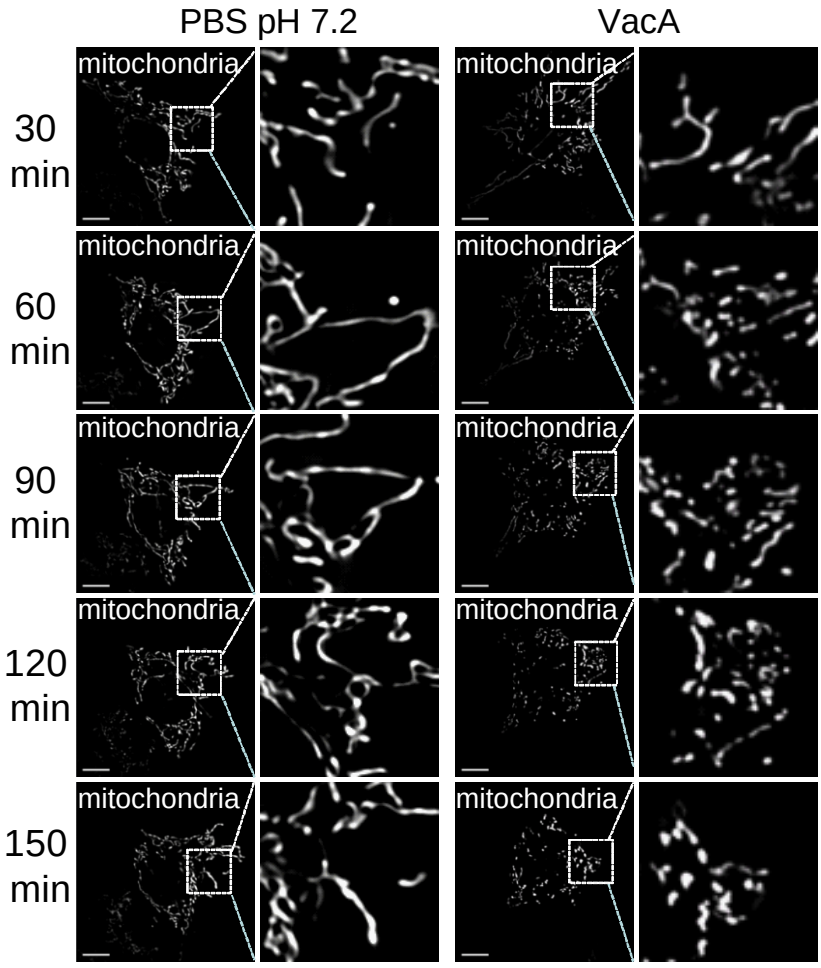

Figure 2.16 VacA induces mitochondrial fragmentation within 1 h of intoxication in AZ-521 cells.

AZ-521 cells transfected with pDsRed2-Mito were incubated at 37 °C and under 5% CO_2 with purified VacA (250 nM) or mock-treated with PBS pH 7.2. Mitochondria within each representative cell were monitored for the indicated time periods using live cell imaging. Images reveal the morphology of fluorescently stained mitochondria and are representative of those collected from 2 independent experiments. Scale bar = 5 µm.

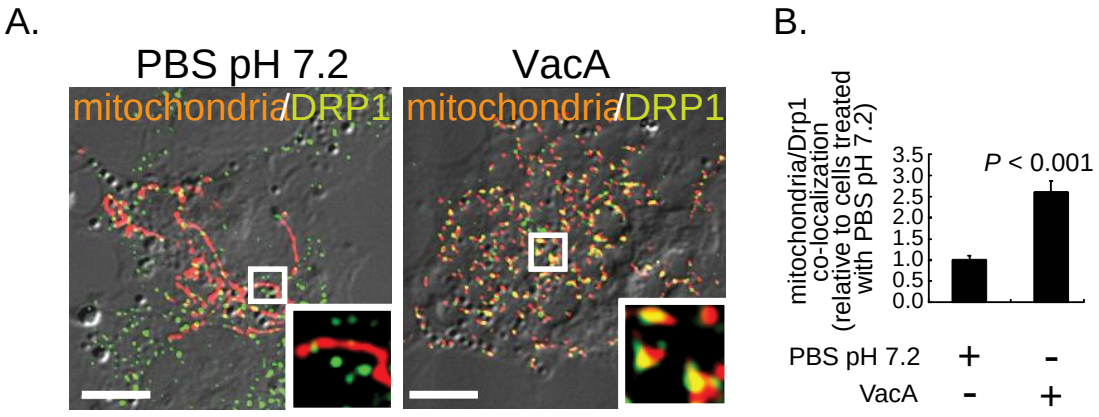

Figure 2.17 VacA induces mitochondrial targeting of the cellular fission protein Drp1.

(A) AZ-521 cells transfected with pDsRed2-Mito were incubated at 37 °C and under 5% CO_2 for 4 h with purified VacA (250 nM) or mock-treated with PBS pH 7.2. The cells were fixed, permeabilized and immunostained for Drp1. Colocalization of Drp1 to mitochondria was studied using DIC-epifluorescence microscopy. Images reveal the morphology of fluorescently stained mitochondria (in red), as well as cellular location of Drp1 (in green). Images are representative of those collected from 3 independent experiments. Scale bar = 5 µm.

(B) Mitochondrial-Drp1 co-localization index determined by combining data obtained from 3 independent experiments. Error bars indicate standard deviations. Statistical difference was calculated for differences in mitochondrial-Drp1 co-localization index between VacA treated cells or cells treated with PBS pH 7.2.

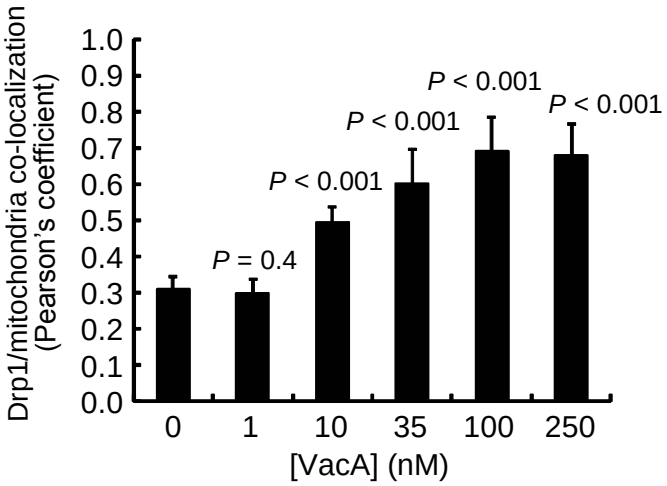

Figure 2.18 VacA induces mitochondrial targeting of the cellular fission protein Drp1 in a toxin dose dependent manner.

AZ-521 cells that had been previously transfected with pDsRed2-Mito were incubated at 37 °C and under 5% CO_2 with VacA (at the indicated concentrations), or mock-intoxicated with PBS pH 7.2. After 4 h, the cells were fixed, permeabilized, and immunostained for cellular Drp1. Localization of Drp1 to mitochondria was determined using DIC-epifluorescence microscopy followed by co-localization analysis. The data are rendered as the average Drp1-mitochondrial co-localization obtained by combining data from two independent experiments. In each independent experiment, 15 randomly chosen, pDsRed2-Mito transfected cells were analyzed. Error bars indicate standard deviations. Statistical significance was calculated for differences in co-localization indices between cells incubated with VacA at the indicated concentrations and those cells mock intoxicated with PBS pH 7.2.

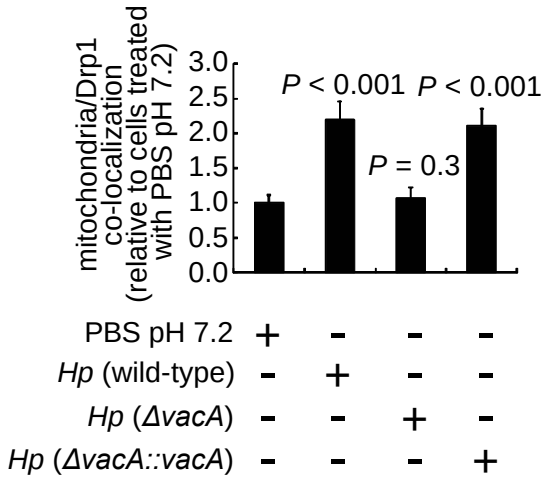

Figure 2.19 VacA is important for *Hp* induced mitochondrial targeting of the cellular fission protein Drp1 in AZ-521 cells.

AZ-521 cells that had been previously transfected with pDsRed2-Mito were incubated at 37 °C and under 5% CO_2 with *Hp* 60190, *Hp* VM022 (*⊿vacA*), *Hp* VM084 (*⊿vacA::vacA*) (all at MOI 100), or mock-infected with PBS pH 7.2. After 4 h, the cells were fixed, permeabilized, and immunostained for cellular Drp1. Localization of Drp1 to mitochondria was determined using DIC-epifluorescence microscopy followed by co-localization analysis. The data are rendered as the average Drp1-mitochondrial co-localization obtained by combining data from three independent experiments. In each independent experiment, 15 randomly chosen, pDsRed2-Mito transfected cells were analyzed. Error bars indicate standard deviations. Statistical significance was calculated for differences in co-localization indices between cells infected with *Hp* and cells mock infected with PBS pH 7.2.

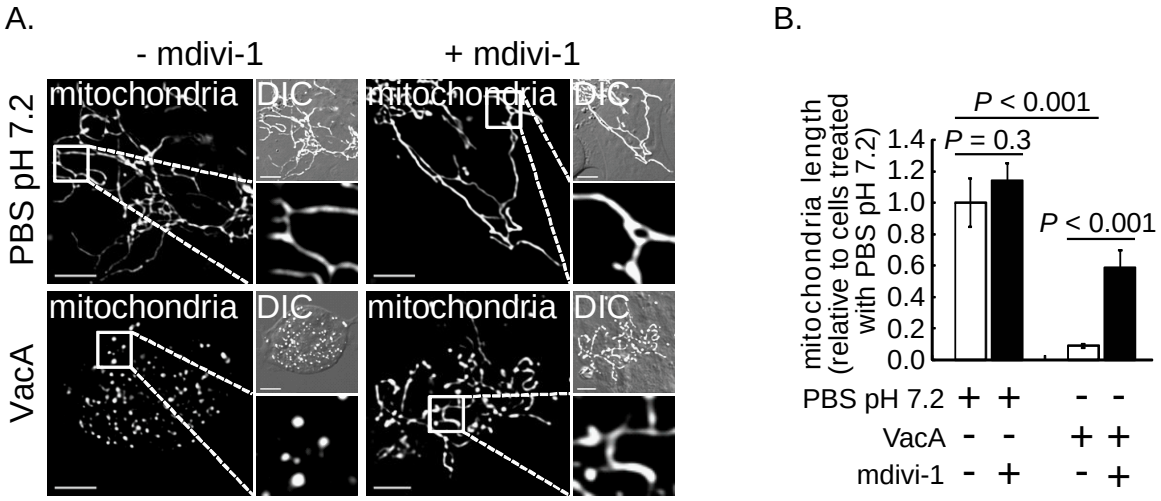

Figure 2.20 Drp1 is important for VacA induced mitochondrial fragmentation in AZ-521 cells.

(A) AZ-521 cells previously transfected with pDsRed2-Mito were incubated at 37 °C and under 5% CO_2 with VacA (250 nM) or mock-treated with PBS pH 7.2, both in the absence or presence of the small molecule Drp1 inhibitor mdivi-1 (50 μM). After 4 h the cells were fixed and cellular mitochondria were visualized by DIC-epifluorescence microscopy. The images reveal the morphology of fluorescently stained mitochondria and are representative of those collected from three independent experiments. Scale bar = 5 μm.

(B) Mitochondrial lengths were measured using Imaris 5.7 (Bitplane) software. The data are rendered as the average mitochondrial length obtained by combining data from three independent experiments where, in each, 45 randomly chosen mitochondria were analyzed (3 mitochondria in each of the 15 cells). Error bars indicate standard deviations.

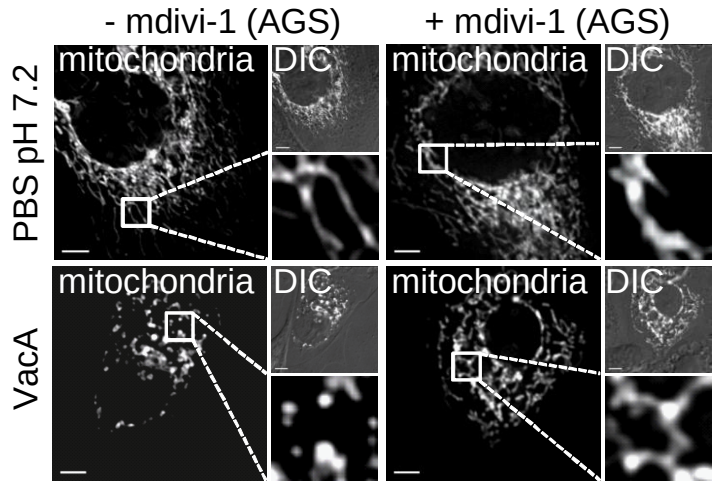

Figure 2.21 Drp1 is important for VacA induced mitochondrial fragmentation in AGS cells.

AGS cells previously transfected with pDsRed2-Mito were incubated at 37 °C and under 5% CO_2 with VacA (250 nM) or mock-treated with PBS pH 7.2, both in the absence or presence of the small molecule Drp1 inhibitor mdivi-1 (50 μM). After 4 h the cells were fixed and cellular mitochondria were visualized by DIC-epifluorescence microscopy. The images reveal the morphology of fluorescently stained mitochondria and are representative of those collected from three independent experiments. Scale bar = 5 μm.

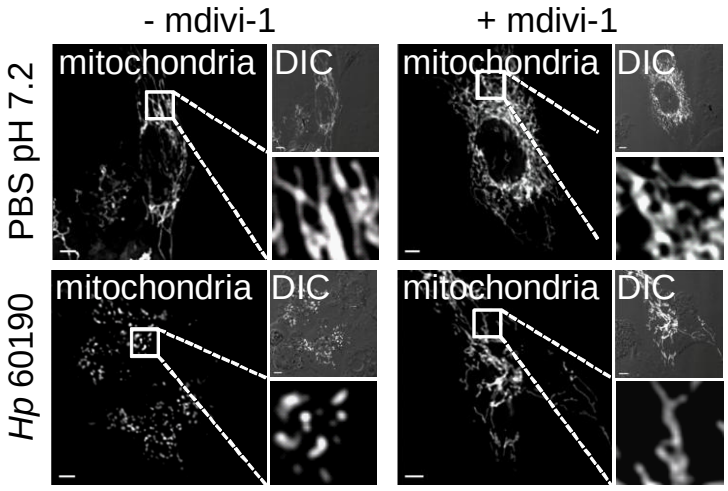

Figure 2.22 Drp1 is important for *Hp* induced mitochondrial fragmentation in AZ-521 cells.

AZ-521 cells previously transfected with pDsRed2-Mito were incubated at 37 °C and under 5% CO_2 with *Hp* 60190 (MOI 100) or mock-treated with PBS pH 7.2, both in the absence or presence of the small molecule Drp1 inhibitor mdivi-1 (50 μM). After 8 h the cells were fixed and cellular mitochondria were visualized by DIC-epifluorescence

Figure 2.22 (cont.) microscopy. The images reveal the morphology of fluorescently stained mitochondria and are representative of those collected from three independent experiments. Scale bar = 5 μm.

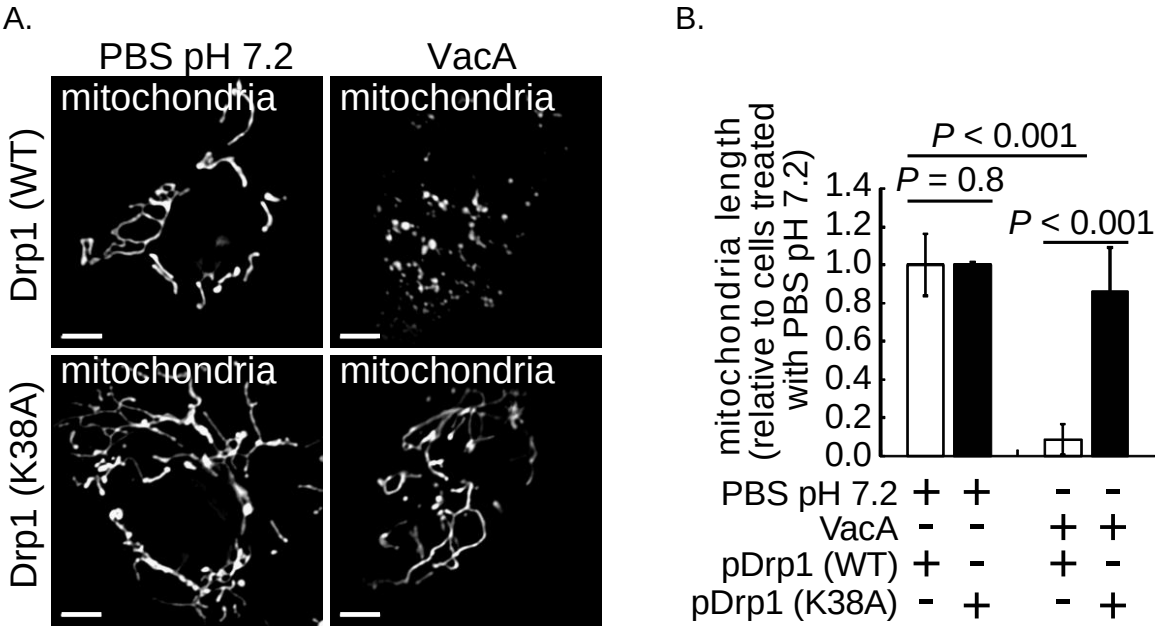

Figure 2.23 Drp1 is important for VacA induced mitochondrial fragmentation in AZ-521 cells.

(A) AZ-521 cells previously transfected with pDsRed2-Mito and co-transfected with either pEGFP-Drp1 or pEGFP-DN-Drp1 (K38A), were incubated at 37 °C and under 5% CO_2 with VacA (250 nM) or mock-treated with PBS pH 7.2. After 4 h the cells were fixed and cellular mitochondria were visualized by DIC-epifluorescence microscopy. The images reveal the morphology of fluorescently stained mitochondria and are representative of those collected from three independent experiments. Scale bar = 5 μm.

(B) Mitochondrial lengths were measured using Imaris 5.7 (Bitplane) software. The data are rendered as the average mitochondrial length obtained by combining data from three independent experiments. Error bars indicate standard deviations.

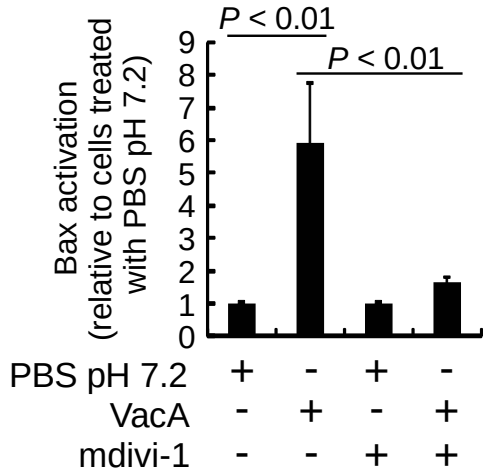

Figure 2.24 Drp1 is important for VacA induced Bax activation in AZ-521 cells.

AZ-521 cells were incubated at 37 °C and under 5% CO_2 with VacA (250 nM) or mock-treated with PBS pH 7.2, both in the absence or presence of the small molecule Drp1 inhibitor mdivi-1 (50 μM). After 18 h the cells were fixed, permeabilized and immunostained for active Bax. Cellular fluorescence, indicative of active Bax was quantified using flow cytometry. The data were combined from three independent experiments. Error bars indicate standard deviations.

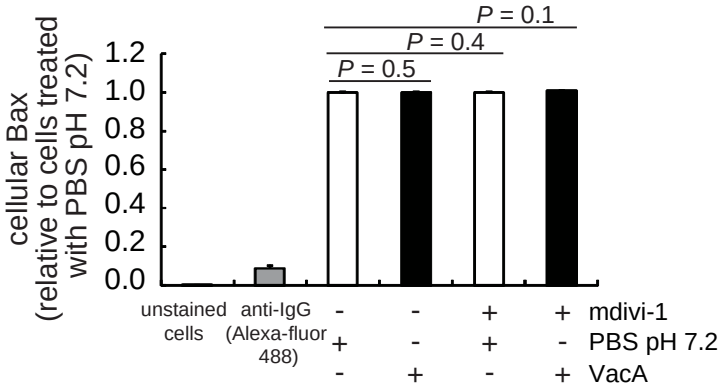

Figure 2.25 Treatment with the Drp1 inhibitor mdivi-1 does not alter endogenous Bax levels within AZ-521 cells.

AZ-521 cells were incubated at 37 °C and under 5% CO_2 with VacA (250 nM) or mock-treated with PBS pH 7.2, both in the absence or presence of the small molecule Drp1 inhibitor mdivi-1 (50 μM). After 8 h the cells were fixed, permeabilized and immunostained for endogenous Bax. Cellular fluorescence, indicative of intracellular Bax (total cellular Bax) levels was quantified using flow cytometry. The data were rendered as the fold change in total cellular Bax between cells incubated with VacA, and those mock-intoxicated with PBS pH 7.2, both in the presence or absence of mdivi-1 and were obtained by combining data from two independent experiments, each conducted in triplicate. Error bars indicate standard deviations. Statistical significance was calculated for fold differences in Bax levels between cells incubated with PBS pH 7.2 alone versus cells pre-treated with mdivi-1 or cells treated with VacA in the presence or absence of mdivi-1.

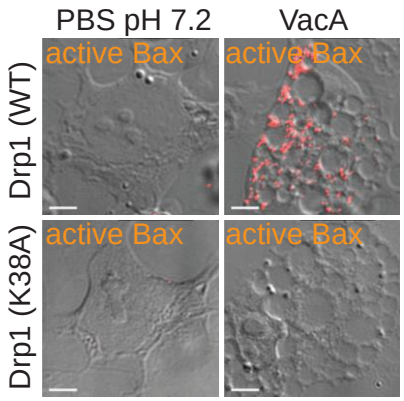

Figure 2.26 Drp1 is important for VacA induced Bax activation in AZ-521 cells.

AZ-521 cells transfected with either pEGFP-Drp1 or pEGFP-DN-Drp1 (K38A) were incubated at 37 °C and under 5% CO_2 with VacA (250 nM) or mock-treated with PBS pH 7.2. After 18 h the cells were fixed, permeabilized and immunostained for active Bax. Intracellular active Bax within each cell was visualized by DIC-epifluorescence microscopy. The images are representative of those collected from three independent experiments. Scale bar = 5 μm.

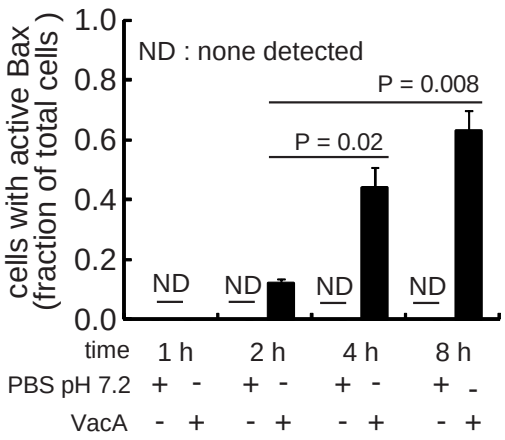

Figure 2.27 Time dependent Bax activation within AZ-521 cells following VacA intoxication.

AZ-521 cells were incubated at 37 °C and under CO_2 with VacA (250 nM) or mock-treated with PBS pH 7.2. After the indicated time periods, the cells were fixed, permeabilized and immunostained for active Bax. Intracellular active Bax within each cell was visualized by DIC-epifluorescence microscopy. Data were rendered as the fraction of entire population of cells incubated with VacA or PBS pH 7.2 that display active Bax, at the indicated time periods. Data were obtained by analyzing over 700 cells from randomly chosen fields over the course of two independent experiments. Error bars indicate standard deviations. Statistical significance was calculated for differences in the fraction of total cells that display Bax activation between cells treated with VacA and those treated with PBS pH 7.2, or between cells intoxicated with VacA for indicated time periods versus those intoxicated for 1 h.

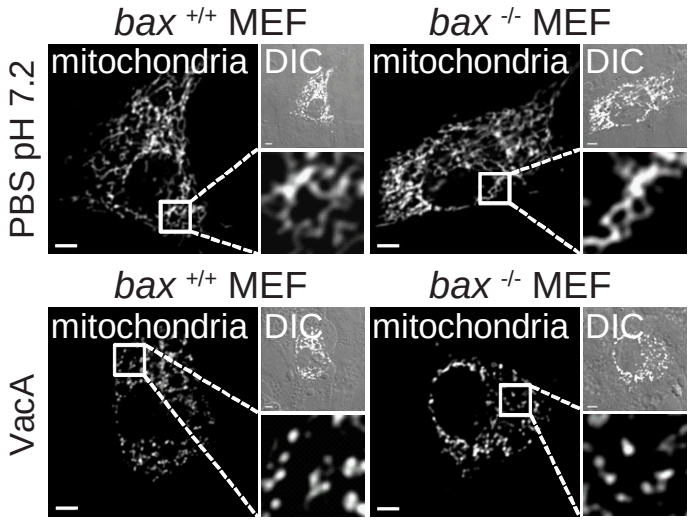

Figure 2.28 Cellular Bax is not required for VacA induced mitochondrial fission.

bax$^{+/+}$ or *bax*$^{-/-}$ MEFs cells previously transfected with pDsRed2-Mito were incubated at 37 °C and under 5% CO_2 with VacA (500 nM) or mock-treated with PBS pH 7.2. After 8 h the cells were fixed and cellular mitochondria were visualized by DIC-epifluorescence microscopy. The images reveal the morphology of fluorescently stained mitochondria and are representative of those collected from three independent experiments. Scale bar = 5 μm.

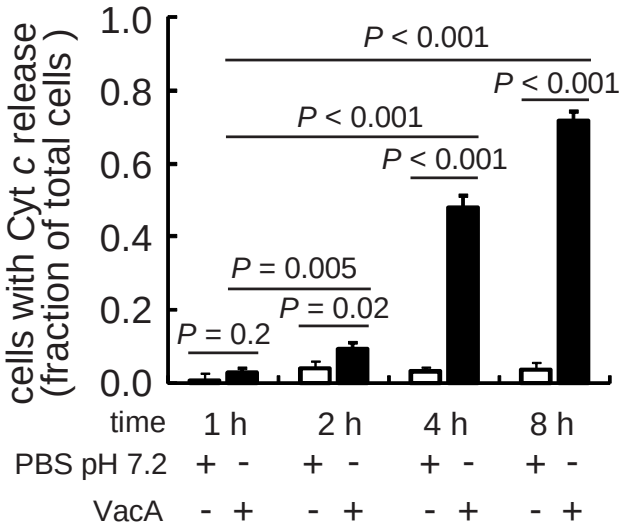

Figure 2.29 Time dependence of VacA induced Cyt *c* release from mitochondria to cytosol within AZ-521 cells.

AZ-521 cells were incubated at 37 °C and under 5% CO_2 with VacA (250 nM) or mock-treated with PBS pH 7.2. After the indicated time periods, the cells were fixed, permeabilized and immunostained for Cyt *c*. Intracellular location of Cyt *c* within each cell was visualized by DIC-epifluorescence microscopy. Data were rendered as the fraction of entire population of cells incubated with VacA or PBS pH 7.2 that display Cyt *c* release, at the indicated time periods. Data were obtained by analyzing over 1000 cells from randomly chosen fields over the course of two independent experiments. Error bars indicate standard deviations. Statistical significance was calculated for differences in the fraction of total cells that display Cyt *c* release between cells intoxicated with VacA and those treated with PBS pH 7.2, or between cells intoxicated with VacA for indicated time periods versus those intoxicated for 1 h.

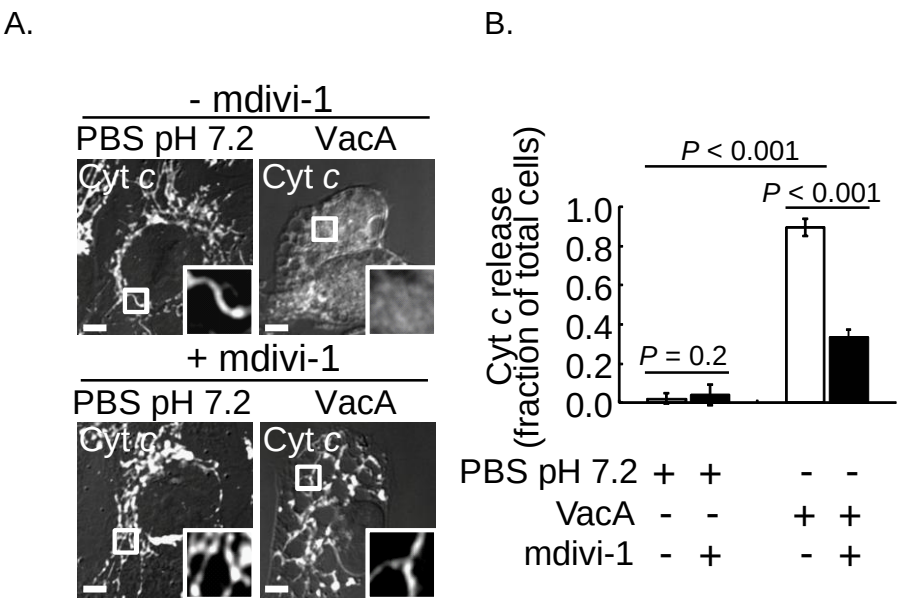

Figure 2.30 Drp1 is important for VacA induced release of Cyt *c* from the mitochondrial inter-membrane space to cytosol.

(A) AZ-521 cells were incubated at 37 °C and under 5% CO_2 with VacA (250 nM) or mock-treated with PBS pH 7.2, both in the absence or presence of the small molecule Drp1 inhibitor mdivi-1 (50 μM). After 8 h the cells were fixed, permeabilized and immunostained for Cyt *c*. Intracellular location of Cyt *c* within each cell was visualized by DIC-epifluorescence microscopy. The images are representative of those collected from three independent experiments. Scale bar = 5 μm.

(B) Data were rendered as the fraction of entire population of cells incubated with VacA or PBS pH 7.2 that display Cyt *c* release. Data were obtained by analyzing over 1000 cells from randomly chosen fields over the course of three independent experiments. Error bars indicate standard deviations.

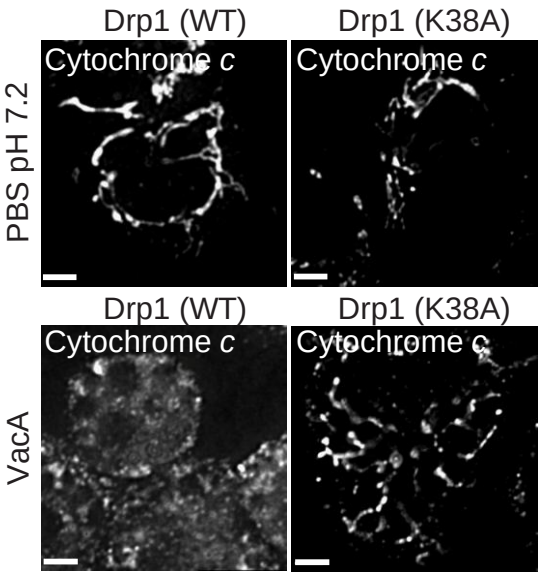

Figure 2.31 Drp1 is important for VacA induced release of Cyt *c* from the mitochondrial inter-membrane space in AZ-521 cells.

AZ-521 cells previously transfected with either pEGFP-Drp1 or pEGFP-DN-Drp1 (K38A) were incubated at 37 °C and under 5% CO_2 with VacA (250 nM) or mock-treated with PBS pH 7.2. After 8 h the cells were fixed, permeabilized and immunostained for Cyt *c*. Intracellular location of Cyt *c* within each cell was visualized by DIC-epifluorescence microscopy. The images are representative of those collected from three independent experiments. Scale bar = 5 μm.

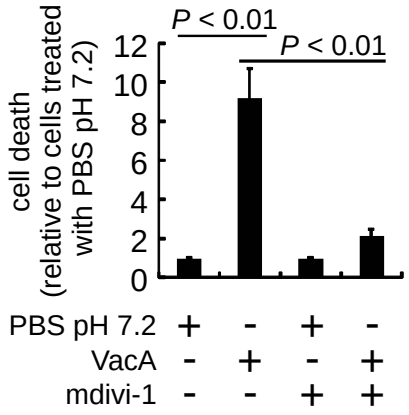

Figure 2.32 Drp1 is important for VacA induced cell death in AZ-521 cells.

AZ-521 cells were incubated at 37 °C and under 5% CO_2 with VacA (250 nM) or mock-treated with PBS pH 7.2, both in the absence or presence of the small molecule Drp1 inhibitor mdivi-1 (50 μM). After 24 h, cell viability was determined with the Live-Dead viability/cytotoxicity assay kit, using flow cytometry. The data were rendered as the fold increase in dead cells following VacA intoxication relative to cells mock-treated with PBS pH 7.2, obtained by combining data collected from three independent experiments, each conducted in triplicate. Error bars indicate standard deviations.

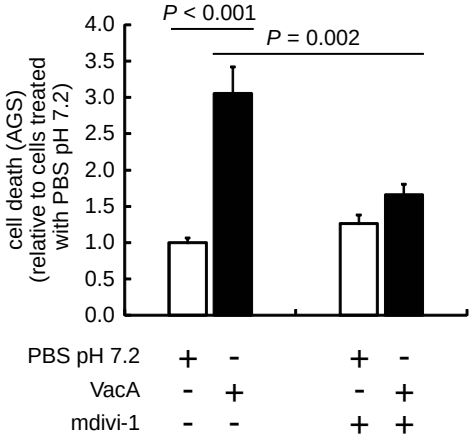

Figure 2.33 Drp1 is important for VacA induced cell death in AGS cells.

AGS cells were incubated at 37 °C and under 5% CO_2 with VacA (250 nM) or mock-treated with PBS pH 7.2, both in the absence or presence of mdivi-1 (50 μM). After 24 h, cell viability was determined with the Live-Dead viability/cytotoxicity assay kit, using flow cytometry. The data were rendered as the fold increase in dead cells following VacA intoxication relative to cells mock-treated with PBS pH 7.2, obtained by combining data collected from two independent experiments, each conducted in triplicate. Error bars indicate standard deviations. Statistical significance was calculated for fold differences in cell death between cells intoxicated with VacA versus cells treated with PBS pH 7.2 in the presence or absence of mdivi-1.

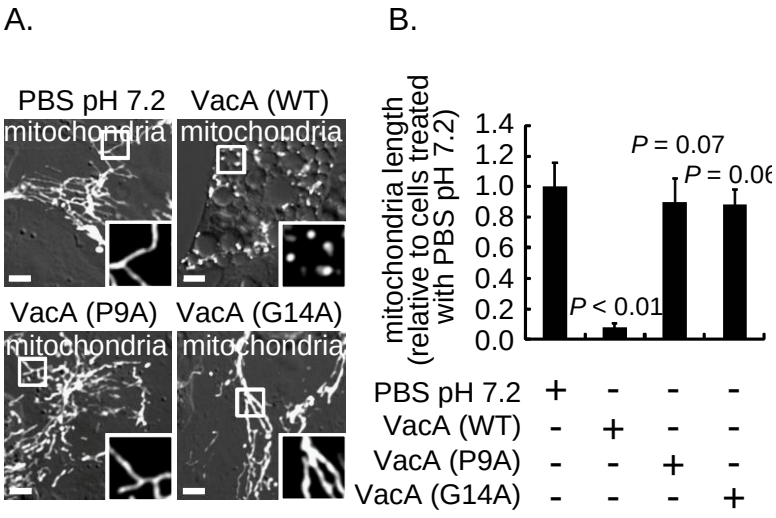

Figure 2.34 VacA anion channel function is important for mitochondrial fragmentation in AZ-521 cells.

(A) AZ-521 cells previously transfected with pDsRed2-Mito were incubated at 37 °C and under 5% CO_2 with *Hp* culture filtrates (0.05 mg/ml) containing wild-type VacA, VacA (P9A), VacA (G14A), or with PBS pH 7.2. After 4 h the cells were fixed and cellular mitochondria were visualized by DIC-epifluorescence microscopy. The images reveal the morphology of fluorescently stained mitochondria and are representative of those collected from three independent experiments. Scale bar = 5 μm.

(B) Mitochondrial lengths were measured using Imaris 5.7 (Bitplane) software. The data are rendered as the average mitochondrial length obtained by combining data from three independent experiments. Error bars indicate standard deviations. Statistical significance was calculated for fold differences in mitochondrial lengths between cells mock-intoxicated with PBS pH 7.2 versus cells that were incubated with VacA (WT), VacA (P9A) or VacA (G14A).

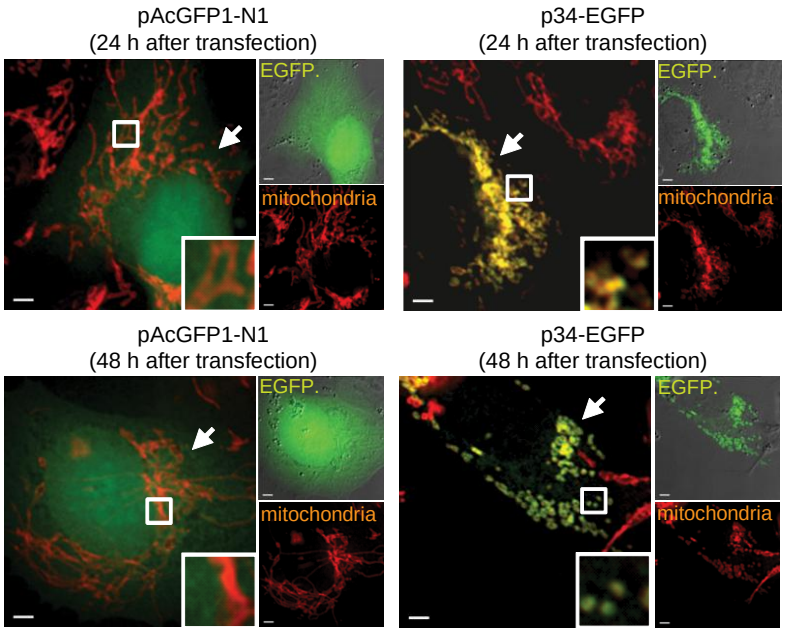

Figure 2.35 The p34 domain of VacA is sufficient to induce mitochondrial fragmentation in AZ-521 cells.

AZ-521 cells were transfected with plasmids encoding p34-EGFP (residues 1-319) or EGFP. After 24 h or 48 h the cells were fixed, permeabilized, and immunostained for Tom-20 as a mitochondrial marker, followed by visualization of cellular mitochondria, as well as p34-EGFP and EGFP using DIC-epifluorescence microscopy. Images include, as indicated, mitochondria (red), p34-EGFP or EGFP (green). Arrows (white) indicate cells positive for p34-EGFP or EGFP expression. Images are representative of those collected over the course of two independent experiments (n=60). Scale bar = 5 μm.

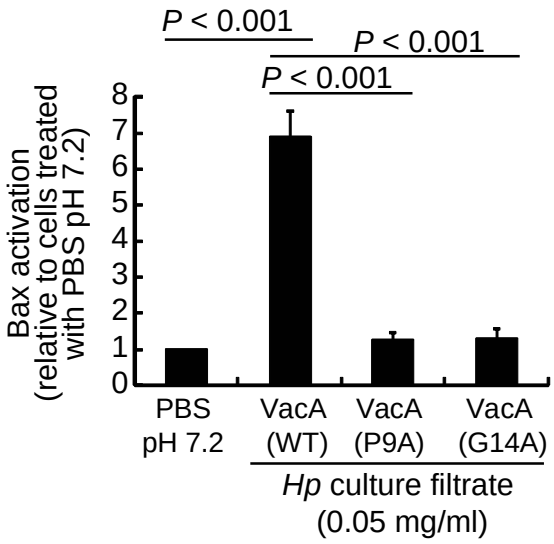

Figure 2.36 VacA anion channel function is important for Bax activation in AZ-521 cells.

AZ-521 cells were incubated at 37 °C and under 5% CO_2 with *Hp* culture filtrates (0.05 mg/ml) containing wild-type VacA, VacA (P9A), VacA (G14A), or with PBS pH 7.2. After 18 h, the cells were fixed, permeabilized, and immunostained for activated Bax. The data were rendered as the fold change in activated Bax levels between cells incubated with the indicated *Hp* culture filtrates compared to monolayers mock-intoxicated with PBS pH 7.2, obtained by combining data collected from three independent experiments, each conducted in triplicate. Error bars indicate standard deviations. Statistical significance was calculated for differences in fold-activated Bax between cells mock-intoxicated with PBS pH 7.2 and those cells incubated with wild-type VacA, VacA (P9A), VacA (G14A).

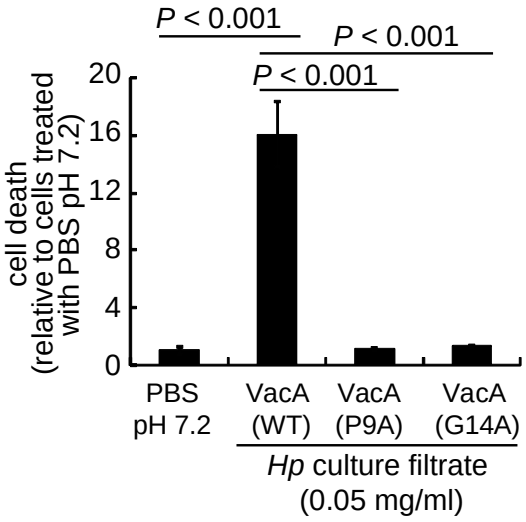

Figure 2.37 VacA anion channel function is important for induction of cell death in AZ-521 cells.

AZ-521 cells were incubated at 37 °C and under 5% CO_2 with *Hp* culture filtrates (0.05 mg/ml) containing wild-type VacA, VacA (P9A), VacA (G14A), or with PBS pH 7.2. After 24 h, the percentage of dead cells was determined using the Live-Dead viability/cytotoxicity assay kit. The data were rendered as the fold increase in dead cells between monolayers incubated with the indicated HPCF relative to monolayers mock-intoxicated with PBS pH 7.2, obtained by combining data collected from three independent experiments, each conducted in triplicate. Error bars indicate standard deviations. Statistical significance was calculated for differences in relative cell death between cells mock-intoxicated with PBS pH 7.2 and those cells incubated with wild-type VacA, VacA (P9A), VacA (G14A).

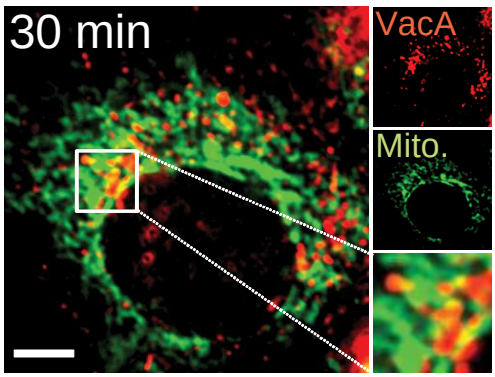

Figure 2.38 VacA localizes to mitochondria within AZ-521 cells.

AZ-521 cells were incubated with VacA (100 nM) at 37 °C and under 5% CO_2. After 30 min, the cells were fixed, permeabilized, and immunostained for VacA, as well as Tom-20 as a mitochondrial marker and analyzed for localization of VacA to mitochondria. Image includes, as indicated, mitochondria (red), VacA (green), and VacA co-localized to mitochondria (yellow). Image is representative of those collected over the course of three independent experiments. Scale bar = 5 μm.

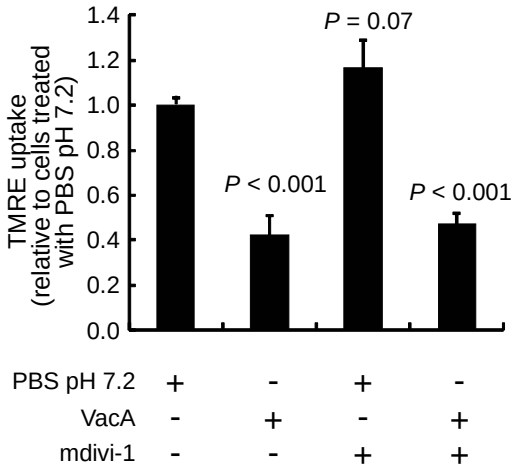

Figure 2.39 Drp1 dependent mitochondrial fission does not influence VacA induced mitochondrial dysfunction within AZ-521 cells.

AZ-521 cells were incubated at 37 °C and under 5% CO_2 with VacA (250 nM) or mock-treated with PBS pH 7.2, both in the absence or presence of mdivi-1 (50 μM). After 4 h, the relative $\Delta\Psi_m$ was determined using flow cytometry analysis of TMRE (50 nM)-stained cells. The data are rendered as the fold change in TMRE uptake in cells intoxicated with VacA relative to cells mock-intoxicated with PBS pH 7.2, obtained by combining data collected from three independent experiments, each conducted in triplicate. Error bars indicate standard deviations. Statistical significance was calculated for differences in $\Delta\Psi_m$ between cells mock-intoxicated with PBS pH 7.2 versus cells incubated with mdivi-1 or cells incubated with VacA in the presence or absence of mdivi-1.

References

1. **Arnoult, D., N. Rismanchi, A. Grodet, R. G. Roberts, D. P. Seeburg, J. Estaquier, M. Sheng, and C. Blackstone.** 2005. Bax/Bak-dependent release of DDP/TIMM8a promotes Drp1-mediated mitochondrial fission and mitoptosis during programmed cell death. Curr Biol **15:**2112-8.

2. **Ashktorab, H., S. Frank, A. R. Khaled, S. K. Durum, B. Kifle, and D. T. Smoot.** 2004. Bax translocation and mitochondrial fragmentation induced by *Helicobacter pylori*. Gut **53:**805-13.

3. **Autret, A., and S. J. Martin.** 2009. Emerging role for members of the Bcl-2 family in mitochondrial morphogenesis. Mol Cell **36:**355-63.

4. **Blanke, S. R.** 2005. Micro-managing the executioner: pathogen targeting of mitochondria. Trends Microbiol **13:**64-71.

5. **Brandon, M., P. Baldi, and D. C. Wallace.** 2006. Mitochondrial mutations in cancer. Oncogene **25:**4647-62.

6. **Brooks, C., Q. Wei, L. Feng, G. Dong, Y. Tao, L. Mei, Z. J. Xie, and Z. Dong.** 2007. Bak regulates mitochondrial morphology and pathology during apoptosis by interacting with mitofusins. Proc Natl Acad Sci U S A **104:**11649-54.

7. **Calore, F., C. Genisset, A. Casellato, M. Rossato, G. Codolo, M. D. Esposti, L. Scorrano, and M. de Bernard.** 2010. Endosome-mitochondria juxtaposition during apoptosis induced by *H. pylori* VacA. Cell Death Differ **17:**1707-16.

8. **Cassidy-Stone, A., J. E. Chipuk, E. Ingerman, C. Song, C. Yoo, T. Kuwana, M. J. Kurth, J. T. Shaw, J. E. Hinshaw, D. R. Green, and J. Nunnari.** 2008. Chemical inhibition of the mitochondrial division dynamin reveals its role in Bax/Bak-dependent mitochondrial outer membrane permeabilization. Dev Cell **14:**193-204.

9. **Cereghetti, G. M., A. Stangherlin, O. Martins de Brito, C. R. Chang, C. Blackstone, P. Bernardi, and L. Scorrano.** 2008. Dephosphorylation by calcineurin regulates translocation of Drp1 to mitochondria. Proc Natl Acad Sci U S A **105:**15803-8.

10. **Cho, D. H., T. Nakamura, and S. A. Lipton.** 2010. Mitochondrial dynamics in cell death and neurodegeneration. Cell Mol Life Sci **67:**3435-47.

11. **Cover, T. L., and S. R. Blanke.** 2005. *Helicobacter pylori* VacA, a paradigm for toxin multifunctionality. Nat Rev Microbiol **3:**320-32.

12. **Cover, T. L., and M. J. Blaser.** 2009. *Helicobacter pylori* in health and disease. Gastroenterology **136:**1863-73.

13. **Cover, T. L., P. I. Hanson, and J. E. Heuser.** 1997. Acid-induced dissociation of VacA, the *Helicobacter pylori* vacuolating cytotoxin, reveals its pattern of assembly. J Cell Biol **138:**759-69.

14. **Cover, T. L., U. S. Krishna, D. A. Israel, and R. M. Peek, Jr.** 2003. Induction of gastric epithelial cell apoptosis by *Helicobacter pylori* vacuolating cytotoxin. Cancer Res **63:**951-7.

15. **Cover, T. L., W. Puryear, G. I. Perez-Perez, and M. J. Blaser.** 1991. Effect of urease on HeLa cell vacuolation induced by *Helicobacter pylori* cytotoxin. Infect Immun **59:**1264-70.

16. **de Bernard, M., A. Cappon, L. Pancotto, P. Ruggiero, J. Rivera, G. Del Giudice, and C. Montecucco.** 2005. The *Helicobacter pylori* VacA cytotoxin activates RBL-2H3 cells by inducing cytosolic calcium oscillations. Cell Microbiol **7:**191-8.

17. **Domanska, G., C. Motz, M. Meinecke, A. Harsman, P. Papatheodorou, B. Reljic, E. A. Dian-Lothrop, A. Galmiche, O. Kepp, L. Becker, K. Gunnewig, R. Wagner, and J. Rassow.** 2010. *Helicobacter pylori* VacA toxin/subunit p34: targeting of an anion channel to the inner mitochondrial membrane. PLoS Pathog **6:**e1000878.

18. **Fannjiang, Y., W. C. Cheng, S. J. Lee, B. Qi, J. Pevsner, J. M. McCaffery, R. B. Hill, G. Basanez, and J. M. Hardwick.** 2004. Mitochondrial fission proteins regulate programmed cell death in yeast. Genes Dev **18:**2785-97.

19. **Foo, J. H., J. G. Culvenor, R. L. Ferrero, T. Kwok, T. Lithgow, and K. Gabriel.** 2010. Both the p33 and p55 subunits of the *Helicobacter pylori* VacA toxin are targeted to mammalian mitochondria. J Mol Biol **401:**792-8.

20. **Fujikawa, A., D. Shirasaka, S. Yamamoto, H. Ota, K. Yahiro, M. Fukada, T. Shintani, A. Wada, N. Aoyama, T. Hirayama, H. Fukamachi, and M. Noda.** 2003. Mice deficient in protein tyrosine phosphatase receptor type Z are resistant to gastric ulcer induction by VacA of *Helicobacter pylori*. Nat Genet **33:**375-81.

21. **Fukushima, N. H., E. Brisch, B. R. Keegan, W. Bleazard, and J. M. Shaw.** 2001. The GTPase effector domain sequence of the Dnm1p GTPase regulates self-assembly and controls a rate-limiting step in mitochondrial fission. Mol Biol Cell **12:**2756-66.

22. **Galmiche, A., J. Rassow, A. Doye, S. Cagnol, J. C. Chambard, S. Contamin, V. de Thillot, I. Just, V. Ricci, E. Solcia, E. Van Obberghen, and P. Boquet.** 2000. The N-terminal 34 kDa fragment of *Helicobacter pylori* vacuolating cytotoxin targets mitochondria and induces cytochrome c release. EMBO J **19:**6361-70.

23. **Gonzalez-Rivera, C., K. A. Gangwer, M. S. McClain, I. M. Eli, M. G. Chambers, M. D. Ohi, D. B. Lacy, and T. L. Cover.** 2010. Reconstitution of *Helicobacter pylori* VacA toxin from purified components. Biochemistry **49:**5743-52.

24. **Goyal, G., B. Fell, A. Sarin, R. J. Youle, and V. Sriram.** 2007. Role of mitochondrial remodeling in programmed cell death in Drosophila melanogaster. Dev Cell **12:**807-16.

25. **Grandemange, S., S. Herzig, and J. C. Martinou.** 2009. Mitochondrial dynamics and cancer. Semin Cancer Biol **19:**50-6.

26. **Green, D. R., and G. Kroemer.** 2004. The pathophysiology of mitochondrial cell death. Science **305:**626-9.

27. **Gupta, V. R., H. K. Patel, S. S. Kostolansky, R. A. Ballivian, J. Eichberg, and S. R. Blanke.** 2008. Sphingomyelin functions as a novel receptor for *Helicobacter pylori* VacA. PLoS Pathog **4:**e1000073.

28. **Gupta, V. R., B. A. Wilson, and S. R. Blanke.** 2010. Sphingomyelin is important for the cellular entry and intracellular localization of *Helicobacter pylori* VacA. Cell Microbiol **12:**1517-33.

29. **Ingerman, E., E. M. Perkins, M. Marino, J. A. Mears, J. M. McCaffery, J. E. Hinshaw, and J. Nunnari.** 2005. Dnm1 forms spirals that are structurally tailored to fit mitochondria. J Cell Biol **170:**1021-7.

30. **James, D. I., P. A. Parone, Y. Mattenberger, and J. C. Martinou.** 2003. hFis1, a novel component of the mammalian mitochondrial fission machinery. J Biol Chem **278:**36373-9.

31. **Jones, N. L., A. S. Day, H. Jennings, P. T. Shannon, E. Galindo-Mata, and P. M. Sherman.** 2002. Enhanced disease severity in *Helicobacter pylori*-infected mice deficient in Fas signaling. Infect Immun **70:**2591-7.

32. **Karbowski, M., Y. J. Lee, B. Gaume, S. Y. Jeong, S. Frank, A. Nechushtan, A. Santel, M. Fuller, C. L. Smith, and R. J. Youle.** 2002. Spatial and temporal association of Bax with mitochondrial fission sites, Drp1, and Mfn2 during apoptosis. J Cell Biol **159:**931-8.

33. **Karbowski, M., A. Neutzner, and R. J. Youle.** 2007. The mitochondrial E3 ubiquitin ligase MARCH5 is required for Drp1 dependent mitochondrial division. J Cell Biol **178:**71-84.

34. **Kimura, M., S. Goto, A. Wada, K. Yahiro, T. Niidome, T. Hatakeyama, H. Aoyagi, T. Hirayama, and T. Kondo.** 1999. Vacuolating cytotoxin purified from *Helicobacter pylori* causes mitochondrial damage in human gastric cells. Microb Pathog **26:**45-52.

35. **Kuck, D., B. Kolmerer, C. Iking-Konert, P. H. Krammer, W. Stremmel, and J. Rudi.** 2001. Vacuolating cytotoxin of *Helicobacter pylori* induces apoptosis in the human gastric epithelial cell line AGS. Infect Immun **69:**5080-7.

36. **Lin, M. T., and M. F. Beal.** 2006. Mitochondrial dysfunction and oxidative stress in neurodegenerative diseases. Nature **443:**787-95.

37. **McClain, M. S., P. Cao, H. Iwamoto, A. D. Vinion-Dubiel, G. Szabo, Z. Shao, and T. L. Cover.** 2001. A 12-amino-acid segment, present in type s2 but not type s1 *Helicobacter pylori* VacA proteins, abolishes cytotoxin activity and alters membrane channel formation. J Bacteriol **183:**6499-508.

38. **McClain, M. S., H. Iwamoto, P. Cao, A. D. Vinion-Dubiel, Y. Li, G. Szabo, Z. Shao, and T. L. Cover.** 2003. Essential role of a GXXXG motif for membrane channel formation by *Helicobacter pylori* vacuolating toxin. J Biol Chem **278:**12101-8.

39. **Montessuit, S., S. P. Somasekharan, O. Terrones, S. Lucken-Ardjomande, S. Herzig, R. Schwarzenbacher, D. J. Manstein, E. Bossy-Wetzel, G. Basanez, P. Meda, and J. C. Martinou.** 2010. Membrane remodeling induced by the dynamin-related protein Drp1 stimulates Bax oligomerization. Cell **142:**889-901.

40. **Moss, S. F., J. Calam, B. Agarwal, S. Wang, and P. R. Holt.** 1996. Induction of gastric epithelial apoptosis by *Helicobacter pylori*. Gut **38:**498-501.

41. **Oldani, A., M. Cormont, V. Hofman, V. Chiozzi, O. Oregioni, A. Canonici, A. Sciullo, P. Sommi, A. Fabbri, V. Ricci, and P. Boquet.** 2009. *Helicobacter pylori* counteracts the apoptotic action of its VacA toxin by injecting the CagA protein into gastric epithelial cells. PLoS Pathog **5:**e1000603.

42. **Parone, P. A., D. I. James, S. Da Cruz, Y. Mattenberger, O. Donze, F. Barja, and J. C. Martinou.** 2006. Inhibiting the mitochondrial fission machinery does not prevent Bax/Bak-dependent apoptosis. Mol Cell Biol **26:**7397-408.

43. **Peek, R. M., Jr., H. P. Wirth, S. F. Moss, M. Yang, A. M. Abdalla, K. T. Tham, T. Zhang, L. H. Tang, I. M. Modlin, and M. J. Blaser.** 2000. *Helicobacter pylori* alters gastric epithelial cell cycle events and gastrin secretion in Mongolian gerbils. Gastroenterology **118:**48-59.

44. **Rudel, T., O. Kepp, and V. Kozjak-Pavlovic.** 2010. Interactions between bacterial pathogens and mitochondrial cell death pathways. Nat Rev Microbiol **8:**693-705.

45. **Salama, N. R., G. Otto, L. Tompkins, and S. Falkow.** 2001. Vacuolating cytotoxin of *Helicobacter pylori* plays a role during colonization in a mouse model of infection. Infect Immun **69:**730-6.

46. **Santel, A., and S. Frank.** 2008. Shaping mitochondria: The complex posttranslational regulation of the mitochondrial fission protein DRP1. IUBMB Life **60:**448-55.

47. **Stavru, F., F. Bouillaud, A. Sartori, D. Ricquier, and P. Cossart.** 2010. *Listeria monocytogenes* transiently alters mitochondrial dynamics during infection. Proc Natl Acad Sci U S A.

48. **Stein, M., R. Rappuoli, and A. Covacci.** 2000. Tyrosine phosphorylation of the *Helicobacter pylori* CagA antigen after cag-driven host cell translocation. Proc Natl Acad Sci U S A **97:**1263-8.

49. **Szabo, I., S. Brutsche, F. Tombola, M. Moschioni, B. Satin, J. L. Telford, R. Rappuoli, C. Montecucco, E. Papini, and M. Zoratti.** 1999. Formation of anion-selective channels in the cell plasma membrane by the toxin VacA of *Helicobacter pylori* is required for its biological activity. Embo J **18:**5517-27.

50. **Tan, S., L. S. Tompkins, and M. R. Amieva.** 2009. *Helicobacter pylori* usurps cell polarity to turn the cell surface into a replicative niche. PLoS Pathog **5:**e1000407.

51. **Torres, V. J., S. E. Ivie, M. S. McClain, and T. L. Cover.** 2005. Functional properties of the p33 and p55 domains of the *Helicobacter pylori* vacuolating cytotoxin. J Biol Chem **280:**21107-14.

52. **Twig, G., B. Hyde, and O. S. Shirihai.** 2008. Mitochondrial fusion, fission and autophagy as a quality control axis: the bioenergetic view. Biochim Biophys Acta **1777:**1092-7.

53. **Vinion-Dubiel, A. D., M. S. McClain, D. M. Czajkowsky, H. Iwamoto, D. Ye, P. Cao, W. Schraw, G. Szabo, S. R. Blanke, Z. Shao, and T. L. Cover.** 1999. A dominant negative mutant of *Helicobacter pylori* vacuolating toxin (VacA) inhibits VacA-induced cell vacuolation. J Biol Chem **274:**37736-42.

54. **Wasiak, S., R. Zunino, and H. M. McBride.** 2007. Bax/Bak promote sumoylation of DRP1 and its stable association with mitochondria during apoptotic cell death. J Cell Biol **177:**439-50.

55. **Westermann, B.** 2010. Mitochondrial fusion and fission in cell life and death. Nat Rev Mol Cell Biol **11:**872-84.

56. **Willhite, D. C., and S. R. Blanke.** 2004. *Helicobacter pylori* vacuolating cytotoxin enters cells, localizes to the mitochondria, and induces mitochondrial membrane permeability changes correlated to toxin channel activity. Cell Microbiol **6:**143-54.

57. **Willhite, D. C., T. L. Cover, and S. R. Blanke.** 2003. Cellular vacuolation and mitochondrial cytochrome c release are independent outcomes of *Helicobacter pylori* vacuolating cytotoxin activity that are each dependent on membrane channel formation. J Biol Chem **278:**48204-9.

58. **Xia, H. H., and N. J. Talley.** 2001. Apoptosis in gastric epithelium induced by *Helicobacter pylori* infection: implications in gastric carcinogenesis. Am J Gastroenterol **96:**16-26.

59. **Yahiro, K., T. Niidome, M. Kimura, T. Hatakeyama, H. Aoyagi, H. Kurazono, K. Imagawa, A. Wada, J. Moss, and T. Hirayama.** 1999. Activation of *Helicobacter pylori* VacA toxin by alkaline or acid conditions increases its binding to a 250-kDa receptor protein-tyrosine phosphatase beta. J Biol Chem **274:**36693-9.

60. **Yahiro, K., A. Wada, M. Nakayama, T. Kimura, K. Ogushi, T. Niidome, H. Aoyagi, K. Yoshino, K. Yonezawa, J. Moss, and T. Hirayama.** 2003. Protein-tyrosine phosphatase alpha, RPTP alpha, is a *Helicobacter pylori* VacA receptor. J Biol Chem **278:**19183-9.

61. **Yamasaki, E., A. Wada, A. Kumatori, I. Nakagawa, J. Funao, M. Nakayama, J. Hisatsune, M. Kimura, J. Moss, and T. Hirayama.** 2006. *Helicobacter pylori* vacuolating cytotoxin induces activation of the proapoptotic proteins Bax and Bak, leading to cytochrome c release and cell death, independent of vacuolation. J Biol Chem **281:**11250-9.

62. **Ye, D., and S. R. Blanke.** 2000. Mutational analysis of the *Helicobacter pylori* vacuolating toxin amino terminus: identification of amino acids essential for cellular vacuolation. Infect Immun **68:**4354-7.

63. **Ye, D., D. C. Willhite, and S. R. Blanke.** 1999. Identification of the minimal intracellular vacuolating domain of the *Helicobacter pylori* vacuolating toxin. J Biol Chem **274:**9277-82.

64. **Yoshimura, T., T. Shimoyama, M. Tanaka, Y. Sasaki, S. Fukuda, and A. Munakata.** 2000. Gastric mucosal inflammation and epithelial cell turnover are associated with gastric cancer in patients with *Helicobacter pylori* infection. J Clin Pathol **53:**532-6.

65. **Zhou, R., A. S. Yazdi, P. Menu, and J. Tschopp.** 2011. A role for mitochondria in NLRP3 inflammasome activation. Nature **469:**221-5.

Chapter 3: *Helicobacter pylori* VacA induces Bax activation through activation and mitochondrial recruitment of the cell stress sensor 'Bid'

3.1 INTRODUCTION

Chronic infection of the human gastric mucosa with the gastric pathogen *Helicobacter pylori* (*Hp*) is a significant risk factor for the development of peptic ulcer disease or gastric cancer (13). *Hp* infection is strongly associated with increased apoptosis within the gastric mucosa of humans (48), mice (32), and Mongolian gerbil models (53) and is considered as important for *Hp* persistence and disease pathophysiology (12, 13). The induction of cell death following *Hp* infection is influenced by a complex interplay between several host and *Hp* factors. The vacuolating cytotoxin A or VacA, a multi-functional virulence factor produced by *Hp*, is shown to be both essential (38) and sufficient (15) for inducing gastric epithelial cell death. Earlier studies have reported that the cellular pro-death effector Bcl-2 associated X factor or Bax, is essential for VacA induced mitochondrial outer membrane permeabilization and cell death (75). In a recent study, we demonstrated that VacA intoxication resulted in the fragmentation of cellular mitochondrial network through excessive activation of the mitochondrial fission protein Drp1 (31). Drp1 mediated mitochondrial fission preceded and was required for Bax activation and cell death mechanism. However, the complete mechanism underlying VacA mediated Bax activation, particularly the nature of cellular changes initiated by VacA that linked the de-

regulation of mitochondrial network dynamics to engagement of host apoptotic machinery, was not entirely clear.

Our study here demonstrates that VacA induces the activation and mitochondrial recruitment of the endogenous stress sensor protein Bid (BH3 interacting death domain agonist), a BH3 domain-only protein of the Bcl2 family which is known directly activate Bax in certain cell death mechanisms (19, 20). Within VacA intoxicated cells, Bid was important for the activation of Bax and mitochondrial cell death mechanism. Importantly, Drp1 GTPase activity was required for Bid activation within VacA intoxicated cells. Our results therefore indicate that cellular stress as a result of excessive fission is possibly translated to Bax mediated mitochondrial outer membrane permeabilization through the stress sensor Bid. Furthermore, Drp1 dependent mitochondrial fission also resulted in the increase in cytosolic calcium levels, which was required for the activation of the calcium dependent cysteine protease called calpain. The proteolytic activity of calpain was required for processing of Bid to yield the mitochondrial targeting active fragment called t-Bid (truncated Bid).

Studies here identify the molecular mechanism underlying the activation of the cellular pro-death effector Bax, following VacA induced Drp1 mediated mitochondrial fission. Our results indicate that excessive mitochondrial fission following VacA intoxication results in activation and mitochondrial recruitment of the “direct-activator” of Bax called Bid, by a mechanism dependent on disruption of cellular calcium homeostasis and activation of calcium depend protease calpain.

3.2 MATERIALS AND METHODS

Bacterial Strains. *Hp* 60190 (*cag* PAI^{+}, *vacA* s1/m1; 49503; ATCC; Manassas, VA) was cultured in bisulfite- and sulfite-free brucella broth (BSFB) containing 5 μg vancomycin/mL (Sigma Aldrich; St. Louis, MO), on a rotary platform shaker for 48 h at 37 °C, under 5% CO_2 and 10% O_2. *Hp* VM022 (*ΔvacA*) (69) was a kind gift from Dr. Timothy Cover (Vanderbilt University Medical Center; Nashville, TN). *Hp* 60190 derived strains producing VacA (P9A) and VacA (G14A) were constructed and cultivated as described previously (42, 73).

Cell Lines. AZ-521 cells (3940; Japan Health Science Foundation) were maintained in minimum essential medium (MEM; Sigma Aldrich), which when supplemented with glutamine (2 mM), penicillin (100 U/mL), streptomycin sulfate (1 mg/mL) (Sigma Aldrich) and 10% fetal bovine calf serum (JRH Biosciences; Lenexa, KS), was referred to as “supplemented MEM”. The cells were maintained at 37 °C within a humidified atmosphere and under 5% CO_2.

Plasmids. The plasmid pDsRed2-Mito was obtained from Clontech Laboratories (Mountain View, CA). The plasmid pBABE Bid p22 GFP was obtained from addgene (Cambridge, MA).

Transfection. Cells were transfected with the indicated plasmids using Lipofectamine-2000 transfection reagent (Invitrogen; Carlsbad, CA), according to manufacturer's instructions.

***H. pylori* culture filtrates (HPCF).** The indicated *Hp* strains were grown in 200 mL bisulfite- and sulfite-free brucella broth (BSFB) containing 5 μg vancomycin/mL, in 1 L culture flasks, on a rotary platform shaker at 37 °C, under 5% CO_2 and 10% O_2. After 48 h, *Hp* cultures were harvested by centrifugation at 8,000 g for 30 min at 4 °C. The supernatants were collected, and pellets were decontaminated by autoclaving. The supernatants were cooled to 4 °C, and the total protein was precipitated by slowly dissolving ammonium sulfate (Sigma Aldrich) to 90% saturation with stirring, followed by stirring overnight at 4 °C. The precipitates were collected by centrifugation at 8,000 g for 30 min at 4 °C, and the pellets were resuspended in 10 mM sodium phosphate buffer pH 7.0. The samples were dialyzed at 4 °C into 10 mM sodium phosphate buffer pH 7.0 using the Spectra/Por® membrane (molecular weight cut-off (MWCO) 50,000 Daltons (Da); Spectrum Laboratories; Rancho Dominguez, CA), concentrated approximately 5-fold using an Amicon Ultra Centrifugal Filter Unit (MWCO 50,000 Da; Sigma Aldrich), and filter sterilized using a 0.2 μm vacuum filtration unit (Corning), to obtain the final HPCF. The presence of full-length VacA within the HPCFs was confirmed by Western blot analysis, using VacA rabbit antiserum (Rockland Immunochemicals; Gilbertsville, PA), followed by incubation with HRP

conjugated anti-rabbit IgG secondary antibody (Cell Signaling Technology; Danvers, MA). The presence of VacA was detected by chemiluminescence using the Super-signal West Femto chemiluminescence detection kit (Thermo Scientific; Waltham, MA). VacA concentrations were normalized using densitometry analysis (UN-SCAN-IT gel analysis software; Silk Scientific Inc.; Orem, Utah) to compare the total pixels of each band against those obtained using known concentrations of purified VacA. The HPCFs were used within several days of preparation, during which time there was no detectable loss of VacA-induced vacuolation of AZ-521 cells, as determined by quantification of cellular vacuolation (16, 29).

VacA Purification. VacA (s1m1) from *Hp* 60190 (49503; ATCC), was purified and activated, as previously described (14). *H. pylori* 60190 was cultured, and VacA was purified from *Hp* culture filtrate (HPCF; from *Hp* broth culture described earlier) by anion exchange chromatography using Diethyl amino ethyl Sephacel resin (Sigma Aldrich). VacA was then eluted using 10 mM phosphate buffer pH 7.0, containing 200 mM sodium chloride. All eluted fractions were collected and analyzed by sodium dodecyl sulfate (SDS)-polyacrylamide gel electrophoresis followed by Coomassie brilliant blue staining and immunoblot analysis using rabbit anti-VacA polyclonal antibody, and purity of the full length toxin in VacA containing fractions was assessed to be on an average of 90-95 % pure. Fractions demonstrating the greatest degree of purity were pooled and stored at 4 °C until use.

Heat Inactivation of *Hp.* *Hp* 60190 (12.5 X 10^8 CFU/mL in 1 mL PBS pH 7.2) were incubated in a 37 °C or 65 °C water bath for 30 min, and then further incubated for 10 min at 37 °C. Immediately, 37 °C- or 65 °C-pretreated *Hp* were incubated with AZ-521 cells (MOI 100) or, alternatively, enumerated by serially diluting in PBS pH 7.2, followed by spread-plating onto fresh F-12 agar plates (supplemented with 5% FBS and 5 μg vancomycin/mL) and incubating the plates at 37 °C, and under 5% CO_2 and 10% O_2. After 72 h, CFU/mL was determined by direct counting of colonies on the F-12 plates and back calculating the appropriate dilution factor.

Heat Inactivation of VacA. Purified VacA (4 μM) was incubated in a 37 °C or 95 °C water bath, followed by further incubation of both samples at 37 °C for 10 min. Immediately, VacA was activated as described previously (14, 28, 73), and incubated with AZ-521 cells (at a final concentration of 250 nM). At the indicated times, the processing of Bid to t-Bid was determined within lysates of AZ-521 cells that were intoxicated with VacA or mock intoxicated with PBS pH 7.2.

Preparation of Whole Cell Lysates. The cultured mammalian epithelial cells were collected following brief trypsinization. Cells were pelleted at 400 g for 5 min at 4 °C and washed two times in ice cold PBS pH 7.2. The cells were incubated on ice in lysis buffer (20 mM HEPES pH 7.5, 10 mM KCl, 150 mM

Sucrose, 1.5 mM $MgCl_2$, 1 mM EDTA, 1 mM EGTA) supplemented with protease inhibition cocktail set III (539134; EMD chemicals; Gibbstown, NJ) for 30 min. The cell suspension in lysis buffer was then passed 25 times through a 30 ½ gauge needle to break open the cells. Cell lysate was centrifuged at 1000 g for 5 min at 4 °C to remove unbroken cells, membrane and nuclear debris. Supernatant was collected and protein concentrations were determined using Bradford assay.

Analysis of processing of Bid to t-Bid. Proteins within whole cell lysates were resolved in 12-15% SDS-polyacrylamide gels and transferred onto Immobilon PVDF transfer membrane with a pore size of 0.2 µm (ISEQ08100; Millipore; Billerica, MA). The PVDF membranes were incubated with blocking buffer (5% nonfat milk in tris buffered saline or TBS) to block nonspecific binding sites. Membranes were incubated with anti-Bid monoclonal antibody (BD Biosciences; San Jose, CA) diluted in blocking buffer for overnight at 4 °C. Membranes were washed with TBS plus 0.1 % Tween-20 (TBS-T) and incubated with species specific HRP-conjugated secondary antibody for 1 h at RT. Membranes were washed with TBS-T and developed using Super-signal West Femto chemiluminescence detection kit.

Analysis of Bid Localization to Mitochondria. AZ-521 cells were transiently transfected with pBABE p22 GFP. After 24 h, cells were incubated purified VacA (at the indicated concentrations). At the indicated times, the

monolayers were stained with mitotracker red (Invitrogen) to visualize mitochondria, washed 3 times with PBS pH 7.2 and fixed by incubation with paraformaldehyde (4%) for 20 min at 37 °C. The cells were imaged using DIC-epifluorescence microscopy. Bid localization to mitochondria was quantified using the co-localization module of the DeltaVision SoftWoRx 3.5.1 software suite. Results were expressed as the co-localization index, derived from calculating the Pearson's coefficient of correlation, which in this study was a measure of co-localization between Bid and mitochondria in each z plane of the cell. For each cell, images from an average of 10-20 z planes at a thickness of 0.2 μm were collected. A co-localization index of 1.0 indicates 100% co-localization of Bid to mitochondria, whereas a co-localization index of 0.0 indicates the absence of detectable co-localization between Bid and mitochondria. Data were rendered as the average co-localization index obtained from analyzing 30 cells from over the course of three independent experiments. In each independent experiment, 10 cells were analyzed from at least 4 randomly chosen fields for each treatment.

Bid siRNA knock-down. AZ-521 cells were transfected with siRNA targeted against Bid (Human) or scrambled AllStars negative control siRNA (Qiagen; Valencia, CA) in Opti-MEM (Invitrogen) without antibiotics (Penicillin/Streptomycin) and serum (10% FBS), using lipofectamine 2000 transfection reagent (Invitrogen). The siRNA-liposome mixture was applied to the cells at ~80% confluence in a 6 well cell culture dish (Corning; Corning, NY)

containing 1.5 ml of Opti-MEM. Cells were further incubated at 37 °C within a humidified environment and 5% CO_2 atmosphere for 6 h, following which opti-MEM was replaced with supplemented minimum essential medium (supplemented MEM). Cells were incubated at 37 °C within a humidified environment and 5% CO_2 atmosphere for additional 48 h. The expression levels of Bid were analyzed by western blot within whole cell lysates, as described earlier.

Determination of cytosolic calcium. AZ-521 cells were pre-loaded with 10 µM Fluo-3 AM (Sigma Aldrich) for 30 min in PBS pH 7.2 (Sigma Aldrich) containing 0.02% Pluronic F-127 (Invitrogen) at 37 °C and 5% CO_2 in dark. The PBS used in this study was devoid of Ca^{2+} or Mg^{2+} salts. The cells were washed twice with PBS pH 7.2 and resuspended in fresh supplemented MEM (containing 0.2 g/L dissolved $Cacl_2.2H_2O$). The cells were further incubated for 30 min at 37 °C and 5% CO_2 in dark to allow for de-esterification of Fluo-3 AM. The cells were treated with VacA or PBS pH 7.2 and cellular calcium levels were monitored by flow cytometry analysis of Fluo-3 fluorescence in the FL1 channel. Cell counts in all samples were normalized to 10000 cells.

Determination of cellular calpain activity. AZ-521 cells were pre-loaded with 1 µM CMAC t-Boc-Leu-Met (Sigma Aldrich), a specific cell permeable substrate for calpain, for 30 min. Cells were then treated with VacA or PBS pH 7.2 and further incubated at 37 °C and 5% CO_2 for required periods of time.

Analysis of AMC fluorescence, generated as a result of substrate cleavage by active calpain was carried out in a Synergy 2 BioTek fluorescence plate reader (BioTek; Winooski, VT) using band pass filter with EX 360/40 and EM 460/40.

Determination of Cellular Bax Activation. AZ-521 cells were detached from tissue culture wells by mild trypsinization for 3 min at 37 °C with Trypsin EDTA (Cellgro), fixed by incubation with paraformaldehyde (4%) for 20 min at 37 °C, followed by permeabilization with saponin (0.1 %) in PBS pH 7.2 containing BSA (0.5%) and anti-Bax Clone 3 mAb (1 μg/mL; BD Biosciences) in order to stain for activated Bax. After 45 min, the cells were washed 3 times with PBS pH 7.2, followed by incubation with mouse anti-IgG conjugated to Alexa Fluor 488 (1 μg/mL) in PBS pH 7.2 containing saponin (0.1 %) and BSA (0.5%) for 30 min on ice and in the dark. As a negative control, cells were incubated in the presence of mouse anti-IgG conjugated to Alexa Fluor 488 (1 μg/mL) alone. Cells were washed in PBS pH 7.2 containing saponin (0.1 %) and BSA (0.5%) and resuspended in PBS pH 7.2. Alexa Fluor 488 fluorescence was quantified by flow cytometry in the FL1 channel (525/40 nm band pass filter). 10,000 cells were analyzed for each sample.

Quantitative measurement of VacA mediated cellular caspase-8 activation. AZ-521 cells were cultured overnight at a seeding density of $2X10^5$ cells/ml in 37 °C and under 5% CO_2 atmosphere and were treated with purified VacA or PBS pH 7.2. After appropriate time periods of incubation, the cells were

collected by brief trypsinization, washed 2 times with PBS pH 7.2 and incubated with CaspGLOW Fluorescein active caspase 8 staining kit (BioVision) for 30 min at 37 °C and under 5% CO_2 atmosphere, according to manufacturer's instructions. The cells were washed 3 times with PBS pH 7.2 and the fluorescein signal was quantified by flow cytometry in the FL1 channel (525/40 nm band pass filter). 10,000 cells were analyzed for each sample.

Determination of Cell Death. Cell death was measured by flow cytometry, using the Live-Dead viability/cytotoxicity assay kit (Invitrogen) according to manufacturer's instructions.

DIC-Epifluorescence Microscopy. Fluorescence and DIC images were collected using a Delta Vision RT microscope (Applied Precision), EX 490/20 and EM 528/38, EX 555/28 and EM 617/73, EX 640/20 and EM 685/40 using Olympus Plan Apo 60X oil objective with NA 1.42 and working distance of 0.17 nm. Images were processed using DeltaVision SoftWoRx 3.5.1 software suite.

Flow Cytometry. Analytical flow cytometry was carried out using a BD FACSCanto II flow analyzer (BD Biosciences) located at the R. J. Carver Biotechnology Center Flow Cytometry Facility (University of Illinois at Urbana-Champaign). The flow cytometer was equipped with 70-μm nozzle, 488 nm line of an air-cooled argon-ion laser, and 400 mV output. The band pass filters used for analysis were 525/40 nm, 575/30 nm and 675/30 nm. Cell analysis was

standardized for scatter and fluorescence by using a suspension of fluorescent beads (Beckman Coulter; Miami, FL). Events were recorded on a log fluorescence scale and the geometric mean as well as percent events was determined using FCS Express analysis software (De Novo Software; Los Angeles, CA). Forward and side scatter properties were considered to exclude non-cellular (debris) events from viable and (or) dead cell populations.

Statistical Analysis. Unless otherwise indicated, each experiment was performed at least three independent times. For those data requiring statistical analysis, data were combined from 2 or 3 independent experiments, as indicated, with each independent experiment carried out in triplicate. Statistical analyses were performed using Microsoft Excel (Version 11.0; Microsoft Corporation; Redmond, WA). Unless otherwise noted, error bars represent standard deviations. All *P* values were calculated with the Student's *t* test using paired, two-tailed distribution. $P < 0.05$ indicates statistical significance.

3.3 RESULTS

3.3.1 *Hp* infection results in the activation of the pro-apoptotic cell stress sensor protein 'Bid'.

Our earlier work demonstrated that the deregulation of mitochondrial dynamics by the vacuolating cytotoxin (VacA) produced by *Hp*, was important for activation of the pro-apoptotic effector protein 'Bax' (31). The activation of Bax is an important step towards commitment of a cell to undergo cell death following

VacA intoxication (75). However, the mechanism underlying Bax activation following VacA induced mitochondrial fragmentation remained unclear. Earlier studies have clearly indicated that the stress sensor protein, BH3 interacting-domain death agonist 'Bid' which belongs to the BH3 domain-only sub-family of Bcl2 proteins is typically associated with the activation of Bax following the receipt of stress related death inducing signals (19, 20, 34). Bid is processed to 't-Bid', a mitochondrial targeted fragment which induces conformational changes within Bax at the mitochondrial outer membrane, resulting in Bax oligomerization and channel formation (20, 27, 37, 39, 40, 63). Therefore we hypothesized that metabolic stress resulting from excessive mitochondrial fission could result in a Bid mediated Bax activation.

To evaluate this possibility, we characterized the processing of Bid to t-Bid within whole cell lysates prepared from cultured AZ-521 gastric epithelial cells that were intoxicated with *Hp*. We observed significant increase in t-Bid cross reactive material within 8 h of infection in the lysates obtained from cells that were infected with *Hp* 60190 (MOI 100), when compared to cells that were treated with *Hp* 60190 (MOI 100) that were pre-incubated at 65 °C for 30 min or with PBS pH 7.2 under similar conditions (Fig. 3.1).

3.3.2 VacA is essential for the processing of Bid to t-Bid.

Our earlier work had demonstrated that VacA was essential for *Hp* induced mitochondrial fission and cellular Bax activation (31). To evaluate the importance of VacA in *Hp* mediated generation of t-Bid, we infected AZ-521 cells

with an isogenic *Hp* 60190 mutant strain lacking a functional *vacA* gene [*Hp* (*⊿vacA*)] (MOI 100). Interestingly, compared to detectable and significant increase in the generation of t-Bid within lysates of cells infected with *Hp* 60190, we did not detect any t-Bid cross reactive material within lysates of cells intoxicated with the mutant strain [*Hp* (*⊿vacA*)], within 8 h of infection (Fig. 3.2). These data indicate VacA was important for *Hp* mediated processing of Bid to t-Bid.

3.3.3 VacA is sufficient to induce the processing of Bid to t-Bid.

Studies to evaluate the sufficiency of VacA in *Hp* mediated processing of Bid to t-Bid revealed that VacA, when purified from *Hp* culture filtrate, induced significant increase in generation of t-Bid within 8 h of intoxication in AZ-521 cells (Fig. 3.3). However, the generation of t-Bid was not observed following intoxication of AZ-521 cells with VacA that had been pre-incubated at 95 °C within 8 h of intoxication (Fig.3.3). Detectable processing of Bid to t-bid was observed within 4 h of VacA treatment (Fig. 3.4). These data clearly indicate that VacA was sufficient in inducing the processing of Bid to t-Bid.

3.3.4 VacA induces mitochondrial localization of Bid.

Bid is a cytosolic protein that is recruited to mitochondrial outer membrane following receipt of death inducing signal(s), where it is believed to activate the death effector protein Bax, by a mechanism that is still not completely understood (51). In order to evaluate the intracellular distribution of Bid, AZ-521 cells were

transfected with a plasmid encoding Bid-GFP (pBABE Bid p22 GFP). Additionally, to visualize mitochondria, the cells were co-transfected with a plasmid encoding a mitochondrial targeted RFP (pDsRed2-mito). The cells were treated with either purified VacA (250 nM) or PBS pH 7.2 and Bid-GFP, as well as mitochondrial-RFP fluorescence was monitored by epi-fluorescence microscopy. After 4 h of incubation, while cells treated with PBS pH 7.2 displayed a predominantly diffuse GFP fluorescence indicative of a cytosolic distribution of Bid-GFP, cells intoxicated with VacA displayed highly distinct GFP puncta, that predominantly colocalized with mitochondria within cells, indicative of the targeting of Bid-GFP to mitochondria (Fig. 3.5 A, B).

3.3.5 VacA induced activation and mitochondrial targeting of Bid is important for toxin mediated Bax activation and cell death.

Our data thus far indicated that VacA was both essential and sufficient to induce the processing of Bid to t-Bid. To evaluate the importance of VacA induced processing to Bid to t-Bid in the mitochondrial cell death mechanism, we monitored VacA induced Bax activation in AZ-521 cells following partial knockdown of Bid expression using Bid specific siRNA (Fig. 3.6). AZ-521 cells that were transfected with Bid specific siRNA, displayed significant reduction in Bax activation within 18 h of intoxication with VacA (250 nM), compared to cells that were transfected with a non-specific siRNA (Fig. 3.7). Furthermore, significant reduction in Bax activation was also observed within cells that were intoxicated with VacA (250 nM) for 18 h in the presence of a small molecule

chemical inhibitor BI6C9, which specifically blocks the association of t-Bid to the mitochondria (36), compared to cells intoxicated with VacA in the absence of BI6C9 (Fig. 3.8). Finally, there was significantly less Bax activation in Bid knock-out MEFs ($MEF^{bid-/bid-}$) incubated with VacA than in wild-type MEFs ($MEF^{bid+/bid+}$) incubated with the toxin (Fig. 3.9). These data support a model that VacA mediated Bax activation occurs by a Bid-dependent mechanism.

Earlier studies have clearly indicated that Bax activation is important for the commitment of cells to undergo cell death following VacA intoxication (75). Consistent with this idea, AZ-521 cells that were transfected with Bid siRNA, displayed significant reduction in cell death within 24 h of intoxication with VacA (250 nM), compared to cells that were transfected with a non-specific siRNA (Fig. 3.10). Additionally, significant reduction in cell death was also observed within cells that were intoxicated with VacA (250 nM) for 24 h in the presence BI6C9, compared to cells intoxicated with VacA in the absence of BI6C9 (Fig. 3.11).

3.3.6 VacA induced activation of the mitochondrial fission factor Drp1 is important for the processing of Bid to t-Bid.

Our earlier work had demonstrated that Drp1 mediated mitochondrial fragmentation was important for VacA induced Bax activation within AZ-521 cells (31). However, the underlying mechanism by which Drp1 influences Bax activation was not clear. Our data thus far indicate a critical role of Bid in inducing Bax activation within VacA intoxicated cells. Therefore, we wished to evaluate

the causal relationship between VacA induced Drp1 activation and the processing of Bid to t-Bid.

While investigating the role of Drp1 in Bid processing following *Hp* infection, we observed considerable reduction in the generation of t-Bid within cells infected with *Hp* 60190 (MOI 10 and 100) for 8 h in the presence of the Drp1 GTPase inhibitor Mdivi-1, compared with cells infected with *Hp* 60190 in the absence of Mdivi-1 (50 µM) (Fig. 3.12). Additionally, intoxication of AZ-521 cells with VacA (100 and 250 nM) for 4 h in the presence of Mdivi-1 (50 µM) resulted in considerable reduction in the processing of Bid to t-Bid (Fig. 3.13). These data therefore indicate that VacA induced Drp1 dependent mitochondrial fission is important for the processing of Bid to t-Bid.

3.3.7 VacA anion channel activity is important for the processing of Bid to t-Bid.

Earlier studies clearly indicate that the ability of VacA to form anion channels in host cell membranes is important for several changes induced within cells following VacA intoxication, including mitochondrial dysfunction, Bax activation and Cyt *c* release (8, 73, 74). Previously, we had demonstrated that VacA anion channel activity is important for the Drp1 dependent mitochondrial fission mechanism (31). Since our data thus far suggest that VacA induced mitochondrial fission is important for the generation of t-Bid, we wished to evaluate the importance of VacA anion channel function in the processing of Bid to t-Bid. AZ-521 cells were intoxicated with *Hp* culture filtrates (HPCF; 0.05

mg/mL) from *Hp* strains expressing wild-type VacA, or 2 mutant forms of toxin, VacA (P9A) or VacA (G14A), each of which had been previously shown to be attenuated in membrane channel-forming ability (43). We observed almost a complete absence of detectable Bid processing in cells that were intoxicated with HPCF containing VacA(P9A) or VacA(G14A), while cells intoxicated HPCF containing wild-type VacA demonstrated robust processing of Bid to t-Bid, within 8 h of intoxication (Fig. 3.14).

3.3.8 Cellular calpain activity is important for VacA induced processing of Bid to t-Bid.

Processing of full-length Bid to t-Bid is known to occur following activation of different classes of proteases (10, 20, 27, 39, 41, 55, 62-64). The aspartate-specific cysteine protease, capsase-8, has been commonly associated with Bid processing within cells during the death receptor mediated or extrinsic cell death mechanism (20, 27). In fact, we did observe significant increase in activated caspase-8 within AZ-521 cells that were intoxicated with purified VacA (250 nM) relative to cells treated with PBS pH 7.2. However, significant increase in detection of activated caspase-8 was observed only after 8 h of treatment with VacA (Fig. 3.15), whereas the processing of Bid was detected within 4 h of VacA intoxication(Fig. 3.4). Our data, therefore suggested that within the context of VacA intoxication, the processing of Bid was not likely initiated by caspase-8.

Several studies have suggested that the calcium dependent cysteine protease, calpain is also capable of processing Bid, but at a site distinct from the

one recognized by caspase-8 (10, 41). In fact, earlier studies have demonstrated an increase in cellular calpain activity following *Hp* infection (50, 71). Notably, we observed significant increase in cellular calpain activity in AZ-521 cells, within 1 h of intoxication with purified VacA (250 nM), relative of cells treated with PBS pH 7.2 (Fig. 3.16). Additionally, cells that were intoxicated with increasing concentrations of VacA for 4 h, demonstrated significant increase in calpain activity at VacA concentration as low as 10 nM, but not at 1 nM, relative to cells treated with PBS pH 7.2 (Fig. 3.17). To evaluate the importance of cellular calpain activity in VacA mediated Bid activation and mitochondrial targeting, we investigated the cellular location of Bid within AZ-521 cells that were intoxicated with VacA (250 nM), in the presence or absence of the N-acetyl-L-leucine-L-leucine-L-methionine peptide or ALLM (20 μM) (calbiochem), which is a specific chemical inhibitor of calpains (49). The cellular location of Bid within AZ-521 cells was predominantly cytosolic in the presence of ALLM, even after 4 h of intoxication with VacA (250 nM), as compared to visible localization of Bid-GFP puncta with the mitochondria in cells intoxicated with VacA in the absence of ALLM (Fig. 3.18). Our results therefore indicate that calpain function is required for the mitochondrial translocation of Bid.

3.3.9 VacA mediated rise in cytosolic calcium levels is important for cellular calpain activity and Bid processing.

Studies evaluating cellular effects of VacA within multiple cell lines have clearly demonstrated that VacA disrupts the cellular calcium homeostasis (17,

71). Calcium concentration within cells is tightly regulated (3, 7). Disruption of calcium homeostasis could result in activation of various calcium dependent enzymes and proteases, thereby activating the molecular switch initiating signaling processes whose effects range from alteration in gene expression to regulation of cellular metabolism and cell death. Notably, calpain activation is known to occur in the presence of elevated concentrations of calcium (45, 56). Additionally, calcium independent mechanism of calpain activation has also been reported (26, 60). Within this study, intoxication of AZ-521 cells with purified VacA (250 nM) resulted in significant rise in cytosolic calcium levels within 2 h of intoxication (Fig. 3.19). Furthermore, significant increases in cytosolic calcium levels was observed within 4 h following intoxication with VacA at concentrations as low as 10 nM, but not at 1 nM (Fig. 3.20). To evaluate the importance of VacA induced elevation of calcium levels in cellular calpain function, we monitored cellular calpain activity in the presence or absence of a specific cell membrane permeable chemical chelator of calcium called BAPTA-AM (Calbiochem). Following 4 h of VacA treatment, we observed a significant reduction in cellular calpain activity within cells intoxicated in the presence of BAPTA-AM than in the absence of the chelator (Fig. 3.21).

3.3.10 VacA induced rise in cellular calcium levels and calpain activity are important for toxin mediated Bax activation.

Our data thus far indicated that VacA induced processing of Bid to t-Bid is important for the activation of Bax and host cell death mechanism. Additionally,

we have shown that VacA mediated translocation of Bid to mitochondria is directly influenced by a calcium dependent calpain activation mechanism. To evaluate the role of cytosolic calcium rise in VacA induced Bax activation we monitored the levels of active Bax within AZ-521 cells intoxicated with VacA (250 nM) in the presence or absence of the cell permeable calcium chelator BAPTA-AM. Following 18 h of VacA treatment, we observed a significant reduction in cellular Bax activation within cells intoxicated in the presence of BAPTA-AM than in the absence of the chelator (Fig. 3.22). Furthermore, we observed a significant reduction in cell death within AZ-521 cells that were intoxicated with VacA (250 nM) for 24 h in the presence of BAPTA-AM than in the absence of the chelator (Fig. 3.23). Notably, we also observed a significant reduction in Bax activation (Fig. 3.24) within cells that were intoxicated with VacA (250 nM), for 18 h in the presence of the calpain inhibitor ALLM than in the absence of the inhibitor. These results are consistent with our model in which VacA induced elevation in cytosolic calcium levels is important for Bax activation through an increase in calpain mediated activation of Bid.

3.3.11 Drp1 activity is important for VacA mediated rise in cytosolic calcium levels and calpain activity.

Our data thus far characterizes the mechanism of VacA mediated activation of Bax, which involves the activation of Bid in a calcium and calpain dependent manner. We have also shown that processing of Bid to t-Bid was influenced by the activity of the mitochondrial fission factor, Drp1. However, it

was not clear whether Drp1 influences Bid activation through a mechanism involving calcium dependent calpain activation. To evaluate the relationship between cellular Drp1 activity and rise in calcium levels following VacA intoxication, we monitored cellular calcium levels within AZ-521 cells intoxicated with VacA (250 nM) in the presence or absence of the Drp1 inhibitor Mdivi-1. After 8 h of VacA treatment, we observed a significant reduction in cellular calcium levels within cells intoxicated in the presence of Mdivi-1 than in the absence of the inhibitor (Fig. 3.25). Consistent with the important role of cytosolic calcium in cellular calpain activity, we observed a significant reduction in calpain activity within cells that were intoxicated with VacA (250 nM) for 8 h in the presence of Mdivi-1 than in the absence of the inhibitor (Fig. 3.26). These data strongly suggest that Drp1 mediated fragmentation of mitochondrial network clearly influences the cellular calcium homeostasis, thereby resulting in calpain activation and processing of Bid to t-Bid.

3.4 DISCUSSION

Mitochondria, besides being the center for generation of metabolic energy within cells (22), are also known to function as central sensors and executioners of programmed cell death mechanism (5). The vacuolating cytotoxin produced by *Helicobacter pylori*, VacA, is known to directly target the mitochondria and activate mitochondrial cell death mechanism within host cells (23, 44, 73, 75). Studies evaluating the mechanism underlying VacA mediated cell death indicate a critical role of the multi-domain (BH1-3) pro-death effector Bax in the

permeabilization of the mitochondrial outer membrane, thereby committing the cell to undergo cell death (75). However, the exact mechanism underlying VacA induced Bax activation remained unclear. Previously, we showed that VacA intoxication resulted in excessive activation of the mitochondrial fission factor Drp1 within host cells, resulting in the deregulation of mitochondrial network dynamics, favoring increased mitochondrial fragmentation. Drp1 mediated mitochondrial fragmentation occurred within 1 h of VacA cellular intoxication and was important for subsequent Bax activation and induction of mitochondrial cell death mechanism (31). However, the molecular mechanism linking the early mitochondrial effects of VacA, i.e. mitochondrial dysfunction and network fragmentation, to subsequent activation of Bax and cellular commitment to undergo cell death remained unclear.

Current models of Bax activation indicate that changes in Bax leading to mitochondrial outer membrane permeabilization are critically influenced by members of the BH3 (Bcl-2 homology domain)-only Bcl2 (B cell lymphoma) family, which belong to either the “sensitizer” or “direct activator” class of BH3-only proteins (11). Within these models, key events that lead to activation of Bax involve either association of BH3 domain-only proteins to members of the anti-apoptotic Bcl2 proteins, thereby alleviating repression on Bax, or direct activation of Bax, leading to homo-oligomerization of Bax at the mitochondrial outer membrane. While “sensitizer” BH3 domain-only proteins activate Bax via binding with anti-apoptotic Bcl2 protein, “direct activator” BH3 domain-only proteins are

known to directly activate Bax oligomerization at the mitochondrial outer membrane.

Our results here indicate that VacA induced Bax activation is mediated by the activation and mitochondrial recruitment of the cellular stress sensor protein Bid (BH3 interacting death domain agonist) which belongs to the “direct activator” sub-family of BH3 domain-only proteins (72). The involvement of Bid in Bax activation, although widely reported, is dependent on the nature of death activating signal. For example, during T-cell apoptosis following staurosporine treatment (4), or TRAIL induced cell death within human rhabdomyosarcoma (RMS) cells (54), cellular Bax was activated by Cathepsin D or sphingosine, respectively, in a Bid-independent manner. However, in this study we have demonstrated that activation of Bid is critical to VacA induced Bax activation and cell death. Within Bid knock-out mouse embryonic fibroblasts, as well as in AZ-521 gastric epithelial cells where Bid levels were knocked down using Bid specific siRNA, we observed significant reduction in VacA induced Bax activation and cell death, suggesting a vital role of Bid in VacA induced mitochondrial cell death mechanism.

Unlike many Bcl-2 family proteins, full length Bid (fl-Bid), a 22 kDa protein, lacks the C-terminal hydrophobic membrane targeting domain and therefore is predominantly localized to the cytosol in healthy cells. However, following receipt of stress/death stimuli, fl-Bid is proteolytically processed by specific proteases to yield a smaller ~15 kDa NH_2-terminal truncated fragment, called t-Bid (truncated-Bid), which inserts into the mitochondrial outer membrane via the exposed

membrane interacting domain (65). The mitochondrial targeting of t-Bid has been shown to be important for Bax activation, possibly through direct interaction with Bax at the mitochondrial membrane (19, 70), but so far, the mechanism remains largely unclear. In certain instances, for example in mammary epithelial cells undergoing anoikis following detachment from extra-cellular matrix (ECM), membrane association of fl-Bid has also been reported (68). Therefore, the exact role of mitochondrial targeting of t-Bid in mitochondrial cell death mechanism is not entirely clear. Within our study we demonstrate that fl-Bid is processed to t-Bid within AZ-521 cells that were either infected with *Hp* or intoxicated with purified VacA. Furthermore, we show that t-Bid progressively targets the cellular mitochondria at time periods earlier to detectable mitochondrial outer membrane permeabilization within VacA treated cells. Importantly, experiments conducted with a small molecule Bid inhibitor, BI6C9, which specifically inhibits the targeting of t-Bid to mitochondria (2), significantly reduced Bax activation as well as the induction of cell death, indicating the importance of Bid activation and mitochondrial targeting in the activation of mitochondrial cell death mechanism following VacA intoxication.

How might Bid influence VacA's ability to induce Drp1 mediated mitochondrial fragmentation within cells, which we had earlier reported to be important for Bax activation (31)? The relationship between Bid induced mitochondrial damage and activation of mitochondrial fission mechanism is not very clear. Bid is shown to be required for induction of mitochondrial fission during oxidative stress induced mitochondrial damage (66). Similarly, Bik, an ER

localized BH3 domain-only protein was shown to induce Drp1 mediated inner mitochondrial cristae reorganization (25). Additionally, Drp1 was required for t-Bid dependent Bax oligomerization, but in a mechanism independent of Drp1 GTPase activity (47). However, it has also been reported that components of mitochondrial fission machinery are a part of multi-molecular signaling complexes within mitochondrial membrane in which t-Bid and Bax are recruited (24). Furthermore, BH3 peptides derived from Bid and Bim, another BH3 domain-only protein, were shown to be sufficient in inducing mitochondrial dysfunction and network fragmentation (61). Within our study, inhibition of mitochondrial translocation of Bid by the small molecule Bid inhibitor BI6C9 did not affect VacA induced mitochondrial fragmentation. However, inhibition of mitochondrial fission by the small molecule Drp1 inhibitor mdivi-1 visibly reduced the processing of fl-Bid to t-Bid following infection with *Hp*, as well as intoxication with purified VacA, indicating that mitochondrial fragmentation was required for Bid activation. While it was clear that Drp1 mediated mitochondrial fission occurred earlier to and was required for Bid activation, the underlying molecular mechanism remained unclear.

Studies so far have indicated that Bid processing can occur following processing by a variety of cellular proteases depending on the stress/death inducing signal. Cellular apoptosis initiated following the engagement of the Fas (CD-95 or APO-1) receptor results in the activation of initiator cysteine-aspartate protease, caspase 8 which acts residue Asp 59 of fl-Bid to generate t-Bid (62). Our studies indicated significant increase in the activation of caspase 8 following

VacA intoxication of AZ-521 cells, however caspase 8 activity was observed at time points much later to those observed for Bid processing and mitochondrial targeting, therefore ruling out the involvement of caspase-8 in the initiation of Bid processing. An alternate mechanism of Bid processing, typically observed under conditions of elevated cytosolic calcium levels involves the calcium dependent protease calpain, which processes fl-Bid between residues Gly-70 and Arg-71 (41). Within our study, we observed a significant increase in calpain activity following VacA intoxication, at time points similar to that observed for Bid activation. Importantly, inhibition of calpain function within cells resulted in significant decrease in the mitochondrial targeting of Bid, as well as Bax activation and cell death, underscoring the importance of calpain activity in VacA mediated mitochondrial cell death mechanism. Calpains are ubiquitous cytosolic cysteine proteases, which undergo conformational change following calcium binding that allows for proper realignment of the protease active-site residues (46). However, calcium independent mechanisms for calpain activation have also been reported (1). Studies conducted thus far to investigate the relationship between VacA and changes in cellular calcium homeostasis have primarily focused on effects of VacA intoxication in immune cells. VacA has been shown to induce rise in cytosolic calcium levels within RBL-2H3 mast cells (17) and human eosinophils (35), leading to production and secretion of pro-inflammatory cytokines and chemokines, respectively. Interestingly, VacA intoxication did not induce changes in cytosolic calcium levels within primary human B cells and Th cells (67). In fact, VacA prevented the influx of calcium from extracellular milieu

into intoxicated T-cells by virtue of VacA anion channels formed in the cell membrane (6). Therefore, the effect of VacA on cellular calcium homeostasis seems to depend on the type and function of the cells being studied. Within our study, we observed a significant increase in cytosolic calcium levels within 2 h of VacA intoxication in AZ-521 gastric epithelial cells. Importantly, chelation of cytosolic calcium by BAPTA-AM, resulted in significant inhibition of cellular calpain function, Bid processing, Bax activation and cell death. These results therefore indicate that early changes in cellular calcium levels play a critical role in the engagement of cellular apoptotic machinery following VacA treatment. Notably, we did not observe any significant increase in cytosolic calcium levels within AZ-521 cells that were intoxicated with VacA anion channel activity deficient mutants. Previously, we had reported that VacA anion channel forming ability is required for the toxin's ability to induce excessive activation of the cellular mitochondrial fission machinery, and was important for subsequent Bax activation and mitochondrial cell death mechanism (31). Our results thus far indicate that the deregulation of cellular calcium homeostasis and mitochondrial dynamics by membrane channels formed by VacA are critical for activation of cell death program within AZ-521 cells.

But what is the causal relationship between VacA induced rise in cytosolic calcium levels and activation of Drp1 mediated mitochondrial fission? Earlier studies have identified significant trafficking of calcium from ER to mitochondria through multiple contact sites between the organelles (52). In fact mitochondria are considered to play an important role in cellular calcium buffering. Additionally,

studies have indicated an important role of calcium in the maintenance of mitochondrial network dynamics within cells. Rise in cytosolic calcium levels has been shown to inhibit mitochondrial movement along microtubules, thereby mediating redistribution of the network (30, 59). Interestingly, mitochondrial calcium overload was shown to induce mitochondrial fission within prostate cancer cells (33). Studies investigating the molecular mechanism of calcium induced mitochondrial fission have demonstrated significant crosstalk between calcium dependent phosphatases or kinases, and Drp1. The activation of phosphatase calcineurin under conditions of sustained calcium increase has been shown to result in the activation of Drp1 through dephosphorylation at the Ser 637 residue within Drp1 (9). Also, the activation of CaMKIalpha following rise in cellular calcium was shown to mediate Drp1 activation through phosphorylation at Ser 600 residue within Drp1 (30). However, within our studies we observed that inhibition of mitochondrial fragmentation within cells resulted in a significant decrease in the ability of VacA to mediate an increase of cytosolic calcium levels, indicating that Drp1 mediated mitochondrial fission was required for increase in cellular calcium. The molecular mechanism underlying fission induced rise in cytosolic calcium is presently not clear. Earlier studies have revealed significant cross-talk between mitochondria and endoplasmic reticulum (ER) which is the main intra-cellular calcium store within a cell (18). The ER-mitochondria connections are known to play an important role in the buffering of cytosolic calcium levels (57, 58). Additionally, a recent study suggested that ER wraps around the mitochondria at specific contact sites (21). Furthermore, the

study also indicates that the fission protein Drp1 targets the mitochondria specifically at the contact sites with ER. It is therefore possible that increased fragmentation of the mitochondrial network may decrease ER-mitochondria cross-talk within cells due to loss of contact sites, therefore decreasing the calcium buffering capacity of the cell. It is also possible that Drp1 targeted to the ER-mitochondrial contact sites may actively participate in the remodeling of ER membranes, thereby mediating calcium release from ER. The role of ER-mitochondria association in VacA induced rise in cytosolic calcium is not yet clear and is currently under investigation.

Our study here provides critical insights into the mechanism by which VacA induces the activation of Bax, a critical mediator of mitochondrial cell death. Our data indicates that the activation and mitochondrial recruitment of the cell stress sensor protein Bid is critical to activation of Bax following VacA induced Drp1 mediated mitochondrial fission.

Figures

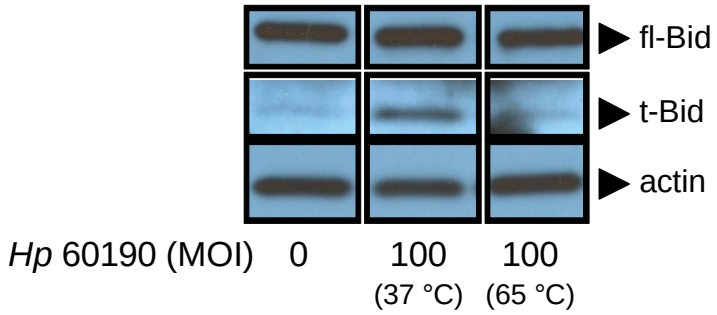

Figure 3.1 VacA is important for *Hp* induced Bid processing.

AZ-521 cells were incubated at 37 °C and under 5% CO_2 with *Hp* 60190 (MOI 100) that were pre-incubated at 37 °C or 65 °C for 30 min, or mock-infected with PBS pH 7.2. After 8 h, the cells were lysed and proteins within the whole cell lysates were resolved on a 15 % SDS-poly acrylamide gel, transferred onto 0.2 µm PVDF membranes and immnostained with polyclonal anti-Bid antibody to detect full-length Bid (Fl-Bid; 22 kDa) or truncated Bid (t-Bid; 15 kDa). Lysates were immunostained with monoclonal anti-actin antibody to confirm equal loading between wells. Data are representative of results obtained from 2 independent experiments.

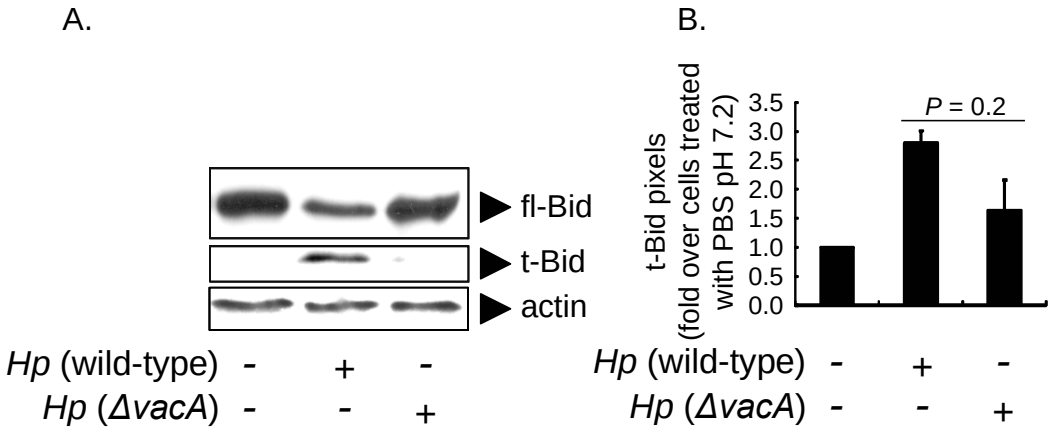

Figure 3.2 VacA is important for *Hp* induced Bid processing.

(A) AZ-521 cells were incubated at 37 °C and under 5% CO_2 with *Hp* 60190 and *Hp* VM022 (*ΔvacA*) or mock-infected with PBS pH 7.2. After 8 h, the cells were lysed and proteins within the whole cell lysates were resolved on a 15 % SDS-poly acrylamide gel, transferred onto 0.2 µm PVDF membranes and immnostained with polyclonal anti-Bid antibody to detect full-length Bid (Fl-Bid; 22 kDa) or truncated Bid (t-Bid; 15 kDa). Lysates were immunostained with monoclonal anti-actin antibody to confirm equal loading between wells. Data are representative of results obtained from 3 independent experiments.

(B) Densitometry analysis was carried out on the western blots using UN-SCAN-IT Gel analysis software (Silk Scientific, Orem, Utah). The pixel region of each t-Bid cross-reactive material band was analyzed, the background subtracted. Average pixels were determined over the course of 3 independent experiments. Error bars indicate standard deviations.

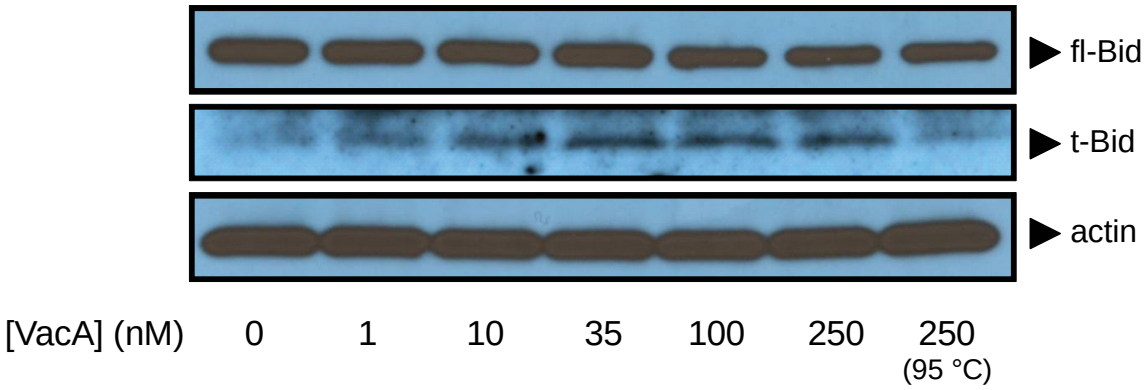

Figure 3.3 VacA induces Bid processing in AZ-521 cells.

AZ-521 cells were incubated at 37 °C and under 5% CO_2 with purified VacA (at the indicated concentrations) or with purified VacA (250 nM) pre-incubated at 95 °C, or mock-intoxicated with PBS pH 7.2. After 8 h, the cells were lysed and proteins within the whole cell lysates were resolved on a 15 % SDS-poly acrylamide gel, transferred onto 0.2 µm PVDF membranes and immnostained with polyclonal anti-Bid antibody to detect full-length Bid (Fl-Bid; 22 kDa) or truncated Bid (t-Bid; 15 kDa). Lysates were immunostained with monoclonal anti-actin antibody to confirm equal loading between wells. Data are representative of results obtained from 2 independent experiments.

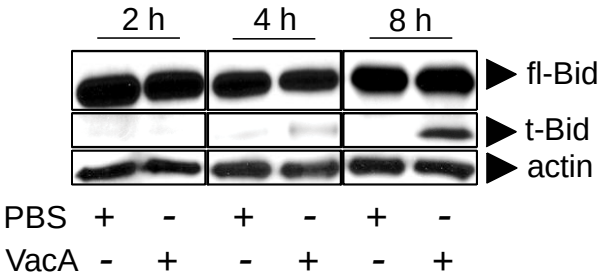

Figure 3.4 VacA induces Bid processing in AZ-521 cells within 4 h of intoxication.

AZ-521 cells were incubated at 37 °C and under 5% CO_2 with purified VacA (250 nM) or mock-intoxicated with PBS pH 7.2. At the indicated time periods, the cells were lysed and proteins within the whole cell lysates were resolved on a 15 % SDS-poly acrylamide gel, transferred onto 0.2 µm PVDF membranes and immnostained with polyclonal anti-Bid antibody to detect full-length Bid (Fl-Bid; 22 kDa) or truncated Bid (t-Bid; 15 kDa). Lysates were immunostained with monoclonal anti-actin antibody to confirm equal loading between wells. Data are representative of results obtained from 3 independent experiments.

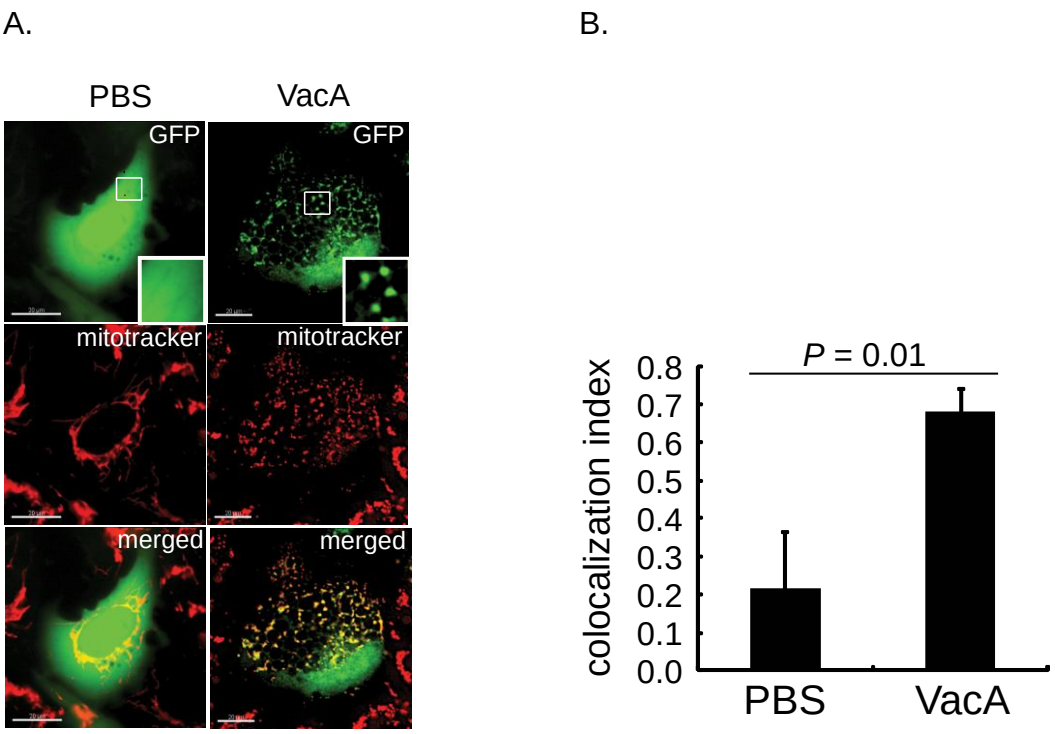

Figure 3.5 VacA intoxication results in the mitochondrial targeting of Bid.

(A) AZ-521 cells transfected with pBABE Bid-GFP and stained with mitotracker red were incubated at 37 °C and under 5% CO_2 with purified VacA (250 nM) or mock-intoxicated with PBS pH 7.2. After 4 h, the cellular location of Bid (green) and mitochondria (red) were visualized by DIC-epifluorescence microscopy. Images are representative of those collected from 3 independent experiments. Scale bar = 20 µm.

(B) Localization of Bid-GFP to mitochondria was quantified by co-localization analysis. The data are rendered as the average Bid-GFP-mitochondrial colocalization index obtained from combining data from three independent experiments. In each independent experiment, 15 randomly chosen, pBABE Bid GFP transfected cells were analyzed. Error bars indicate standard deviations. Statistical significance was calculated for differences in colocalization indices between cells mock-intoxicated with PBS pH 7.2 versus cells incubated with VacA.

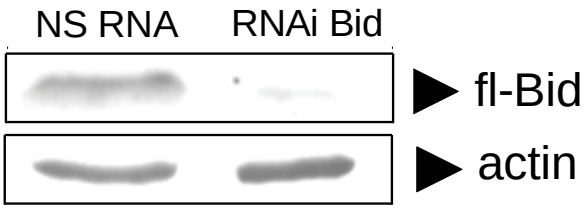

Figure 3.6 siRNA mediated knock-down of endogenous Bid expression in AZ-521 cells.

AZ-521 cells were transfected with Bid specific siRNA or a non-specific (scrambled) siRNA and incubated at 37 °C and under 5% CO_2. After 48 h, the cells were lysed and proteins within the whole cell lysates were resolved on a 15 % SDS-poly acrylamide gel, transferred onto 0.2 µm PVDF membranes and immnostained with polyclonal anti-Bid antibody to detect full-length Bid (Fl-Bid; 22 kDa). Lysates were immunostained with monoclonal anti-actin antibody to confirm equal loading between wells. Data are representative of results obtained from 2 independent experiments.

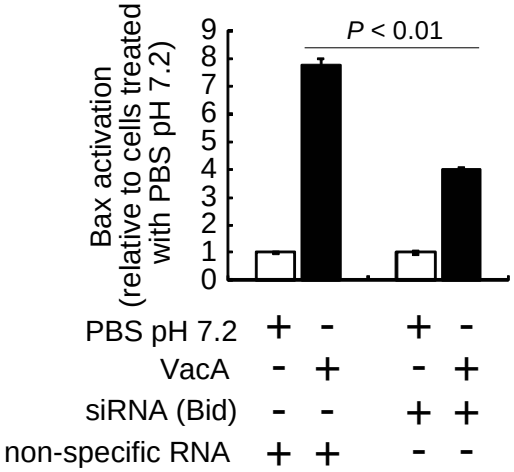

Figure 3.7 Bid is important for VacA induced Bax activation in AZ-521 cells.

AZ-521 cells were transfected with Bid specific siRNA or a non-specific (scrambled) siRNA and incubated at 37 °C and under 5% CO_2. After 48 h, the cells were incubated at 37 °C and under 5% CO_2 with VacA (250 nM) or mock-treated with PBS pH 7.2. After 18 h the cells were fixed, permeabilized and immunostained for active Bax. Cellular fluorescence, indicative of active Bax was quantified using flow cytometry. The data were combined from three independent experiments. Error bars indicate standard deviations. Statistical significance was calculated for differences in VacA induced Bax activation between non-specific siRNA transfected cells versus cells that were transfected with Bid specific siRNA.

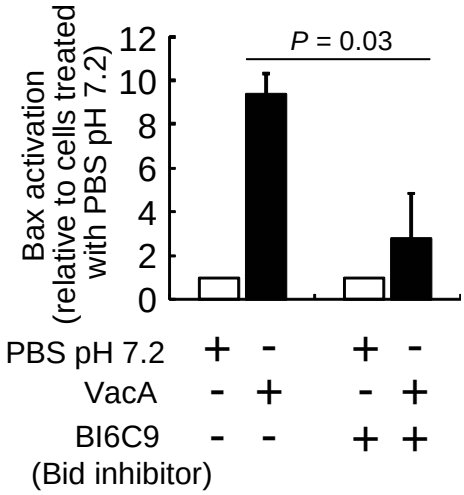

Figure 3.8 Mitochondrial targeting of Bid is important for VacA induced Bax activation in AZ-521 cells.

AZ-521 cells were incubated at 37 °C and under 5% CO_2 with VacA (250 nM) or mock-treated with PBS pH 7.2, in the presence or absence of the small molecule inhibitor of Bid, BI6C9 (25 µM). After 18 h the cells were fixed, permeabilized and immunostained for active Bax. Cellular fluorescence, indicative of active Bax was quantified using flow cytometry. The data were combined from three independent experiments. Error bars indicate standard deviations. Statistical significance was calculated for differences in Bax activation between cells treated with VacA in the absence of BI6C9 versus cells that were treated with VacA in the presence of BI6C9.

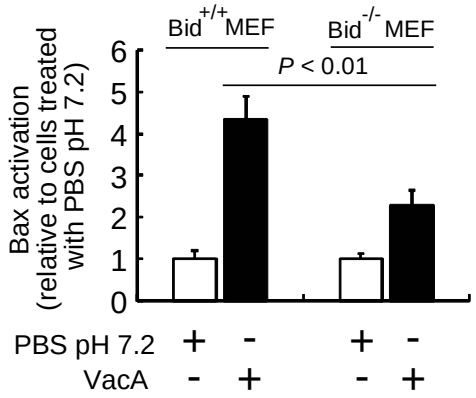

Figure 3.9 Bid is required for VacA induced Bax activation.

Wild-type and Bid knock-out mouse embryonic fibroblasts (MEFs) were incubated at 37 °C and under 5% CO_2 with purified VacA (250 nM). After 24 h, the cells were fixed, permeabilized and immunostained for active Bax. Cellular fluorescence, indicative of active Bax was quantified using flow cytometry. The data were combined from three independent experiments. Error bars indicate standard deviations. Statistical significance was calculated for differences in VacA induced Bax activation within wild-type MEFs versus Bid knock-out MEFs.

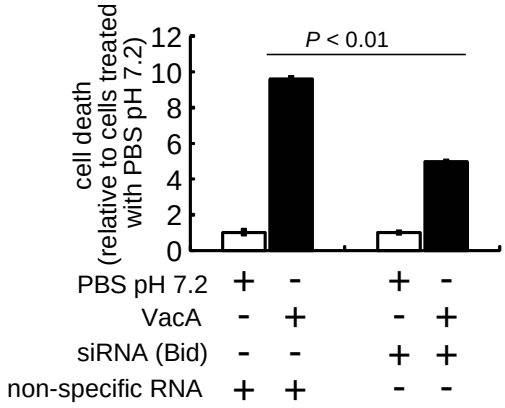

Figure 3.10 Bid is important for VacA induced cell death in AZ-521 cells.

AZ-521 cells were transfected with Bid specific siRNA or a non-specific (scrambled) siRNA and incubated at 37 °C and under 5% CO_2. After 48 h, the cells were incubated at 37 °C and under 5% CO_2 with VacA (250 nM) or mock-treated with PBS pH 7.2. After 24 h, cell death was determined using the Live-Dead viability/cytotoxicity assay kit and quantified using flow cytometry. The data were combined from three independent experiments. Error bars indicate standard deviations. Statistical significance was calculated for differences in VacA induced cell death between non-specific siRNA transfected cells versus cells that were transfected with Bid specific siRNA.

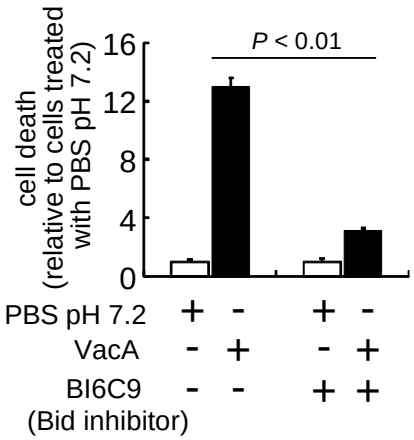

Figure 3.11 Mitochondrial targeting of Bid is important for VacA induced cell death in AZ-521 cells.

AZ-521 cells were incubated at 37 °C and under 5% CO_2 with VacA (250 nM) or mock-treated with PBS pH 7.2, in the presence or absence of the small molecule inhibitor of Bid, BI6C9 (25 µM). After 24 h, the percentage of dead cells was determined using the Live-Dead viability/cytotoxicity assay kit and quantified using flow cytometry. The data were combined from three independent experiments. Error bars indicate standard deviations. Statistical significance was calculated for differences in cell death between cells treated with VacA in the absence of BI6C9 versus cells that were treated with VacA in the presence of BI6C9.

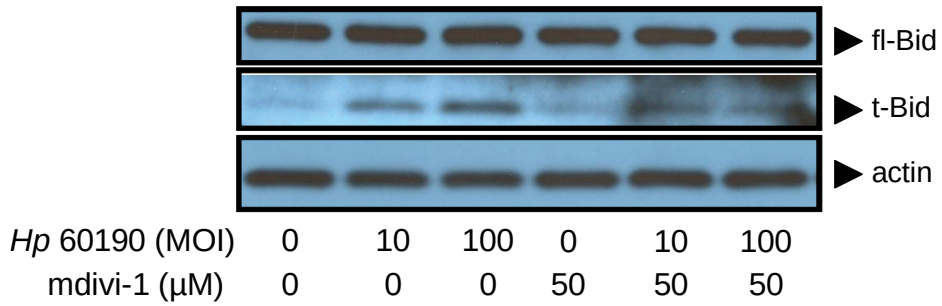

Figure 3.12 GTPase function of the cellular fission protein Drp1 is required for *Hp* induced Bid processing in AZ-521 cells.

AZ-521 cells were incubated at 37 °C and under 5% CO_2 with *Hp* 60190 (MOI 10 and 100) or mock-infected with PBS pH 7.2, in the presence or absence of the small molecule Drp1 inhibitor, mdivi-1. After 8 h, the cells were lysed and proteins within the whole cell lysates were resolved on a 15 % SDS-poly acrylamide gel, transferred onto 0.2 µm PVDF membranes and immnostained with polyclonal anti-Bid antibody to detect full-length Bid (Fl-Bid; 22 kDa) or truncated Bid (t-Bid; 15 kDa). Lysates were immunostained with monoclonal anti-actin antibody to confirm equal loading between wells. Data are representative of results obtained from 2 independent experiments.

Figure 3.13 GTPase function of the cellular fission protein Drp1 is required for VacA induced Bid processing in AZ-521 cells.

AZ-521 cells were incubated at 37 °C and under 5% CO_2 with purified VacA (250 nM) or mock-intoxicated with PBS pH 7.2, in the presence or absence of the small molecule Drp1 inhibitor, mdivi-1. After 8 h, the cells were lysed and proteins within the whole cell lysates were resolved on a 15 % SDS-poly acrylamide gel, transferred onto 0.2 µm PVDF membranes and immnostained with polyclonal anti-Bid antibody to detect full-length Bid (Fl-Bid; 22 kDa) or truncated Bid (t-Bid; 15 kDa). Lysates were immunostained with monoclonal anti-actin antibody to confirm equal loading between wells. Data are representative of results obtained from 2 independent experiments.

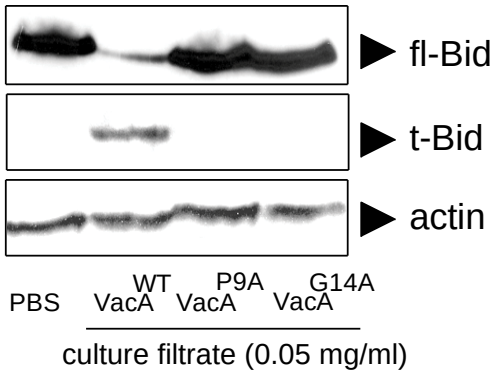

Figure 3.14 VacA anion channel function is required for Bid processing in AZ-521 cells.

AZ-521 cells were incubated at 37 °C and under 5% CO_2 with 0.5 mg/ml HPCF containing VacA (WT), VacA(P9A) or VacA(G14A) or mock-intoxicated with PBS pH 7.2. After 8 h, the cells were lysed and proteins within the whole cell lysates were resolved on a 15 % SDS-poly acrylamide gel, transferred onto 0.2 µm PVDF membranes and immnostained with polyclonal anti-Bid antibody to detect full-length Bid (Fl-Bid; 22 kDa) or truncated Bid (t-Bid; 15 kDa). Lysates were immunostained with monoclonal anti-actin antibody to confirm equal loading between wells. Data are representative of results obtained from 3 independent experiments.

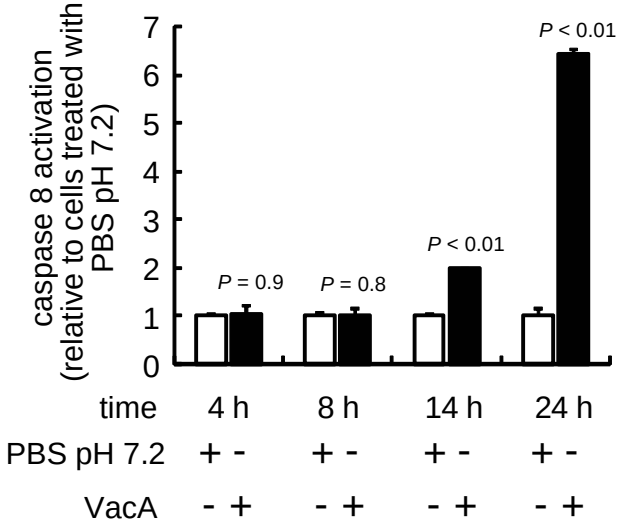

Figure 3.15 VacA intoxication results in caspase 8 activation.

AZ-521 cells were incubated at 37 °C and under 5% CO_2 with purified VacA (250 nM) or mock-intoxicated with PBS pH 7.2. At the indicated time periods, the cells were collected by brief trypsinization, washed 2 times with PBS pH 7.2 and incubated with CaspGLOW Fluorescein active caspase 8 staining kit (BioVision) for 30 min at 37 °C and under 5% CO_2 atmosphere, according to manufacturer's instructions. The fluorescein signal within cells was quantified by flow cytometry in the FL1 channel (525/40 nm band pass filter). 10,000 cells were analyzed for each sample. Error bars indicate standard deviations. Statistical significance was calculated for fold differences in mean fluorescence values between cells mock-intoxicated with PBS pH 7.2 versus cells incubated with VacA for each of the time periods tested.

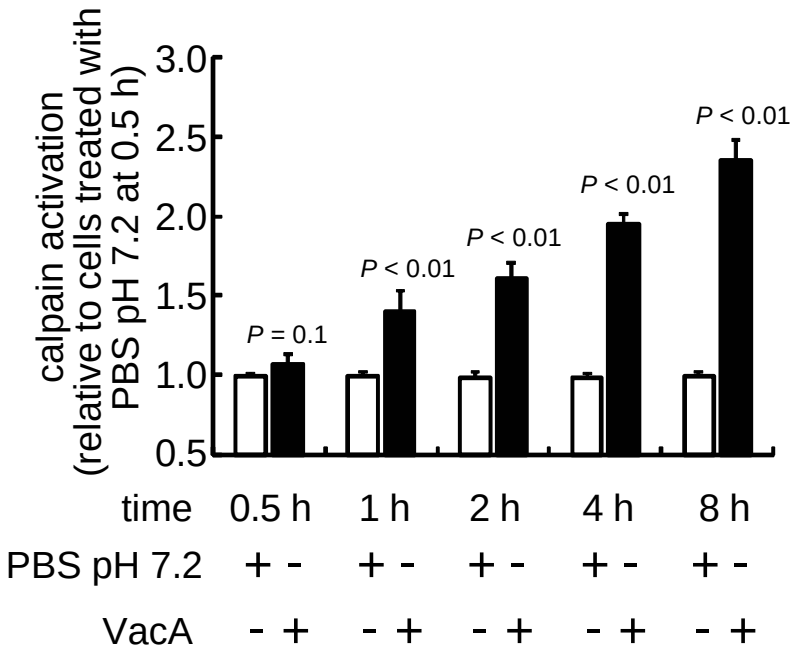

Figure 3.16 VacA induces increase in cellular calpain activity.

AZ-521 cells were incubated at 37 °C and under 5% CO_2 with purified VacA (250 nM) or mock-intoxicated with PBS pH 7.2, in the presence of fluorogenic calpain substrate t-Boc-LLVY-AMC to detect calpain activity. At the indicated time periods, generation of fluorogenic product AMC was quantified using a microplate reader with appropriate filters. The data are rendered as the fold change in relative fluorescence unit (RFU) in VacA treated cells, relative to cells treated with PBS pH 7.2 and were obtained from combining data from three independent experiments. Error bars indicate standard deviations. Statistical significance was calculated for fold differences in RFU between cells mock-intoxicated with PBS pH 7.2 versus cells incubated with VacA at each of the time periods tested.

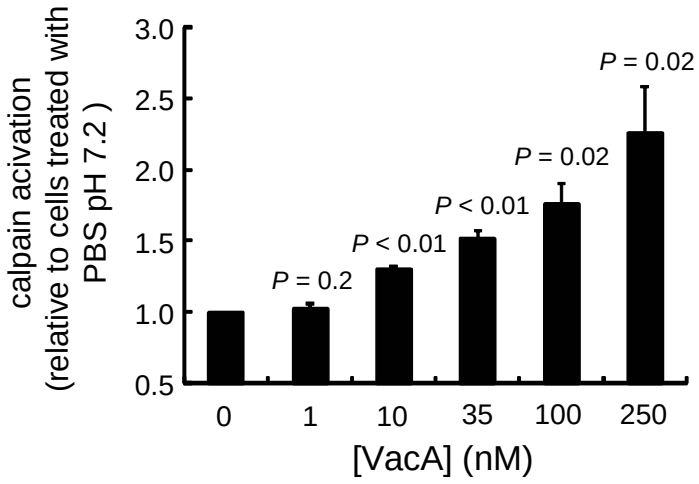

Figure 3.17 VacA induces increase in cellular calpain activity in a toxin dose dependent manner.

AZ-521 cells were incubated at 37 °C and under 5% CO_2 with purified VacA (at the indicated concentrations) or mock-intoxicated with PBS pH 7.2, in the presence of fluorogenic calpain substrate t-Boc-LLVY-AMC to detect calpain activity. After 4 h, the generation of fluorogenic product AMC was quantified using a microplate reader with appropriate filters. The data are rendered as the fold change in relative fluorescence unit (RFU) in VacA treated cells, relative to cells treated with PBS pH 7.2 and were obtained from combining data from three independent experiments. Error bars indicate standard deviations. Statistical significance was calculated for fold differences in RFU between cells mock-intoxicated with PBS pH 7.2 versus cells incubated with VacA for each of the concentrations tested.

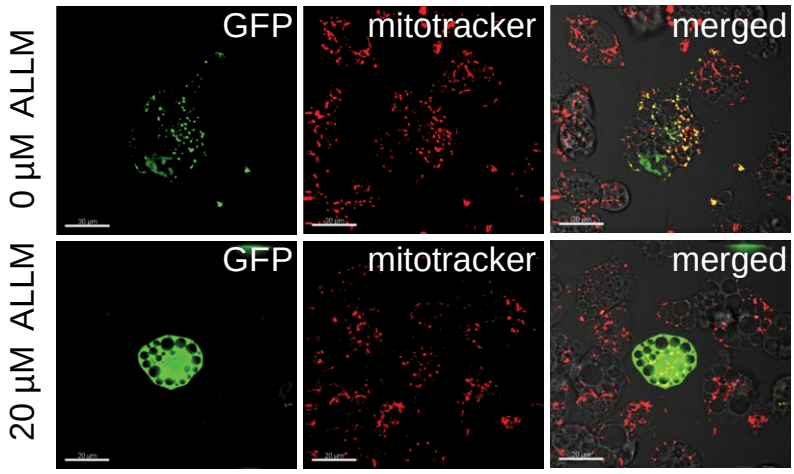

Figure 3.18 Calpain activity is important for VacA induced targeting of Bid to mitochondria.

AZ-521 cells transfected with pBABE Bid-GFP and stained with mitotracker red were incubated at 37 °C and under 5% CO_2 with purified VacA (250 nM) or mock-intoxicated with PBS pH 7.2, in the presence of absence of the calpain inhibitor ALLM (20 µM). After 4 h, the cellular location of Bid (green) and mitochondria (red) were visualized by DIC-epifluorescence microscopy. Images are representative of those collected from 3 independent experiments. Scale bar = 30 µm.

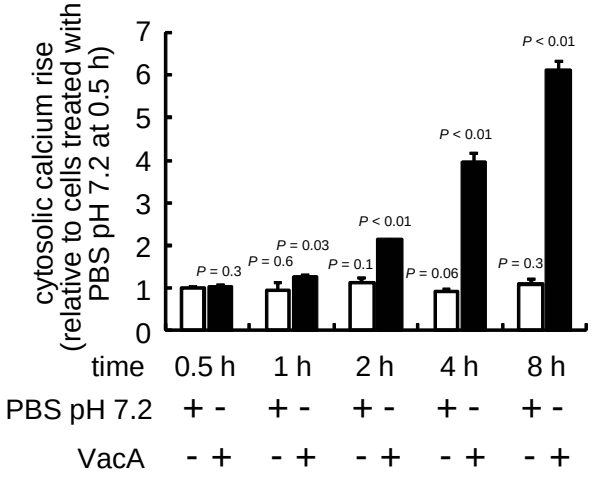

Figure 3.19 VacA induces rise in cytosolic calcium levels.

AZ-521 cells that were preloaded with calcium sensitive fluorescence probe Fluo-3 AM, were incubated at 37 °C and under 5% CO_2 with purified VacA (250 nM) or mock-intoxicated with PBS pH 7.2. At the indicated time periods, cellular fluorescence was quantified by flow cytometry in the FL1 channel (525/40 nm band pass filter). 10,000 cells were analyzed for each sample. Error bars indicate standard deviations. Statistical significance was calculated for fold differences in mean fluorescence values between cells mock-intoxicated with PBS pH 7.2 at 0.5 h versus cells incubated with PBS pH 7.2 or VacA for all the time periods tested.

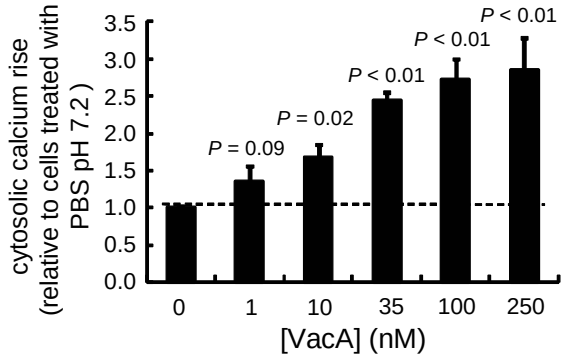

Figure 3.20 VacA induces rise in cytosolic calcium levels in a toxin dose dependent manner.

AZ-521 cells that were preloaded with calcium sensitive fluorescence probe Fluo-3 AM, were incubated at 37 °C and under 5% CO_2 with purified VacA (at the indicated concentrations) or mock-intoxicated with PBS pH 7.2. After 4 h, cellular fluorescence was quantified by flow cytometry in the FL1 channel (525/40 nm band pass filter). 10,000 cells were analyzed for each sample. Error bars indicate standard deviations. Statistical significance was calculated for fold differences in mean fluorescence values between cells mock-intoxicated with PBS pH 7.2 versus cells incubated with each of the indicated concentrations of VacA.

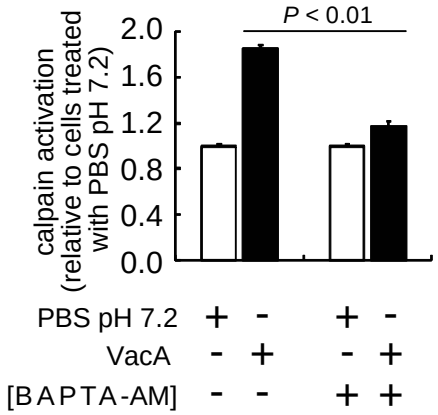

Figure 3.21 Cellular calcium is required for VacA induced calpain activation.

AZ-521 cells were incubated at 37 °C and under 5% CO_2 with purified VacA (250 nM) or mock-intoxicated with PBS pH 7.2, in the presence of the fluorogenic calpain substrate t-Boc-LLVY-AMC, as well as in the presence or absence of the cell permeable calcium chelator BAPTA-AM (10 µM). After 4 h, generation of fluorogenic product AMC was quantified using a microplate reader with appropriate filters. The data are rendered as the fold change in relative fluorescence unit (RFU) in VacA treated cells, relative to cells treated with PBS pH 7.2 and were obtained from combining data from two independent experiments. Error bars indicate standard deviations. Statistical significance was calculated for fold differences in RFU between cells intoxicated with VacA in the absence of BAPTA-AM versus cells intoxicated with VacA in the presence of BAPTA-AM.

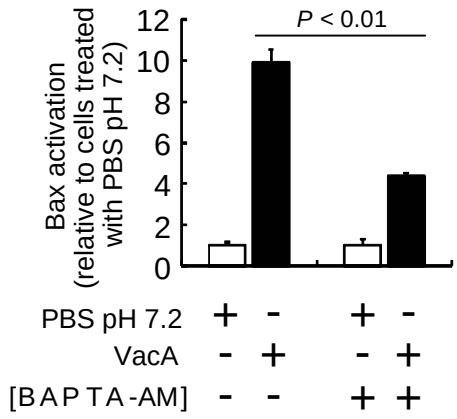

Figure 3.22 Cellular calcium is required for VacA induced Bax activation.

AZ-521 cells were incubated at 37 °C and under 5% CO_2 with purified VacA (250 nM) or mock-intoxicated with PBS pH 7.2, in the presence or absence of the calcium chelator BAPTA-AM (10 µM). After 18 h, the cells were fixed, permeabilized and immunostained for active Bax. Quantification of Bax activation was carried out by flow cytometry analysis. The data were rendered as the fold increase in Bax activation following VacA intoxication relative to cells mock-treated with PBS pH 7.2, obtained from combining data collected from three independent experiments, each conducted in triplicate. Error bars indicate standard deviations. Statistical significance was calculated for fold differences in Bax activation following VacA intoxication in the presence of BAPTA-AM versus the activation of Bax following VacA intoxication in the absence of BAPTA-AM.

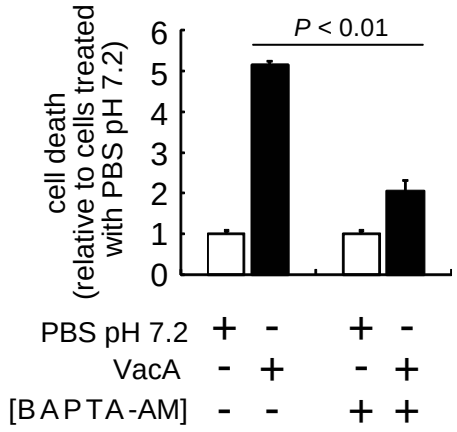

Figure 3.23 Cellular calcium is required for VacA induced cell death.

AZ-521 cells were incubated at 37 °C and under 5% CO_2 with purified VacA (250 nM) or mock-intoxicated with PBS pH 7.2, in the presence of the calcium chelator BAPTA-AM (10 µM). After 24 h, the cells were evaluated for cell death using Live-Dead viability/cytotoxicity assay kit. Quantification of cell death was carried out by flow cytometry analysis. The data were rendered as the fold increase in cell death following VacA intoxication relative to cells mock-treated with PBS pH 7.2, obtained from combining data collected from three independent experiments, each conducted in triplicate. Error bars indicate standard deviations. Statistical significance was calculated for fold differences in cell death following VacA intoxication in the presence of BAPTA-AM versus cell death induced following VacA intoxication in the absence of BAPTA-AM.

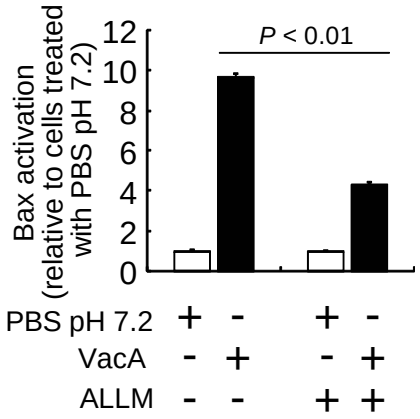

Figure 3.24 Cellular calpain activity is required for VacA induced Bax activation.

AZ-521 cells were incubated at 37 °C and under 5% CO_2 with purified VacA (250 nM) or mock-intoxicated with PBS pH 7.2, in the presence of the calpain inhibitor ALLM (20 µM). After 18 h, the cells were fixed, permeabilized and immunostained for active Bax. Quantification of Bax activation was carried out by flow cytometry analysis. The data were rendered as the fold increase in Bax activation following VacA intoxication relative to cells mock-treated with PBS pH 7.2. Error bars indicate standard deviations. Statistical significance was calculated for fold differences in Bax activation following VacA intoxication in the presence of ALLM versus the activation of Bax following VacA intoxication in the absence of ALLM.

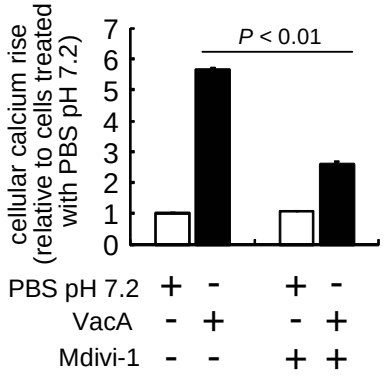

Figure 3.25 Drp1 activity is required for VacA induced rise in cytosolic calcium.

AZ-521 cells that were preloaded with calcium sensitive fluorescence probe Fluo-3 AM, were incubated at 37 °C and under 5% CO_2 with purified VacA (at the indicated concentrations) or mock-intoxicated with PBS pH 7.2, in the presence or absence of the Drp1 inhibitor mdivi-1 (50 µM). After 4 h, cellular fluorescence was quantified by flow cytometry in the FL1 channel (525/40 nm band pass filter). 10,000 cells were analyzed for each sample. Error bars indicate standard deviations. Statistical significance was calculated for fold differences in mean fluorescence values between cells intoxicated with VacA in the presence of mdivi-1 versus those intoxicated with VacA in the absence of mdivi-1.

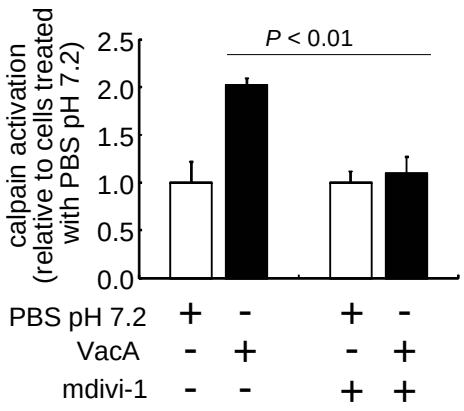

Figure 3.26 Drp1 activity is required for VacA induced activation of cellular calpain.

AZ-521 cells were incubated at 37 °C and under 5% CO_2 with purified VacA (at the indicated concentrations) or mock-intoxicated with PBS pH 7.2, in the presence of fluorogenic calpain substrate t-Boc-LLVY-AMC, as well as in the presence or absence of the Drp1 inhibitor mdivi-1 (50 µM). After 4 h, the generation of fluorogenic product AMC was quantified using a microplate reader with appropriate filters. The data are rendered as the fold change in relative fluorescence unit (RFU) in VacA treated cells, relative to cells treated with PBS pH 7.2 and were obtained from combining data from two independent experiments. Error bars indicate standard deviations. Statistical significance was calculated for fold differences in RFU between cells intoxicated with VacA in the presence of mdivi-1 versus those intoxicated with VacA in the absence of mdivi-1.

References

1. **Arora, A. S., P. de Groen, Y. Emori, and G. J. Gores.** 1996. A cascade of degradative hydrolase activity contributes to hepatocyte necrosis during anoxia. Am J Physiol **270:**G238-45.

2. **Becattini, B., C. Culmsee, M. Leone, D. Zhai, X. Zhang, K. J. Crowell, M. F. Rega, S. Landshamer, J. C. Reed, N. Plesnila, and M. Pellecchia.** 2006. Structure-activity relationships by interligand NOE-based design and synthesis of antiapoptotic compounds targeting Bid. Proc Natl Acad Sci U S A **103:**12602-6.

3. **Berridge, M. J., M. D. Bootman, and H. L. Roderick.** 2003. Calcium signalling: dynamics, homeostasis and remodelling. Nat Rev Mol Cell Biol **4:**517-29.

4. **Bidere, N., H. K. Lorenzo, S. Carmona, M. Laforge, F. Harper, C. Dumont, and A. Senik.** 2003. Cathepsin D triggers Bax activation, resulting in selective apoptosis-inducing factor (AIF) relocation in T lymphocytes entering the early commitment phase to apoptosis. J Biol Chem **278:**31401-11.

5. **Blanke, S. R.** 2005. Micro-managing the executioner: pathogen targeting of mitochondria. Trends Microbiol **13:**64-71.

6. **Boncristiano, M., S. R. Paccani, S. Barone, C. Ulivieri, L. Patrussi, D. Ilver, A. Amedei, M. M. D'Elios, J. L. Telford, and C. T. Baldari.** 2003. The *Helicobacter pylori* vacuolating toxin inhibits T cell activation by two independent mechanisms. J Exp Med **198:**1887-97.

7. **Brini, M., and E. Carafoli.** 2011. The plasma membrane Ca(2)+ ATPase and the plasma membrane sodium calcium exchanger cooperate in the regulation of cell calcium. Cold Spring Harb Perspect Biol **3**.

8. **Calore, F., C. Genisset, A. Casellato, M. Rossato, G. Codolo, M. D. Esposti, L. Scorrano, and M. de Bernard.** 2010. Endosome-mitochondria juxtaposition during apoptosis induced by *H. pylori* VacA. Cell Death Differ **17:**1707-16.

9. **Cereghetti, G. M., A. Stangherlin, O. Martins de Brito, C. R. Chang, C. Blackstone, P. Bernardi, and L. Scorrano.** 2008. Dephosphorylation by calcineurin regulates translocation of Drp1 to mitochondria. Proc Natl Acad Sci U S A **105:**15803-8.

10. **Chen, M., H. He, S. Zhan, S. Krajewski, J. C. Reed, and R. A. Gottlieb.** 2001. Bid is cleaved by calpain to an active fragment in vitro and during myocardial ischemia/reperfusion. J Biol Chem **276:**30724-8.

11. **Chipuk, J. E., and D. R. Green.** 2008. How do BCL-2 proteins induce mitochondrial outer membrane permeabilization? Trends Cell Biol **18:**157-64.

12. **Cover, T. L., and S. R. Blanke.** 2005. *Helicobacter pylori* VacA, a paradigm for toxin multifunctionality. Nat Rev Microbiol **3:**320-32.

13. **Cover, T. L., and M. J. Blaser.** 2009. *Helicobacter pylori* in health and disease. Gastroenterology **136:**1863-73.

14. **Cover, T. L., P. I. Hanson, and J. E. Heuser.** 1997. Acid-induced dissociation of VacA, the *Helicobacter pylori* vacuolating cytotoxin, reveals its pattern of assembly. J Cell Biol **138:**759-69.

15. **Cover, T. L., U. S. Krishna, D. A. Israel, and R. M. Peek, Jr.** 2003. Induction of gastric epithelial cell apoptosis by *Helicobacter pylori* vacuolating cytotoxin. Cancer Res **63:**951-7.

16. **Cover, T. L., W. Puryear, G. I. Perez-Perez, and M. J. Blaser.** 1991. Effect of urease on HeLa cell vacuolation induced by *Helicobacter pylori* cytotoxin. Infect Immun **59:**1264-70.

17. **de Bernard, M., A. Cappon, L. Pancotto, P. Ruggiero, J. Rivera, G. Del Giudice, and C. Montecucco.** 2005. The *Helicobacter pylori* VacA cytotoxin activates RBL-2H3 cells by inducing cytosolic calcium oscillations. Cell Microbiol **7:**191-8.

18. **de Brito, O. M., and L. Scorrano.** 2010. An intimate liaison: spatial organization of the endoplasmic reticulum-mitochondria relationship. EMBO J **29:**2715-23.

19. **Desagher, S., A. Osen-Sand, A. Nichols, R. Eskes, S. Montessuit, S. Lauper, K. Maundrell, B. Antonsson, and J. C. Martinou.** 1999. Bid-induced conformational change of Bax is responsible for mitochondrial cytochrome *c* release during apoptosis. J Cell Biol **144:**891-901.

20. **Eskes, R., S. Desagher, B. Antonsson, and J. C. Martinou.** 2000. Bid induces the oligomerization and insertion of Bax into the outer mitochondrial membrane. Mol Cell Biol **20:**929-35.

21. **Friedman, J. R., L. L. Lackner, M. West, J. R. DiBenedetto, J. Nunnari, and G. K. Voeltz.** 2011. ER tubules mark sites of mitochondrial division. Science **334:**358-62.

22. **Fulda, S., L. Galluzzi, and G. Kroemer.** 2010. Targeting mitochondria for cancer therapy. Nat Rev Drug Discov **9:**447-64.

23. **Galmiche, A., J. Rassow, A. Doye, S. Cagnol, J. C. Chambard, S. Contamin, V. de Thillot, I. Just, V. Ricci, E. Solcia, E. Van Obberghen, and P. Boquet.** 2000. The N-terminal 34 kDa fragment of *Helicobacter pylori* vacuolating cytotoxin targets mitochondria and induces cytochrome c release. EMBO J **19:**6361-70.

24. **Garofalo, T., A. M. Giammarioli, R. Misasi, A. Tinari, V. Manganelli, L. Gambardella, A. Pavan, W. Malorni, and M. Sorice.** 2005. Lipid microdomains contribute to apoptosis-associated modifications of mitochondria in T cells. Cell Death Differ **12:**1378-89.

25. **Germain, M., J. P. Mathai, H. M. McBride, and G. C. Shore.** 2005. Endoplasmic reticulum BIK initiates DRP1-regulated remodelling of mitochondrial cristae during apoptosis. EMBO J **24:**1546-56.

26. **Glading, A., F. Uberall, S. M. Keyse, D. A. Lauffenburger, and A. Wells.** 2001. Membrane proximal ERK signaling is required for M-calpain activation downstream of epidermal growth factor receptor signaling. J Biol Chem **276:**23341-8.

27. **Gross, A., X. M. Yin, K. Wang, M. C. Wei, J. Jockel, C. Milliman, H. Erdjument-Bromage, P. Tempst, and S. J. Korsmeyer.** 1999. Caspase cleaved BID targets mitochondria and is required for cytochrome *c* release, while BCL-XL prevents this release but not tumor necrosis factor-R1/Fas death. J Biol Chem **274:**1156-63.

28. **Gupta, V. R., H. K. Patel, S. S. Kostolansky, R. A. Ballivian, J. Eichberg, and S. R. Blanke.** 2008. Sphingomyelin functions as a novel receptor for *Helicobacter pylori* VacA. PLoS Pathog **4:**e1000073.

29. **Gupta, V. R., B. A. Wilson, and S. R. Blanke.** 2010. Sphingomyelin is important for the cellular entry and intracellular localization of *Helicobacter pylori* VacA. Cell Microbiol **12:**1517-33.

30. **Han, X. J., Y. F. Lu, S. A. Li, T. Kaitsuka, Y. Sato, K. Tomizawa, A. C. Nairn, K. Takei, H. Matsui, and M. Matsushita.** 2008. CaM kinase I alpha-induced phosphorylation of Drp1 regulates mitochondrial morphology. J Cell Biol **182:**573-85.

31. **Jain, P., Z. Q. Luo, and S. R. Blanke.** 2011. *Helicobacter pylori* vacuolating cytotoxin A (VacA) engages the mitochondrial fission machinery to induce host cell death. Proc Natl Acad Sci U S A **108:**16032-7.

32. **Jones, N. L., A. S. Day, H. Jennings, P. T. Shannon, E. Galindo-Mata, and P. M. Sherman.** 2002. Enhanced disease severity in *Helicobacter pylori*-infected mice deficient in Fas signaling. Infect Immun **70:**2591-7.

33. **Kaddour-Djebbar, I., V. Choudhary, C. Brooks, T. Ghazaly, V. Lakshmikanthan, Z. Dong, and M. V. Kumar.** 2010. Specific mitochondrial calcium overload induces mitochondrial fission in prostate cancer cells. Int J Oncol **36:**1437-44.

34. **Kim, H., M. Rafiuddin-Shah, H. C. Tu, J. R. Jeffers, G. P. Zambetti, J. J. Hsieh, and E. H. Cheng.** 2006. Hierarchical regulation of mitochondrion-dependent apoptosis by BCL-2 subfamilies. Nat Cell Biol **8:**1348-58.

35. **Kim, J. M., J. S. Kim, J. Y. Lee, Y. S. Sim, Y. J. Kim, Y. K. Oh, H. J. Yoon, J. S. Kang, J. Youn, N. Kim, H. C. Jung, and S. Kim.** 2010. Dual effects of *Helicobacter pylori* vacuolating cytotoxin on human eosinophil apoptosis in early and late periods of stimulation. Eur J Immunol **40:**1651-62.

36. **Kohler, B., S. Anguissola, C. G. Concannon, M. Rehm, D. Kogel, and J. H. Prehn.** 2008. Bid participates in genotoxic drug-induced apoptosis of HeLa cells and is essential for death receptor ligands' apoptotic and synergistic effects. PLoS One **3:**e2844.

37. **Korsmeyer, S. J., M. C. Wei, M. Saito, S. Weiler, K. J. Oh, and P. H. Schlesinger.** 2000. Pro-apoptotic cascade activates BID, which oligomerizes BAK or BAX into pores that result in the release of cytochrome *c*. Cell Death Differ **7:**1166-73.

38. **Kuck, D., B. Kolmerer, C. Iking-Konert, P. H. Krammer, W. Stremmel, and J. Rudi.** 2001. Vacuolating cytotoxin of *Helicobacter pylori* induces apoptosis in the human gastric epithelial cell line AGS. Infect Immun **69:**5080-7.

39. **Li, H., H. Zhu, C. J. Xu, and J. Yuan.** 1998. Cleavage of BID by caspase 8 mediates the mitochondrial damage in the Fas pathway of apoptosis. Cell **94:**491-501.

40. **Luo, X., I. Budihardjo, H. Zou, C. Slaughter, and X. Wang.** 1998. Bid, a Bcl2 interacting protein, mediates cytochrome *c* release from mitochondria in response to activation of cell surface death receptors. Cell **94:**481-90.

41. **Mandic, A., K. Viktorsson, L. Strandberg, T. Heiden, J. Hansson, S. Linder, and M. C. Shoshan.** 2002. Calpain-mediated Bid cleavage and calpain-independent Bak modulation: two separate pathways in cisplatin-induced apoptosis. Mol Cell Biol **22:**3003-13.

42. **McClain, M. S., P. Cao, H. Iwamoto, A. D. Vinion-Dubiel, G. Szabo, Z. Shao, and T. L. Cover.** 2001. A 12-amino-acid segment, present in type s2 but not type s1 *Helicobacter pylori* VacA proteins, abolishes cytotoxin activity and alters membrane channel formation. J Bacteriol **183:**6499-508.

43. **McClain, M. S., H. Iwamoto, P. Cao, A. D. Vinion-Dubiel, Y. Li, G. Szabo, Z. Shao, and T. L. Cover.** 2003. Essential role of a GXXXG motif for membrane channel formation by *Helicobacter pylori* vacuolating toxin. J Biol Chem **278:**12101-8.

44. **Menaker, R. J., P. J. Ceponis, and N. L. Jones.** 2004. *Helicobacter pylori* induces apoptosis of macrophages in association with alterations in the mitochondrial pathway. Infect Immun **72:**2889-98.

45. **Moldoveanu, T., C. M. Hosfield, D. Lim, J. S. Elce, Z. Jia, and P. L. Davies.** 2002. A Ca(2+) switch aligns the active site of calpain. Cell **108:**649-60.

46. **Moldoveanu, T., Z. Jia, and P. L. Davies.** 2004. Calpain activation by cooperative Ca2+ binding at two non-EF-hand sites. J Biol Chem **279:**6106-14.

47. **Montessuit, S., S. P. Somasekharan, O. Terrones, S. Lucken-Ardjomande, S. Herzig, R. Schwarzenbacher, D. J. Manstein, E. Bossy-Wetzel, G. Basanez, P. Meda, and J. C. Martinou.** 2010. Membrane remodeling induced by the dynamin-related protein Drp1 stimulates Bax oligomerization. Cell **142:**889-901.

48. **Moss, S. F., J. Calam, B. Agarwal, S. Wang, and P. R. Holt.** 1996. Induction of gastric epithelial apoptosis by *Helicobacter pylori*. Gut **38:**498-501.

49. **Nottrott, S., J. Schoentaube, H. Genth, I. Just, and R. Gerhard.** 2007. *Clostridium difficile* toxin A-induced apoptosis is p53-independent but depends on glucosylation of Rho GTPases. Apoptosis **12:**1443-53.

50. **O'Connor, P. M., T. K. Lapointe, S. Jackson, P. L. Beck, N. L. Jones, and A. G. Buret.** 2011. *Helicobacter pylori* activates calpain via toll-like receptor 2 to disrupt adherens junctions in human gastric epithelial cells. Infect Immun **79:**3887-94.

51. **Ott, M., E. Norberg, B. Zhivotovsky, and S. Orrenius.** 2009. Mitochondrial targeting of tBid/Bax: a role for the TOM complex? Cell Death Differ **16:**1075-82.

52. **Patergnani, S., J. M. Suski, C. Agnoletto, A. Bononi, M. Bonora, E. De Marchi, C. Giorgi, S. Marchi, S. Missiroli, F. Poletti, A. Rimessi, J. Duszynski, M. R. Wieckowski, and P. Pinton.** 2011. Calcium signaling around Mitochondria Associated Membranes (MAMs). Cell Commun Signal **9:**19.

53. **Peek, R. M., Jr., H. P. Wirth, S. F. Moss, M. Yang, A. M. Abdalla, K. T. Tham, T. Zhang, L. H. Tang, I. M. Modlin, and M. J. Blaser.** 2000. *Helicobacter pylori* alters gastric epithelial cell cycle events and gastrin secretion in Mongolian gerbils. Gastroenterology **118:**48-59.

54. **Petak, I., R. Vernes, K. S. Szucs, M. Anozie, K. Izeradjene, L. Douglas, D. M. Tillman, D. C. Phillips, and J. A. Houghton.** 2003. A caspase-8-independent component in TRAIL/Apo-2L-induced cell death in human rhabdomyosarcoma cells. Cell Death Differ **10:**729-39.

55. **Reiners, J. J., Jr., J. A. Caruso, P. Mathieu, B. Chelladurai, X. M. Yin, and D. Kessel.** 2002. Release of cytochrome *c* and activation of pro-caspase-9 following lysosomal photodamage involves Bid cleavage. Cell Death Differ **9:**934-44.

56. **Reverter, D., S. Strobl, C. Fernandez-Catalan, H. Sorimachi, K. Suzuki, and W. Bode.** 2001. Structural basis for possible calcium-induced activation mechanisms of calpains. Biol Chem **382:**753-66.

57. **Rizzuto, R., M. Brini, M. Murgia, and T. Pozzan.** 1993. Microdomains with high Ca2+ close to IP3-sensitive channels that are sensed by neighboring mitochondria. Science **262:**744-7.

58. **Rizzuto, R., P. Pinton, W. Carrington, F. S. Fay, K. E. Fogarty, L. M. Lifshitz, R. A. Tuft, and T. Pozzan.** 1998. Close contacts with the endoplasmic reticulum as determinants of mitochondrial Ca2+ responses. Science **280:**1763-6.

59. **Saotome, M., D. Safiulina, G. Szabadkai, S. Das, A. Fransson, P. Aspenstrom, R. Rizzuto, and G. Hajnoczky.** 2008. Bidirectional Ca2+-dependent control of mitochondrial dynamics by the Miro GTPase. Proc Natl Acad Sci U S A **105:**20728-33.

60. **Shiraha, H., A. Glading, J. Chou, Z. Jia, and A. Wells.** 2002. Activation of m-calpain (calpain II) by epidermal growth factor is limited by protein kinase A phosphorylation of m-calpain. Mol Cell Biol **22:**2716-27.

61. **Shroff, E. H., C. M. Snyder, G. R. Budinger, M. Jain, T. L. Chew, S. Khuon, H. Perlman, and N. S. Chandel.** 2009. BH3 peptides induce mitochondrial fission and cell death independent of BAX/BAK. PLoS One **4:**e5646.

62. **Slee, E. A., S. A. Keogh, and S. J. Martin.** 2000. Cleavage of BID during cytotoxic drug and UV radiation-induced apoptosis occurs downstream of the point of Bcl-2 action and is catalysed by caspase-3: a potential feedback loop for amplification of apoptosis-associated mitochondrial cytochrome c release. Cell Death Differ **7:**556-65.

63. **Stoka, V., B. Turk, S. L. Schendel, T. H. Kim, T. Cirman, S. J. Snipas, L. M. Ellerby, D. Bredesen, H. Freeze, M. Abrahamson, D. Bromme, S. Krajewski, J. C. Reed, X. M. Yin, V. Turk, and G. S. Salvesen.** 2001. Lysosomal protease pathways to apoptosis. Cleavage of bid, not pro-caspases, is the most likely route. J Biol Chem **276:**3149-57.

64. **Sutton, V. R., J. E. Davis, M. Cancilla, R. W. Johnstone, A. A. Ruefli, K. Sedelies, K. A. Browne, and J. A. Trapani.** 2000. Initiation of apoptosis by granzyme B requires direct cleavage of bid, but not direct granzyme B-mediated caspase activation. J Exp Med **192:**1403-14.

65. **Tait, S. W., E. de Vries, C. Maas, A. M. Keller, C. S. D'Santos, and J. Borst.** 2007. Apoptosis induction by Bid requires unconventional ubiquitination and degradation of its N-terminal fragment. J Cell Biol **179:**1453-66.

66. **Tobaben, S., J. Grohm, A. Seiler, M. Conrad, N. Plesnila, and C. Culmsee.** 2011. Bid-mediated mitochondrial damage is a key mechanism in glutamate-induced oxidative stress and AIF-dependent cell death in immortalized HT-22 hippocampal neurons. Cell Death Differ **18:**282-92.

67. **Torres, V. J., S. E. VanCompernolle, M. S. Sundrud, D. Unutmaz, and T. L. Cover.** 2007. *Helicobacter pylori* vacuolating cytotoxin inhibits activation-induced proliferation of human T and B lymphocyte subsets. J Immunol **179:**5433-40.

68. **Valentijn, A. J., and A. P. Gilmore.** 2004. Translocation of full-length Bid to mitochondria during anoikis. J Biol Chem **279:**32848-57.

69. **Vinion-Dubiel, A. D., M. S. McClain, D. M. Czajkowsky, H. Iwamoto, D. Ye, P. Cao, W. Schraw, G. Szabo, S. R. Blanke, Z. Shao, and T. L. Cover.** 1999. A dominant negative mutant of *Helicobacter pylori* vacuolating toxin (VacA) inhibits VacA-induced cell vacuolation. J Biol Chem **274:**37736-42.

70. **Walensky, L. D., K. Pitter, J. Morash, K. J. Oh, S. Barbuto, J. Fisher, E. Smith, G. L. Verdine, and S. J. Korsmeyer.** 2006. A stapled BID BH3 helix directly binds and activates BAX. Mol Cell **24:**199-210.

71. **Wang, F., P. Xia, F. Wu, D. Wang, W. Wang, T. Ward, Y. Liu, F. Aikhionbare, Z. Guo, M. Powell, B. Liu, F. Bi, A. Shaw, Z. Zhu, A. Elmoselhi, D. Fan, T. L. Cover, X. Ding, and X. Yao.** 2008. *Helicobacter pylori* VacA disrupts apical membrane-cytoskeletal interactions in gastric parietal cells. J Biol Chem **283:**26714-25.

72. **Wang, K., X. M. Yin, D. T. Chao, C. L. Milliman, and S. J. Korsmeyer.** 1996. BID: a novel BH3 domain-only death agonist. Genes Dev **10:**2859-69.

73. **Willhite, D. C., and S. R. Blanke.** 2004. *Helicobacter pylori* vacuolating cytotoxin enters cells, localizes to the mitochondria, and induces mitochondrial membrane permeability changes correlated to toxin channel activity. Cell Microbiol **6:**143-54.

74. **Willhite, D. C., T. L. Cover, and S. R. Blanke.** 2003. Cellular vacuolation and mitochondrial cytochrome *c* release are independent outcomes of *Helicobacter pylori* vacuolating cytotoxin activity that are each dependent on membrane channel formation. J Biol Chem **278:**48204-9.

75. **Yamasaki, E., A. Wada, A. Kumatori, I. Nakagawa, J. Funao, M. Nakayama, J. Hisatsune, M. Kimura, J. Moss, and T. Hirayama.** 2006. *Helicobacter pylori* vacuolating cytotoxin induces activation of the proapoptotic proteins Bax and Bak, leading to cytochrome *c* release and cell death, independent of vacuolation. J Biol Chem **281:**11250-9.

Chapter 4: Characterization of mitochondrial outer membrane permeabilization and nature of cell death following intoxication of AZ-521 gastric epithelial cells with VacA

4.1 INTRODUCTION

Infection with the gastric pathogen *H. pylori* is routinely associated with host cell mitochondrial damage and activation of programmed cell death within gastric epithelial cells (5, 19, 23, 25, 27, 32, 34, 39). For *Hp*, an increase in cell death within the gastric mucosa may alter the host niche in several ways, including the loss of specialized cells, such as gastric parietal cells, but also an increase in cellular proliferation, and gastric atrophy that precedes metaplasia, dysplasia, and ultimately cancer (7, 8). Earlier studies have clearly identified the vacuolating cytotoxin (VacA) as a critical mediator of *H. pylori* induced host cell death. VacA induces mitochondrial damage which results in the activation of mitochondria dependent cell death mechanism. In fact, studies have indicated that VacA is both essential (21) and sufficient (10) to activate the mitochondrial cell death mechanism within the host cells. VacA has been shown to induce an early depolarization of mitochondria, resulting in mitochondrial dysfunction, followed by the release of the pro-death effector Cyt *c* from mitochondrial intermembrane space to cytosol (36), which is an important step that irreversibly commits the cell to undergo cell death. Interestingly, although VacA was shown to be sufficient in inducing mitochondrial depolarization, it requires the cellular pro-death effector Bax to induce mitochondrial outer membrane permeabilization

and activation of downstream cell death mechanism (38). However, the extent to which VacA induces damage at the mitochondrial outer membrane, as well as the nature of cell death mechanism induced following VacA intoxication is not completely understood.

Based on morphological and biochemical features exhibited by a dying cell, several modalities of cell death have been described which include caspase dependent and independent apoptosis, programmed necrosis, autophagic cell death and mitotic catastrophe (16). Induction of programmed cell death or apoptosis following pathogen infection provides the pathogen with means to remodel the host environment by inducing cell death in an immunologically silent manner. Studies have identified distinct cellular changes which act as markers that enable the differentiation of apoptotic cell death from other forms of cell death. A widely used marker used in identifying apoptotic cells is the exposure of Phosphatidylserine (PtdSer or PS) from the inner leaflet of plasma membrane, to the outer leaflet in apoptotic cells (14, 15), which can be fluorescently tagged using fluorescently tagged Annexin V, a protein known to bind with high affinity to PS (29). Annexin V labeling of PS is commonly used in combination with the DNA binding fluorescent dye propidium iodide, which enters cells following plasma membrane permeabilization during late stages of apoptosis (18). Our studies here demonstrate a time and VacA dose dependent increase in PS exposure, as well as plasma membrane permeabilization within VacA intoxicated AZ-521 cells. These results therefore indicate that VacA induces the activation of programmed cell death or apoptosis. Additionally, we demonstrate that the

presence of the weak base ammonium chloride (NH_4Cl) in cell culture medium potentiated VacA mediated exposure of PS, as well as permeabilization of plasma membrane within host cells.

Studies to characterize the extent of VacA induced mitochondrial damage demonstrated that VacA induced extensive permeabilization of mitochondrial outer membrane (MOMP) within AZ-521 cells. VacA induced mitochondrial outer membrane permeabilization resulted in the release of multiple pro-death effectors from the mitochondrial inter-membrane space including Cytochrome *c*, Smac/DIABLO (Second mitochondria derived activator of caspase) and AIF (Apoptosis inducing factor). However, Cyt *c* and Smac/DIABLO were released into the cytosol considerably earlier than AIF, indicating that the release of pro-death effectors from mitochondria was temporally regulated. While Cyt *c* and Smac/DIABLO are known mediators of caspase dependent cell death mechanism (31), AIF is known to translocate directly to the nucleus and induce DNA damage resulting in cell death in a caspase independent manner (22, 30). Consistent with the known consequences of Cyt *c* and Smac/DIABLO release from mitochondrial inter-membrane space to cytosol, we demonstrate significant activation of both initiator caspases 8 and 9, as well as the effector caspase 3 following VacA induced mitochondrial outer membrane permeabilization. Notably, the release of pro-death effectors from mitochondria to cytosol, as well as activation of caspases is further indicative of apoptotic cell death mechanism.

The induction of cell death at the site of infection can sometimes be beneficial for the invading pathogen, allowing efficient colonization and

persistence, as well as access to nutrients from the dead cells. Furthermore, mitochondrial damage and cell death could incapacitate the innate and adaptive immune responses mounted against the pathogen. Our data indicates that VacA induces the activation of apoptotic cell death program within host cells through extensive, but regulated permeabilization of mitochondrial outer membrane.

4.2 MATERIALS AND METHODS

Bacterial Strains. *Hp* 60190 (*cag* PAI^{+}*, vacA* s1/m1; 49503; ATCC; Manassas, VA) was cultured in bisulfite- and sulfite-free brucella broth (BSFB) containing 5 μg vancomycin/mL (Sigma Aldrich; St. Louis, MO), on a rotary platform shaker for 48 h at 37 °C, under 5% CO_2 and 10% O_2.

Cell Lines. AZ-521 cells (3940; Japan Health Science Foundation) were maintained in minimum essential medium (MEM; Sigma Aldrich), which when supplemented with glutamine (2 mM), penicillin (100 U/mL), streptomycin sulfate (1 mg/mL) (Sigma Aldrich) and 10% fetal bovine calf serum (JRH Biosciences; Lenexa, KS), was referred to as “supplemented MEM”. The cells were maintained at 37 °C within a humidified atmosphere and under 5% CO_2.

VacA Purification. *Helicobacter pylori* 60190 were cultured, and VacA was purified from HPCF as described previously (9).

Determination of Cell Death. AZ-521 cells were cultured overnight at a seeding density of $2X10^5$ cells/ml in 37 °C and under 5% CO_2 atmosphere and were treated with purified VacA at indicated concentrations or mock-intoxicated with PBS pH 7.2. At the indicated time periods, the cells were collected by brief trypsinization, washed 2 times with PBS pH 7.2 and incubated with Annexin-V conjugated to alexa fluor 488 and propidium iodide provided in the apoptosis detection kit (Molecular probes, V13241) and analyzed by flow cytometry in the FL1 and FL3 channels respectively. Live and dead cell were differentiated as follows: Viable cells (Annexin V-, PI -), early apoptotic cells (Annexin V+, PI -) and late apoptotic cells (Annexin V+, PI +). Cell counts in all samples were normalized to 10000 cells.

Quantitative measurement of VacA mediated mitochondrial IMS factor release. AZ-521 cells were cultured overnight at a seeding density of $2X10^5$ cells/ml in 37 °C and under 5% CO_2 atmosphere and were treated with purified VacA at indicated concentrations or mock-intoxicated with PBS pH 7.2. At the indicated time periods, the cells were permeabilized with 0.05% digitonin (500 µg/ml in PBS pH 7.2 with 100 mM KCl) for 10 min on ice. Cells were fixed in 4% paraformaldehyde for 20 min at room temperature, washed 2 times in PBS pH 7.2 and incubated in blocking buffer (3% BSA and 0.05% saponin in PBS pH 7.2) for 1h. Cells were incubated for overnight at 4 °C with anti-Cyt *c* antibody (6H2.B4) (BD Biosciences), anti-AIF antibody (Epitomics) and anti-Smac/DIABLO FITC antibody (Assay Designs) in blocking buffer. Cells were

washed twice in PBS pH 7.2 and incubated with goat anti rabbit IgG (H+L) alexa 488 conjugate (Molecular probes) to quantify AIF and with goat anti mouse IgG (H+L) alexa 488 conjugate (Molecular probes) to quantify Cyt *c*, for 1h at room temperature. Alexa 488 and FITC fluorescence was quantified by flow cytometry in the FL1 channel. Cells with low alexa 488 fluorescence were regarded as having increased cytoplasmic levels of Cyt *c* or AIF and cells with low FITC fluorescence were regarded as having increased cytoplasmic levels of Smac/DIABLO. Cells with high fluorescence were regarded as having intact mitochondrial outer membrane with little to no release of mitochondrial IMS factors into the cytosol. Cell counts in all samples were normalized to 10000 cells.

Quantitative measurement of VacA mediated cellular caspase activation. AZ-521 cells were cultured overnight at a seeding density of $2X10^5$ cells/ml in 37 °C and under 5% CO_2 atmosphere and were treated with purified VacA at indicated concentrations or mock-intoxicated with PBS pH 7.2. At the indicated time periods, the cells were collected by brief trypsinization, washed 2 times with PBS pH 7.2 and incubated with CaspGLOW Fluorescein active caspase 8, 9 or 3 staining kit (BioVision) for 30 min at 37 °C and under 5% CO_2 atmosphere, according to manufacturer's instructions. The cells were washed 3 times with PBS pH 7.2 and the fluorescein signal was quantified by flow cytometry in the FL1 channel (525/40 nm band pass filter). 10,000 cells were analyzed for each sample.

Flow Cytometry. Analytical flow cytometry was carried out using a BD FACSCanto II flow analyzer (BD Biosciences) located at the R. J. Carver Biotechnology Center Flow Cytometry Facility (University of Illinois at Urbana-Champaign). The flow cytometer was equipped with 70-μm nozzle, 488 nm line of an air-cooled argon-ion laser, and 400 mV output. The band pass filters used for analysis were 525/40 nm, 575/30 nm and 675/30 nm. Cell analysis was standardized for scatter and fluorescence by using a suspension of fluorescent beads (Beckman Coulter; Miami, FL). Events were recorded on a log fluorescence scale and the geometric mean as well as percent events was determined using FCS Express analysis software (De Novo Software; Los Angeles, CA). Forward and side scatter properties were considered to exclude non-cellular (debris) events from viable and (or) dead cell populations.

Statistical Analysis. Unless otherwise indicated, each experiment was performed at least three independent times. For those data requiring statistical analysis, data were combined from 2 or 3 independent experiments, as indicated, with each independent experiment carried out in triplicate. Statistical analyses were performed using Microsoft Excel (Version 11.0; Microsoft Corporation; Redmond, WA). Unless otherwise noted, error bars represent standard deviations. All *P* values were calculated with the Student's *t* test using paired, two-tailed distribution. $P < 0.05$ indicates statistical significance.

4.3 RESULTS

4.3.1 VacA induces the activation of apoptotic cell death mechanism within AZ-521 gastric epithelial cells.

In order to explore the mechanism underlying VacA mediated cell death, we evaluated AZ-521 cells for the presence of known markers of cellular apoptosis. Early indications of cellular apoptosis involve the dramatic increase in the exposure of Phosphatidylserine (PtdSer or PS), normally found in the inner leaflet of plasma membrane, to the outer leaflet in apoptotic cells (14, 15). The exposure of PS occurs very early during apoptosis and enables recognition of apoptotic cells by phagocytes through interaction with specific receptors on phagocyte cell surface. Interestingly, cells in early stages of apoptosis still retain their membrane integrity. However, the integrity of plasma membrane becomes increasingly compromised during late stages of apoptotic cell death. We therefore evaluated the presence of the markers of early and late stages of apoptosis in AZ-521 cells. Monolayers of AZ-521 cells were incubated at 37 °C, and under 5% CO_2 with purified VacA (250 nM) or PBS pH 7.2. After 24 h, the cells were stained with alexa 488 conjugated Annexin V, a Ca^{2+} dependent PS binding protein, to detect PS exposed on cell surface, as well as the DNA binding dye Propidium Iodide (PI), that specifically enters the cells in which the membrane integrity is compromised. Cells with increased Annexin V labeling alone indicated early apoptosis, and cells with increased labeling with both Annexin V and PI indicated late apoptosis. We observed a significant increase in

Annexin V labeling and PI uptake within cells intoxicated with purified VacA, compared to cells that were treated with PBS pH 7.2 alone, suggesting that VacA induced the activation of apoptotic cell death mechanism (Fig. 4.1). Additionally, significant increases in Annexin V labeling and PI uptake was observed in cells intoxicated with purified VacA at concentration as low as 10 nM, but not at 1 nM (Fig. 4.2).

4.3.2 Role of serum (10% FBS) in VacA induced cellular apoptosis.

To evaluate the requirements of VacA induced cell death in AZ-521 cells, we investigated the relationship between serum (10% FBS) present in the cell culture medium and the capacity of the toxin to induce cellular apoptosis. Notably, an earlier study had demonstrated that a high molecular weight factor present within Fetal calf serum (FCS) attenuated the binding of VacA to its putative receptor RPTP-β on the surface of AZ-521 cells, thereby significantly inhibiting toxin mediated cellular vacuolation (20). In order to evaluate the relationship between VacA induced cell death and serum, AZ-521 cells were incubated at 37 °C, and under 5% CO_2 for overnight in cell culture medium containing 10 % FBS and following 3 washes with PBS pH 7.2, the cells were incubated at 37 °C, and under 5% CO_2 with either fresh medium containing 10% FBS or with medium devoid of serum. After 30 min, the cells were further incubated with purified VacA (250 nM) or PBS pH 7.2. After 24 h, the cells were stained with alexa fluor 488 conjugated Annexin V, as well as Propidium Iodide (PI). We observed a significant increase in Annexin V labeling and PI uptake

within cells intoxicated with purified VacA at concentrations as low as 10 nM, both in the presence and absence of 10% FBS, compared to cells that were treated with PBS pH 7.2 alone (Fig. 4.3). However, the role of serum in VacA induced activation of cell death remains in-conclusive due to the lack of a clear trend within the preliminary data obtained so far (Fig. 4.3).

4.3.3 VacA induced activation of cellular apoptosis is potentiated in the presence of ammonium chloride (NH_4Cl).

Previous studies have also reported that the degree of cellular vacuolation is enhanced in the presence of ammonium chloride (11, 24), which is proposed to enhance the swelling of the vacuoles induced by VacA. To explore whether ammonium chloride also enhances VacA mediated apoptosis, AZ-521 cells were incubated at 37 °C, and under 5% CO_2 with different concentrations of purified VacA or with PBS pH 7.2, in the presence or absence of 5 mM ammonium chloride. After 24 h, the cells were stained with alexa fluor 488 conjugated Annexin V, as well as Propidium Iodide (PI). We observed a significant decrease in Annexin V labeling and PI uptake within cells intoxicated with purified VacA at concentrations as low as 10 nM, in the absence of ammonium chloride than in the presence of ammonium chloride (Fig. 4.4). Our data therefore indicates that ammonium chloride is important for efficient induction of cell death within AZ-521 cells following VacA intoxication.

4.3.4 VacA induces extensive permeabilization of mitochondrial outer membrane, resulting in the release of multiple pro-apoptotic effectors from mitochondrial inter-membrane space to cytosol.

Mitochondrial inter-membrane space (IMS) is a storehouse for multiple cell death effector proteins like Cytochrome *c* (Cyt *c*), Second mitochondria derived activator of caspase (Smac/DIABLO) and Apoptosis inducing factor (AIF). After release into the cytosol, these proteins activate cell death pathways, by both caspase dependent and independent mechanisms. While Cyt *c* (4) and Smac/DIABLO (13) are known to participate in caspase dependent cell death pathways, AIF is known to translocate directly to the nucleus and induce DNA damage resulting in cell death in a caspase independent manner (33). Cyt *c* release is considered as a critical step for the activation of cellular caspases like caspase 3 and caspase 9, the release of other IMS factors like Smac/DIABLO has been shown to further enhance Cyt *c* mediated caspase activation, by relieving inhibition of caspase activity by a group of proteins called Inhibitor of Apoptosis proteins or IAPs (13). Moreover, in certain cases of cell death, activation of caspases also leads to further increase in MOMP and causes the release of additional IMS factors like AIF (2, 17), which can further potentiate cell death in a caspase-independent manner. The extent of permeabilization of the mitochondrial outer membrane (MOMP) therefore determines not only the rate at which cell death is induced, but also the mechanism of cell death that follows the release of any or all of the IMS proteins. To determine the extent of VacA mediated MOMP and to explore the role of MOMP as a possible mechanism of

VacA induced cell death, we studied the release Cyt *c*, Smac/DIABLO and AIF following incubation of cells with VacA. AZ-521 cells were incubated at 37 °C, and under 5% CO_2 with purified VacA or PBS pH 7.2. The cells were differentially permeabilized to wash off the cytosolic contents, while maintaining the integrity of the mitochondrial membranes. The cells were fixed, mitochondrial membrane permeabilized and immunostained for Cyt *c* and AIF using primary antibodies against each of these proteins, followed by detection with secondary antibody conjugated to alexa fluor 488 dye. Detection of Smac/DIABLO was carried out by intracellular staining with anti-Smac/DIABLO antibody conjugated to FITC (Assay Designs). A decrease in alexa-488 and FITC fluorescence indicated the release of proteins from mitochondrial IMS into cytosol. These experiments revealed that VacA induced extensive permeabilization of mitochondrial outer membrane, resulting in the release of Cyt *c*, Smac/DIABLO and AIF from the mitochondrial intermembrane space to cytosol (Fig. 4.5). Furthermore, these results also suggest that VacA induced cell death probably involves both caspase dependent and independent mechanisms.

It has been reported that MOMP as a result of certain death stimuli can be a highly regulated process and can lead to activation of diverse cell death pathways depending on the release of specific IMS factors to the cytosol. In order to explore the relationship between Cyt *c* release and the release of other IMS factors and their role in VacA induced cell death, we studied VacA induced Cyt *c* release and release of other mitochondrial IMS factors like Smac/DIABLO, and AIF, at different VacA concentrations after 24 h of intoxication. AZ-521 cells

were incubated at 37 °C, and under 5% CO_2 with increasing concentrations of purified VacA or PBS pH 7.2. After 24 h, the cells were immunostained as described earlier for Cyt *c* and AIF using primary antibodies against each of these proteins, followed by detection with secondary antibody conjugated to alexa fluor 488 dye. The release of Smac/DIABLO was quantified by intracellular staining of AZ-521 cells with anti-Smac/DIABLO-FITC conjugated antibody (Assay Designs), followed by monitoring the FITC fluorescence within cells by flow cytometry. Our data indicated a progressive increase in the release of Cyt *c*, Smac/DIABLO and AIF in a VacA dose dependent manner (Fig. 4.6 A-C). These data therefore suggest that VacA intoxication results in extensive release of mitochondrial inter-membrane space effectors to cytosol.

4.3.5 VacA induced permeabilization of mitochondrial outer membrane results in a temporally regulated release of different mitochondrial inter-membrane space effectors to the cytosol.

In order to further characterize the relationship between Cyt *c* release and the release of other IMS factors and their role in VacA induced cell death, we studied the temporal relationship between VacA induced Cyt *c* release and the release of Smac/DIABLO and AIF, at different time periods following VacA intoxication. AZ-521 cells were incubated at 37 °C, and under 5% CO_2 with purified VacA (250 nM) or PBS pH 7.2 for different time periods followed by analysis of Cyt *c*, Smac/DIABLO and AIF release. Our data indicate that VacA induced MOMP results in release of Cyt *c* and Smac/DIABLO much earlier to AIF

release (Fig. 4.7). We hypothesize that Cyt *c* and Smac/DIABLO release could probably result in activation of cellular proteases such as caspases or cysteine proteases like calpains that could result in further permeabilization of mitochondrial outer membrane and release of AIF, which could further enhance the activation of mitochondria dependent cell death mechanism.

4.3.6 VacA induces activation of caspases 8, 9 and 3 within AZ-521 cells.

Our earlier results suggested that VacA induces the activation of a caspase dependent cell death mechanism. We therefore wished to directly evaluate the activation of caspases 8, 9 and 3 within AZ-521 cells following VacA intoxication. Caspases 8 and 9 belong to the “Initiator” family of caspases, which are activated during the “death receptor” mediated cell death mechanism and “mitochondrial” cell death mechanism, respectively. Caspase 3 belongs to the “Executioner” family of caspases, and is activated by the “Initiator” caspase 8 or 9 (26, 37). AZ-521 cells were incubated at 37 °C, and under 5% CO_2 with increasing concentration of purified VacA or PBS pH 7.2. After 18 h, the cells were incubated with CaspGLOW in situ caspase staining reagent, specific for each of caspase 8, 9 or 3. The assay utilized specific caspase inhibitors that were conjugated with Fluorescein Isothiocyanate (FITC), which bound specifically with only the active caspases within each cell. Increase in caspase activity therefore resulted in increased FITC labeling of the cell, which could be quantified by flow cytometry. We observed a significant, VacA dose dependent increase in the activation of Caspase 8, 9 and 3 within AZ-521 cells intoxicated

with VacA, compared to cells treated with PBS pH 7.2 (Fig.4.8). Our data therefore indicated that VacA intoxication resulted in cellular caspase activation.

4.4 DISCUSSION

Our experiments support the model that VacA induces cell death primarily through an apoptotic mechanism. Cells exposed to VacA almost always demonstrated exposure of phosphatidyl serine to the outer leaflet of plasma membrane, as well as increase in plasma membrane permeability by 24 h. We could not detect an appreciable number of cells with increased PI uptake in the absence of PS exposure, which could occur by non-apoptotic mechanisms.

Previous studies have reported that the supplementation of 5 mM ammonium chloride in the tissue culture medium significantly enhances the degree of cellular vacuolation within VacA intoxicated cells (11, 24). We therefore evaluated the effects of ammonium chloride on VacA induced cell death. In the absence of ammonium chloride, significant decrease in VacA induced PS exposure and PI uptake were observed when compared to cells that were intoxicated with VacA in the presence of ammonium chloride. These results indicate that the presence of 5 mM ammonium chloride was required for efficient activation of cellular apoptosis following VacA intoxication. The presence of serum has also been shown to influence the cellular effects of VacA intoxication. An earlier study indicated that VacA induced cellular vacuolation was potentiated under reduced serum concentrations (12). This study hypothesized that VacA associates with an unidentified serum component, thereby reducing the effective

concentration of the active molecule. However, inhibitory effects of serum were seen only at VacA concentrations below 10 nM. Furthermore, it has been demonstrated that a high molecular weight factor present within Fetal calf serum (FCS) attenuated the binding of VacA to its putative receptor RPTP-β on the surface of AZ-521 cells, thereby significantly inhibiting toxin mediated cellular vacuolation (20). However, the results of our experiments studying the effect of serum on VacA induced cell death have so far been inconclusive. Preliminary data, thus far, have not indicated a significant difference in the ability of VacA to induce cell death in the presence or absence of serum.

An important consequence of VacA induced mitochondrial damage is the permeabilization of mitochondrial outer membrane (MOMP) and release of Cyt *c* from the mitochondrial inter membrane space to cytosol. The release of Cyt *c* is required for the formation of the multi-protein complex called apoptosome which acts as a platform for caspase activation, and therefore commits the cell to undergo cell death (1). Besides Cyt *c*, the mitochondrial inter membrane space is also a reservoir of other pro-death effectors like Smac/DIABLO (Second mitochondria derived activator of caspase) and AIF (Apoptosis inducing factor). While Cyt *c* and Smac/DIABLO are known to participate in caspase dependent cell death pathways, AIF is known to translocate directly to the nucleus and induce DNA damage resulting in cell death in a caspase independent manner (22). Although the mechanism of VacA induced MOMP and Cyt *c* release has been studied earlier, the extent of mitochondrial outer membrane permeabilization was not entirely understood. Our study demonstrates that VacA

induced mitochondrial outer membrane permeabilization resulted in release of Smac/DIABLO, as well as AIF, in addition to Cyt *c*. Consistent with the role of Cyt *c* and Smac/DIABLO in caspase activation within cells, we observed significant increases in the activation of caspases 8, 9 and 3 within VacA intoxicated AZ-521 cells. Interestingly, AIF release was observed at considerably later time periods when compared to the release of Cyt *c* and Smac/DIABLO. Earlier studies have indicated the involvement of the cellular protease calpain in AIF release from mitochondria (6, 28), although calpain independent AIF release has also been reported (35). Additionally, AIF release from mitochondria is also shown to be mediated by caspase activation (3). Our studies have demonstrated that VacA intoxication results in significant increases in cellular calpain activity within 1 h of intoxication (Chapter 3) as well as caspase activation within AZ-521 cells. However, the involvement of either calpains or caspases in VacA induced AIF release within AZ-521 cells is not entirely clear and would be evaluated in future studies.

Our data demonstrates that VacA induces extensive and temporally regulated permeabilization of mitochondrial outer membrane, resulting in the release of multiple pro-death effectors to the cytosol. These results suggest the involvement of both caspase-dependent and -independent cell death mechanisms in VacA induced cellular apoptosis. Further studies are needed to identify the essentiality of these effectors in VacA induced cell death, as well as identify the molecular mechanism underlying their release from mitochondria.

Figures

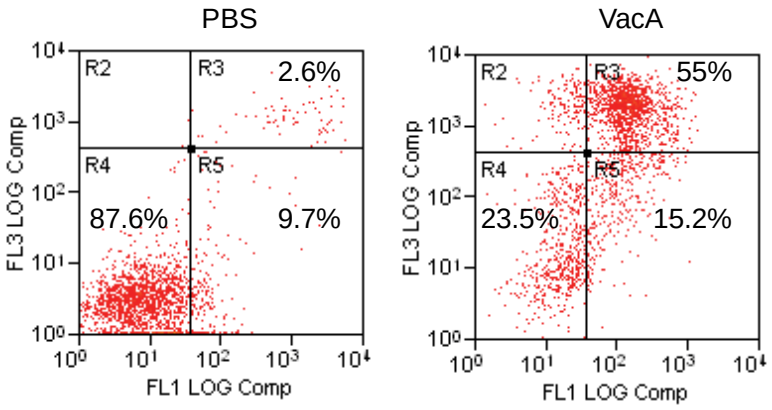

Figure 4.1 VacA induces cellular apoptosis.

AZ-521 cells were incubated at 37 °C and under 5% CO_2 with purified VacA (250 nM) or mock-intoxicated with PBS pH 7.2. After 24 h, the cells were incubated with Annexin-V conjugated to alexa fluor 488 and propidium iodide provided in the apoptosis detection kit (Molecular probes, V13241) and analyzed by flow cytometry in the FL1 and FL3 channels respectively. Live and dead cell were differentiated as follows: Viable cells (Annexin V-, PI -), early apoptotic cells (Annexin V+, PI -) and late apoptotic cells (Annexin V+, PI +). Cell counts in all samples were normalized to 10000 cells. Data are representative of results obtained from at least 4 independent experiments.

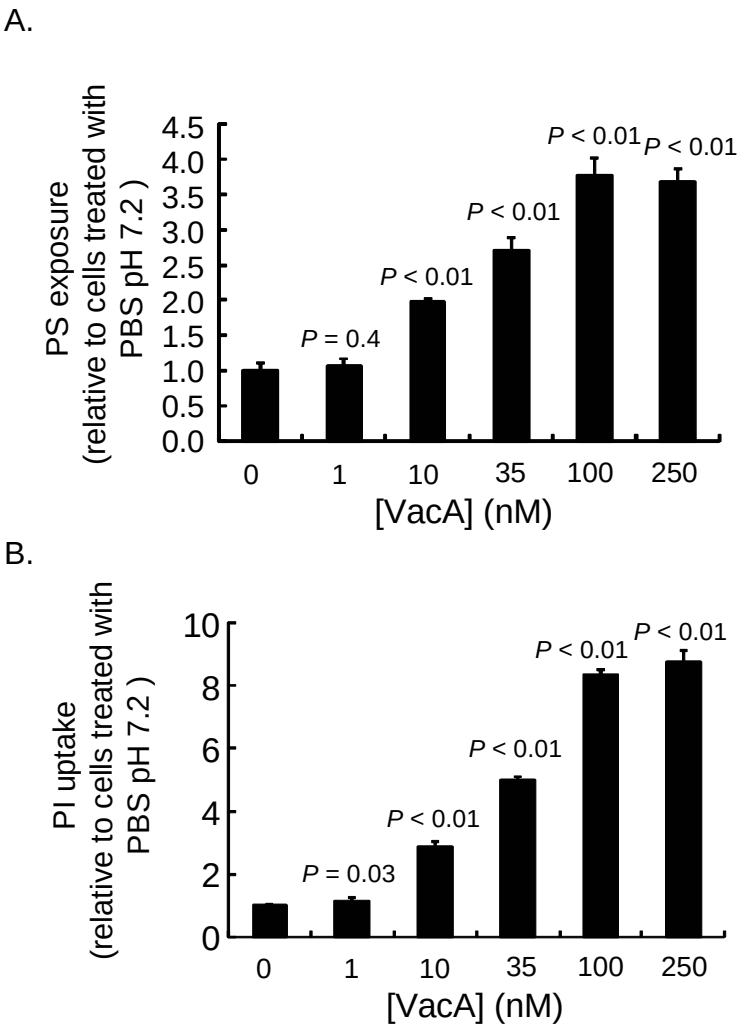

Figure 4.2 VacA induces cellular apoptosis in a toxin dose dependent manner.

AZ-521 cells were incubated at 37 °C and under 5% CO_2 with purified VacA (at the indicated concentrations) or mock-intoxicated with PBS pH 7.2. After 24 h, the cells were incubated with (A) Annexin-V conjugated to alexa fluor 488 to determine PS exposed in the outer leaflet of the plasma membrane and (B) propidium iodide to monitor permeabilization of plasma membrane, provided in the apoptosis detection kit (Molecular probes, V13241). All samples were analyzed by flow cytometry in the FL1 (A) and FL3 (B) channels. Cell counts in all samples were normalized to 10000 cells. Data are representative of results obtained from at least 4 independent experiments. Error bars indicate standard deviations. Statistical significance was calculated for fold differences in PS exposure (A) or PI uptake (B) between cells mock-intoxicated with PBS pH 7.2 versus cells incubated with indicated concentrations of VacA.

A.

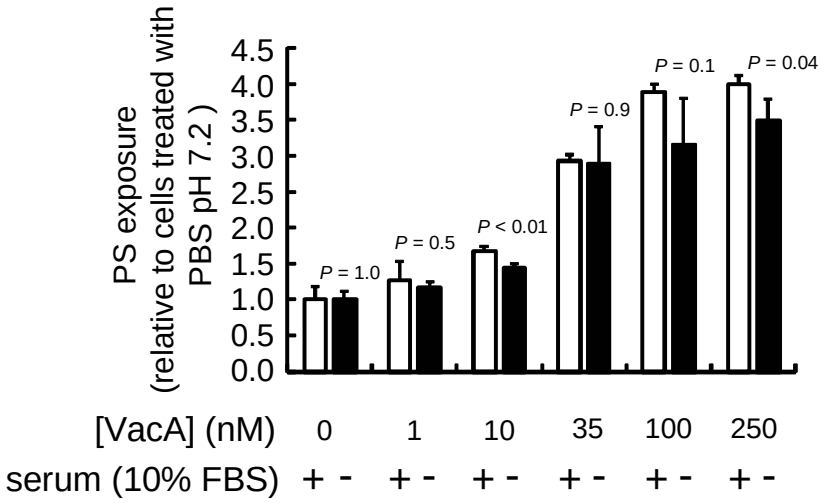

B.

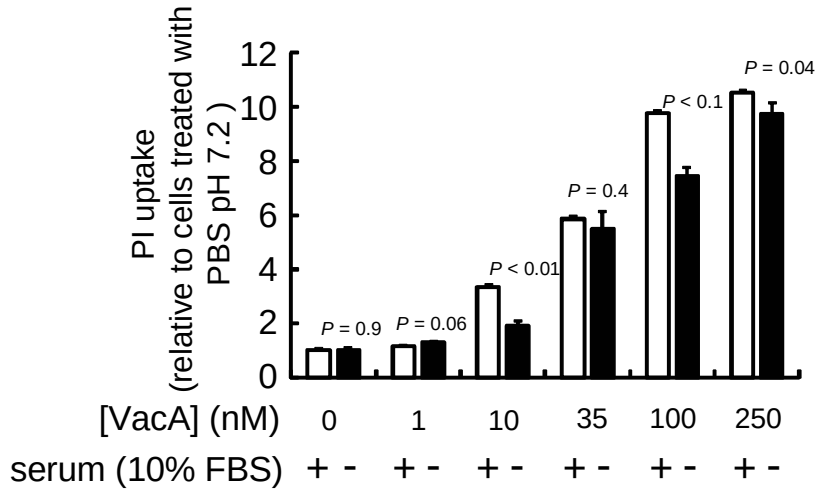

Figure 4.3 Effect of serum on VacA induced cellular apoptosis.

AZ-521 cells were incubated at 37 °C and under 5% CO_2 with purified VacA (at the indicated concentrations) or mock-intoxicated with PBS pH 7.2, in the presence or absence of serum (10% FBS). After 24 h, the cells were incubated with (A) Annexin-V conjugated to alexa fluor 488 to determine PS exposed in the outer leaflet of the plasma membrane and (B) propidium iodide to monitor permeabilization of plasma membrane, provided in the apoptosis detection kit (Molecular probes, V13241). All samples were analyzed by flow cytometry in the FL1 (A) and FL3 (B) channels. Cell counts in all samples were normalized to 10000 cells. Data are representative of results obtained from at least 3 independent experiments. Error bars indicate standard deviations. Statistical significance was calculated for fold differences in PS exposure (A) or PI uptake (B) between cells intoxicated with VacA in the presence of serum versus those intoxicated in the absence of serum.

A.

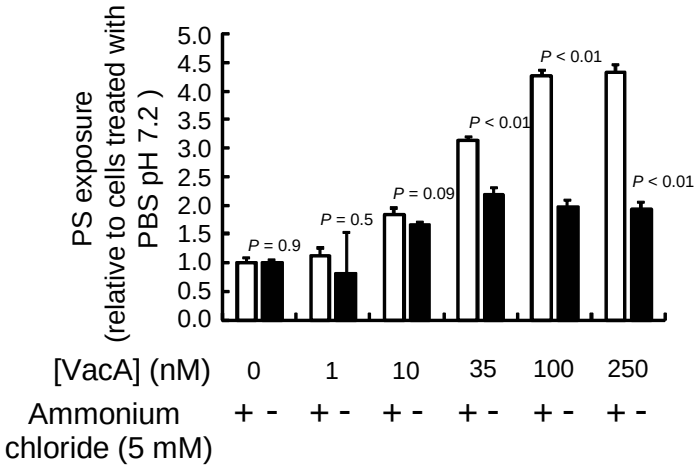

B.

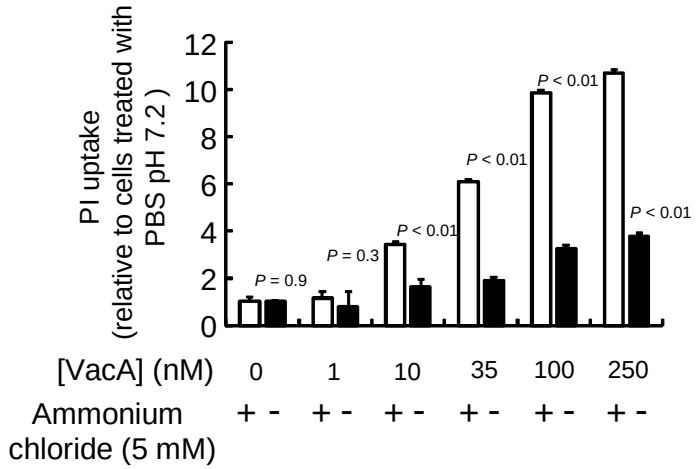

Figure 4.4 Effect of ammonium chloride on VacA induced cellular apoptosis.

AZ-521 cells were incubated at 37 °C and under 5% CO_2 with purified VacA (at the indicated concentrations) or mock-intoxicated with PBS pH 7.2, in the presence or absence of ammonium chloride (5 mM). After 24 h, the cells were incubated with (A) Annexin-V conjugated to alexa fluor 488 to determine PS exposed in the outer leaflet of the plasma membrane and (B) propidium iodide to monitor permeabilization of plasma membrane, provided in the apoptosis detection kit (Molecular probes, V13241). All samples were analyzed by flow cytometry in the FL1 (A) and FL3 (B) channels. Cell counts in all samples were normalized to 10000 cells. Data are representative of results obtained from at least 3 independent experiments. Error bars indicate standard deviations. Statistical significance was calculated for fold differences in PS exposure (A) or PI uptake (B) between cells intoxicated with VacA in the presence of ammonium chloride versus those intoxicated in the absence of ammonium chloride.

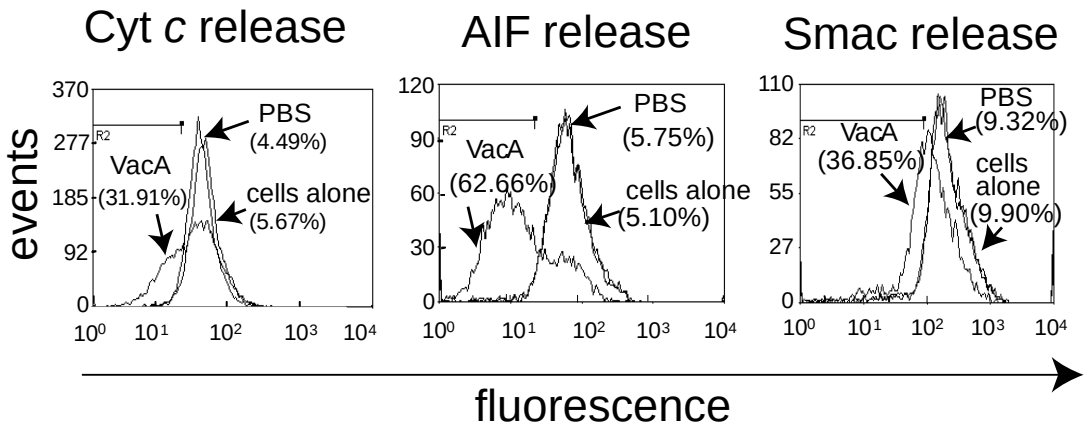

Figure 4.5 VacA intoxication results in the release of Cyt *c*, Smac/DIABLO and AIF from the mitochondrial inter-membrane space to cytosol.

AZ-521 cells were incubated at 37 °C and under 5% CO_2 with purified VacA (250 nM) or mock-intoxicated with PBS pH 7.2. After 24 h, the cells were permeabilized with 0.05% digitonin (500 µg/ml in PBS pH 7.2 with 100 mM KCl), fixed in 4% paraformaldehyde and incubated in blocking buffer (3% BSA and 0.05% saponin in PBS pH 7.2) for 1h. Cells were immunostained with anti-Cyt *c* antibody (6H2.B4; BD) or anti-AIF antibody (Epitomics) followed by incubation with goat anti rabbit IgG (H+L) alexa 488 conjugate (Molecular probes) to detect Cyt *c* or AIF, respectively. To detect Smac/DIABLO, cells were incubated with anti-Smac/DIABLO FITC antibody (Assay Designs) in blocking buffer. Alexa 488 and FITC fluorescence was quantified by flow cytometry in the FL1 channel. Cells with low alexa 488 fluorescence were regarded as having increased cytoplasmic levels of Cyt *c* or AIF and cells with low FITC fluorescence were regarded as having increased cytoplasmic levels of Smac/DIABLO. Cells with high fluorescence were regarded as having intact mitochondrial outer membrane with little to no release of mitochondrial IMS factors into the cytosol. Cell counts in all samples were normalized to 10000 cells. Data are representative of results obtained from at least 3 independent experiments.

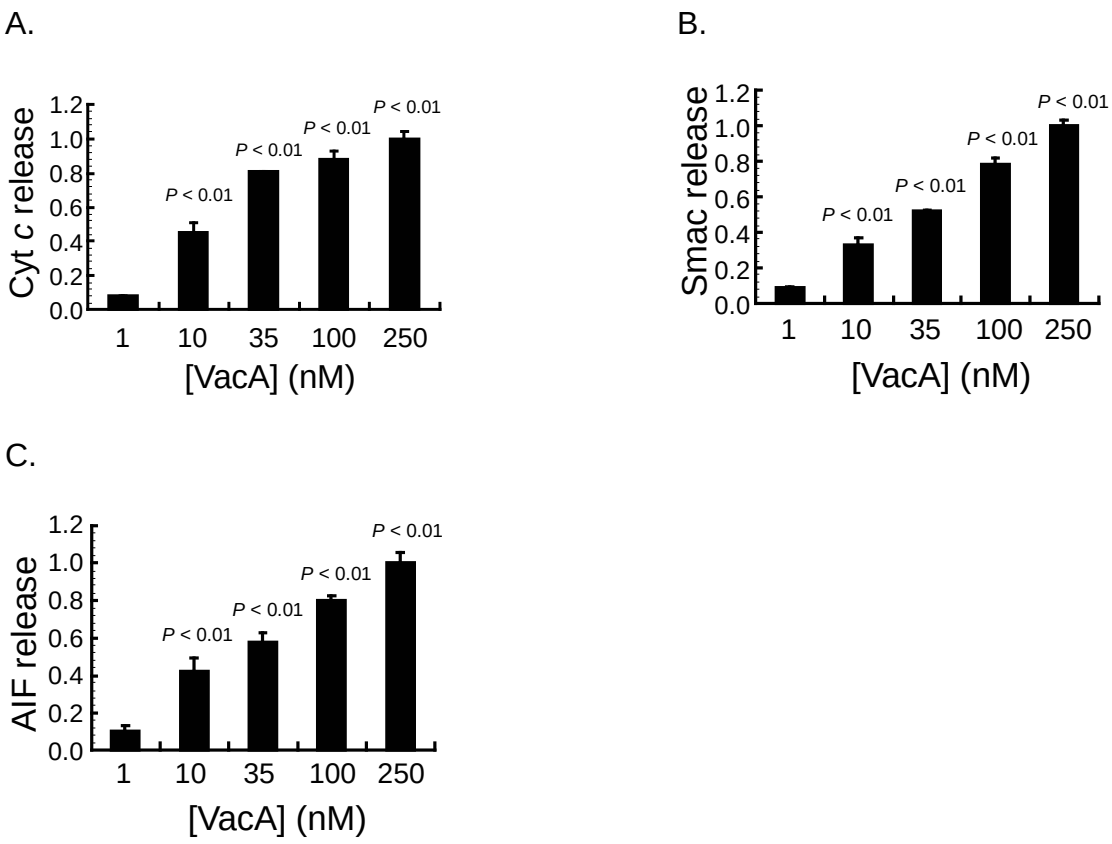

Figure 4.6 VacA intoxication results in the release of Cyt *c*, Smac/DIABLO and AIF from the mitochondrial inter-membrane space to cytosol in a toxin dose dependent manner.

AZ-521 cells were incubated at 37 °C and under 5% CO_2 with purified VacA (at the indicated concentrations) or mock-intoxicated with PBS pH 7.2. After 24 h, the cells were permeabilized with 0.05% digitonin (500 µg/ml in PBS pH 7.2 with 100 mM KCl), fixed in 4% paraformaldehyde and incubated in blocking buffer (3% BSA and 0.05% saponin in PBS pH 7.2) for 1h. (A, C) Cells were immunostained with anti-Cyt *c* antibody (6H2.B4; BD) or anti-AIF antibody (Epitomics) followed by incubation with goat anti rabbit IgG (H+L) alexa 488 conjugate (Molecular probes) to detect (A) Cyt *c* or (C) AIF, respectively. (B) To detect Smac/DIABLO, cells were incubated with anti-Smac/DIABLO FITC antibody (Assay Designs) in blocking buffer. (A, C) Alexa 488 and (B) FITC fluorescence was quantified by flow cytometry in the FL1 channel. Cells with low alexa 488 fluorescence were regarded as having increased cytoplasmic levels of Cyt *c* or AIF and cells with low FITC fluorescence were regarded as having increased cytoplasmic levels of Smac/DIABLO. Cells with high fluorescence were regarded as having intact mitochondrial outer membrane with little to no release of mitochondrial IMS factors into the cytosol. Cell counts in all samples were normalized to 10000 cells. Data are representative of results obtained from at least 2 independent experiments. Error bars indicate standard deviations. Statistical significance was calculated for fold differences in Cyt *c* (A), Smac/DIABLO (B) or AIF release (C) between cells intoxicated with 1 nM VacA versus those intoxicated with increasing concentrations of VacA.

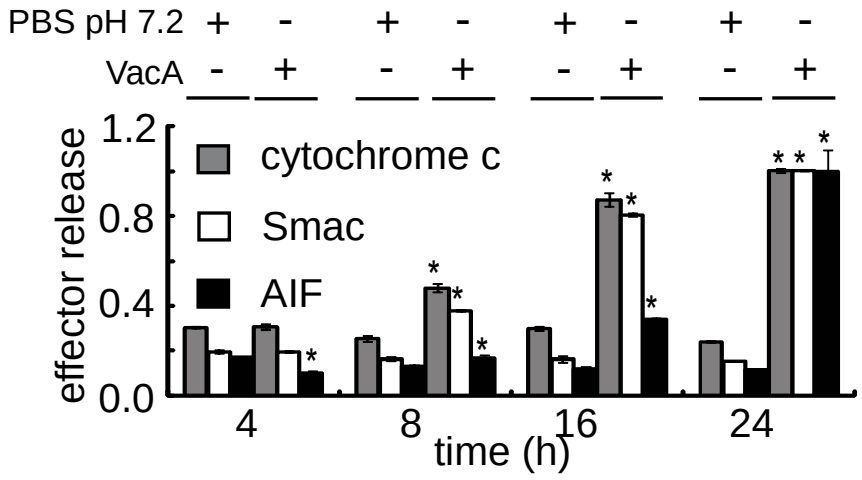

Figure 4.7 VacA intoxication results in a temporally ordered release of Cyt *c*, Smac/DIABLO and AIF from the mitochondrial inter-membrane space to cytosol.

AZ-521 cells were incubated at 37 °C and under 5% CO_2 with purified VacA (250 nM) or mock-intoxicated with PBS pH 7.2. At the indicated time periods, the cells were permeabilized with 0.05% digitonin (500 µg/ml in PBS pH 7.2 with 100 mM KCl), fixed in 4% paraformaldehyde and incubated in blocking buffer (3% BSA and 0.05% saponin in PBS pH 7.2) for 1h. Cells were immunostained with anti-Cyt *c* antibody (6H2.B4; BD) or anti-AIF antibody (Epitomics) followed by incubation with goat anti rabbit IgG (H+L) alexa 488 conjugate (Molecular probes) to detect Cyt *c* or AIF, respectively. To detect Smac/DIABLO, cells were incubated with anti-Smac/DIABLO FITC antibody (Assay Designs) in blocking buffer. Alexa 488 and FITC fluorescence was quantified by flow cytometry in the FL1 channel. Cells with low alexa 488 fluorescence were regarded as having increased cytoplasmic levels of Cyt *c* or AIF and cells with low FITC fluorescence were regarded as having increased cytoplasmic levels of Smac/DIABLO. Cells with high fluorescence were regarded as having intact mitochondrial outer membrane with little to no release of mitochondrial IMS factors into the cytosol. Cell counts in all samples were normalized to 10000 cells. Data are representative of results obtained from at least 3 independent experiments. Error bars indicate standard deviations. Statistical significance was calculated for fold differences in Cyt *c*, Smac/DIABLO or AIF release between cells mock-intoxicated with PBS pH 7.2 versus those intoxicated with VacA at each time period tested.

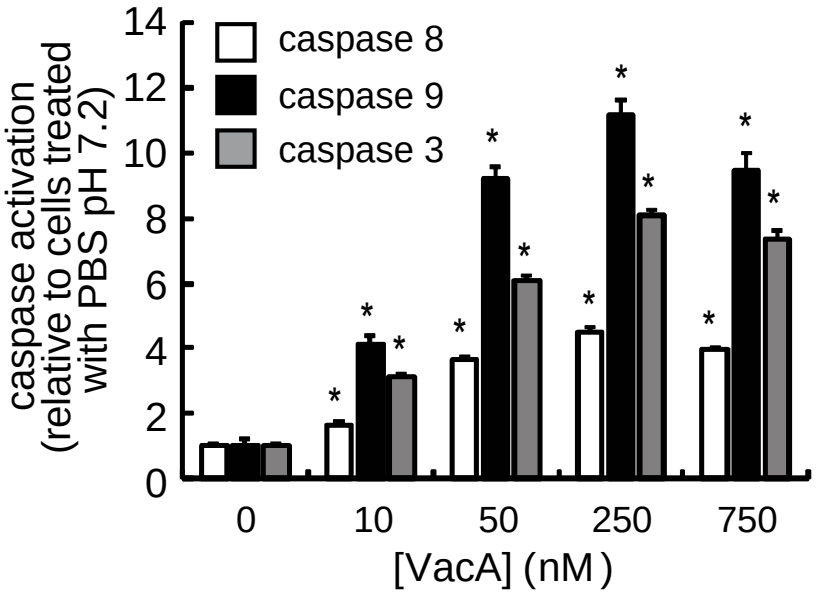

Figure 4.8 VacA induces activation of caspases 8, 9 and 3 in AZ-521 cells.

AZ-521 cells were incubated at 37 °C and under 5% CO_2 with purified VacA (250 nM) or mock-intoxicated with PBS pH 7.2. After 24 h, the cells were incubated with CaspGLOW Fluorescein active caspase 8, 9 or 3 staining kit (BioVision) and cellular fluorescence associated with active caspases was quantified by flow cytometry in the FL1 channel (525/40 nm band pass filter). Cell counts in all samples were normalized to 10000 cells. Data are representative of results obtained from at least 2 independent experiments. Error bars indicate standard deviations. Statistical significance was calculated for fold differences in caspase 8, 9 or 3 activation between cells mock-intoxicated with PBS pH 7.2 versus those intoxicated with each of the indicated concentrations of VacA.

References

1. **Acehan, D., X. Jiang, D. G. Morgan, J. E. Heuser, X. Wang, and C. W. Akey.** 2002. Three-dimensional structure of the apoptosome: implications for assembly, procaspase-9 binding, and activation. Mol Cell **9**:423-32.

2. **Arnoult, D., B. Gaume, M. Karbowski, J. C. Sharpe, F. Cecconi, and R. J. Youle.** 2003. Mitochondrial release of AIF and EndoG requires caspase activation downstream of Bax/Bak-mediated permeabilization. EMBO J **22**:4385-99.

3. **Arnoult, D., P. Parone, J. C. Martinou, B. Antonsson, J. Estaquier, and J. C. Ameisen.** 2002. Mitochondrial release of apoptosis-inducing factor occurs downstream of cytochrome *c* release in response to several proapoptotic stimuli. J Cell Biol **159**:923-9.

4. **Cai, J., J. Yang, and D. P. Jones.** 1998. Mitochondrial control of apoptosis: the role of cytochrome *c*. Biochim Biophys Acta **1366**:139-49.

5. **Calvino-Fernandez, M., S. Benito-Martinez, and T. Parra-Cid.** 2008. Oxidative stress by *Helicobacter pylori* causes apoptosis through mitochondrial pathway in gastric epithelial cells. Apoptosis **13**:1267-80.

6. **Cao, G., J. Xing, X. Xiao, A. K. Liou, Y. Gao, X. M. Yin, R. S. Clark, S. H. Graham, and J. Chen.** 2007. Critical role of calpain I in mitochondrial release of apoptosis-inducing factor in ischemic neuronal injury. J Neurosci **27**:9278-93.

7. **Cover, T. L., and S. R. Blanke.** 2005. *Helicobacter pylori* VacA, a paradigm for toxin multifunctionality. Nat Rev Microbiol **3**:320-32.

8. **Cover, T. L., and M. J. Blaser.** 2009. *Helicobacter pylori* in health and disease. Gastroenterology **136**:1863-73.

9. **Cover, T. L., P. I. Hanson, and J. E. Heuser.** 1997. Acid-induced dissociation of VacA, the *Helicobacter pylori* vacuolating cytotoxin, reveals its pattern of assembly. J Cell Biol **138**:759-69.

10. **Cover, T. L., U. S. Krishna, D. A. Israel, and R. M. Peek, Jr.** 2003. Induction of gastric epithelial cell apoptosis by *Helicobacter pylori* vacuolating cytotoxin. Cancer Res **63**:951-7.

11. **Cover, T. L., S. G. Vaughn, P. Cao, and M. J. Blaser.** 1992. Potentiation of *Helicobacter pylori* vacuolating toxin activity by nicotine and other weak bases. J Infect Dis **166**:1073-8.

12. **de Bernard, M., M. Moschioni, E. Papini, J. Telford, R. Rappuoli, and C. Montecucco.** 1998. Cell vacuolization induced by *Helicobacter pylori* VacA toxin: cell line sensitivity and quantitative estimation. Toxicol Lett **99**:109-15.

13. **Du, C., M. Fang, Y. Li, L. Li, and X. Wang.** 2000. Smac, a mitochondrial protein that promotes cytochrome *c*-dependent caspase activation by eliminating IAP inhibition. Cell **102**:33-42.

14. **Fadok, V. A., A. de Cathelineau, D. L. Daleke, P. M. Henson, and D. L. Bratton.** 2001. Loss of phospholipid asymmetry and surface exposure of phosphatidylserine is required for phagocytosis of apoptotic cells by macrophages and fibroblasts. J Biol Chem **276**:1071-7.

15. **Fadok, V. A., D. R. Voelker, P. A. Campbell, J. J. Cohen, D. L. Bratton, and P. M. Henson.** 1992. Exposure of phosphatidylserine on the surface of apoptotic lymphocytes triggers specific recognition and removal by macrophages. J Immunol **148**:2207-16.

16. **Galluzzi, L., I. Vitale, J. M. Abrams, E. S. Alnemri, E. H. Baehrecke, M. V. Blagosklonny, T. M. Dawson, V. L. Dawson, W. S. El-Deiry, S. Fulda, E. Gottlieb, D. R. Green, M. O. Hengartner, O. Kepp, R. A. Knight, S. Kumar, S. A. Lipton, X. Lu, F. Madeo, W. Malorni, P. Mehlen, G. Nunez, M. E. Peter, M. Piacentini, D. C. Rubinsztein, Y. Shi, H. U. Simon, P. Vandenabeele, E. White, J. Yuan, B. Zhivotovsky, G. Melino, and G. Kroemer.** 2012. Molecular definitions of cell death subroutines: recommendations of the Nomenclature Committee on Cell Death 2012. Cell Death Differ **19**:107-20.

17. **Guo, Y., S. M. Srinivasula, A. Druilhe, T. Fernandes-Alnemri, and E. S. Alnemri.** 2002. Caspase-2 induces apoptosis by releasing proapoptotic proteins from mitochondria. J Biol Chem **277**:13430-7.

18. **Hamel, W., P. Dazin, and M. A. Israel.** 1996. Adaptation of a simple flow cytometric assay to identify different stages during apoptosis. Cytometry **25**:173-81.

19. **Jones, N. L., A. S. Day, H. Jennings, P. T. Shannon, E. Galindo-Mata, and P. M. Sherman.** 2002. Enhanced disease severity in *Helicobacter pylori*-infected mice deficient in Fas signaling. Infect Immun **70**:2591-7.

20. **Kimura, T., A. Wada, M. Nakayama, K. Ogushi, Y. Nishi, B. B. De Guzman, J. Moss, and T. Hirayama.** 2003. High molecular weight factor in FCS inhibits *Helicobacter pylori* VacA-binding to its receptor, RPTPbeta, on AZ-521. Microbiol Immunol **47**:105-7.

21. **Kuck, D., B. Kolmerer, C. Iking-Konert, P. H. Krammer, W. Stremmel, and J. Rudi.** 2001. Vacuolating cytotoxin of *Helicobacter pylori* induces apoptosis in the human gastric epithelial cell line AGS. Infect Immun **69**:5080-7.

22. **Lorenzo, H. K., S. A. Susin, J. Penninger, and G. Kroemer.** 1999. Apoptosis inducing factor (AIF): a phylogenetically old, caspase-independent effector of cell death. Cell Death Differ **6**:516-24.

23. **Menaker, R. J., P. J. Ceponis, and N. L. Jones.** 2004. *Helicobacter pylori* induces apoptosis of macrophages in association with alterations in the mitochondrial pathway. Infect Immun **72**:2889-98.

24. **Morbiato, L., F. Tombola, S. Campello, G. Del Giudice, R. Rappuoli, M. Zoratti, and E. Papini.** 2001. Vacuolation induced by VacA toxin of *Helicobacter pylori* requires the intracellular accumulation of membrane permeant bases, Cl(-) and water. FEBS Lett **508**:479-83.

25. **Moss, S. F., J. Calam, B. Agarwal, S. Wang, and P. R. Holt.** 1996. Induction of gastric epithelial apoptosis by *Helicobacter pylori*. Gut **38**:498-501.

26. **Oberst, A., C. Bender, and D. R. Green.** 2008. Living with death: the evolution of the mitochondrial pathway of apoptosis in animals. Cell Death Differ **15**:1139-46.

27. **Peek, R. M., Jr., H. P. Wirth, S. F. Moss, M. Yang, A. M. Abdalla, K. T. Tham, T. Zhang, L. H. Tang, I. M. Modlin, and M. J. Blaser.** 2000. *Helicobacter pylori* alters gastric epithelial cell cycle events and gastrin secretion in Mongolian gerbils. Gastroenterology **118**:48-59.

28. **Polster, B. M., G. Basanez, A. Etxebarria, J. M. Hardwick, and D. G. Nicholls.** 2005. Calpain I induces cleavage and release of apoptosis-inducing factor from isolated mitochondria. J Biol Chem **280**:6447-54.

29. **Reutelingsperger, C. P., and W. L. van Heerde.** 1997. Annexin V, the regulator of phosphatidylserine-catalyzed inflammation and coagulation during apoptosis. Cell Mol Life Sci **53**:527-32.

30. **Sevrioukova, I. F.** 2011. Apoptosis-inducing factor: structure, function, and redox regulation. Antioxid Redox Signal **14**:2545-79.

31. **Shi, Y.** 2001. A structural view of mitochondria-mediated apoptosis. Nat Struct Biol **8**:394-401.

32. **Singh, M., K. N. Prasad, A. Saxena, and S. K. Yachha.** 2006. *Helicobacter pylori* induces apoptosis of T- and B-cell lines and translocates mitochondrial apoptosis-inducing factor to nucleus. Curr Microbiol **52**:254-60.

33. **Susin, S. A., H. K. Lorenzo, N. Zamzami, I. Marzo, B. E. Snow, G. M. Brothers, J. Mangion, E. Jacotot, P. Costantini, M. Loeffler, N. Larochette, D. R. Goodlett, R. Aebersold, D. P. Siderovski, J. M. Penninger, and G. Kroemer.** 1999. Molecular characterization of mitochondrial apoptosis-inducing factor. Nature **397**:441-6.

34. **Wagner, S., W. Beil, J. Westermann, R. P. Logan, C. T. Bock, C. Trautwein, J. S. Bleck, and M. P. Manns.** 1997. Regulation of gastric epithelial cell growth by *Helicobacter pylori*: offdence for a major role of apoptosis. Gastroenterology **113**:1836-47.

35. **Wang, Y., N. S. Kim, X. Li, P. A. Greer, R. C. Koehler, V. L. Dawson, and T. M. Dawson.** 2009. Calpain activation is not required for AIF translocation in PARP-1-dependent cell death (parthanatos). J Neurochem **110**:687-96.

36. **Willhite, D. C., and S. R. Blanke.** 2004. *Helicobacter pylori* vacuolating cytotoxin enters cells, localizes to the mitochondria, and induces mitochondrial membrane permeability changes correlated to toxin channel activity. Cell Microbiol **6**:143-54.

37. **Wolf, B. B., and D. R. Green.** 1999. Suicidal tendencies: apoptotic cell death by caspase family proteinases. J Biol Chem **274**:20049-52.

38. **Yamasaki, E., A. Wada, A. Kumatori, I. Nakagawa, J. Funao, M. Nakayama, J. Hisatsune, M. Kimura, J. Moss, and T. Hirayama.** 2006. *Helicobacter pylori* vacuolating cytotoxin induces activation of the proapoptotic proteins Bax and Bak, leading to cytochrome c release and cell death, independent of vacuolation. J Biol Chem **281**:11250-9.

39. **Zhang, H., D. C. Fang, C. H. Lan, and Y. H. Luo.** 2007. *Helicobacter pylori* infection induces apoptosis in gastric cancer cells through the mitochondrial pathway. J Gastroenterol Hepatol **22**:1051-6.

Chapter 5: Conclusions and Future Work

The overall objective of the work described in this dissertation was to evaluate and characterize the mechanism underlying the activation of programmed cell death within host cell following *Helicobacter pylori* (*Hp*) infection. Chronic infection with *Hp* is associated with increased cell death within the gastric mucosa of humans (24), mice (18), and Mongolian gerbil models (25). *Hp* induced gastric epithelial cell death contributes towards remodeling of the gastric mucosa in a manner which favors *Hp* persistence (4), while at the same time, could eventually contribute towards generation of gastric disease, including peptic ulcers and gastric adenocarcinoma (5). The vacuolating cytotoxin (VacA), an *Hp* virulence factor, has been shown to be critical for *Hp* colonization (28) and disease pathogenesis (12). Notably, VacA has been shown to be both essential (20) and sufficient (6) for inducing gastric epithelial cell death.

Studies that aimed at identifying the mechanism of VacA mediated host cell death, have demonstrated that VacA is a mitochondrial acting toxin. Subsequent to binding plasma membrane sphingomyelin (16, 17), and potentially additional protein components (36, 37), VacA is internalized and localizes to mitochondria (13, 35). Furthermore, studies have shown that isolated mitochondria rapidly import purified VacA beyond the outer membrane (10, 13). Studies thus far have identified significant changes in the mitochondrial inner and outer membrane integrity following VacA intoxication, which resulted in mitochondrial dysfunction and release of pro-apoptotic factor Cyt *c* into cytosol,

respectively, prior to detectible increase in host cell death (35, 38). These studies therefore indicated that VacA induced the activation of mitochondria dependent cell death mechanism. Importantly, while VacA is sufficient to induce mitochondrial inner membrane permeabilization which leads to mitochondrial dysfunction, the activation of the endogenous host cell death-effector Bcl-2–associated X (Bax) protein or Bax, was required for toxin mediated mitochondrial outer membrane permeabilization and Cyt *c* release (38). However, the mechanism underlying Bax activation remained poorly understood.

Within our study, we report that VacA disrupts the morphological dynamics of mitochondria as a mechanism to induce gastric epithelial cell death. Cellular mitochondria exist as highly interconnected network of extended strands throughout the cell. The mitochondrial network is known to change in a dynamic fashion through frequent and repetitive cycles of fission and fusion that occur in response to cellular energy demands and environmental challenges (32). Therefore, changes in the mitochondrial morphology are emerging as reliable indicators of cellular health. Our results indicate that VacA intoxication resulted in the hyper-activation and mitochondrial targeting of the cellular fission protein Drp1, a dynamin-related GTPase which induces the fragmentation of mitochondrial strands under conditions of prolonged mitochondrial dysfunction or cellular stress (31). Importantly, Drp1 activity was important for VacA mediated cell death within cultured gastric epithelial cells. Investigations into the relationship between Drp1 activity and cellular Bax activation, which is also important for VacA induced cell death mechanism, indicated that Drp1 mediated

mitochondrial fragmentation was required for Bax activation. To evaluate the mechanism of Drp1 activation, we investigated the relationship between Drp1 activity and VacA induced mitochondrial depolarization (dysfunction). Earlier studies have reported that Drp1 dependent mitochondrial fission is required for efficiently weeding out dysfunctional regions from the functional mitochondrial network, thereby maintaining the overall functionality of the network (31). Within our study, we found that inhibition of cellular Drp1 function did not have any significant effect on VacA induced mitochondrial dysfunction. These data therefore suggest that VacA induced mitochondrial inner membrane permeabilization and prolonged dysfunction, could be the trigger for increased activation of Drp1. Our study therefore identified a possible mechanism that links VacA induced mitochondrial dysfunction and disruption of mitochondrial network dynamics to Bax dependent mitochondrial outer membrane permeabilization. Furthermore, our study provides critical insights into the mechanism by which VacA engages the cell death-effector Bax to activate the mitochondrial cell death mechanism. The de-regulation of mitochondrial dynamics has increasingly been linked to the pathologies resulting from inflammatory and neurodegenerative disorders (3), as well as several cancers (14). However, the extent to which the morphological dynamics of mitochondria may be targeted by pathogenic microbes during host infection, or are associated with the pathophysiology of some infectious diseases, has so far been largely unexplored. The disruption of mitochondrial dynamics during *Hp* infection is a here-to-fore unrecognized strategy by which a pathogenic microbe engages the host's apoptotic machinery.

Although our study demonstrated the importance of Drp1 mediated mitochondrial fission in Bax activation following VacA intoxication, the nature of cellular changes initiated by VacA following the de-regulation of mitochondrial network dynamics which resulted in the engagement of host apoptotic machinery, particularly Bax, was not entirely clear. Due to the importance of mitochondrial network in cellular energy production and distribution, increased fragmentation of the mitochondrial network could result in decreased energy production and metabolic stress within cells. In order to evaluate the possibility of a mechanism linking cellular stress as a result of excessive mitochondrial fission to VacA induced Bax activation, we studied the involvement of known Bcl2 family proteins that directly influence Bax activation under conditions of cell stress. Current models of Bax activation indicate that changes in Bax leading to MOMP are critically influenced by members of the BH3 (Bcl-2 homology domain)-only Bcl2 (B cell lymphoma) family, which belong to either the “sensitizer” or “direct activator” class of BH3-only proteins (2). While “sensitizer” BH3-only proteins activate Bax via binding with anti-apoptotic Bcl2 protein, “direct activator” BH3-only proteins are known to directly activate Bax oligomerization at the mitochondrial outer membrane.

Our results demonstrated that the cellular stress sensor protein Bid (BH3 interacting death domain agonist) which belongs to the “direct activator” sub-family of BH3 domain-only proteins (34) played an important role in VacA induced Bax activation. VacA intoxication resulted in the processing of Bid to its mitochondria targeted active fragment called t-Bid (truncated Bid) (9, 15, 19, 21,

22, 29). Inhibition of Bid processing and mitochondrial translocation prevented VacA induced Bax activation and cell death. Importantly, inhibition of Drp1 mediated mitochondrial fission led to significantly decreased Bid processing within VacA intoxicated cells. Our results therefore indicate a mechanism where de-regulation of mitochondrial dynamics results in the activation of Bax through the activation and mitochondrial recruitment of the cell stress sensor protein Bid.

Bid processing can occur following processing by a variety of cellular proteases, such as the cysteine-aspartate protease, caspase 8 or the calcium dependent cysteine protease, calpain, depending on the stress/death inducing signal (1, 9, 15, 23). Within VacA intoxicated cells, we observed the activation of both caspase 8 and calpain. However, while calpain activation occurred at time periods similar to those observed for Bid processing, the activation of caspase 8 was observed at significantly later time periods. Importantly, the mitochondrial translocation of Bid was considerably reduced following inhibition of cellular calpain activity. Studies to further characterize the mechanism of VacA induced calpain activation revealed significant elevation in cytosolic calcium levels at time points similar to detectable calpain activation. Notably, chemical chelation of cytosolic calcium resulted in significant inhibition of VacA induced calpain activation, Bax activation and cell death. These results therefore indicated that early rise in cytosolic calcium levels following VacA intoxication was important for engaging the mitochondrial cell death machinery.

Significantly, studies which aimed at evaluating the relationship between VacA induced de-regulation of mitochondrial network dynamics and disruption of

cellular calcium homeostasis demonstrated that Drp1 mediated mitochondrial fission was required for VacA induced rise in cytosolic calcium levels. The mechanism underlying Drp1 dependent rise in cytosolic calcium is not currently understood. Studies have revealed significant cross-talk between mitochondria and endoplasmic reticulum (ER) which is the main intra-cellular calcium store within a cell (7). The ER-mitochondria connections are known to play an important role in the buffering of cytosolic calcium levels (26, 27). Additionally, a recent study suggested that ER wraps around the mitochondria at specific contact sites (11). Furthermore, the study also indicates that the fission protein Drp1 targets the mitochondria specifically at the contact sites with ER. Future studies would evaluate the effects of VacA induced mitochondrial network fragmentation on ER-mitochondria connections and related capacity of cells to buffer changes in cytosolic calcium levels. Additionally, the relationship between Drp1 and ER morphology would also be investigated.

Thus far, our results indicate that the BH3 domain-only protein Bid is important for VacA mediated Bax activation. Bid belongs to an important class of cellular proteins called BH3 domain-only Bcl2 proteins that act as sentinels for stress signals and are responsible for relaying the stress signal to pro-death effectors such as Bax, thereby inducing Bax mediated mitochondrial outer membrane permeabilization (8, 30, 33). BH3 domain-only proteins can be classified into either “sensitizers” or “de-repressors”, which include proteins like Bad and Noxa, or “direct activators” which include proteins like Bid and Bim (2). Within these models, key events that lead to activation of Bax involve either

association of BH3-only proteins to members of the anti-apoptotic Bcl2 proteins, thereby alleviating repression on Bax, or direct activation of Bax, leading to homo-oligomerization of Bax at the mitochondrial outer membrane. While sensitizer (de-repressor) BH3-only proteins activate Bax via binding with anti-apoptotic Bcl2 protein, direct activator BH3-only proteins are known to directly activate Bax oligomerization at the mitochondrial outer membrane. However, the relative contribution of the different members of the BH3 domain-only proteins in VacA induced mitochondrial outer membrane permeabilization remains poorly understood. Future work would aim to evaluate the importance of the various BH3 domin-only proteins in VacA induced Bax activation. Particularly, it would be interesting to see whether certain degree of functional cross-talk exists between the different BH3 domain-only proteins.

Figure

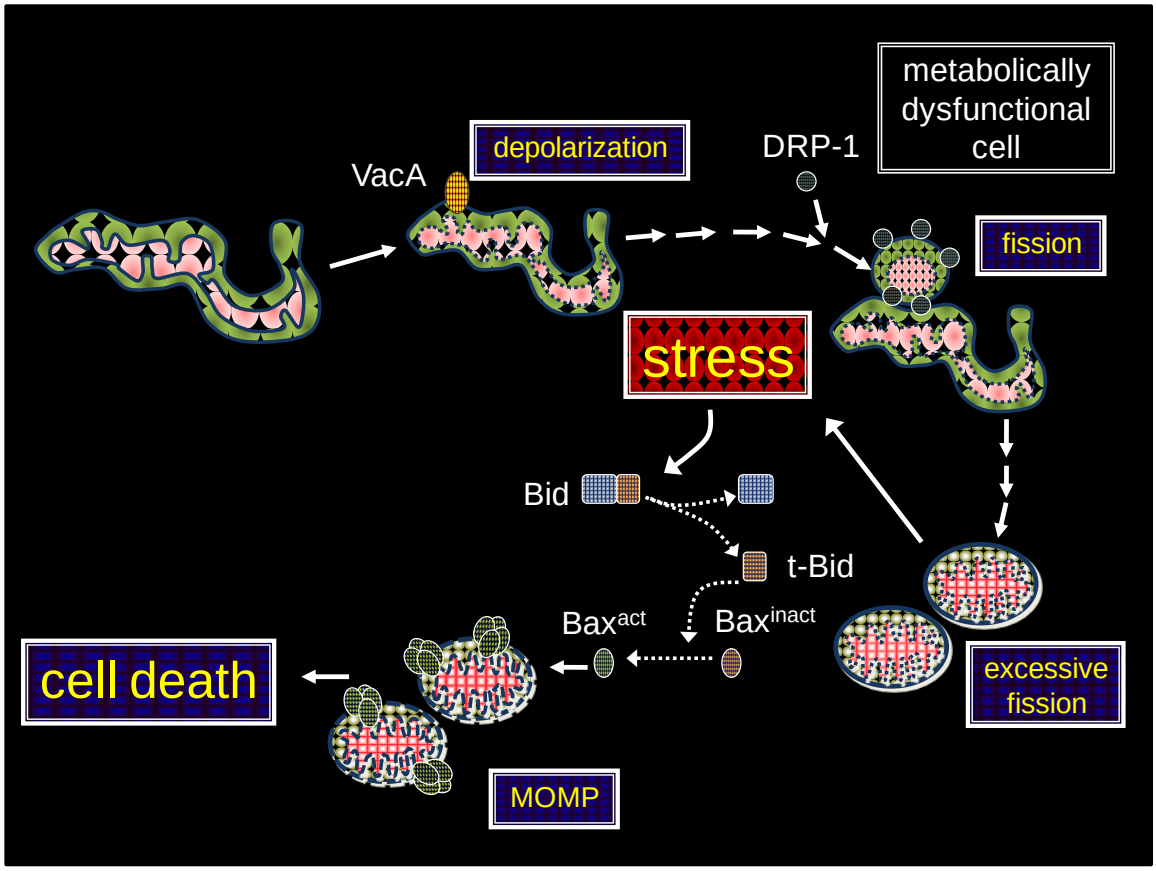

Figure 5.1 Model illustrating the proposed mechanism for VacA induced activation of mitochondria dependent host cell death.

References

1. **Chen, M., H. He, S. Zhan, S. Krajewski, J. C. Reed, and R. A. Gottlieb.** 2001. Bid is cleaved by calpain to an active fragment in vitro and during myocardial ischemia/reperfusion. J Biol Chem **276:**30724-8.

2. **Chipuk, J. E., and D. R. Green.** 2008. How do BCL-2 proteins induce mitochondrial outer membrane permeabilization? Trends Cell Biol **18:**157-64.

3. **Cho, D. H., T. Nakamura, and S. A. Lipton.** 2010. Mitochondrial dynamics in cell death and neurodegeneration. Cell Mol Life Sci **67:**3435-47.

4. **Cover, T. L., and S. R. Blanke.** 2005. *Helicobacter pylori* VacA, a paradigm for toxin multifunctionality. Nat Rev Microbiol **3:**320-32.

5. **Cover, T. L., and M. J. Blaser.** 2009. *Helicobacter pylori* in health and disease. Gastroenterology **136:**1863-73.

6. **Cover, T. L., U. S. Krishna, D. A. Israel, and R. M. Peek, Jr.** 2003. Induction of gastric epithelial cell apoptosis by *Helicobacter pylori* vacuolating cytotoxin. Cancer Res **63:**951-7.

7. **de Brito, O. M., and L. Scorrano.** 2010. An intimate liaison: spatial organization of the endoplasmic reticulum-mitochondria relationship. EMBO J **29:**2715-23.

8. **Desagher, S., A. Osen-Sand, A. Nichols, R. Eskes, S. Montessuit, S. Lauper, K. Maundrell, B. Antonsson, and J. C. Martinou.** 1999. Bid-induced conformational change of Bax is responsible for mitochondrial cytochrome c release during apoptosis. J Cell Biol **144:**891-901.

9. **Eskes, R., S. Desagher, B. Antonsson, and J. C. Martinou.** 2000. Bid induces the oligomerization and insertion of Bax into the outer mitochondrial membrane. Mol Cell Biol **20:**929-35.

10. **Foo, J. H., J. G. Culvenor, R. L. Ferrero, T. Kwok, T. Lithgow, and K. Gabriel.** 2010. Both the p33 and p55 subunits of the *Helicobacter pylori* VacA toxin are targeted to mammalian mitochondria. J Mol Biol **401:**792-8.

11. **Friedman, J. R., L. L. Lackner, M. West, J. R. DiBenedetto, J. Nunnari, and G. K. Voeltz.** 2011. ER tubules mark sites of mitochondrial division. Science **334:**358-62.

12. **Fujikawa, A., D. Shirasaka, S. Yamamoto, H. Ota, K. Yahiro, M. Fukada, T. Shintani, A. Wada, N. Aoyama, T. Hirayama, H. Fukamachi, and M. Noda.** 2003. Mice deficient in protein tyrosine phosphatase receptor type Z are resistant to gastric ulcer induction by VacA of *Helicobacter pylori*. Nat Genet **33:**375-81.

13. **Galmiche, A., J. Rassow, A. Doye, S. Cagnol, J. C. Chambard, S. Contamin, V. de Thillot, I. Just, V. Ricci, E. Solcia, E. Van Obberghen, and P. Boquet.** 2000. The N-terminal 34 kDa fragment of *Helicobacter pylori* vacuolating cytotoxin targets mitochondria and induces cytochrome c release. EMBO J **19:**6361-70.

14. **Grandemange, S., S. Herzig, and J. C. Martinou.** 2009. Mitochondrial dynamics and cancer. Semin Cancer Biol **19:**50-6.

15. **Gross, A., X. M. Yin, K. Wang, M. C. Wei, J. Jockel, C. Milliman, H. Erdjument-Bromage, P. Tempst, and S. J. Korsmeyer.** 1999. Caspase cleaved BID targets mitochondria and is required for cytochrome c release, while BCL-XL prevents this release but not tumor necrosis factor-R1/Fas death. J Biol Chem **274:**1156-63.

16. **Gupta, V. R., H. K. Patel, S. S. Kostolansky, R. A. Ballivian, J. Eichberg, and S. R. Blanke.** 2008. Sphingomyelin functions as a novel receptor for *Helicobacter pylori* VacA. PLoS Pathog **4:**e1000073.

17. **Gupta, V. R., B. A. Wilson, and S. R. Blanke.** 2010. Sphingomyelin is important for the cellular entry and intracellular localization of *Helicobacter pylori* VacA. Cell Microbiol **12:**1517-33.

18. **Jones, N. L., A. S. Day, H. Jennings, P. T. Shannon, E. Galindo-Mata, and P. M. Sherman.** 2002. Enhanced disease severity in *Helicobacter pylori*-infected mice deficient in Fas signaling. Infect Immun **70:**2591-7.

19. **Korsmeyer, S. J., M. C. Wei, M. Saito, S. Weiler, K. J. Oh, and P. H. Schlesinger.** 2000. Pro-apoptotic cascade activates BID, which oligomerizes BAK or BAX into pores that result in the release of cytochrome c. Cell Death Differ **7:**1166-73.

20. **Kuck, D., B. Kolmerer, C. Iking-Konert, P. H. Krammer, W. Stremmel, and J. Rudi.** 2001. Vacuolating cytotoxin of *Helicobacter pylori* induces apoptosis in the human gastric epithelial cell line AGS. Infect Immun **69:**5080-7.

21. **Li, H., H. Zhu, C. J. Xu, and J. Yuan.** 1998. Cleavage of BID by caspase 8 mediates the mitochondrial damage in the Fas pathway of apoptosis. Cell **94:**491-501.

22. **Luo, X., I. Budihardjo, H. Zou, C. Slaughter, and X. Wang.** 1998. Bid, a Bcl2 interacting protein, mediates cytochrome *c* release from mitochondria in response to activation of cell surface death receptors. Cell **94:**481-90.

23. **Mandic, A., K. Viktorsson, L. Strandberg, T. Heiden, J. Hansson, S. Linder, and M. C. Shoshan.** 2002. Calpain-mediated Bid cleavage and calpain-independent Bak modulation: two separate pathways in cisplatin-induced apoptosis. Mol Cell Biol **22:**3003-13.

24. **Moss, S. F., J. Calam, B. Agarwal, S. Wang, and P. R. Holt.** 1996. Induction of gastric epithelial apoptosis by *Helicobacter pylori*. Gut **38:**498-501.

25. **Peek, R. M., Jr., H. P. Wirth, S. F. Moss, M. Yang, A. M. Abdalla, K. T. Tham, T. Zhang, L. H. Tang, I. M. Modlin, and M. J. Blaser.** 2000. *Helicobacter pylori* alters gastric epithelial cell cycle events and gastrin secretion in Mongolian gerbils. Gastroenterology **118:**48-59.

26. **Rizzuto, R., M. Brini, M. Murgia, and T. Pozzan.** 1993. Microdomains with high Ca2+ close to IP3-sensitive channels that are sensed by neighboring mitochondria. Science **262:**744-7.

27. **Rizzuto, R., P. Pinton, W. Carrington, F. S. Fay, K. E. Fogarty, L. M. Lifshitz, R. A. Tuft, and T. Pozzan.** 1998. Close contacts with the endoplasmic reticulum as determinants of mitochondrial Ca2+ responses. Science **280:**1763-6.

28. **Salama, N. R., G. Otto, L. Tompkins, and S. Falkow.** 2001. Vacuolating cytotoxin of *Helicobacter pylori* plays a role during colonization in a mouse model of infection. Infect Immun **69:**730-6.

29. **Stoka, V., B. Turk, S. L. Schendel, T. H. Kim, T. Cirman, S. J. Snipas, L. M. Ellerby, D. Bredesen, H. Freeze, M. Abrahamson, D. Bromme, S. Krajewski, J. C. Reed, X. M. Yin, V. Turk, and G. S. Salvesen.** 2001. Lysosomal protease pathways to apoptosis. Cleavage of bid, not pro-caspases, is the most likely route. J Biol Chem **276:**3149-57.

30. **Tait, S. W., E. de Vries, C. Maas, A. M. Keller, C. S. D'Santos, and J. Borst.** 2007. Apoptosis induction by Bid requires unconventional ubiquitination and degradation of its N-terminal fragment. J Cell Biol **179:**1453-66.

31. **Twig, G., A. Elorza, A. J. Molina, H. Mohamed, J. D. Wikstrom, G. Walzer, L. Stiles, S. E. Haigh, S. Katz, G. Las, J. Alroy, M. Wu, B. F. Py, J. Yuan, J. T. Deeney, B. E. Corkey, and O. S. Shirihai.** 2008. Fission and selective fusion govern mitochondrial segregation and elimination by autophagy. EMBO J **27:**433-46.

32. **Twig, G., B. Hyde, and O. S. Shirihai.** 2008. Mitochondrial fusion, fission and autophagy as a quality control axis: the bioenergetic view. Biochim Biophys Acta **1777:**1092-7.

33. **Walensky, L. D., K. Pitter, J. Morash, K. J. Oh, S. Barbuto, J. Fisher, E. Smith, G. L. Verdine, and S. J. Korsmeyer.** 2006. A stapled BID BH3 helix directly binds and activates BAX. Mol Cell **24:**199-210.

34. **Wang, K., X. M. Yin, D. T. Chao, C. L. Milliman, and S. J. Korsmeyer.** 1996. BID: a novel BH3 domain-only death agonist. Genes Dev **10:**2859-69.

35. **Willhite, D. C., and S. R. Blanke.** 2004. *Helicobacter pylori* vacuolating cytotoxin enters cells, localizes to the mitochondria, and induces mitochondrial membrane permeability changes correlated to toxin channel activity. Cell Microbiol **6:**143-54.

36. **Yahiro, K., T. Niidome, M. Kimura, T. Hatakeyama, H. Aoyagi, H. Kurazono, K. Imagawa, A. Wada, J. Moss, and T. Hirayama.** 1999. Activation of *Helicobacter pylori* VacA toxin by alkaline or acid conditions increases its binding to a 250-kDa receptor protein-tyrosine phosphatase beta. J Biol Chem **274:**36693-9.

37. **Yahiro, K., A. Wada, M. Nakayama, T. Kimura, K. Ogushi, T. Niidome, H. Aoyagi, K. Yoshino, K. Yonezawa, J. Moss, and T. Hirayama.** 2003. Protein-tyrosine phosphatase alpha, RPTP alpha, is a *Helicobacter pylori* VacA receptor. J Biol Chem **278:**19183-9.

38. **Yamasaki, E., A. Wada, A. Kumatori, I. Nakagawa, J. Funao, M. Nakayama, J. Hisatsune, M. Kimura, J. Moss, and T. Hirayama.** 2006. *Helicobacter pylori* vacuolating cytotoxin induces activation of the proapoptotic proteins Bax and Bak, leading to cytochrome c release and cell death, independent of vacuolation. J Biol Chem **281:**11250-9.